Mutational Analysis of Hsp110 Suggests an Integral Role for the Chaperone in Yeast Prion Propagation

NUI MAYNOOTH

Ollscoil na hÉireann Má Nuad

A thesis submitted to the

National University of Ireland Maynooth

For the degree of

DOCTOR OF PHILOSOPHY

BY

Ciara Moran B.Sc.

Supervisor:

Dr. Gary Jones,

Yeast Genetics Laboratory,

NUI Maynooth,

Co. Kildare.

Head of Department:

Professor Kay Ohlendieck

November 2010

TABLE OF CONTENTS

Chapter 1. Introduction

Chapter 2. Materials and Methods

Chapter 3. Isolation and characterisation of *sse1* mutants that impair prion propagation

Chapter 4. Investigation into the temperature-sensitive effects of *sse1* mutants

Chapter 5. Comparative analysis of *SSE1* and *SSE2* in ability to propagate prions and an initial introduction into posttranslational modification of Hsp110

Chapter 6. Discussion

LIST OF FIGURES

Chapter 1 Figures

Chapter 2 Figures

Chapter 3 Figures

Chapter 4 Figures

Chapter 5 Figures

Chapter 6 Figures

LIST OF TABLES

Chapter 1 Tables

Chapter 2 Tables

Chapter 3 Tables

Chapter 4 Tables

Chapter 5 Tables

Chapter 6 Tables

ABBREVIATIONS

(3HBD)	3-helical bundle domain
(5-FOA)	5-fluoroorotic acid
(ADP)	adenosine diphosphate
(ATP)	adenosine triphosphate
(APS)	alkaline phosphatase
(bp)	base pair
(BSA)	bovine serum albumin
($CaCl_2.2H_2O$)	calcium chloride dihydrate
(cAMP)	cyclic adenosine monophosphate
(Cip)	calf intestinal protein
(CWI)	cell wall integrity
(dH_2O)	distilled water
(DNA)	deoxyribonucleic acid
(DTT)	dithiothreitol
(EDTA)	ethylenediaminetetraacetic acid
(EtOH)	ethanol
(GdnHCl)	guanidine hydrochloride
(GT)	generation time
(HB)	hydrogen bond
(HF)	high fidelity
(H_2O_2)	hydrogen peroxide
(HOG)	high osmolarity glycerol
(Hsps)	heat shock proteins

(ISCMs)	inactivating stop codon mutations
(KAc)	potassium acetate
(K-Acetate)	potassium acetate
(Kb)	kilobase
(kDa)	kilodalton
(KO)	knockout
(l)	litre
(LB)	Luria broth
(LiAc)	lithium acetate
(M)	mole
(mM)	millimole
(MAP)	mitogen-activated protein
(MeOH)	methanol
($MgCl_2$)	magnesium chloride
(mg)	milligram
($MgSO_4$)	magnesium sulfate
(ml)	millilitre
(mm)	millimetre
($MnCl_2.4H_2O$)	manganese chloride tetrahydrate
(NaCl)	sodium chloride
(NaOH)	sodium hydroxide
(NBD)	nucleotide binding domain
(NEB)	new england biolabs
(NEF)	nucleotide exchange factor
(ng)	nanogram

(nm)	nanometre
(OD)	optical density
(ORFs)	open reading frames
(PCR)	polymerase chain reaction
(PEG)	polyethylene glycol
(PKA)	protein kinase A
(pmol)	picomole
(PVDF)	polyvinylidene
(RbCl)	rubidium chloride
(SBD)	substrate binding domain
(SC)	synthetic complete
(SD)	synthetic dextrose
(SDS)	sodium dodecyl sulfate
(SMM)	supplemented minimal media
(SNP)	single nucleotide polymorphism
(Sss)	second site suppressor
(TAE)	tris-acetate-EDTA
(TBS)	tris buffered saline
(TBS-t)	tris buffered saline-tween
(TOR)	target of rapamycin
(ts)	temperature sensitive
(v-src)	viral sarcoma
(v/v)	volume per total volume
(WT)	wild type
(w/v)	weight per total volume

(YPD)	yeast peptone dextrose
(YPG)	yeast peptone glycerol
(μg)	microgram
(μl)	microlitre
(μM)	micromolar

Presentations

Isolation of Hsp110 (Sse1) mutants that impair prion propagation. The Society for General Microbiology Meeting, University College Cork, April 2009. (Poster presentation).

Isolation of Hsp110 (Sse1) mutants that impair prion propagation. The Irish Fungal Meeting, Conway Institute, University College Dublin, June 2009. (Poster presentation).

Isolation of Hsp110 (Sse1) mutants that impair prion propagation. Royal Academy of Medicine in Ireland Annual Meeting, NUI Maynooth, June 2009. (Poster presentation).

Mutational Analysis of Sse1 (Hsp110) Suggests an Integral Role for the Chaperone in Yeast Prion Propagation. The Irish Fungal Meeting, University College Cork, June 2010. (Poster presentation).

The role of chaperones in yeast prion propagation. Presentation at NUI Maynooth department of Biology seminar, June 2008. (Oral presentation).

The role of Hsp110 in the regulation of yeast prion propagation. Presentation at NUI Maynooth department of Biology seminar, June 2009. (Oral presentation).

Abstract

Prions are highly aggregated infectious proteins that have been identified in mammals and in some fungal species. The discovery that prions exist in the yeast species *S. cerevisiae* has enabled researchers to explore the characteristics of these unusual proteins and how they propagate within the cell. Heat shock proteins are implicated as having a major role in the propagation of prions. The work presented in this thesis focuses on the heat shock protein Hsp110. Recent reports have demonstrated how the Hsp110 proteins Sse1 and Sse2 are necessary for promoting the propagation of the yeast prions [*PSI*$^{+}$] and [*URE3*]. A group of Sse1 mutants with impaired ability to propagate [*PSI*$^{+}$] were created. These mutants were characterised according to the degree in which they affect [*PSI*$^{+}$]. Molecular modeling of the mutants onto the Sse1 structure allowed us to assess the potential structural affects the mutants are having on Sse1. These changes could affect normal Sse1 functions necessary for [*PSI*$^{+}$] propagation such as nucleotide exchange factor function and interaction with the molecular chaperone Hsp70. *SSE1* and *SSE2* are an essential gene pair and have been implicated in yeast cellular homeostasis. The Sse1 mutants disrupted cellular thermostability at 37^{o}C and 39^{o}C. Mutant G616D displayed osmoremedial temperature sensitivity at 37^{o}C. Disruption to cell wall integrity signaling was explored as a possible reason for this phenotype but evidence from this study suggests that G616D may disrupt PKA signaling. Comparative analysis of Sse1 and Sse2 reveals that Sse1 is more thermostable than Sse2 and Sse1 propagates [*PSI*$^{+}$] efficiently whereas Sse2 fails to promote [*PSI*$^{+}$] propagation. Small structural differences between the proteins may be responsible for this. However, differentially phosphorylating Sse2 may impact its ability to act as a [*PSI*$^{+}$] promoting factor.

Overall, this work further highlights the important role Sse1 plays in yeast prion propagation and in cellular homeostasis.

Acknowledgements

I would first and foremost like to thank my supervisor Dr Gary Jones for all his help and guidance over the past three years. I would also like to thank my fourth year research project supervisor Dr Kevin Kavanagh for his encouragement and advice on pursuing a PhD. I would like to thank my colleagues from the Yeast Genetics Lab, Harriet, Emma, Sarah, Jen and Naushaba. Thanks to Harriet and Emma for their help with my experiments and for helping me settle into the lab all those years ago. Thanks girls for all the laughs we've had and hopefully we will stay friends for a very long time! Thanks to all the friends I've made in the department, particularly from the Biotech and Medical Mycology Lab, we have really had an interesting three years through the difficult and the fun times! I would especially like to thank the Biology department and IRCSET for their funding and thankyou to the technical staff for all their help. I would like to thank those who have contributed to the work in this thesis, to Gemma Kinsella (Membrane Protein Lab, NUIM) for her help with the molecular modeling, to Zhai Chao (Dr Panaratou Lab, Kings College London) for his help with the Hsp90 experiments and to all my past fourth year and UREKA students who have contributed to this work.

Thankyou to all my family and friends for their support and encouragement over the past three years. I would like to thank all my grandparents, in particular my granddad Moran who helped me throughout school, college and my PhD and who would have loved to see this thesis. My deepest thanks go to my parents Fran and Philip who have encouraged and supported me throughout my years of learning and whose advice and love has helped me in every way. Thankyou for helping me chose Maynooth to pursue my undergraduate degree and thanks Mam for all the unexpected car lifts when I was stuck at the bus stop! I would like to thank my wonderful

boyfriend Derek, who has been my rock throughout this PhD. Thankyou for dropping and collecting me to and from the lab at awkward times and for being my personal alarm clock in the morning! Thanks for putting up with my rants over the past few months and for all the cooking and cleaning you have had to do as I was totally useless! Without your support, love and good humour I could never have done this PhD.

Declaration of Authorship

This thesis has not been submitted in whole or in part, to this or any other University, for any degree and is except otherwise stated the original work of the author.

_____

Ciara Moran B.Sc.

CHAPTER ONE
INTRODUCTION

1.1 An introduction to amyloids

An amyloid is a filamentous protein aggregate with cross β-sheet structure. The β-strands are stacked perpendicular to the fibril axis (Dobson, 2003). Protein amyloid deposition in the central nervous system causes human neurodegenerative disorders such as Alzheimer's, Huntington's and Parkinson's disease. Despite much research into protein amyloid formation, little is understood about how they cause their toxic effects. To date, more than 20 human proteins have been identified which form amyloid aggregates, including the protein responsible for a group of diseases termed 'prions' (Caughey and Lansbury, 2003).

1.2 Prion disease in mammalian systems

Prions are infectious proteins that cause a group of neurodegenerative diseases termed transmissible spongiform encephalopathies (TSEs) (Weissmann and Aguzzi, 2005). In a review article by Aguzzi (2003) it states that mammalian prion transmission is usually taken up orally. Prions enter the GI tract where they travel through the gut and invade the peripheral nervous system, finally ascending to the central nervous system (CNS) (Aguzzi, 2003). Mammalian prion disease results in spongiform degeneration and astrocytic gliosis in the central nervous system of the patient (Zlotnik and Stamp, 1961). Mammalian disease caused by prions include Creutzfeldt-Jakob disease (CJD), Gerstmann-Straussler-Scheinker syndrome (GSS) and kuru in man; chronic wasting disease (CWD) in deer and elk; scrapie in sheep and Bovine Spongiform Encephalopathy (BSE) in cattle, as reviewed in Collinge (2001) and Collinge (2005). TSEs were first recognised as scrapie of sheep in Western Europe in the 1700s but evidence suggests they may have existed much earlier (M'Gowan, 1914; Wickner, 2005).

1.2.1 Isolation and characterisation of the infectious agent

In 1966 Alper *et al*. sought to determine the nature of the scrapie infectious agent. From inactivation studies using ionizing and UV irradiation they concluded that the infectious agent was too small to be a viral particle and it displayed protein-like properties. Many questions were left unanswered until the early 1980s when Stanley Prusiner performed a number of chemical, physical and enzymatic studies on this disease. Once believed to be a viral particle, Prusiner proved that the infectious agent was extremely resistant to chemical viral inactivation but sensitive to protein damaging agents, suggesting it had a structure completely different from viruses. He hypothesised that this enigmatic disease may have a requirement for protein in order to cause infectivity. He assigned the name 'prion' to the disease, derived from proteinaceous and infectious (Prusiner, 1982). He later defined a prion as a 'proteinaceous infectious agent that lacks nucleic acid' (Prusiner, 1997).

In a review article by Riesner (2003) it states that in order to confirm that prions were proteinaceous, the protein had to be purified and characterised (Riesner, 2003). The discovery that PrP protein was associated with prion disease transformed prion-related research progress. PrP was first isolated from homogenised animal brain tissue purified by precipitation. Prion forms of PrP are resistant to proteinase K digestion and this step was crucial in the isolation of the prion protein (Figure 1.1) (McKinley *et al*., 1991; Riesner, 2003).

PrP is a highly conserved mammalian glycoprotein essential for prion disease infectivity in all TSEs (Weissmann, 1995). PrP is ubiquitously expressed and anchored to the surface of cell membranes by a glycosylphosphatidyl inositol (Stahl *et al*., 1987; Prusiner, 2004). Prion disease is composed of a modified PrP^{c} protein called PrP^{sc} (Prusiner, 1998). PrP^{sc} and PrP^{c} are indistinguishable in their amino acid sequence but

differ in conformation (Stahl *et al*., 1993). Normal cellular protein PrP^{c} is α-helical in structure. PrP^{c} is converted to the PrP^{sc} infectious form by posttranslational modification by which the protein acquires a highly aggregated β-sheet rich content (Pan *et al*., 1993; Prusiner, 1997). PrP^{sc} differs from its normal isoform in that it is detergent insoluble (Meyer *et al*., 1986), resistant to proteinase K digestion (McKinley *et al*., 1991) and to inactivation by radiation (Gibbs *et al*., 1978). They also differ in their monomer conformation and state of aggregation (Riesner, 2003; Weissmann, 2004).

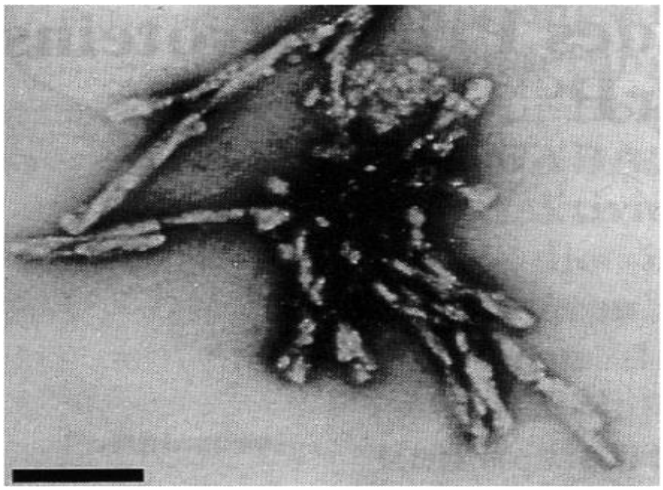

Figure 1.1. Electron micrograph of purified PrP^{sc} amyloid shows the presence of prion rods. Prion protein was purified with detergent and proteinase K resulting in insoluble aggregates visible by Congo red staining (Riesner, 2003).

In a review article, by Shorter and Lindquist (2005), it states that prions are unusual proteins that can exist in diverse conformations. One of these conformations is self-replicating. Prion PrP^{sc} replicates by converting endogenous PrP^{c} into the aggregated prion form, therefore infectivity only requires PrP protein templates (Shorter and Lindquist, 2005). Prions are an unusual subclass of amyloid protein as they replicate their altered conformation by generating infectious prion 'seeds', which are transmitted to new daughter cells. However, since Prusiner (1982) first proposed the

theory that prions are infectious forms of PrP, we are still unclear about the exact mechanisms by which a prion is first generated and propagated (Tuite and Koloteva-Levin, 2004).

1.2.2 Prion disease classification

As reviewed in Prusiner (1989) and Collinge (2005), prion disease can be divided into inherited, sporadic or acquired forms. The best example of acquired prion disease in humans is kuru. In this disease prions were transmitted by ritualistic cannibalism in the Fore people of Papau New Guinea (Gajdusek, 1977). The first case was recorded in the 1920s and interestingly the disease mainly affected women and children with only 2% of cases being in adult men (Alpers, 1987; Collinge *et al*., 2006). Kuru is an inevitably fatal disease but the type of infection and length of incubation period is dependent upon a PrP polymorphism, which confers certain people less susceptible to the disease (Lee *et al*., 2001). Collinge *et al*. (2006) analysed 11 patients from New Guinea, who had kuru, and found that men exhibited long prion incubation periods, some for up to 56 years. Acquired prion diseases are now rare but the 1990s saw a rise in iatrogenic CJD. This was caused by contamination of medical instruments, corneal transplantations and pituitary hormone treatment (Brown *et al*., 1992; Brown *et al*., 2000; Weissmann and Aguzzi, 2005).

BSE and CJD are some of the most notable CNS degenerative disorders caused by prion disease. It is believed that BSE originated through cannibalism in which prion contaminated food was prepared for cattle, as reviewed in Prusiner (1997). Sporadic forms of prion disease constitute most human CJD cases. 85% of human prion disease is caused by sporadic CJD with a rate of 1-2 cases per million occurring every year (Brown *et al*., 1987; Wadsworth *et al*., 2003; Collinge, 2005). Variant CJD (vCJD)

Another characteristic of prion disease is that they can exist as different strains. Each strain can vary in its incubation time, disease symptoms and its neuropathological lesion profile (Bruce *et al*., 1997). The distinct strains are not due to different PrP sequences but differences in amyloid conformations (Wickner *et al*., 2007a). Amyloid plaques are notable in kuru and GSS patients but less notable in sporadic CJD sufferers who show a diffuse pattern of PrP deposition (Budka *et al*., 1995). In a review article by Ironside and Head (2004) it discusses how vCJD histopathological features are distinguishable from other human prion diseases. vCJD is characterised by having abundant florid plaques with the surrounding tissue having a microvacuolated appearance (Figure 1.2) (Ironside and Head, 2004).

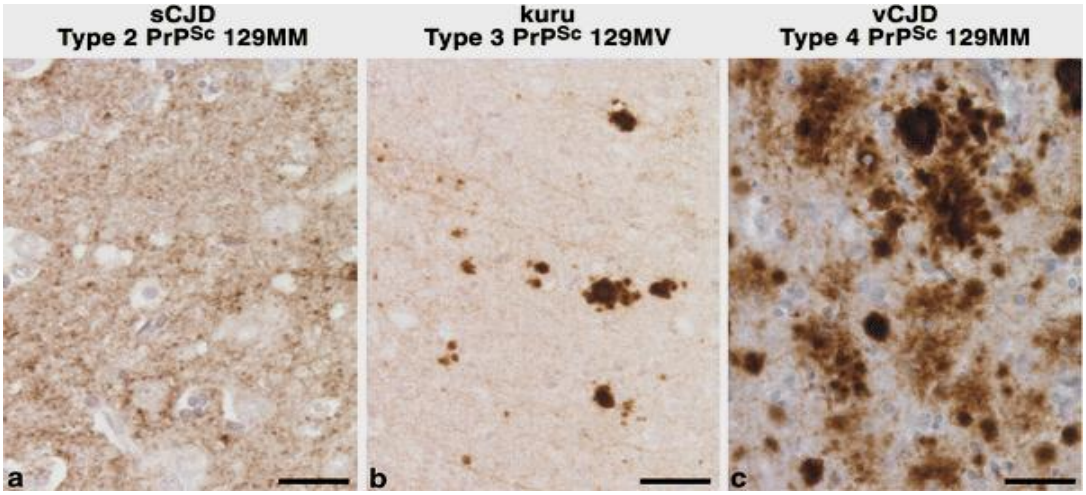

Figure 1.2. Distinct pattern of PrP deposition in human diseased brain tissue. (a) sporadic CJD shows a diffuse, synaptic pattern of PrP deposition (b) kuru shows a diffuse pattern of PrP deposition and the formation of amyloid plaques at various locations (c) In vCJD PrP plaques are often surrounded by vacuolation designated 'florid plaques'. *Scale bars* a, c 25μm; b 50μm. MV = methionine or valine at *PRNP* codon 129 (Wadsworth and Collinge, 2010).

The following review articles discuss the nature of mammalian prion disease and the importance of understanding their complex molecular composition in order to progress prion disease therapeutics. Prion diseases have attracted much research interest

for many years because of their unique composition and their impact on public health (Collinge, 2001). Understanding the molecular biology behind prion disease processes would highlight key aspects of protein misfolding and aggregation and the biological entities which regulate them (Wadsworth and Collinge, 2010). Research into prion biology is also essential to elucidate a prion curing treatment for patients suffering from cerebral degeneration. Early diagnosis is essential as drugs that retard or eliminate the prion amyloid will not reverse neuronal loss in the patient. No definite drugs or treatments are available as of yet but much research is ongoing into diagnostics and therapeutics (Collinge, 2005). Prion research could also prevent the onslaught of another BSE endemic.

1.3 Prions exist in yeast *S. cerevisiae*

Saccharomyces cerevisiae is a budding yeast species that has been used for decades as a model organism in the study of genetic and biochemical processes common to all eukaryotes. It is often referred to as ‘baker’s’ or ‘brewer’s’ yeast as it has been used in the food industry as a fermenting agent. It is a single celled eukaryotic organism containing approximately 6000 genes and it was the first eukaryote to have its genome completely sequenced. Many of its genes have been fully characterised which has enabled scientists to investigate fundamental aspects of biology in this simple eukaryotic organism (Watson *et al*., 2008).

1.3.1 The discovery of prions in yeast

In 1994 Reed Wickner extended the prion concept to explain how two non-mendelian elements in yeast *S. cerevisiae* could propagate without nucleic acid (Wickner, 1994). He referred to them as ‘proteins acting like genes’. These prions were

is a novel form of human CJD and experimental data has confirmed that vCJD and cattle BSE are caused by the same prion strain (Bruce *et al*., 1997; Hill *et al*., 1997). In 1994 the first case of vCJD was identified in young adults in Britain (Will *et al*., 1996). This led to the discovery that prions could be transmitted from cattle to humans through the food chain (Prusiner, 2004). The large-scale BSE epidemic affected approximately 2 million cows (Donnelly *et al*., 2002) and cases were reported in almost all EU states. In the UK approximately 200 cases of vCJD have been identified (Mead, 2009). The total vCJD epidemic may be relatively small as the incidence of vCJD has been stabilising and gradually falling in the UK since the early 2000s (Valleron *et al*., 2001; Ghani *et al*., 2003). In the review articles by Collinge (2005) and Mead (2006) they discuss how the clinical presentation of human prion diseases tends to vary. The main clinical difference between vCJD and CJD is the PrP^{sc} tissue distribution. vCJD involves lymphoreticular tissues and most prominently the tonsils (Hill *et al*., 1999; Wadsworth *et al*., 2001).

In review articles by Prusiner (1998) and Collinge (2005) they discuss how familial or genetic prion diseases are generally associated with mutations to PrP. Approximately 10-15% of human prion diseases are associated with mutations to the gene which encodes PrP (PRNP) (Collinge, 2005). A polymorphism at PrP residue 129 affects susceptibility to human prion disease (Palmer *et al*., 1991; Lee *et al*., 2001). All cases of vCJD so far have been in individuals homozygous for methionine at position 129 in PrP (Mead *et al*., 2009). Humans that are heterozygous for this allele are mostly protected from CJD (Mead *et al*., 2003). This could account for how only a small number of people contracted vCJD when it is likely that a lot more were exposed to BSE (Mead *et al*., 2009). To date, over 30 other autosomal dominant mutations have been described in PRNP (Collinge, 2005).

[*PSI*$^{+}$] and [*URE3*], discovered prior to Wickner by Brian Cox in 1965 and Francois Lacroute in 1971, respectively. [*PSI*$^{+}$] was originally discovered by serendipity, as a mutant that suppressed nonsense mutations in *S. cerevisiae.* Cox was monitoring the inheritance of a dominant nonsense suppressor called *SUQ5*, using an *ade2-1* allele, at the time of the discovery. *SUQ5* is a weak tRNA anticodon mutant that inserts serine residues at ochre stop codon sites. This enhancement of nonsense suppression produced by [*PSI*$^{+}$] was not restricted to a single tRNA suppressor but was later shown to be an 'omnipotent' suppressor causing readthrough at various nonsense stop codons (Liebman and Sherman, 1979). Lacroute was screening for *ura2* mutants able to incorporate ureidosuccinate when he identified a second class of mutant he termed [*URE3*]. Both Cox and Lacroute demonstrated that [*URE3*] and [*PSI*$^{+}$] were dominant and demonstrated non-mendelian segregation (4:0) when crossed with another yeast strain.

These two elements satisfied the criteria to be defined as a fungal prion. Wickner (1994) proposed three genetic traits that distinguish prions from nucleic acid replicons; (1) if a prion is cured it can arise again as the protein is still present (2) overproduction of the protein increases the prion frequency and (3) mutation of the gene encoding the protein should have the same phenotype as the prion (Wickner, 1994).

1.3.2 Linking proteins Ure2 and Sup35 with yeast prion induction

The molecular basis of [*URE3*] and [*PSI*$^{+}$] was a long puzzle. [*URE3*] and [*PSI*$^{+}$] were shown to be prions of Ure2 and Sup35 proteins, respectively (Chernoff *et al*., 1993; Wickner, 1994).

Ure2 is involved in nitrogen catabolite repression. In the presence of rich nitrogen sources, such as ammonia, Ure2 mediates the repression of genes that encode the enzymes and transporters for poor nitrogen uptake, reviewed in Cooper (2002). [*URE3*] prion is an inactive aggregated amyloid form of Ure2 (Wickner, 1994). [*URE3*] prion disrupts Ure2 function, similarly to *ure2* mutants, resulting in the inappropriate expression of genes and unnecessary nitrogen uptake (Lacroute, 1971; Brachmann *et al*., 2005). The link between Ure2 and [*URE3*] prion was confirmed when the over-expression of Ure2 protein was shown to elevate the frequency of [*URE3*] appearance by 20 to 200 fold (Wickner, 1994).

Sup35 is a protein invoved in stop codon recognition during protein synthesis. [PSI^+] is formed by aggregation of Sup35 monomers resulting in reduced termination activity (Wickner *et al*., 1995). Evidence for the link between Sup35 and [PSI^+] was revealed in independent reports. In 1993 Chernoff *et al*. demonstrated that the over-expression of *SUP35* gene resulted in the *de novo* expression of [PSI^+], later confirmed as the Sup35 protein and not the gene causing the effect (Derkatch *et al*., 1996). In 1994 Ter-Avanesyan *et al*. showed that a deletion to the N-terminus of *SUP35* resulted in loss of [PSI^+]. The 'protein-only' nature of yeast prions has also been demonstrated by groups such as King and Diaz-Avalos (2004) and Tanaka *et al*. (2004). They suggested that [PSI^+] is 'infectious' as *in vitro* studies demonstrate that protein aggregates composed of Sup35 fragments can stimulate *de novo* [PSI^+] formation and lead to distinct prion strains (King and Diaz-Avalos, 2004; Tanaka *et al*., 2004). Since the early 1990s a plethora of biochemical and genetic data substantiates [PSI^+] and [*URE3*] as yeast prions and the 'protein-only' hypothesis is better established in yeast than it is in mammals, reviewed in Serio and Lindquist (2000).

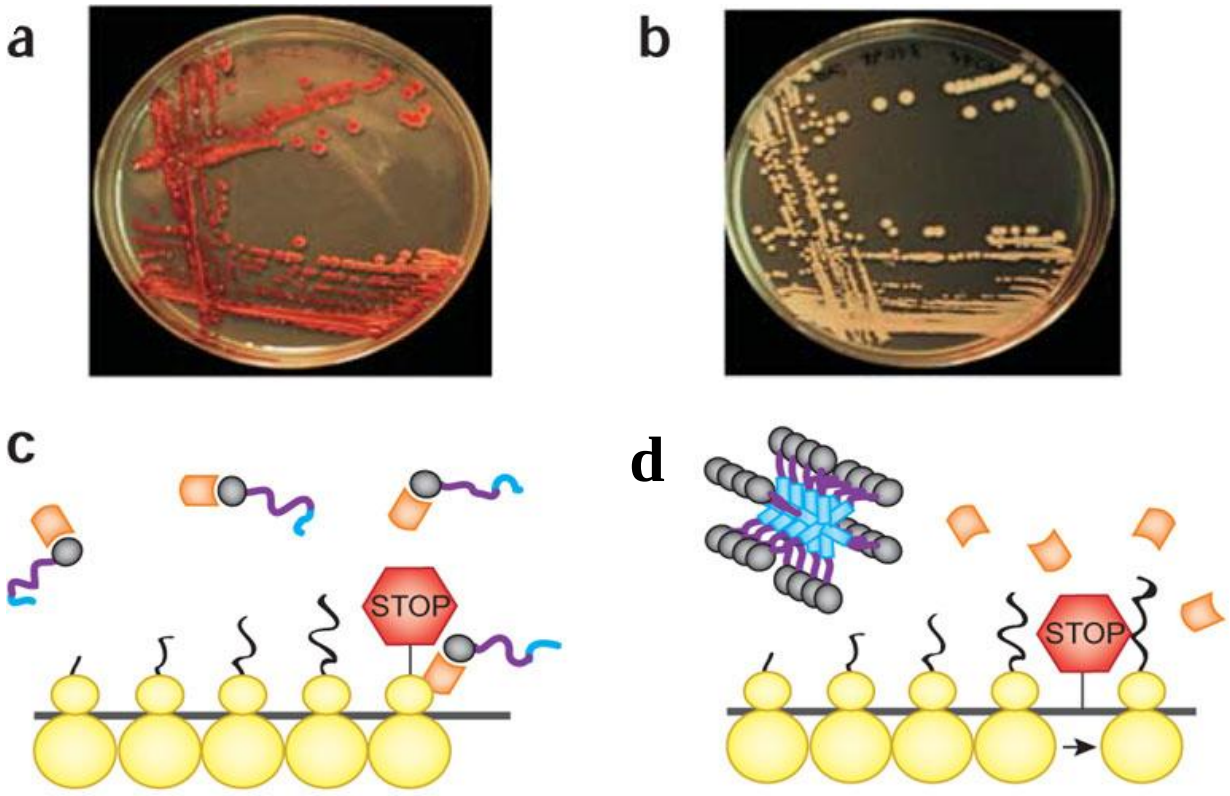

Figure 1.3. Monitoring Sup35 aggregation in yeast using the red/white assay. Plates a and b represent yeast colony colour when cells are (a) [*psi*$^-$] and (b) [*PSI*$^+$]. (c) In [*psi*$^-$] cells eRF1 and eRF3 bind and halt translation at the premature stop codon of *ADE* gene (d) In [*PSI*$^+$] cells Sup35 is aggregated and the termination machinery does not form. This leads to enhanced readthrough at the premature stop codon and *ADE* gene is fully translated (adapted from Tessier and Lindquist 2009).

This red colour screen has been adapted for the [*URE3*] system whereby an *ADE2*-based reporter system is used. The *ADE2* gene is placed under control of the *DAL5* promoter (Schlumpberger *et al*., 2001). Ure2 protein negatively regulates the transcription of the allantoate permease *DAL5*. Functional Ure2 prevents the expression of *DAL5* (Lacroute, 1971; Cooper, 2002). Therefore [*ure-o*] cells with functional Ure2 protein fail to induce *DAL5* leading to Ade$^-$ cells that appear red on limiting adenine medium. [*URE3*] cells fail to halt *DAL5* transcription leading to transcription of *ADE2* and colonies appearing white (Schlumpberger *et al*., 2001; Brachmann *et al*., 2005). The intensity of the red pigment is proportional to the amount of *ADE* gene expression

and [*URE3*] strength variants can be distinguished by colour and stability (Brachmann *et al*., 2005). [*PSI*$^{+}$] variants also exist which are dependent upon efficiency of suppression of the ade2/ade1 nonsense codon (Figure 1.4) (Derkatch *et al*., 1996; Halfmann *et al*., 2010).

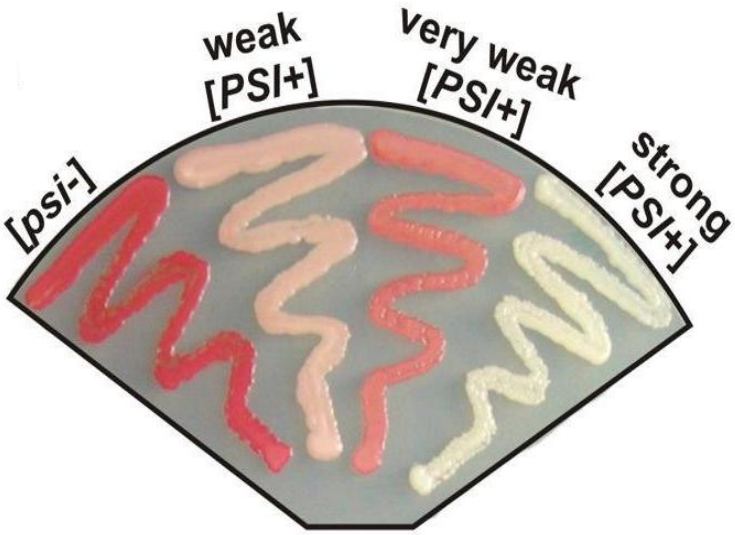

Figure 1.4. [*PSI*$^{+}$] strains differ by their level of nonsense suppression (adapted from Halfman *et al*., 2010).

1.3.4 The adenine biosynthesis pathway

In *S. cerevisiae* the adenine pathway is a seven-step process by which P-ribosyl-PP (PRPP) is converted into adenine monophosphate. The *ADE* genes encode enzymes which catalyse steps in the conversion from PRPP to adenine. The *ADE2* gene encodes phosphoribosylaminoimidazole carboxylase which catalyses the sixth step in the biosynthesis of the purine nucleotide adenine. Mutations in *ADE2* lead to the accumulation of purine precursors in the vacuole, causing colonies to be red in colour. This pigmentation has been used as a marker for selection and screening of [*PSI*$^{+}$] and [*URE3*] prions in yeast (Jones and Fink, 1982). *ADE2* mutants that turn red are blocked in the step forming CAIR and AIR accumulates in the cell. AIR is not red but cells

growing aerobically oxidise it to a red pigment. Figure 1.5 illustrates the steps involved in the adenine biosynthesis pathway.

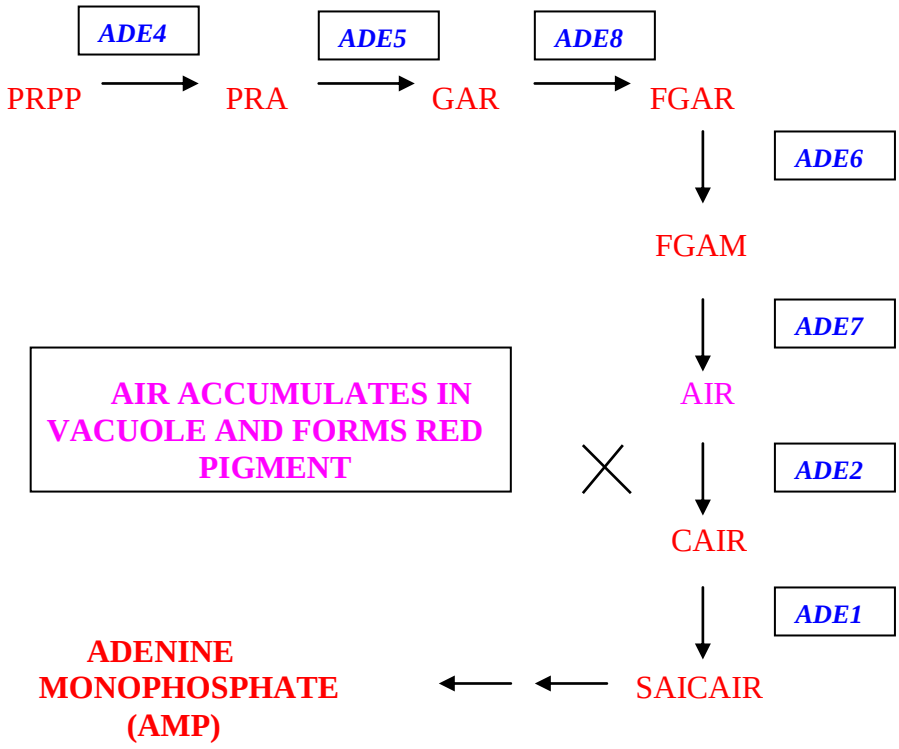

Figure 1.5. The adenine biosynthesis pathway in *S. cerevisiae* (adapted from Jones and Fink, 1982 and the *Saccharomyces* Genome Database (SGD)).

The [*PSI*$^+$] phenotype can also be monitored by means other than the red/white colony assay. A more quantitative means of measuring the level of nonsense suppression at *ade1* or *ade2* mutations is by using plasmid-borne gene fusions in which two assayable open reading frames are separated by a stop codon. For example the PGK-stop-lacZ assay (Firoozan *et al*., 1991) and the lacZ-stop-luc assay (Namy *et al*., 2003). [*PSI*$^+$] can also be monitored by comparing the level of Sup35 degradation when cell lysates are treated with proteases such as proteinase K. [*PSI*$^+$] strains are more

1.3.3 Monitoring yeast prions

It took many years for the 'protein-only' mechanism of prion propagation to be accepted. The discovery of a similar prion process in yeast allowed scientists to study this phenomenon with greater ease, as yeast can be readily manipulated. This was an important factor in confirming the 'protein-only' hypothesis (Wickner, 1994; Patino *et al*., 1996). In a review article by Osherovich and Weissmann (2002) it states that unlike mammalian prions, yeast prions are non-toxic and do not cause cell death, therefore there are no obvious 'sick' phenotypes like in TSE patients.

In a review article by Tuite and Cox (2007) it states that the most straightforward measurement of cellular [*PSI*$^{+}$] is by colony analysis of strains carrying a nonsense allele of either *ADE1* or *ADE2*. In *S. cerevisiae SUP35* encodes a release factor called eRF3. In [*psi*$^{-}$] (normal) cells eRF3 functions with eRF1 (Sup45) to promote protein synthesis termination at in-frame stop codons (Stansfield *et al*., 1995). In [*PSI*$^{+}$] cells protein synthesis termination machinery is defective due to the aggregated nature of Sup35 (Patino *et al*., 1996; Paushkin *et al*., 1996) thus preventing essential eRF1-eRF3 functional interaction (Tuite and Cox, 2007). Laboratory yeast strains can be created with aberrant stop codons in adenine biosynthesis genes *ADE1* or *ADE2*. In [*psi*$^{-}$] cells functional Sup35 promotes translation termination of the gene which leads to production of a red pigment due to oxidation of an accumulated precursor (Cox, 1965). In contrast, [*PSI*$^{+}$] cells express Sup35 in a highly aggregated insoluble state leading to loss of Sup35 function and enhanced readthrough of nonsense mutations (Paushkin *et al*., 1996). Functional Ade1/Ade2 is produced and cells therefore produce white colonies and grow on medium lacking adenine. This red/white assay is convenient and widely used in [*PSI*$^{+}$] research (Figure 1.3), as reviewed in Shorter and Lindquist (2005).

resistant to protease digestion due to their highly aggregated structure (Paushkin *et al*., 1996). [*PSI*$^{+}$] and [*psi*$^{-}$] strains also differ in their solubility. Sedimentation assays by differential centrifugation analysis can be a useful technique to detect strains with insoluble forms of the Sup35 protein. Microscopic localisation of a Sup35-green fluorescent protein fusion can also be informative about the cellular location and aggregated state of the Sup35 protein (Patino *et al*., 1996).

1.3.5 Structures of Sup35 and Ure2 and their prion counterparts

Sup35 is composed of an N-terminal (N) prion domain (123 residues) which is normally involved in mRNA turnover (Hosoda *et al*., 2003), a 129 residue highly charged middle region (M) and a 432 residue C-terminal translation termination domain (Ter-Avanesyan *et al*., 1994). The Ure2 protein is composed of an 80 amino acid N-terminal (N) prion domain and a C-terminal domain necessary for nitrogen regulation (Figure 1.6) (Coschigano and Magasanik, 1991; Tuite and Cox, 2003).

Yeast prion proteins share the same feature of having an abundance of polar uncharged residues in their N-terminus prion forming domains. In general less than 10% of yeast proteins contain glutamine or asparagine residues. In contrast, yeast prion proteins, such as Sup35 and Ure2, have regions containing up to 40% glutamine or asparagine (Michelitsch and Weissman, 2000; Sondheimer and Lindquist, 2000). In a review article by Shorter and Lindquist (2005) it states how Ure2 and Sup35 contain these Q/N rich regions in their N-terminus and are referred to as ‘prion forming domains’ (PrDs). The PrD of both Ure2 and Sup35 are necessary for prion activity (Shorter and Lindquist, 2005). Prion domains are flexible, a characteristic believed to be critical in the switch to a prion conformation (Scheibel and Lindquist, 2001).

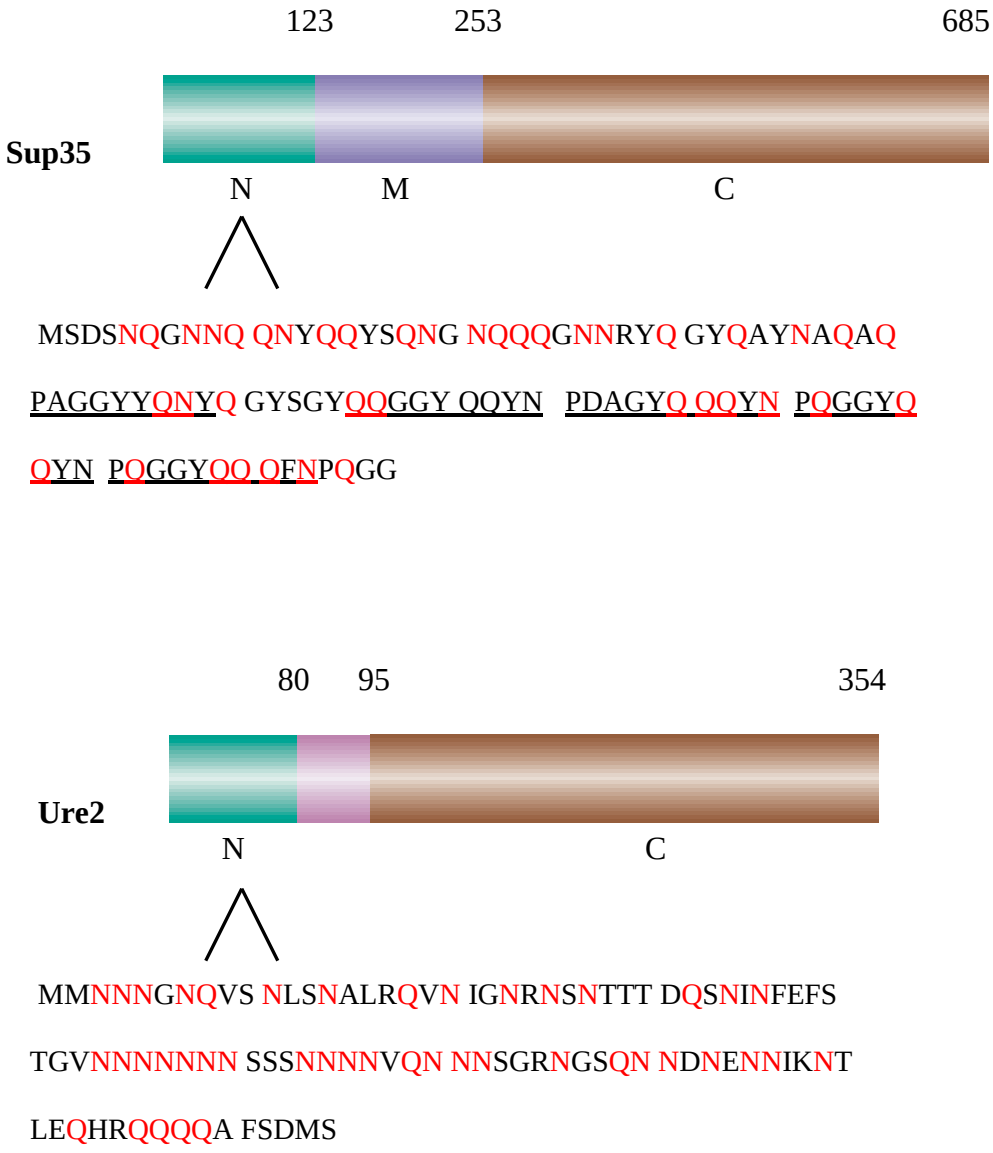

Figure 1.6. The linear structure of yeast prion proteins Sup35 and Ure2**.** Sup35 has three regions, an amino terminal N region, followed by a middle M region and carboxy terminal C region. The prion forming domain spans from residue one to 97 in the N-terminus and is rich in Q/N residues (highlighted in red). Ure2 consists of an amino terminal N domain and a C-terminal carboxy domain. The prion forming domain spans the first 65 residues of the N-terminus and like Sup35 is also rich in Q/N residues. The Sup35 octapeptide repeats are underlined (adapted from Tuite and Cox, 2003).

The Sup35 PrD function is transferable as it can successfully induce prion behaviour when fused to other proteins such as GFP, leading to the accumulation of visible prion aggregates (Patino *et al*., 1996; Li and Lindquist, 2000). The prion forming domain is

necessary for both induction and propagation of the prion state as prion proteins lacking their PrD cannot convert to the prion state spontaneously or when induced by the presence of other prions (Ter-Avanesyan *et al*., 1994; Masison and Wickner, 1995). Sup35 N-terminus also contains five imperfect repeats of an octapeptide (YQQYNPQGG) with resemblance to an octapeptide repeat found in mammalian PrP (PHGGGWGQ) (Figure 1.6). Deletion of these repeats in yeast Sup35 disrupts [PSI^{+}] propagation (Ter-Avanesyan *et al*., 1994; Li and Lindquist, 2000).

As reviewed in Lindquist *et al*. (2001) yeast prions do not cause cell death but simply alter the metabolic state of the organism. However, like mammalian prions, the protein responsible undergoes changes in conformation which alters its ability to function normally (Lindquist *et al*., 2001). Yeast prions adopt highly aggregated conformations with a fibrillar structure and have partial protease resistance (Figure 1.7.a) (Patino *et al*., 1996; Paushkin *et al*., 1996). X-ray diffraction and solid state NMR have been extensively used to study their structure. However, there has been much controversy over the proposed structure of prion amyloids.

The most prominent model for Sup35NM amyloids and the Ure2 prion domain is the in-register parallel β-sheet conformation. This conformation means that the adjacent peptide chains line up in the same orientation with corresponding residues opposite one another (Figure 1.7.b) (Kajava *et al*., 2004; Shewmaker *et al*, 2006; Baxa *et al*., 2007). Another prominent model for the structure of Sup35NM amyloids is the β-helix whereby amino acid residues are arranged in a rung with a central pore, thus preventing close contact between β-sheets (Krishnan and Lindquist, 2005). Resolving the controversy surrounding these models will probably depend on new independent methods of amyloid structural analysis (Tessier and Lindquist, 2009).

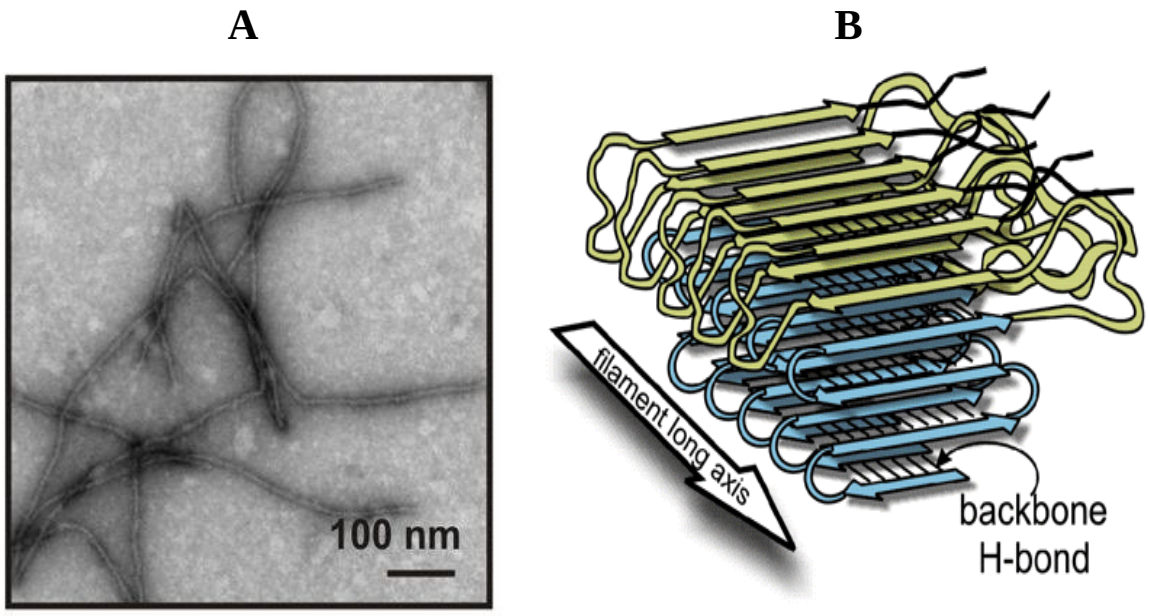

Figure 1.7. Yeast prions have a fibrillar compact structure**.**
A. Transmission electron microscopy of the prion conformation. Prions are highly ordered amyloids with a fibrillar nature (adapted from Halfmann *et al*., 2010).
B. A schematic model of Sup35NM amyloid protein in the in-register parallel β-sheet conformation. The N domain (blue) is mainly composed of β-sheet and the M domain (green) is composed of both β-sheet and non-β-sheet components (adapted from Shewmaker *et al*., 2006).

Loss of the prion conformation results in a return of functional soluble Sup35 and Ure2 protein (Masison and Wickner, 1995; Patino *et al*., 1996). These alternating states can be tracked by tagging each protein with GFP. Fluorescence of Sup35NM GFP is diffusely distributed throughout the cell in a [*psi*$^{-}$] state (Figure 1.8). In contrast [*PSI*$^{+}$] cells exhibit Sup35NM-GFP fluorescence at specific foci due to the formation of aggregates. These aggregates are cytoplasmically transmitted during cell division (Figure 1.8) (Patino *et al*., 1996; Serio and Lindquist, 2000; Halfmann *et al*., 2010).

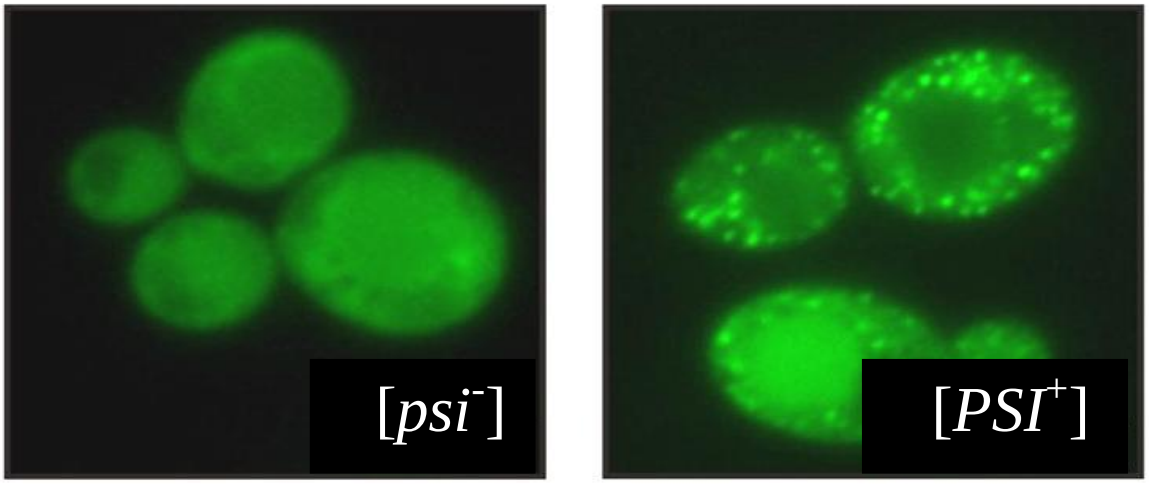

Figure 1.8. GFP-Sup35 fluorescence in [*PSI*$^{+}$] and [*psi*$^{-}$] cells (adapted from Halfmann *et al*., 2010).

1.3.6 Initiation of prion formation and polymerisation

What triggers Sup35 and Ure2 to become an amyloid infectious prion is complicated and involves a number of cellular and environmental factors. Sup35NM converts to amyloid fibres by a nucleated conformational conversion (Scheibel *et al*., 2004). Amyloid polymerisation usually starts with the formation of a 'nucleus' or a 'seed' of protein with different conformation to the normal soluble form. This nucleus promotes the conversion of the rest of the protein monomers to polymerise into the prion conformation (Jarrett *et al*., 1993; Wickner *et al*., 2000; Tuite, 2000; Scheibel *et al*., 2004). *In vitro* kinetic models have been established for how Sup35 forms amyloids. Collins *et al*. (2004) determined that *de novo* amyloid polymerisation occurs very slowly by the addition of monomers to the fibre ends of Sup35NM. Once established, fibres grow rapidly and efficiently by the addition of Sup35NM monomers followed by fibre fragmentation (Collins *et al*., 2004). The partition of these prion 'propagons' onto daughter cells occurs by passive transfer via cytoplasm distribution. It is estimated that approximately 500-1000 propagons can exist per cell (Byrne *et al*., 2009). As reviewed in Halfmann *et al*. (2010), a number of protein remodelling factors

and chaperone proteins interact with prions during the propagation process. Details of the role of chaperones in prion propagation will be discussed in section 1.5.

1.3.7 Other fungal prions

A third well documented yeast prion is [*PIN*$^+$], the amyloid form of Rnq1 protein (Derkatch *et al*., 2001). [*PIN*$^+$] was discovered by Susan Liebman's laboratory in 1997 (Derkatch *et al*., 1997) and it stands for [*PSI*$^+$] inducibility. The transient over-expression and subsequent *de novo* appearance of [*PSI*$^+$] depends upon the presence of [*PIN*$^+$] (Derkatch *et al*., 2001).

[*Het-s*] is a well documented prion form of the protein HET-s found in the filamentous fungal species *Podospora anserina* (Coustou *et al*., 1997). This prion is involved in heterokaryon incompatibility whereby the aggregated prion form [*Het-s*] facilitates programmed cell death when incompatible strain fusions occur (Coustou *et al*., 1997). As discussed in the review article by Benkemoun and Saupe (2006), both [*Het-s*] and [*PIN*$^+$] differ from [*PSI*$^+$] and [*URE3*] in that their transition to the prion state results in no detectable loss of function in the corresponding protein.

Until recently the prion field has been confined to this small group of proteins but discoveries over the past few years have expanded it. Four additional yeast prions [*SWI*$^+$] (Du *et al*., 2008), [*MOT3*$^+$] (Alberti *et al*., 2009), [*OCT*$^+$] (Patel *et al*., 2009) and [*MCA*] (Nemecek *et al*., 2009) have been reported recently. However, [*MCA*] was not confirmed by Alberti *et al*. (2009) as a yeast prion and Erhardt *et al*. (2010) have suggested that the prion-like properties of Mca1 protein is dependent upon an N-terminus peptide stretch, an isoform not consistently expressed. A genome-wide analysis of yeast was carried out by Alberti *et al*. (2009) whereby they discovered many potential prions with protein compositions similar to known yeast prions (Q/N rich).

But prion proteins may not be restricted to proteins with rich Q/N structure as both PrP and HET-s are not rich in glutamine and asparagine residues. It is intriguing to consider how many more fungal prions possibly exist (Tessier and Lindquist, 2009). Table 1.1 summarises the confirmed mammalian and fungal prions, their functions and prion manifestations.

1.3.8 Evolutionary significance of yeast prions

Research groups have focused much attention on the evolutionary significance of yeast prions. Amyloid conformers are disfavoured by natural selection and in mammals are usually associated with age-related disorders such as late-onset amyloidoses (Alzheimers and Parkinsons disease), as reviewed in Shorter and Lindquist (2005). Most groups believe that yeast prions evolved because they are somehow beneficial to the cell. True and Lindquist (2000) proposed that [*PSI*$^{+}$] must affect yeast survival and adaptation in the wild as it profoundly affects the relationship between genotypes and phenotypes. Many lines of evidence suggest that yeast prions are benign and in some cases beneficial. Eaglestone *et al*., (1999) found that the [*PSI*$^{+}$] state conferred an increased tolerance to heat and ethanol stress possibly due to their defective translation termination. Reduced translational fidelity brought about by [*PSI*$^{+}$] could, in the short run, be advantageous by allowing cells to grow in the presence of antibiotics and metals or with different carbon and nitrogen sources, depending on the strain background, as reviewed in Halfman *et al*. (2010). True and Lindquist (2000) compared various [*PSI*$^{+}$] and [*psi*$^{-}$] strains in their preference for certain growth conditions. They found that some conditions favoured a [*PSI*$^{+}$] state whilst others favoured [*psi*$^{-}$]. True and Lindquist (2000) referred to [*PSI*$^{+}$] as an ‘evolutionary capacitator’ by facilitating the evolution of new genetic traits. In the review article by

Table 1.1. Prions of mammals, yeast and the filamentous fungus *Podospora anserina*

Organism	Prion	Protein	Normal function	Prion manifestation
Mammals	TSEs	PrP	Not known	Transmissible spongiform encephalopathy
Saccharomyces cerevisiae	[*URE3*]	Ure2	Nitrogen catabolite repression	Derepression of nitrogen catabolism enzymes and transporters
	[*PSI*$^+$]	Sup35	Translation termination	Read-through of stop codons
	[*PIN*$^+$]	Rnq1	Not known	Rare seeding of [*PSI*$^+$], other prions
	[*SWI*$^+$]	Swi1	Chromatin remodeling	Poor growth on glycerol, raffinose, galactose
	[*MCA*]	Mca1	Metacaspase (suspected function in apoptosis)	Unknown
	[*OCT*$^+$]	Cyc8	Repression of *CYC7* and other genes	Derepression of transcription
	[*MOT3*$^+$]	Mot3	Transcription factor	Cell-wall changes
Podospora anserina	[*Het-s*]	HET-s	Heterokaryon incompatibility; meiotic drive (as a prion)	Heterokaryon incompatibility; meiotic drive (as a prion)

(Wickner *et al*., 2009).

Shorter and Lindquist (2005) they discuss how [*PSI*$^+$] is perhaps being maintained due to the fluctuating environment which yeast are accustomed to. Or, that perhaps the self-

perpetuating state of modern prions is just a vestige of a once functional mechanism in early life forms (Shorter and Lindquist (2005).

One group believes that yeast prions are disadvantageous and are actual yeast diseases. Wickner believes that yeast prions are non-beneficial and that any prion not found in wild yeast strains must be disadvantageous to the host (Nakayashiki *et al*., 2005; Wickner *et al*., 2007b). They analysed 70 wild yeast isolates and failed to find [*URE3*] or [PSI^+] in any of them (Wickner *et al*., 2007b). Much of their theory stems from the fact that the beneficial prion [*Het-s*] was found in 80% of *P. anserina* wild isolates (Dalstra *et al*., 2003). The first description of a yeast prion in a natural isolate was [PIN^+], as reported by Resende *et al*. (2003). Out of thirteen clinical isolates of *S. cerevisiae* two were [PIN^+] with none containing either [PSI^+] or [*URE3*].

If the [PSI^+] conformation provided no benefit to the cell then you would predict that it would have been lost over time. Even single point mutations to the Sup35 prion domain dramatically affect [PSI^+] propagation (Doel *et al*., 1994; DePace *et al*., 1998; Osherovich and Weissman, 2002).

1.4 Structural and functional similarities between yeast and mammalian prions

There are a number of unifying features of mammalian and fungal prions which supports why prion generation and propagation patterns can be modeled in yeast. These similar characteristics have been discussed in the following review articles:

- Mammalian and yeast prions both assemble into self-propagating amyloid conformations *in vitro* (Shorter and Lindquist, 2005).
- They both form structurally related but distinct prion strains (Tessier and Lindquist, 2009).

- They both exhibit strong species barriers (Tessier and Lindquist, 2009).
- Mammalian and yeast prions are composed of tightly packed β-sheets which are protease resistant and SDS insoluble (Shorter and Lindquist, 2005).
- They both rely on cellular chaperones to propagate their abnormal conformation (Jones and Tuite, 2005).

1.5 Yeast prion propagation and chaperones

The generally accepted model for yeast prion propagation is that prions are transmitted from mother to daughter cell during cell division. The term 'propagon' or 'seed' has been coined for these small transmissible particles (Cox *et al*., 2003). Molecular chaperones have been implicated in playing a major role in the replication of these prion particles (Chernoff *et al*., 1995; Kryndushkin *et al*., 2003; Allen *et al*., 2005; Sadlish *et al*., 2008).

1.5.1 The role of chaperones in protein folding

In order for a protein to reach its final 3D folded form and avoid misfolding, many proteins use chaperone proteins to assist them (Walter and Buchner, 2002). In the review article by Jones and Tuite (2005) it discusses how proteins are formed in a step-wise manner with small segments of the protein being produced at a time. This leads to many chances of misfolding. Chaperones interact non-covalently with polypeptide chains in order to stabilise their folds and prevent them from forming an incorrect structure and in doing so they accelerate the folding steps. Chaperones also rescue misfolded or highly aggregated proteins by refolding them back into their native active state (Jones and Tuite, 2005). Many chaperones are classed as heat shock proteins as their expression is up-regulated in response to stress (Perrett and Jones, 2008). In a

review article by Parsell and Lindquist (1993) the induction of heat shock protein expression is discussed. A mild non-lethal heat shock induces heat shock protein (Hsp) synthesis and enhances cell survival to severe heat shock exposure. This is known as induced thermotolerance (Parsell and Lindquist, 1993). Most heat shock proteins facilitate protein folding, assembly and translocation across intracellular membranes. In the past decade heat shock proteins have received much attention in their role in maintaining and propagating yeast prions (Rikhvanov *et al*., 2007).

1.5.2 How Hsps assist prion formation and propagation

S. cerevisiae has been widely used to study eukaryotic protein folding pathways and all the major chaperones involved in these pathways have been extensively characterised in this yeast species. Prion proteins appear to have evolved to exploit the molecular chaperone machinery in mammals and fungi. Once proteins have established the prion form they use chaperones to remodel their structure in a way that can be transmitted and propagated onto daughter cells. Genetic studies have identified a number of chaperones which interact with and modulate yeast prions (reviewed in Jones and Tuite, 2005).

Three classes of chaperone protein (Hsp40, Hsp70 and Hsp100), along with a number of co-chaperones, have been extensively analysed in their role in prion propagation. Hsp104 is a protein disaggregase responsible for recovering cells from environmental stresses, such as extreme heat, by dissolving protein aggregates and with help from Hsp70 and Hsp40 it reactivates and refolds them (Parsell *et al*., 1994b; Glover and Lindquist, 1998; True, 2006). Hsp104 plays a dual role in both the generation and propagation of yeast prions as it has been implicated in initial Ure2 and Sup35 nucleation events and fragmentation of their prion counterparts (Shorter and

Lindquist, 2006). In the review article by Perrett and Jones (2008) they suggest that Hsp104 can distinguish the difference between heat-denatured and prion substrates and can also recognise differences in prion substrates. They based this theory on a study done by Doyle *et al*. (2007) who highlighted that Hsp104 has different requirements for ATP hydrolysis depending on the type of protein substrate it is acting on (Doyle *et al*., 2007).

Hsp104 is a member of the AAA^+ (ATPases associated with various cellular activities) superfamily of proteins (Schirmer *et al*., 2004) which are characterised by assembling into oligomeric ring complexes (usually hexamers) with a central pore, when in the presence of ATP (Parsell *et al*., 1994a). ATP binding results in ATP hydrolysis, which possibly leads to release of the substrate from the chaperone (Bosl *et al*., 2005). Hsp104 has two highly conserved nucleotide binding domains (NBD1/NBD2) that each display a cooperative kinetics of ATP hydrolysis (Parsell *et al*., 1994a: Hattendorf and Lindquist, 2002). Mutational analysis has shown that the structure of the hexamer pore entrance is crucial for Hsp104 function (Lum *et al*., 2004). ATP binding to the NBD1 of Hsp104 is essential for the Hsp104 chaperone to interact with substrate aggregates as mutations that prevent ATP binding to NBD1 impair Hsp104-substrate interactions (Bosl *et al*., 2005). The NBD2 is also important for Hsp104 function as mutations to it severely impair Hsp104 hexamerisation (Schirmer *et al*., 1998).

There have been two separate models describing how Hsp104 disaggregates proteins. The first describes Hsp104 breaking aggregates into smaller fragments in a crowbar-like fashion (Glover and Lindquist, 1998). The other, more accepted model, suggests an unfolding/threading mechanism whereby individual polypeptide chains are removed by passing through the central pore of Hsp104 (Bosl *et al*., 2006). The

mechanism of how this model applies to prion propagation is discussed in the review article by Romanova and Chernoff (2009). Hsp104 breaks prion polymers into small propagons called ‘seeds’. Prions are propagated from yeast generation to generation by the production of these ’seeds’. These are heritable and pass with the cytoplasm from mother to daughter cell. The ‘seeds’ initiate protein aggregation in the new cell (Romanova and Chernoff, 2009).

Hsp104 is conserved in prokaryotes (ClpB) (Squires *et al*., 1991), fungi and plants (Hsp101) (Queitsch *et al*., 2000) and in animal mitochondria but so far no Hsp104 ortholog has been identified in animal cell cytoplasm (Leidhold *et al*, 2006; Romanova and Chernoff, 2009). Induced thermotolerance is evident in mammalian cells, indicating that they may have a functional analog of Hsp104 (Romanova and Chernoff, 2009).

The yeast model provided the first link between chaperones and prions as deletion or over-expression of Hsp104 ‘cures’ [*PSI*$^{+}$] (Chernoff *et al*., 1995). Adding the agent Guanidine HCl to yeast cures prions, presumably by Hsp104 inhibition (Ferreira *et al*., 2001). Deletion or inhibition of Hsp104 activity results in the generation of large prion polymers that are too large to be passed from mother to daughter cell, leading to the eventual loss of [*PSI*$^{+}$] through the cell divisions (Cox *et al*., 2003). When Hsp104 is over-expressed it also results in a loss of [*PSI*$^{+}$]. It is possible that excess Hsp104 eliminates [*PSI*$^{+}$] by dissolving large polymers into monomers that cannot be propagated to daughter cells, but there lacks any direct evidence to confirm this. An alternative model proposes that excess Hsp104 cures [*PSI*$^{+}$] by converting polymers into larger structures that are non-transmissible. Kryndushkin *et al*. (2003) showed, by electrophoretic analysis, that cells over-expressing Hsp104 resulted in Sup35 polymers larger in comparison to extracts from

the same strain expressing normal levels of Hsp104 (Kryndushkin *et al*., 2003). Controversies surrounding the mechanism of [*PSI*$^{+}$] curing by Hsp104 over-expression indicate that despite research progress we do not fully understand the role Hsp104 plays in prion propagation.

Although Hsp104 is the primary factor involved in prion replication, Hsp70, Hsp70 co-factors and Hsp40 act as components of this machinery and also play critical roles in prion propagation (Figure 1.9), as reviewed in Shorter and Lindquist (2008) and Guinan and Jones (2009). Hsp70 and Hsp40 bring denatured protein aggregates to Hsp104 and themselves refold newly misfolded proteins (Glover and Lindquist, 1998). Various studies have shown that shifting the cellular balance of various Hsp70 and Hsp40 chaperones can affect the induction and propagation of [*PSI*$^{+}$] (Chernoff *et al*., 1999; Kryndushkin *et al*., 2002; Allen *et al*., 2005).

Meimaridou *et al*. (2009) extensively summarised the functions provided by Hsp70 proteins in yeast. Hsp70s are universally conserved chaperones that play a role in protein synthesis, translocation across intracellular membranes, sequestration of protein aggregates and provide protection from aggregation in times of cellular stress (Meimaridou *et al*., 2009). All Hsp70 proteins share the property of binding to short hydrophobic segments of unfolded polypeptides and preventing their aggregation (Jones and Tuite, 2005). Hsp70 also interacts directly with Sup35 *in vivo* as Hsp70s and their co-chaperones have been shown to co-purify with [*PSI*$^{+}$] and [*psi*$^{-}$] versions of Sup35 (Allen *et al*., 2005; Bagriantsev *et al*., 2008). Efficient prion propagation is dependent on the cytosolic Hsp70 superfamily (Loovers *et al*., 2007). Mutations in the ATPase domain of Hsp70 and residues important for its interaction with Hsp40, impair [*PSI*$^{+}$] propagation. Two mutations have also been isolated in the Hsp70 substrate

binding domain (SBD) which impair prion propagation. These mutations highlight the importance of Hsp70 ATPase activity and substrate binding efficiency in yeast prion propagation (Jung *et al*., 2000; Jones and Masison, 2003; Loovers *et al*., 2007).

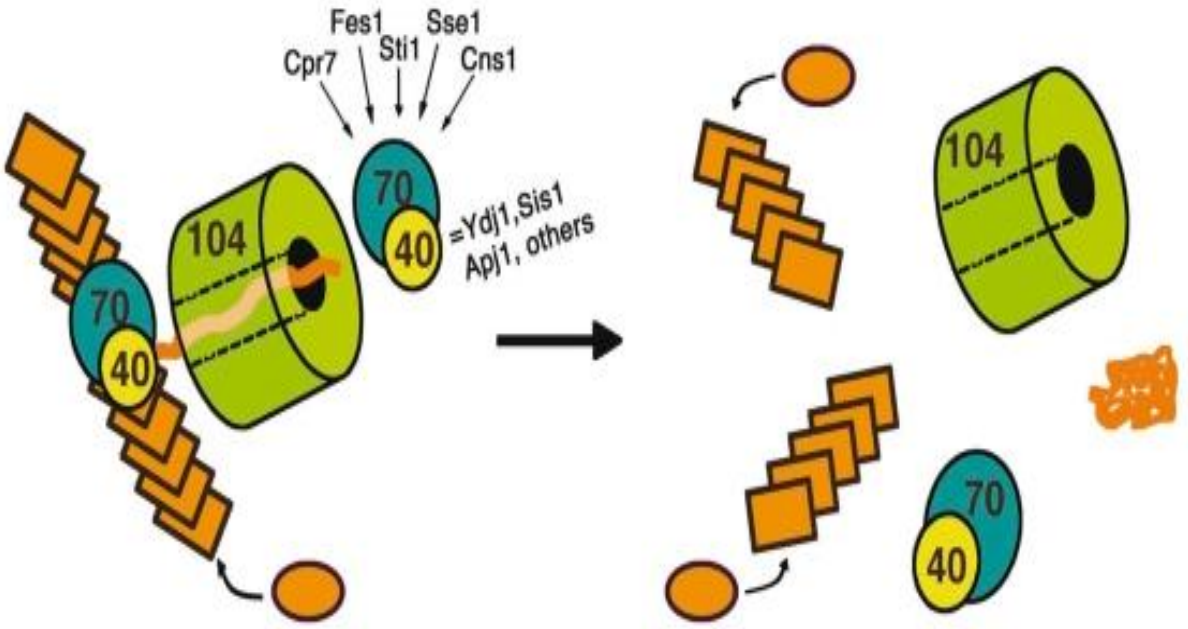

Figure 1.9. Chaperones assist yeast prion replication. Prion polymers (rectangles) grow by the addition of monomers (ovals) to their ends. Chaperones fragment individual polymers into two polymers, each of which can grow and continue the cycle. Hsp70 and Hsp40 interact directly with the polymer and facilitate Hsp104 interaction. Hsp104 fragments polymers into monomers by extruding them through its central channel. Hsp70/Hsp40 may help in refolding these monomers. Many co-chaperones are involved in regulating this process through Hsp70 and thus aid in prion propagation (adapted from Guinan and Jones, 2009).

Hsp70 is a diverse family of proteins 70 kDa in size and in yeast two cytosolic Hsp70 subfamilies are involved in [*PSI*$^{+}$] propagation. The Hsp70 Ssa subfamily (stress-seventy subfamily A) are an essential group represented by four proteins (Ssa1-4), at least one of which must be expressed for viability (Werner-Washburne *et al*., 1987). The Hsp70 Ssb subfamily are ribosome-associated proteins and have two

members, Ssb1 and Ssb2 (Nelson *et al*., 1992). The functions of Ssa and Ssb proteins has been inferred almost entirely by genetic analysis. These two classes of cytosolic Hsp70 are implicated in the *de novo* formation and propagation of prions but have opposing effects. Ssa1 over-expression promotes *de novo* [*PSI*$^{+}$] induction even in the absence of [*PIN*$^{+}$] (Allen *et al*., 2005). Unlike Ssa proteins, the Ssb subfamily has been implicated in yeast prion propagation by antagonising [*PSI*$^{+}$] (Kushnirov *et al*., 2000). Spontaneous [*PSI*$^{+}$] appearance increases 10-fold when Ssb1 and Ssb2 are deleted (Chernoff *et al*., 1999). Also Ssa1 reduces [*PSI*$^{+}$] curing when Hsp104 is over-expressed whereas Ssb1 enhances it (Chernoff *et al*., 1999). These opposing effects may be due to differences in the proteins cellular roles. Ssa1 stabilises misfolded proteins for prion conversion whereas Ssb1 may stimulate proteins to fold to their native state (Allen *et al*., 2005).

In the review articles by Mayer *et al*. (2001) and Mayer and Bukau (2005) the structure and molecular functions of Hsp70 chaperones are discussed. The structure of Hsp70 chaperones are composed of an amino terminal nucleotide/ATP (NBD) binding domain, followed by a substrate binding domain (SBD) and a C-terminal variable domain. The Hsp70 ATPase cycle regulates the chaperones ability to bind non-covalently to a substrate. When bound by ATP Hsp70 is in an ‘open’ conformation and can rapidly bind and release substrates in the SBD. When ATP is hydrolysed to ADP Hsp70 is in a ‘closed’ conformation and substrate is tightly bound to the SBD. Nucleotide exchange restores the ‘open’ conformation (Mayer *et al*., 2001; Mayer and Bukau, 2005). It is the fine tuning of this Hsp70 ATPase cycle that proves crucial for efficient prion propagation by the Ssa proteins. Evidence suggests that the ATP bound ‘open’ conformation is necessary for the propagation of yeast prions (Jones and Masison, 2003; Jones *et al*., 2004; Loovers *et al*., 2007). Hydrolysis of Hsp70 ATP is

influenced by the co-chaperones Ydj1, Sti1, Sis1, Cpr7 and Cns1 (reviewed in Jones and Tuite, 2005) and nucleotide exchange requires Fes1 and Sse1 (Figure 1.10) (Kabani *et al*., 2002; Dragovic *et al*., 2006).

Hsp70 structural data has helped reveal how interdomain communication drives ATP hydrolysis and peptide binding and has allowed other groups to interpret Hsp70 mutant data and their effects on prion propagation (Jiang *et al*., 2005; Loovers *et al*., 2007). Detailed crystallographic data will aid future functional characterisation of Hsp70 and other chaperones in their role in yeast prion propagation (Perrett and Jones, 2008).

In a review article by Jones and Tuite (2005), it discusses how a number of co-chaperones and co-factors have been shown to play a role in yeast prion propagation. Hsp40 proteins Ydj1 and Sis1, Hsp70/Hsp90 cofactors Sti1, Cpr7 and Cns1 and Hsp70 nucleotide exchange factors Sse1 and Fes1 (NEFs) are all implicated in stimulating the Hsp70 peptide binding cycle (Figure 1.10) (Jones and Tuite, 2005). It is not fully understood as to whether these influence [*PSI*$^{+}$] propagation solely through Hsp70 or independently. It is probable that both scenarios are possible, as reviewed by Perrett and Jones (2008). The functions of Hsp104, Hsp70, Hsp40 and their co-chaperones is summarised in Table 1.2.

1.6 The molecular chaperone Hsp110

Hsp110 proteins are a group of eukaryotic proteins that are ubiquitously expressed in mammalian tissue, especially at high levels in the brain (Liu and Hendrickson, 2007). Several cytosolic Hsp110 proteins have been described in eukaryotes, including HSPH1, Apg-1, Apg-2 and Grp170 in mammals (Vos *et al*., 2008; Kampinga *et al*., 2009). Hsp110 is represented by Sse1 and Sse2 in *S. cerevisiae.*

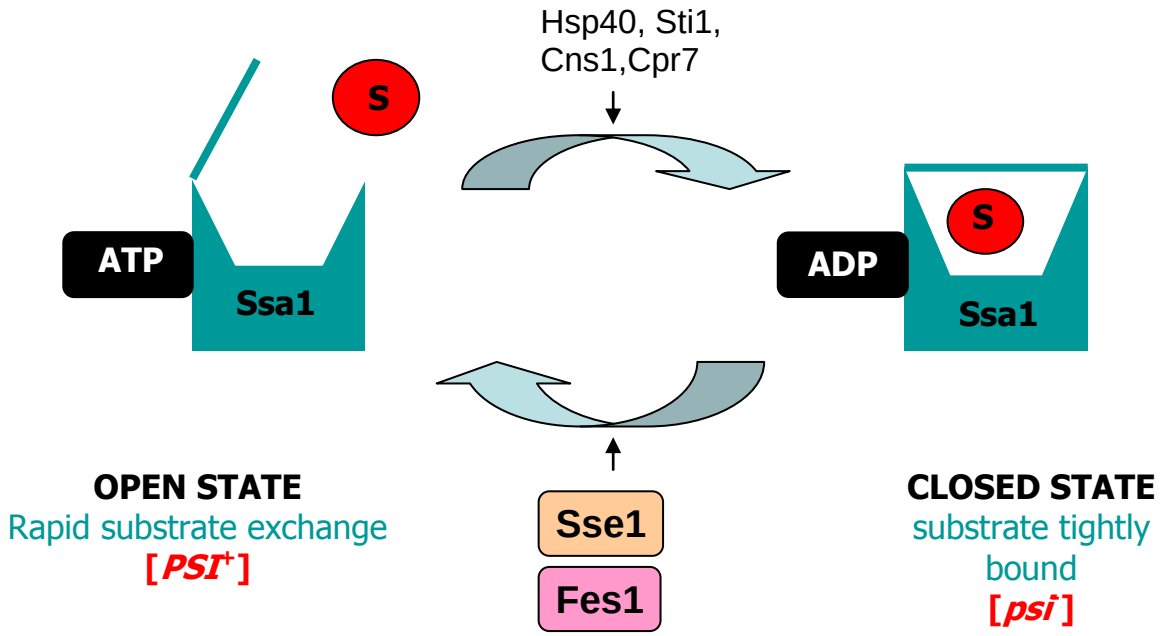

Figure 1.10. Regulation of Ssa peptide binding cycle by co-chaperones. The hydrolysis of Ssa ATP to ADP creates a 'closed' Ssa conformation and protein substrates are tightly bound. Nucleotide exchange by Fes1 and Sse1 promotes an 'open' conformation and [*PSI*$^{+}$] is restored (adapted from Jones and Tuite, 2005).

They constitute an essential gene pair (Trott *et al*., 2005). They are not individually essential but deletion of Sse1 confers a growth defect (Shirayama *et al*., 1993; Mukai *et al*., 1993; Shaner *et al*., 2004). Sse1 was first isolated from yeast biochemically as acalmodulin-binding protein (Mukai *et al*., 1993) and genetically as a suppressor of a protein kinase A (PKA) mutant (Shirayama *et al*., 1993). Sse1 and Sse2 share a high level of sequence homology (~76%) and also share homology with members of the Hsp70 superfamily (Mukai *et al*., 1993). Sse1 is constitutively expressed in yeast and Sse2 is the stress-induced isoform (Polier *et al*., 2008). Sse1 is expressed at moderately high levels under normal growth conditions and is further induced upon heat shock. Sse2 transcripts are nearly undetectable at basal temperatures but are increased more than 20-fold upon heat shock (Mukai *et al*., 1993; Shirayama *et al*., 1993). Little is understood about the cellular functions of Sse1 and Sse2 but they have been recently

Table 1.2. Summary of chaperone effects on prion propagation

Chaperone or co-chaperone	Cellular function	Effects on prion propagation when deleted	Effects on prion propagation when overexpressed
Hsp104	Protein disaggregation and stress tolerance.	Cures all known naturally occurring yeast prions.	Efficiently cures [*PSI*$^+$] but not [*URE3*] or [*PIN*$^+$]/[*RNQ*$^+$].
Hsp70 (Ssa1-4)	Protein folding, stress tolerance, binds denatured proteins and prevents aggregation. Protein translocation and translation.	Deletion of all 4 Ssa members is lethal, constitutes an essential gene family.	Can counteract the [*PSI*$^+$] curing effect of Hsp104 overexpression. Can cure some variants of [*PSI*$^+$]. Ssa1 can cure [*URE3*] while Ssa2 cannot.
Hsp70 (Ssb1/2)	Ribosome associated. Aid in folding of newly synthesised proteins.	10-fold increase in spontaneous appearance of [*PSI*$^+$] in a [*PIN*$^+$] background.	Can cure some weak variants of [*PSI*$^+$].
Hsp40 (Ydj1, Sis1, Apj1)	Deliver peptide substrates. Stimulate ATPase activity of Hsp70 partner. Sis1 is involved in translation initiation.	No effects of *YDJ1* or *APJ1* deletion. *SIS1* is essential.	Ydj1 efficiently cures [*URE3*] but not [*PSI*$^+$]. All three can cure artificial [*PSI*$^+$] variants.
Hsp110 (Sse1/2; related to Hsp70)	Nucleotide exchange factor for Hsp70 (Ssa and Ssb).	Reduced efficiency of propagation for some [*PSI*$^+$] variants. Cures [*URE3*].	Efficiently cures [*URE3*].
Fes1	Nucleotide exchange factor for Hsp70 (Ssa).	Reduced efficiency of propagation for some [*PSI*$^+$] variants. Cures [*URE3*].	Weakens [*PSI*$^+$].
Sti1	Aids in the Hsp70-Hsp90 protein folding cycle. Regulates ATPase activity of both Hsp70 and Hsp90.	Reduced stability of [*URE3*].	Cures artificial [*PSI*$^+$] and weakens wild type variant.

(adapted from Perrett and Jones, 2008).

implicated in playing a role in yeast prion propagation (Fan *et al*., 2007; Kryndushkin and Wickner, 2007; Sadlish *et al*., 2008).

1.6.1 Hsp110 is a divergent member of the Hsp70 superfamily

The Sse1 protein was crystalised by Liu and Hendrickson (2007). They established that Sse1 is modular and built-up from Hsp70-like subdomains. Even though Sse1 and Hsp70 functions have diverged, certain structural vestiges in Hsp70 have been conserved in Sse1. Mutational analysis revealed that certain mutant variants in Sse1 and Ssa1 resulted in similar phenotypic defects, supporting the hypothesis that Sse1 is an evolutionary vestige of Hsp70 (Liu and Hendrickson, 2007). Recent structural analysis studies of complexes formed by Hsp70 and Hsp110 has revealed that residues important for Hsp70 binding and initiation of nucleotide exchange, are almost invariant in the Sse1 protein (Polier *et al*., 2008). A recent report suggests that Sse1, like Ssa1, can recognise and bind hydrophobic peptide sequences with high affinity (Goeckeler *et al*., 2008) and can exhibit ATPase activity (Raviol *et al*., 2006a; Raviol *et al*., 2006b). However the functional similarities end there, as Sse1 cannot functionally refold denatured proteins but instead acts as a 'holdase' by binding denatured proteins and preventing their aggregation (Oh *et al*., 1999). This 'holdase' function may serve a function in the peptide refolding pathway carried out by other chaperones. *SSE1* has been shown to accelerate the refolding of luciferase by Hsp70/Hsp40 machinery (Brodsky *et al*., 1999; Goeckeler *et al*., 2002). Sse1 is the only nucleotide exchange factor (NEF) with a substrate binding domain containing a peptide binding site (Cyr, 2008).

The general domain organisation of Sse1 does reflect that of Hsp70. Sse1 consists of an N-terminal nucleotide binding domain (NBD), a β–sandwich domain

(SBD-β) and a three helical bundle domain (3HBD or SBD-α) in the C-terminus. The Sse1 protein has a compact structure with tight interactions between the NBD and SBD (substrate binding domain). Unlike Hsp70, the Sse1 SBD does not form a lid over its binding pocket but instead interacts with the flank of the Sse1 NBD (Polier *et al*., 2008). Sse1 is larger than Hsp70 due to insertions at its SBD and C-terminus extensions (Figure 1.11) (Easton *et al*., 2000; Liu and Hendrickson, 2007). Sse1 shares ~30% sequence identity with Ssa1 (Yam *et al*., 2005; Shaner *et al*., 2005). Like other Hsp70-Hsp110 interacting components the sequence similarity between Sse1 and Ssa1 is largely confined to the NBD (Goeckeler *et al*., 2008).

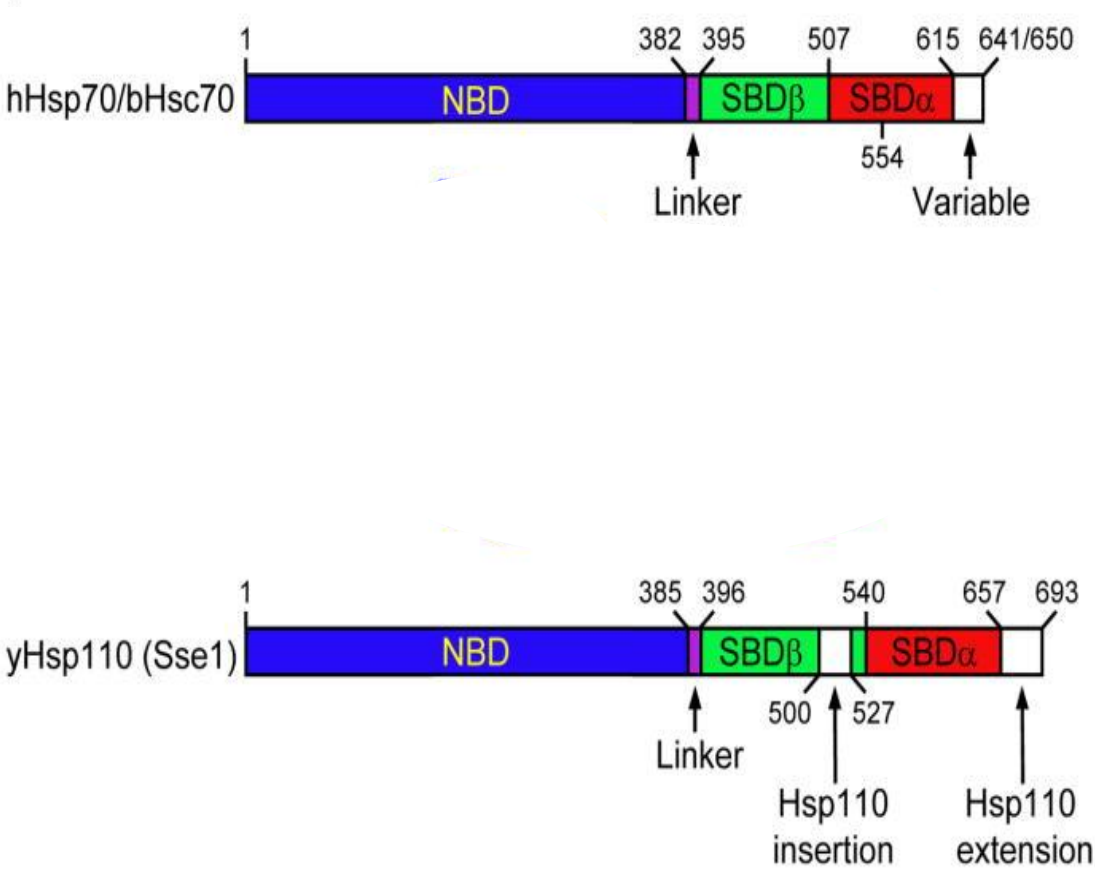

Figure 1.11. The domain organisation of Sse1 is similar to Hsp70. Schematic diagram of h (human)/b (bovine) Hsp70 and y (yeast) Hsp110. Both structures are similar except Hsp110 contains an insertion in the SBDβ and an extended C-terminus (adapted from Liu and Hendrickson, 2007).

Sse1 preferentially associates with Ssa1 *in vivo* (Shaner *et al*., 2005). The Hsp70 NBD is embraced by the NBD and 3HBD (SBD-α) of Sse1 leading to the opening of the Hsp70 nucleotide binding cleft. The Sse1 β-sandwich domain of the substrate binding cleft (SBD-β) alternates away from the Sse1-Ssa1 complex (Polier *et al*., 2010). It appears that almost the entire length of Sse1 is required for complex formation with Hsp70 (Shaner *et al*., 2004; Dragovic *et al*., 2006; Polier *et al*., 2008). Complex formation also requires Sse1 to be ATP bound as this alters the NBD in a way that stabilises Sse1 and allows it to bind Hsp70 (Shaner *et al*., 2006; Polier *et al*., 2008). Yeast Sse1 can also form a functional complex with human Hsp70 which reflects a high degree of conservation in the Hsp70 structure (Shaner *et al*., 2006).

The multidomain architecture of Sse1 suggests that it may play a role as a chaperone similar to Hsp70. However, the protein folding ability of Hsp70 relies heavily on the conformational structural changes between the NBD and SBD upon ATP/ADP binding. This allostery is not present in Sse1. The Sse1 substrate binding pocket remains closed upon ATP binding suggesting that any potential substrate-binding or chaperone activity expressed by Sse1 will potentially function differently to Hsp70 (Andreasson *et al*., 2008).

1.6.2 The nucleotide exchange function of Sse1

Defective regulation of the Hsp70 peptide binding and nucleotide exchange cycle is lethal to *S. cerevisiae* (Raviol *et al*., 2006b). Prion propagation can also become impaired by altering this peptide binding cycle (Jones and Tuite, 2005). Peptide binding and release by Hsp70 is controlled by an ATP hydrolytic cycle (Cyr, 2008). ATP binds tightly to the Hsp70 NBD. In this state, peptides are bound with low affinity to the SBD due to the extensive contacts made between the NBD and SBD (Liu and Hendrickson,

and the Hsp70 NBD is thought to stimulate the release of ADP nucleotide. It has been suggested that when the Sse1 NBD and its SBD-α contact lobes I and II of Hsp70 NBD this leads to the opening of the Hsp70 SBD and subsequent nucleotide release (Figure 1.12) (Cyr, 2008). Mutational analysis supports this and reveals that the Sse1 ATPase domain and C-terminus are important for its NEF function and that complex formation requires ATP binding by Sse1 (Dragovic *et al*., 2006; Shaner *et al*., 2006). Many questions remain unanswered about how this heterodimer functions *in vivo* and whether it is involved in protein folding or if it has specific cellular targets.

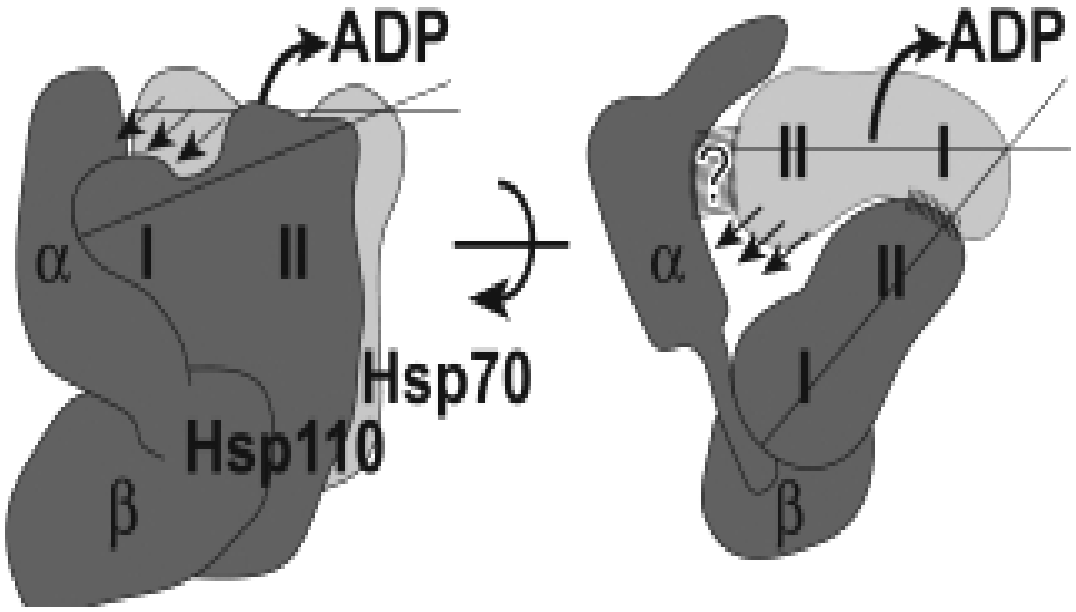

Figure 1.12. Schematic model for Hsp110 (dark grey) and Hsp70 (light grey) interaction and the mechanism of catalysed nucleotide release. The lobes of each NBD are indicated as I and II and subdomains of the SBD are indicates as α and β. The arrows indicate the the outward rotation of Hsp70 NBD lobe II and the triggered release of ADP. Points of interaction are noted as the striped areas. The main contact between the two molecules is via their NBDs which orientate towards one another. The α subdomain in Hsp110 protrudes outwards perhaps to embrace the upper periphery of the Hsp70 SBD (adapted from Andreasson *et al*., 2008).

1.6.3 How the expression of Sse1 affects yeast prion propagation

The initiation and propagation of yeast prions are constituted by folding and remodelling events that require the action of chaperones. Many reports have confirmed that Sse1 is required for the *de novo* formation and the propagation of [*PSI*$^{+}$] (Kryndushkin and Wickner, 2007; Fan *et al*., 2007; Sadlish *et al*., 2008). Sse1 mainly functions in prion propagation due to its NEF activity for Hsp70. However, Sse1 has been suggested to bind to early intermediates in Sup35 prion conversion and thus facilitate prion seed conversion independently of its NEF function. The exact mechanism as to how this occurs is still undiscovered (Sadlish *et al*., 2008). Fan *et al*. (2007) over-expressed Sse1 and observed an increase in the rate of *de novo* [*PSI*$^{+}$] formation compared to a control (Figure 1.13). They also tested the effects of deleting *SSE1* on [*PSI*$^{+}$] *de novo* formation and found a reduction in prion formation. It is possible that when Sse1 is over-produced it forms increased heterodimer complexes with Ssa promoting nucleotide exchange of Ssa (Fan *et al*., 2007). However, the over-production of Sse1 has no effect on pre-existing [*PSI*$^{+}$] (Kryndushkin and Wickner, 2007; Fan *et al*., 2007).

In contrast, the over-production and deletion of *SSE1* has a curing effect on the [*URE3*] prion (Figure 1.14). Mutant analysis indicates that this function depends upon ATP binding and interaction with Hsp70. Deletion of *SSE1* may promote tight binding of Ure2 protein to Hsp70 which could block the addition of monomers to the fibril. Sse1 up-regulation could stimulate an Hsp70 disaggregating activity that shears Ure2 prion polymers or perhaps stabilises Ure2 monomers (Kryndushkin and Wickner, 2007). Sse1 expression does affect yeast prion propagation but the resulting phenotype depends on a number of parameters. It is still unclear as to whether Sse1 has an influence on prion propagation directly or indirectly through Hsp70 but evidence to

date suggests that it mainly functions through its NEF activity.

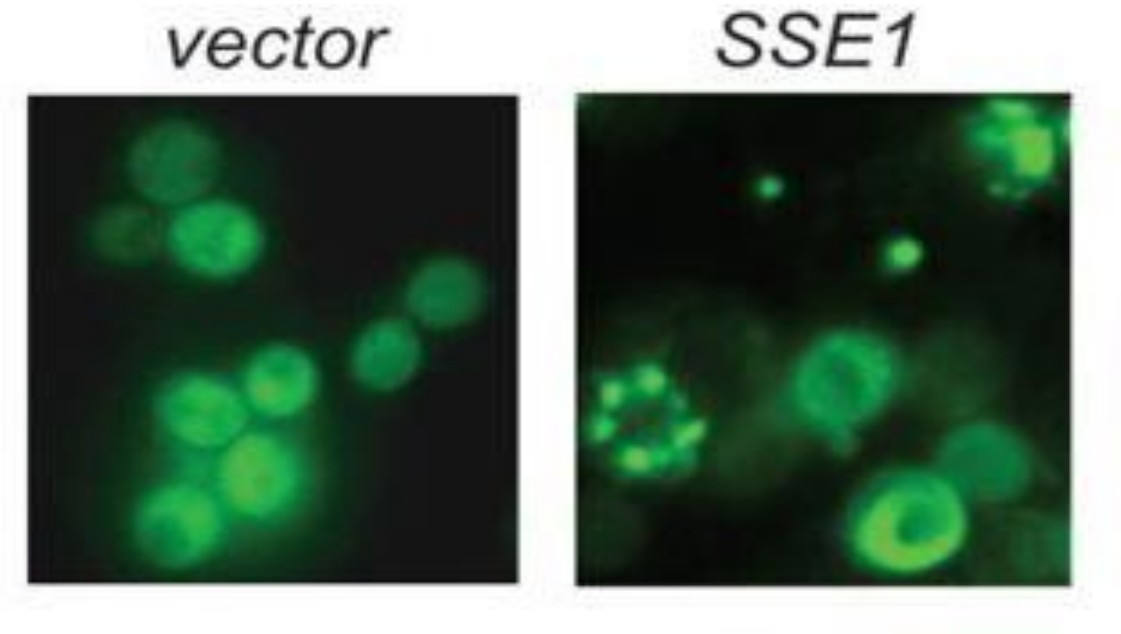

Figure 1.13. Overproduction of Sse1 promotes Sup35 aggregation. Cells either expressed an extra copy of *SSE1* on plasmid DNA or an empty vector control. GFP-Sup35NM is visible evenly distributed under normal conditions (vector) but aggregates into defined foci when Sse1 is over-expressed (*SSE1*) (Fan *et al*., 2007).

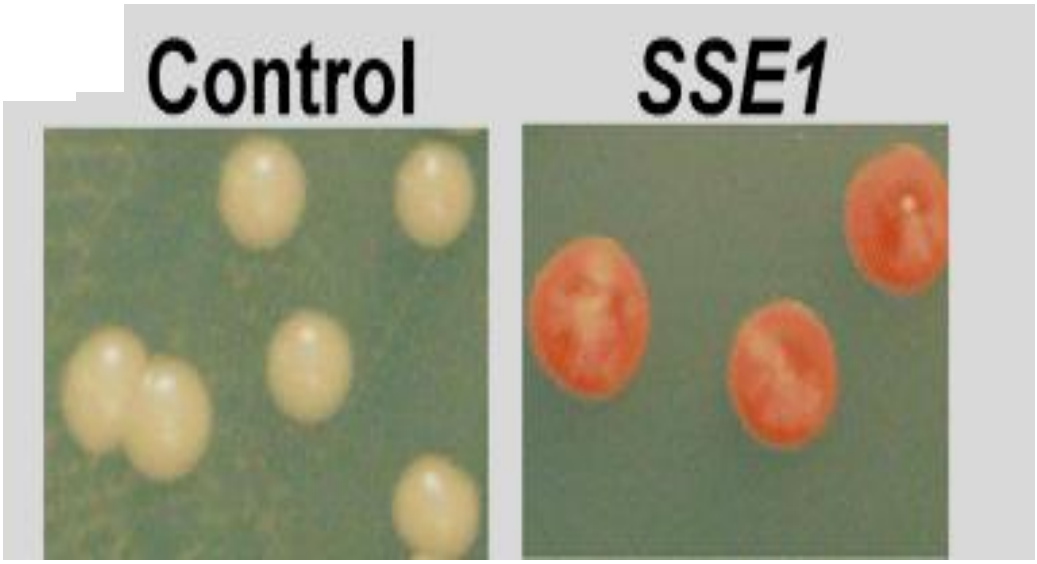

Figure 1.14. BY241 [*URE3*] expressing a control empty vector or a copy of *SSE1* gene. Overproduced Sse1 results in the loss of [*URE3*] (Kryndushkin and Wickner, 2007).

2007). ATP hydrolysis results in ADP-bound Hsp70 leading to the α-SBD closing over the β-SBD and the peptide tightly binding to the complex. Substrate release is then stimulated by nucleotide exchange (Cyr, 2008).

Genetic studies carried out by Jones and Masison (2003) and Jones *et al*. (2004) suggested that promoting the ADP bound form of Hsp70 leads to impaired prion propagation. It is possible that when substrates, such as Sup35, are tightly bound by Hsp70 in its closed state they are unable to be released and converted into the prion state (Loovers *et al*., 2007). Loovers *et al*. (2007) also found that altering the interaction between Hsp70 and its NEFs can affect ATPase cycle regulation and inhibit prion propagation.

Functions of Hsp110 proteins are poorly characterised but it has been recently suggested that they may act as the principal nucleotide exchange factor (NEF) for Hsp70. It has been shown that Sse1 acts as a potent NEF for yeast Hsp70 proteins Ssa1 and Ssa2 (Dragovic *et al*., 2006; Raviol *et al*., 2006b). This discovery followed soon after the discovery that Hsp110 proteins interact physically and functionally with their Hsp70 counterparts (Yamagishi *et al*., 2004; Shaner *et al*., 2005; Yam *et al*., 2005). Previous to these findings Fes1 was the only known Ssa1 NEF (Kabani *et al*., 2002).

The NEF function of Sse1 is to catalyse the exchange of nucleotides on Hsp70, thereby increasing the rate of Hsp70-dependent processes (Polier *et al*., 2008). Therefore Sse1 may indirectly stimulate the release of Sup35 from Hsp70 and in this way promote prion conversion of Sup35. Δ*sse1* strains have a decreased ability to propagate [*PSI*$^{+}$], possibly by limiting the amount of free 'open' Hsp70 with the capacity to bind and release aggregates (Sadlish *et al*., 2008).

The process by which this nucleotide exchange occurs is reliant on the stable Hsp70:Sse1 heterodimeric complex (Shaner *et al*., 2006). The contact between Sse1

1.6.4 Other cellular functions of Sse1

Before Sse1 was ever defined as a NEF and linked with prion propagation it was known as an Hsp90 co-chaperone. Hsp90 is a molecular chaperone that plays a role in protein folding and activation but unlike other chaperones its client proteins are typically transcription factors and kinases that rely on Hsp90 for proper signaling (Pearl and Prodromou, 2001). Sse1 has been physically and genetically linked with Hsp90 and is implicated in the maturation and client fate of Hsp90 substrates, which is possibly dependent on its NEF function (Liu *et al*., 1999; Lee *et al*., 2004; Shaner *et al*., 2008; Mandal *et al*., 2010). Completely separate from its function in protein folding and as a co-chaperone, Sse1 has been implicated in cell wall signaling pathways. In partnership with Hsp90, Sse1 has been suggested as playing a role in the MAP kinase cell integrity signaling pathway. This pathway is responsible for regulating genes involved in cell wall repair and morphogenesis. Evidence suggests that Sse1 may signal in this pathway as a member of a multichaperone complex that supports cell integrity (Shaner *et al*., 2008). Sse1 has also been implicated in the protein kinase A (PKA) pathway, a pathway that responds to alterations in environmental glucose concentrations by changing the magnitude and direction of gene transcription (Broach and Deschenes, 1990; Wang *et al*., 2004; Zaman *et al*., 2009). Sse1 has been linked with PKA signaling and it has been shown that the temperature sensitive effects of Δ*sse1* can be suppressed by decreasing PKA signaling (Trott *et al*., 2005). Trott *et al*. (2005) demonstrated that Δ*sse1* temperature sensitivity can be alleviated by growth on non-fermentable carbon sources suggesting that Sse1 is a negative regulator of PKA signaling.

1.6.5 The relevance of studying Sse1 as a modulator of prion propagation

Despite recent advances in our knowledge of Sse1 and the role it plays in prion propagation it still remains an enigmatic protein. Much is to be discovered about how exactly it interacts with other chaperones, whether it interacts with prion aggregates and how it drives prion propagation. How Hsp110 chaperones regulate prion propagation in yeast can be used as a model for how its mammalian counterparts function in prion disease progression. The fact that yeast Sse1 can functionally interact with mammalian Hsp70 suggests that both mammalian and yeast Hsp110 proteins have conserved functions. Human and yeast Sse1 are 41% identical but share higher homology in their regions forming the protein:protein interface (61%) (Schuermann *et al*., 2008; Polier *et al*., 2008). Human and yeast Hsp110 both function as NEFs for Hsp70 and this function in yeast appears essential for prion propagation (Dragovic *et al*., 2006). Understanding the mechanisms that promote yeast prion propagation could help us determine the underlying features of mammalian prion disease generation.

1.7 Objectives of this study

The primary objective of this study was to investigate the role that Hsp110 plays in yeast prion propagation. The first step undertaken was to create a group of Sse1 mutants with altered ability to propagate [*PSI*$^{+}$] and to express them in an appropriate *sse1* knockout strain. Once these mutants were created we could test what effects they have on prion propagation by using a number of phenotypic and growth tests. Previously within our laboratory, such an approach has been successfully undertaken to isolate Ssa1 mutants that disrupt prion propagation.

From here we could model the mutants on the 3D structure of Sse1 and decipher possible disruptions the mutations cause to protein stability and protein

interaction. Such work could help pinpoint whether Sse1 mutants affecting prion propagation are working directly through Sse1 or indirectly through its function as a NEF.

As Sse1 is an important cellular protein and also plays a role in cell signaling processes we wanted to determine if any of the mutants have effects on normal cellular homeostasis such as thermostability. It was also an objective to investigate the role of Sse1 in activities such as cell wall integrity signaling, Hsp90 signaling and in PKA signaling.

Another objective of this project was to draw a comparative analysis of Sse1 and Sse2. Sse2 is a more enigmatic protein than Sse1 and seems to play a less important role in yeast prion propagation. Little research has been published on the comparative differences in their ability to propagate prions and in their ability to provide cellular homeostasis.

An area we wished to explore was the role phosphorylation plays in the ability of molecular chaperones to function as prion propagators. Differentially inducing and preventing phosphorylation of Sse1 and Sse2 may impact their ability to propagate [*PSI*$^{+}$]. This is a totally new theory that hasn't been investigated in detail by other groups. As Hsp110 has only been recently implicated as a modulator of prion propagation there is much that needs to be determined to further our understanding of the nature of the chaperone and the complexity involved in prion propagation.

CHAPTER TWO
MATERIALS & METHODS

2.1 *S. cerevisiae* strains and plasmids used in this study

2.1.1 *S. cerevisiae* strains

All [*PSI*$^{+}$] strains used in this study are derivatives of strain G600. This strain was originally constructed in the laboratory of Daniel Masison and is a descendent of BSC strains isolated and characterised by Brian Cox.

Table 2.1. *S. cerevisiae* strains used in this study

Strain name	Genotype	Source
G600	*MAT***a**/*MAT*α *ade2.1 SUQ5 kar1-1 his3 leu2 trp1 ura3*	Jones *et al*. (2004)
MYS101	G600 *MAT***a** *sse1*::*kanMX*	Harriet Loovers Yeast Genetics Lab
MYS105	G601 *MAT*α *sse2*::*kanMX*	Harriet Loovers Yeast Genetics Lab
CMK1	G600 *MAT***a** *akl1*::*kanMX*	This study
CMK2	G600 *MAT*α *kin2*::*kanMX*	This study

CMK3	G600 *MAT*α *hsl1*::*kanMX*	This study
CMK4	G600 *hsl1*::*kanMX akl1*::*kanMX*	This study
CMK5	G600 *kin2*::*kanMX hsl1*::*kanMX*	This study
CM01	G600 *MAT***a** *sse1*::*kanMX*	This study
	G601 *MAT*α *sse2*::*kanMX* mated diploid transformed with pRS316*SSE1*	
CM02	*sse1*::*kanMX sse2*::*kanMX* pRS316*SSE1*, isolated as haploid segregant following sporulation of CM01	This study
CM02-*SSE1*	*sse1*::*kanMX sse2*::*kanMX* pRS315*SSE1*	This study
CM02-*SSE2*	*sse1*::*kanMX sse2*::*kanMX* pRS315*SSE2*	This study
CM02-315	*sse1*::*kanMX sse2*::*kanMX* pRS315	This study
CM02-(SMP3-SMG6)	*sse1*::*kanMX sse2*::*kanMX* pRS315*SSE1*mutant (fourteen sse1 mutants- plasmid mutants listed in Table 2.2)	This study

CM02-*FES1*	*sse1*::*kanMX sse2*::*kanMX* pRS423*FES1*	This study
CM02-423	*sse1*::*kanMX sse2*::*kanMX* pRS423	This study
CM02-*HSPH1*	*sse1*::*kanMX sse2*::*kanMX* pC210*HSPH1*	This study
CM02-Q458trunc	*sse1*::*kanMX sse2*::*kanMX* pC210*SSE1* truncated at position 458	This study
CM02F-SM1	*sse1*::*kanMX sse2*::*kanMX* pRS423*FES1* pRS315*SSE1*^{P37L}	This study
CM02F-SM2	*sse1*::*kanMX sse2*::*kanMX* pRS423*FES1* pRS315*SSE1*^{G41D}	This study
CM02F-SM3	*sse1*::*kanMX sse2*::*kanMX* pRS423*FES1* pRS315*SSE1*^{G50D}	This study
CM02F-SM4	*sse1*::*kanMX sse2*::*kanMX* pRS423*FES1* pRS315*SSE1*^{C211Y}	This study
CM02F-SM5	*sse1*::*kanMX sse2*::*kanMX* pRS423*FES1* pRS315*SSE1*^{D236N}	This study

CM02F-SM6	*sse1*::*kanMX sse2*::*kanMX* pRS423*FES1* pRS315*SSE1*^{G342D}	This study
CM02F-SM7	*sse1*::*kanMX sse2*::*kanMX* pRS423*FES1* pRS315*SSE1*^{G343D}	This study
CM02F-SM8	*sse1*::*kanMX sse2*::*kanMX* pRS423*FES1* pRS315*SSE1*^{T365I}	This study
CM02F-SM9	*sse1*::*kanMX sse2*::*kanMX* pRS423*FES1* pRS315*SSE1*^{E370K}	This study
CM02F-SM11	*sse1*::*kanMX sse2*::*kanMX* pRS423*FES1* pRS315*SSE1*^{S440L}	This study
CM02F-SM12	*sse1*::*kanMX sse2*::*kanMX* pRS423*FES1* pRS315*SSE1*^{E504K}	This study
CM02F-SM13	*sse1*::*kanMX sse2*::*kanMX* pRS423*FES1* pRS315*SSE1*^{E554K}	This study
CM02F-SM14	*sse1*::*kanMX sse2*::*kanMX* pRS423*FES1* pRS315*SSE1*^{G616D}	This study

CM02F-*SSE1*	*sse1*::*kanMX sse2*::*kanMX* pRS423*FES1*pRS315*SSE1*	This study
CM02423-SM1	*sse1*::*kanMX sse2*::*kanMX* pRS423 pRS315*SSE1*^{P37L}	This study
CM02423-SM2	*sse1*::*kanMX sse2*::*kanMX* pRS423 pRS315*SSE1*^{G41D}	This study
CM02423-SM3	*sse1*::*kanMX sse2*::*kanMX* pRS423 pRS315*SSE1*^{G50D}	This study
CM02423-SM4	*sse1*::*kanMX sse2*::*kanMX* pRS423 pRS315*SSE1*^{C211Y}	This study
CM02423-SM5	*sse1*::*kanMX sse2*::*kanMX* pRS423 pRS315*SSE1*^{D236N}	This study
CM02423-SM6	*sse1*::*kanMX sse2*::*kanMX* pRS423 pRS315*SSE1*^{G342D}	This study
CM02423-SM7	*sse1*::*kanMX sse2*::*kanMX* pRS423 pRS315*SSE1*^{G343D}	This study
CM02423-SM8	*sse1*::*kanMX sse2*::*kanMX* pRS423 pRS315*SSE1*^{T365I}	This study

CM02423-SM9	*sse1*::*kanMX sse2*::*kanMX* pRS423 pRS315*SSE1*^{E370K}	This study
CM02423-SM11	*sse1*::*kanMX sse2*::*kanMX* pRS423 pRS315*SSE1*^{S440L}	This study
CM02423-SM12	*sse1*::*kanMX sse2*::*kanMX* pRS423 pRS315*SSE1*^{E504K}	This study
CM02423-SM13	*sse1*::*kanMX sse2*::*kanMX* pRS423 pRS315*SSE1*^{E554K}	This study
CM02423-SM14	*sse1*::*kanMX sse2*::*kanMX* pRS423 pRS315*SSE1*^{G616D}	This study
CM02423-*SSE1*	*sse1*::*kanMX sse2*::*kanMX* pRS423 pRS315*SSE1*	This study
CM02-S-*PKC1*	*sse1*::*kanMX sse2*::*kanMX* pRS315*SSE1* p241*PKC1*	This study
CM02-G3-*PKC1*	*sse1*::*kanMX sse2*::*kanMX* pRS315*SSE1*^{G342D} p241*PKC1*	This study
CM02-G6-*PKC1*	*sse1*::*kanMX sse2*::*kanMX* pRS315*SSE1*^{G616D} p241*PKC1*	This study
CM02-S-*BCK1*	*sse1*::*kanMX sse2*::*kanMX* pRS315*SSE1* p636*BCK1*	This study

CM02-G3-*BCK1*	*sse1*::*kanMX sse2*::*kanMX* pRS315*SSE1* ^{G342D} p636*BCK1*	This study
CM02-G6-*BCK1*	*sse1*::*kanMX sse2*::*kanMX* pRS315*SSE1*^{G616D} p636*BCK1*	This study
CM02-S-316	*sse1*::*kanMX sse2*::*kanMX* pRS315*SSE1* pRS316	This study
CM02-G3-316	*sse1*::*kanMX sse2*::*kanMX* pRS315*SSE1* ^{G342D} pRS316	This study
CM02-G6-316	*sse1*::*kanMX sse2*::*kanMX* pRS315*SSE1* ^{G616D} pRS316	This study
CM02-*SSE1*-SSS	*sse1*::*kanMX sse2*::*kanMX* pRS315SSE1$^{G342D\ T100I}$	This study
CM02-*SSE1*SDMA	*sse1*::*kanMX sse2*::*kanMX* pRS315*SSE1*^{S85A}	This study
CM02-*SSE1*SDMB	*sse1*::*kanMX sse2*::*kanMX* pRS315*SSE1*^{S85E}	This study
CM02-*SSE1*SDMC	*sse1*::*kanMX sse2*::*kanMX* pRS315*SSE1*^{S384A}	This study

CM02-*SSE1*SDMD	*sse1*::*kanMX sse2*::*kanMX* pRS315*SSE1*^{S384E}	This study
CM02-*SSE2*SDMA	*sse1*::*kanMX sse2*::*kanMX* pRS315*SSE2*^{S384A}	This study
CM02-*SSE2*SDMB	*sse1*::*kanMX sse2*::*kanMX* pRS315*SSE2*^{S384E}	This study
CM02-*SSE2*SDMC	*sse1*::*kanMX sse2*::*kanMX* pRS315*SSE2*^{S679A}	This study
CM02-*SSE2*SDMD	*sse1*::*kanMX sse2*::*kanMX* pRS315*SSE2*^{S679E}	This study
CM02-*SSE2*SDME	*sse1*::*kanMX sse2*::*kanMX* pRS315*SSE2*^{S682A}	This study
CM02-*SSE2*SDMF	*sse1*::*kanMX sse2*::*kanMX* pRS315*SSE2*^{S682E}	This study
CM02-*SSE2*^{Q504E}	*sse1*::*kanMX sse2*::*kanMX* pRS315*SSE2*^{Q504E}	This study
CM02-*SSE2*^{G616D}	*sse1*::*kanMX sse2*::*kanMX* pRS315*SSE2*^{G616D}	This study
Y02146	*MAT***a** *his3Δ1 leu2Δ0 met15Δ0 ura3Δ0 sse1::kanMX*	EUROSCARF
Y17167	*MAT*α *his3Δ1 leu2Δ0 lys2Δ0 ura3Δ0 sse2*::*kanMX*	EUROSCARF

CMY01	*MAT***a**/α *his3Δ1/his3Δ1 leu2Δ0/leu2Δ0 lys2Δ0/++ / met15Δ0 ura3Δ0 +/sse1*::*kanMX sse2*::*kanMX*+ pRS316*SSE1* (constructed by mating Y02146 and Y17167 and transforming with pRS316*SSE1*)	This study
CM03	*MAT***a** *his3Δ1 leu2Δ0 ura3Δ0 sse1*::*kanMX sse2*::*kanMX* pRS316*SSE1* (isolated as haploid following sporulation of CMY101)	This study
CM03-*SSE1*	*sse1*::*kanMX sse2*::*kanMX* pRS316*SSE1*	This study
CM03-*SSE2*	*sse1*::*kanMX sse2*::*kanMX* pRS315*SSE2*	This study
CM03-315	*sse1*::*kanMX sse2*::*kanMX* pRS315	This study
CM03-(SMP3-SMG6)	*sse1*::*kanMX sse2*::*kanMX* pRS315*SSE1*mutant (14 *sse1* mutants listed in Table 2.2)	This study
CM03-*FES1*	*sse1*::*kanMX sse2*::*kanMX* pRS423*FES1*	This study
CM03-*FES1*P315	*sse1*::*kanMX sse2*::*kanMX* pRS423*FES1*, pRS315	This study
CM03-*HSPH1*	*sse1*::*kanMX sse2*::*kanMX* pC210*HSPH1*	This study

CM03-Q458trunc	*sse1*::*kanMX sse2*::*kanMX* pC210Q458trunc	This study
CM03-Q458*	*sse1*::*kanMX sse2*::*kanMX* pRS315*SSE1*^{Q458*}	This study
CM03Δ*swi6*Δ*sse2*	CM03 *sse1*::*kanMX sse2*::*kanMX swi6::HIS5* pRS315*SSE1*	This study
BY4741Δ*swi6*	BY4741 *swi6:: kanMX*	EUROSCARF
CM03Δ*swi6*Δ*sse1*	CM03 *sse1*::*kanMX sse2*::*kanMX swi6::HIS5* pRS315*SSE2*	This study
CM03Δ*swi6*Δ*sse2*+ G41D	CM03 *sse1*::*kanMX sse2*::*kanMX swi6::HIS5* pRS315*SSE1*^{G41D}	This study
CM03Δ*swi6*Δ*sse2*+ G50D	CM03 *sse1*::*kanMX sse2*::*kanMX swi6::HIS5* pRS315*SSE1*^{G50D}	This study
CM03Δ*swi6*Δ*sse2*+ G342D	CM03 *sse1*::*kanMX sse2*::*kanMX swi6::HIS5* pRS315*SSE1*^{G342D}	This study

CM03Δ*swi6*Δ*sse2*+ T365I	CM03 *sse1*::*kanMX sse2*::*kanMX swi6::HIS5* pRS315*SSE1*^{T365I}	This study
G600 (Ψ^+) + YBRO74W	G600 (Ψ^+) pYCGYBRO74W	This study
G600 (Ψ^+) + pRS316	G600 (Ψ^+) pRS316	This study
G600 (Ψ^-) + YBRO74W	G600 (Ψ^-) pYCGYBRO74W	This study
G600 (Ψ^-) + pRS316	G600 (Ψ^-) pRS316	This study
SB34	*MAT***a**, *trp1-1, ade2-1, leu2-3, 112, his3-11, 15, URA2::HIS3, erg6::TRP1, dal5::ADE2*[*URE3*]	Bach *et al*. (2003)
SB34-*SSE1*	SB34 pRS315*SSE1*	This study
SB34-pRS315	SB34 pRS315	This study

SB34-(SMP3-SMG6)	SB34 pRS315*SSE1*mutant (SB34 expressing 1 of 14 *sse1* mutants SMP3-SMG6-mutants listed in Table 2.2)	This study
Δ*slt2*	BY4741Δ*slt2*	EUROSCARF

2.1.2 Plasmid vectors

Table 2.2. Plasmid vectors used in this study

Plasmid Name	Description	Source
pRS315	Centromeric *Saccharomyces cerevisiae* shuttle vector- *LEU2* marker	Sikorshi and Hieter (1989)
pRS316	Centromeric *Saccharomyces cerevisiae* shuttle vector- *URA3* marker	Sikorski and Hieter (1989)
pC210	*SSA1* under control of *SSA2* promoter-*LEU2* marker	Schwimmer and Masison (2002)

pRS315-*SSE1*	*SSE1*+/-500bp cloned into pRS315, *LEU2* marker	Harriett Loovers
pRS315-*SSE2*	*SSE2* + promoter cloned into pRS315, *LEU2* marker	This study
pRS316-*SSE1*	*SSE1*+/-500bp cloned into pRS316, *URA3* marker	Harriett Loovers
SMP3	Mutation P37L in pRS315*SSE1*	This study
SMG4	Mutation G41D in pRS315*SSE1*	This study
SMG5	Mutation G50D in pRS315*SSE1*	This study
SMC2	Mutation C211Y in pRS315*SSE1*	This study
SMD2	Mutation D236N in pRS315*SSE1*	This study
SMG311	Mutation G342D in pRS315*SSE1*	This study
SMG312	Mutation G343D in pRS315*SSE1*	This study
SMT3	Mutation T365I in pRS315*SSE1*	This study

SME3	Mutation E370K in pRS315*SSE1*	This study
SMS4	Mutation S440L in pRS315*SSE1*	This study
SMQ4	Mutation Q458* in pRS315*SSE1*	This study
SME511	Mutation E504K in pRS315*SSE1*	This study
SME512	Mutation E554K in pRS315*SSE1*	This study
SMG6	Mutation G616D in pRS315*SSE1*	This study
SMG3-T1	Mutation G342D and T100I in pRS315*SSE1*	This study
pRS315-*SSE2*^{G616D}	Site directed mutagenesis of pRS315*SSE2* to produce G616D	This study
pRS315-*SSE2*^{Q504E}	Site directed mutagenesis of pRS315*SSE2* to produce Q504E	This study
pC210-*HSPH1*	*HSPH1* under control of *SSA2* promoter-*LEU2* marker	This study

pRS423-*FES1*	*FES1*+/-500bp cloned into pRS423, *HIS3* marker	Jones *et al*. (2004)
pRS423	pRS423, *HIS3* marker	Addgene
pC210-*SSE1*Q458TRUNC	pRS315*SSE1* truncated at position 458	This study
pUG27	Plasmid expresses *HIS5* gene and *loxP* flanking regions	EUROSCARF
pSH47	Plasmid expresses *cre* recombinase gene under control of GAL promoter	EUROSCARF
p241*PKC1*	Constitutively activated *PKC1* gene - *URA3* marker	Gift from Andy Truman (University of Chicago)
p636*BCK1*	Constitutively activated *BCK1* gene - *URA3* marker	Gift from Andy Truman (University of Chicago)
EP10,11,21,22	pRS315*SSE1* mutagenesis resulting in four ts plasmid mutants-all sequenced as mutant G616D	This study

p20632	YBR074W gene cloned into pYCG vector	EUROSCARF
*SSE1*SDMA	pRS315-*SSE1*^{S85A}	This study
*SSE1*SDMB	pRS315-*SSE1*^{S85E}	This study
*SSE1*SDMC	pRS315-*SSE1*^{S384A}	This study
*SSE1*SDMD	pRS315-*SSE1*^{S384E}	This study
*SSE2*SDMA	pRS315-*SSE2*^{S384A}	This study
*SSE2*SDMB	pRS315-*SSE2*^{S384E}	This study
*SSE2*SDMC	pRS315-*SSE2*^{S679A}	This study
*SSE2*SDMD	pRS315-*SSE2*^{S679E}	This study
*SSE2*SDME	pRS315-*SSE2*^{S682A}	This study
*SSE2*SDMF	pRS315-*SSE2*^{S682E}	This study

2.2 Sterilisation techniques

Sterilisation of growth media and materials required for aseptic techniques was achieved by autoclaving at 121^{o}C for 15 minutes. Any solutions that were susceptible to decomposition during autoclaving were filter sterilised using 0.22 μm Millipore membrane filters. All worktops and benches were washed with 70% (v/v) ethanol prior to carrying out experiments.

2.3 Yeast and bacterial growth media

2.3.1 Media for culturing yeast

All media was adjusted to a final volume of 1000 ml using dH_2O prior to autoclaving, unless otherwise stated. All liquid media was autoclaved and stored at room temperature unless otherwise stated. All agar plates were poured into sterile Petri dishes, allowed to cool and stored at 4^{o}C.

Complete Media (YPD)

10 g Bacteriological yeast extract ((Becton, Dickinson and Company, Le Point de Claix, France) (BD))

20 g Bacteriological peptone (BD)

20 g D-glucose (Sigma Aldrich Chemical Company, St. Louis, USA)

20 g Bacteriological agar (BD) (can be added to the growth media to solidify it)

adjusted to 1000 ml with dH_2O

Dropout Media

6.7 g Bacteriological yeast nitrogen base without amino acids and ammonium sulphate (BD)

20 g D-glucose

2 g Dropout mix (mix of 15 amino acids, the contents of which are described in Table 2.3)

20 g Bacteriological agar (can be added to media to solidify it)

adjusted to 1000 ml with dH_2O

Table 2.3. Amino acid composition of dropout mix

Alanine	Inositol
Isoleucine	Arginine
Lysine	Asparagine
Methionine	Aspartic acid
Aminobenzoic acid	Phenylalanine
Proline	Serine
Threonine	Cysteine
Glutamine	Valine
Glutamic acid	Tyrosine
Glycine	

Dropout mix contains 2 g of each of the amino acid components. Each amino acid was mixed together in a pestle and mortar and the mixture was stored at room temperature.

Synthetic Complete Medium (SC)

Dropout media can be supplemented with one or more additional amino acids to become Synthetic Complete (SC) media. The media is supplemented depending upon the growth requirements of the strain. Amino acids L-Leucine, Adenine sulphate, L-Tryptophan, L-Histidine and Uracil were purchased from Sigma. Stock concentrations of each amino acid were made by adding the appropriate amount indicated in Table 2.4 into 100 ml dH_2O. The stocks were vortexed until the amino acids were completely dissolved and subsequently filter sterilised using 0.22 μm Millipore membrane filters. Adenine and Uracil stocks were stored at room temperature. Tryptophan, Histidine and Leucine stocks were stored at 4^oC. The volume of amino acid stock added to 1 Litre of SC medium is indicated in Table 2.4 along with the final concentrations of the amino acid.

Table 2.4. Amino acid stock concentrations and final concentration of amino acids supplemented into SC media (Synthetic Complete)

AMINO ACID	AMINO ACID CONCENTRATION ADDED TO 100 ML H_2O TO MAKE STOCK SOLUTIONS (G)	VOLUME OF STOCK ADDED TO 1 LITRE SC MEDIA (ML)	FINAL AMINO ACID CONCENTRATION IN 1 LITRE SC MEDIA (μG/ML)
Leucine	1 g	10 ml	100 μg/ml
Adenine	0.2 g	10 ml	20 μg/ml
Histidine	1 g	2 ml	20 μg/ml
Tryptophan	1 g	2 ml	20 μg/ml
Uracil	0.2 g	10 ml	20 μg/ml

Synthetic Dextrose Media (SD)

6.7 g Bacteriological yeast extract

20 g D-glucose

20 g Bacteriological agar (can be added to media to solidify it)

adjusted to 1000 ml with dH_2O

Supplemented Minimal Media (SMM)

SMM is SD to which various growth supplements have been added.

Sporulation Medium

10 g Potassium acetate (Sigma)

1 g Bacteriological yeast extract

0.5 g D-glucose

20 g Bacteriological agar

adjusted to 1000 ml with dH_2O

Minimal Sporulation Medium

10 g Potassium acetate

20 g Bacteriological agar

Amino acid stocks (Table 2.4) were supplemented prior to autoclaving, depending upon strain requirements.

adjusted to 1000 ml with dH_2O

Yeast Peptone Glycerol Medium (YPG)

10 g Bacteriological yeast extract

20 g Bacteriological peptone

20 ml Glycerol (Sigma)

20 g Bacteriological agar

adjusted to 1000 ml with dH_2O

Yeast Peptone Ethanol Medium

10 g Bacteriological yeast extract

20 g Bacteriological peptone

20 ml Ethanol (Sigma)

20 g Bacteriological agar

adjusted to 1000 ml with dH_2O

Yeast Peptone Galactose Medium (YPGal)

10 g Bacteriological yeast extract

20 g Bacteriological peptone

20 g Galactose (Sigma)

20 g Bacteriological agar

adjusted to 1000 ml with dH_2O

5-fluoro-orotic acid Medium (5-FOA)

Amino acid stocks of Leucine (10 ml), Adenine (10 ml), Tryptophan (2 ml) and Histidine (2 ml) were added to 400 ml dH_2O along with 50 mg of Uracil (Sigma). Glucose (20 g), dropout mix (2 g), Bacteriological yeast nitrogen base without amino acids or ammonium sulphate (6.7 g) and 5-FOA (1 g) (Sigma) were also added. The mixture was brought to a final volume of 500 ml with dH_2O and filter sterilised. 20 g of Bacteriological agar was added, in a separate flask, to 500 ml dH_2O and autoclaved. This was allowed to cool and the components of both flasks were combined and mixed before pouring into sterile Petri dishes. The final concentration of 5-FOA was 1 mg/ml.

Guanidine-HCl Medium

10 g Bacteriological yeast extract

20 g Bacteriological peptone

20 g D-glucose

20 g Bacteriological agar

adjusted to 990 ml with dH_2O

The media was cooled to approximately 60^{o}C prior to adding Guanidine HCl. Stock solutions of Guanidine HCl were made by adding 2.9 g of Guanidine HCl (Sigma) to 100 ml of dH_2O (0.029 g/ml stock) followed by filter sterilisation. This made a 300 mM stock. 10 ml of Guanidine HCl stock solution was added to the 990 ml media to make a final concentration of 3 mM.

YPD-Geneticin Medium (G418)

10 g Bacteriological yeast extract

20 g Bacteriological peptone

20 g D-glucose

20 g Bacto agar

adjusted to 1000 ml with dH_2O

The solution was autoclaved and allowed cool to approximately 60^{o}C. 200 mg of Geneticin (Sigma) was added to the media to make a final concentration of 200 μg/ml.

Geldanamycin Medium

10 g Bacteriological yeast extract

20 g Bacteriological peptone

20 g D-glucose

20 g Bacto agar

adjusted to 1000 ml with dH_2O

Geldanamycin (Sigma) was added to flasks of cooled media, making a final concentration of 80 μM or 160 μM. This medium was made by members of Dr Panaratou's laboratory, Kings College London.

YPD-Sorbitol

5 g Bacteriological yeast extract

10 g Bacteriological peptone

10 g D-glucose

10 g Bacto agar

The components of YPD medium listed above were added to a 500 ml flask. In a separate flask 91 g of sorbitol (Sigma) was mixed with 200 ml of warm dH_2O and stirred until the sorbitol dissolved. The sorbitol-dH_2O mix was added to the dry YPD components and the mixture was adjusted to 500 ml with dH_2O. The final sorbitol concentration was 1 M.

Cell wall damaging Medium

All cell wall damaging media was made using YPD with the addition of the following chemicals when media reached approximately 60^oC after autoclaving. Stock solution concentrations and final concentrations are listed in Tables 2.5-2.8.

(a) Caffeine (Sigma): 100 mM caffeine stock was prepared by dissolving 9.6 g caffeine in 500 ml dH_2O. From this a 10 mM stock was made by mixing 10 ml of the 100 mM stock with 90 ml dH_2O. This stock was filter sterilised before adding appropriate volumes to cooled YPD media. The final caffeine concentrations used were 4 μM, 6 μM, 8 μM and 10 μM. Dilutions and concentrations are indicated in Table 2.5.

(b) SDS (Sigma): A 1% SDS stock was made by dissolving 1 g of SDS in a final volume of 100 ml dH_2O. The stock was filter sterilised prior to adding to the media. YPD-SDS plates were made to a final concentration of 0.005%, 0.01% and 0.02%. Dilutions and concentrations are indicated in Table 2.6.

Table 2.5. Concentrations of YPD-caffeine medium for cell wall damage analysis

VOLUME OF YPD MEDIA (ML)	VOLUME OF 10 mM CAFFEINE STOCK ADDED TO YPD MEDIA (μL)	FINAL CONCENTRATION OF CAFFEINE ADDED TO YPD (μM)
499.8 ml	200 μl (1/2500 dilution)	4 μM
499.7 ml	300 μl (1/1666 dilution)	6 μM
499.6 ml	400 μl (1/1250 dilution)	8 μM
499.5 ml	500 μl (1/1000 dilution)	10 μM

Table 2.6. Concentrations of YPD-SDS medium for cell wall damage analysis

VOLUME OF YPD MEDIA (ML)	VOLUME OF 1% SDS STOCK ADDED TO YPD MEDIA (ML)	FINAL CONCENTRATION OF SDS ADDED TO YPD (%)
497.5 ml	2.5 ml (1/200 dilution)	0.005%
495 ml	5 ml (1/100 dilution)	0.01%
490 ml	10 ml (1/50 dilution)	0.02%

(c) Congo red (Sigma): 1000X congo red stocks were made by making four separate stocks to a final volume of 100 ml with dH_2O (Table 2.7). 1000X stocks were filter sterilised and diluted 1/10 in fresh sterile dH_2O to make 100X stocks. YPD-congo red medium was made to a final concentration of 5 μg/ml, 10 μg/ml, 25 μg/ml and 35 μg/ml. Stock concentrations and dilutions made are indicated in Table 2.7.

(d) Calcofluor white (Sigma): 1000X calcofluor white stocks were made by making four separate stocks to a final volume of 100 ml with dH_2O (Table 2.8). 1000X stocks were filter sterilised and diluted 1/10 in fresh sterile dH_2O to make 100X stocks. YPD-calcofluor white medium was made to a final concentration of 5 μg/ml, 10 μg/ml, 15 μg/ml and 25 μg/ml. Stock concentrations and dilutions made are indicated in Table 2.8.

Table 2.7. Concentrations of YPD-congo red medium for cell wall damage analysis

1000X CONGO RED STOCK SOLUTION CONCENTRATIONS IN 100 ML OF dH_2O	100X CONGO RED STOCK SOLUTION CONCENTRATIONS	VOLUME OF 100X CONGO RED STOCK ADDED TO 495 ML OF YPD MEDIA (ML)	FINAL CONCENTRATION OF CONGO RED IN YPD (μG/ML)
0.5 g (0.005 g/ml)	0.0005 g/ml	5 ml	5 μg/ml
1.5 g (0.015 g/ml)	0.0015 g/ml	5 ml	15 μg/ml
2.5 g (0.025 g/ml)	0.0025 g/ml	5 ml	25 μg/ml
3.5 g (0.035 g/ml)	0.0035 g/ml	5 ml	35 μg/ml

Table 2.8. Concentrations of YPD-calcofluor white medium for cell wall damage analysis

1000X CALCOFLUOR WHITE STOCK SOLUTION CONCENTRATIONS IN 100 ML OF dH_2O	100X CALCOFLUOR WHITE STOCK SOLUTION CONCENTRATIONS	VOLUME OF 100X STOCK ADDED TO 495 ML OF YPD MEDIA (ML)	FINAL CONCENTRATION OF CALCOFLUOR WHITE IN YPD (μG/ML)
0.5 g (0.005 g/ml)	0.0005 g/ml	5 ml	5 μg/ml
1.0 g (0.010 g/ml)	0.0010 g/ml	5 ml	10 μg/ml
1.5 g (0.015 g/ml)	0.0015 g/ml	5 ml	15 μg/ml
2.5 g (0.025 g/ml)	0.0025 g/ml	5 ml	25 μg/ml

(e) H_2O_2 (Sigma): 30% liquid H_2O_2 with a molar concentration of 12 M was used to make a stock solution. 300 mM H_2O_2 stocks were made by adding 1 ml of H_2O_2 to 39 ml of H_2O (1/40 dilution). The stock was filter sterilised and 5 ml was added to 495 ml of sterile YPD media to give a final concentration of 3 mM H_2O_2.

2.3.2 Media for culturing *E. coli*

Luria Broth (LB) Media

25 g Luria bertani broth (BD)

Media was supplemented with 20 g (w/v) Bacto agar to solidify it.

adjusted to 1000 ml with dH_2O

LB-ampicillin

LB liquid or solid media was supplemented with ampicillin to make LB-amp. This ensures the selection of ampicillin resistant plasmids incorporated into the cell. Stock solutions of the antibiotic ampicillin (Sigma) were made by adding 5 g of ampicillin into 100 ml dH_2O to give a 50 mg/ml concentration. The stock was filter sterilised, separated into 100 x 1 ml volumes and stored at -20^{o}C until needed. 1 ml of ampicillin stock was thawed and added to 999 ml of LB media after it was autoclaved and cooled to approximately 60^{o}C. This gave a final ampicillin concentration of 50 μg/ml.

2.4 Yeast and bacterial culture conditions

2.4.1 Yeast culture conditions

All parent yeast stocks were stored at -80^{o}C in a sterile mixture of 15% (v/v) glycerol to 85% (v/v) liquid YPD. Yeast strains were grown on YPD or synthetic selective media at 30^{o}C static (BD series, Binder incubator, Mason Technology) for 48 hours and kept at 4^{o}C for short-term storage. Working stocks of yeast strains were maintained on YPD plates at 4^{o}C and were routinely sub-cultured every 2-4 weeks.

For liquid culturing, yeast were grown overnight in 14 ml round bottom falcon tubes (BD). Yeast cultures were grown in an orbital shaker (Innova 4000, New Brunswick Scientific, UK) at 30^{o}C and 200rpm using either YPD or synthetic selective liquid medium.

2.4.2 Bacterial culture conditions

E. coli strain DH5α was stored at -70°C in dH_2O or in 20% (v/v) glycerol to 80% (v/v) liquid LB. Strains were cultured overnight on LB-amp plates at 37°C (B series, Binder incubator, Mason Technology). Liquid culturing involved inoculating a single *E. coli* colony in 5 ml of LB + 5 µl ampicillin stock (final concentration of 50 µg/ml) , in a round bottom falcon (BD), and cultured overnight in an orbital shaker (Innova 44, New Brunswick Scientific) at 37°C and 200rpm.

2.4.3 Harvesting yeast and bacterial liquid cultures

Both yeast and bacterial cultures were harvested by centrifugation (Centrifuge 5810R, Eppendorf) for 5 minutes at 2000rpm (yeast) or 4000rpm (bacteria).

2.5 Determination of yeast and bacterial cell density

2.5.1 Determination of yeast cell density

Yeast overnight cultures were diluted 1/100 with sterile dH_2O and added to a haemocytometer (Bright Line, Hausser Scientific). The cells were counted using a light microscope (INGENIUS, Bio imaging Syngene) at a magnification of X 100. Other experiments required O.D values of yeast growth over a certain time period. In this case cell concentration was determined using a spectrophotometer (Eppendorf) at OD_{600nm}.

2.5.2 Determination of bacterial cell density

The OD_{600nm} of bacterial cultures was determined using a spectrophotometer.

2.6 Comparative growth analysis

Yeast were grown overnight at 30^{o}C shaking in 5 ml selective media. The following morning the cultures were diluted back to OD_{600nm}= 0.1 in 5 ml of fresh media and incubated at 30^{o}C shaking until the cells reached a concentration of 3x10^{6} cells/ml. The cells were harvested by centrifugation and resuspended in selective media to a final concentration of 5x10^{6} cells/ml. 100 µl of culture was placed in well A1 in a 96 well plate (Starstedt) and 80 µl of media added to wells A2-A6. A 1/5 serial dilution was performed on the cells using a multichannel pipette by removing and adding 20 µl of culture from well A1 through to A6. Using a 96 well metal replicator (Sigma) cells were transferred as spots onto appropriate agar plates and left to dry on the bench. The plates were incubated at 30^{o}C and in the case of temperature-sensitive tests plates were also incubated at 37^{o}C and 39^{o}C. The plates were incubated for 48 hours and growth was monitored over that time.

2.7 Yeast growth curve

Yeast strains were inoculated overnight in 5 ml YPD at 30^{o}C shaking. The following morning each cultures concentration was measured at OD_{600nm} and diluted back to an OD_{600nm} of 0.1 (t=0) in 10 ml selective media. The 10 ml cultures were placed in fresh falcons and incubated at 30^{o}C and 37^{o}C shaking. Cell growth was measured at OD_{600nm} at t= 2 h, 4 h, 6 h, 8 h. Each strain was measured in duplicate and the experiment was repeated in triplicate. The data was entered into excel and compiled into linear graphs. The linear graphs were achieved by plotting the log values for the OD values obtained against time. The time points which gave the most linear point on the graph

were used in the following formula to calculate the mean generation time (GT) for each yeast strain;

$$((t1-t0)/(logx1-logx0))/log2$$

2.8 Cell morphology analysis

Cellular morphology was analysed on a Cell^M imaging station using an Olympus IX microscope at 40X magnification. Yeast were prepared by growing fresh cells on selective medium at 30^{o}C for 2 days and spreading on glass slides with dH_2O.

2.9 Transformation of yeast with plasmid DNA

Materials

(a) 1 M Lithium acetate (Sigma) was prepared by dissolving 10.2 g of Lithium acetate in 100 ml of dH_2O, followed by autoclaving the mixture. 100 mM Lithium acetate was prepared by mixing 10 ml of 1 M Lithium acetate with 90 ml of sterile dH_2O. Stocks were stored at room temperature.

(b) 50% polyethylene glycol (PEG) (Sigma) stock solutions were prepared by mixing 50 g PEG in 50 ml of dH_2O and adjusting it to a final volume of 100 ml with dH_2O, followed by autoclaving. PEG Stocks were stored at room temperature.

(c) Carrier DNA was prepared by adding 200 mg of single stranded DNA (Sigma) into 100 ml of 10 mM Tris (Sigma)/1 mM EDTA (Sigma) solution. This gave a final carrier DNA concentration of 2 mg/ml. The 100 ml stocks were separated into 1 ml volumes in fresh 1.5 ml microfuge tubes (Eppendorf) and boiled at 100^{o}C for 5 minutes on a digital dry bath. After boiling, the tubes were cooled on ice and stored at -20^{o}C.

(d) The plasmid DNA to be transformed into the yeast cells is prepared by methods described in sections 2.10.4 and 2.12. DNA concentrations were determined on a Nanodrop Spectrophotometer and 50 µl volumes of DNA/dH_2O were prepared by resuspending plasmid DNA in dH_2O to give a final concentration of approximately 0.1-1.0 ng of DNA. The amount of DNA used depended on the numbers of colonies desired on the transformation plate.

(e) The 10 mM Tris/1 mM EDTA solutions used in **(c)** were prepared by making a 100X stock concentration. 12.14 g Tris and 2.92 g EDTA were added together and adjusted to 100 ml with dH_2O. The pH was adjusted to 7.5. The solution was autoclaved and 1 ml was removed and added to 99 ml sterile dH_2O to give a final concentration of 10 mMTris/1 mM EDTA.

Method

Yeast strains were inoculated and harvested as previously described in sections 2.4.1 and 2.4.3. Following centrifugation, the cells were counted and resuspended in 50 ml of appropriate media to a cell density of $5x10^6$ cells/ml. Yeast cultures were incubated at 30^oC shaking for a further 3-5 h until cell concentrations reached 1-2 x 10^7cells/ml. The cells were harvested by centrifugation at 2000rpm, washed in 25 ml of sterile dH_2O and centrifuged again. The supernatants were disposed of and pellets resuspended in 1 ml 100 mM Lithium acetate. The cells were transferred to 1.5 ml microfuge tubes and cell pellets were harvested in a table top centrifuge (Centrifuge 5415D, Eppendorf AG, Hamburg) at 13000rpm for 5 sec and resuspended in 500 µl of 100 mM Lithium acetate. 50 µl aliquots of the cell suspensions were added to fresh 1.5 ml microfuge tubes and

centrifuged again for 5 sec to remove any residual Lithium acetate. Add this stage the cells could be stored at 4^{o}C for 1-2 weeks or used immediately for transformation. The following components were added to each microfuge tube in the order listed:

240 μl 50% (w/v) PEG

36 μl 1 M Lithium acetate

25 μl single stranded carrier DNA (taken from 2 mg/ml stock)

50 μl mix of dH_2O and plasmid DNA

Cell suspensions were mixed and incubated at 30^{o}C for 30 minutes. The mixtures were heat shocked at 42^{o}C in an Accublock Digital Dry Bath (Labnet International.Inc) for 20-25 minutes. The microfuge tubes were centrifuged at 13000rpm for 15 sec and the pellets were resuspended in 200 μl of dH_2O. Aliquots from each microfuge tube were plated onto separate selective agar plates and the plates were incubated at 30^{o}C for 2-3 days.

2.10 Preparation and transformation of *E. coli*

2.10.1 Procedure for the preparation of electro-competent *E. coli* DH5α

E. coli DH5α were inoculated in 20 ml of LB media and incubated overnight at 200rpm at 37^{o}C. The following morning the 20 ml cell culture was resuspended in 1 Litre LB media and incubated at 37^{o}C shaking until OD_{600nm} = 0.6-1.0. The cell culture was then separated into 4 x 250 ml volumes, centrifuged in a GSA rotor at 6000rpm for 10 minutes at 4^{o}C (Sorvall centrifuge). The pellets were resuspended in 1 Litre of ice cold water and were kept on ice from now on in between each centrifugation. Cell cultures were centrifuged for 10 minutes at 6000rpm and the pellets resuspended in 500 ml cold

dH_2O. The cells were centrifuged at 6000rpm for 10 minutes and the pellets were resuspended 250 ml cold dH_2O then centrifuged again and resuspended in 100 ml cold dH_2O. The cells were centrifuged for a fifth time at 6000rpm for 10 minutes and resuspended in 10 ml of 10% (v/v) glycerol to 90% (v/v) cold dH_2O. The cells were centrifuged at 6000rpm for 10 minutes for the last time and the pellets were pooled and resuspended in 1 ml of 10% (v/v) glycerol to 90% (v/v) cold dH_2O. The cells were then aliquoted into 1.5 ml microfuge tubes in 100 µl suspensions and frozen in liquid nitrogen before storing *E. coli* stocks at -70°C. Care was taken when using liquid nitrogen, by wearing thermal protective gloves and goggles.

2.10.2 Procedure for the preparation of competent *E. coli* DH5α

E. coli DH5α were inoculated in 10 ml of LB media and incubated overnight at 37°C 200rpm. The 10 ml culture was added to 1 L of LB media and incubated for 2 hours at 37°C shaking. The *E. coli* culture was split into 4 x 250 ml centrifugation tubes and cooled on ice for 10 minutes. The cells were centrifuged at 5000rpm for 10 minutes at 4°C. The pellets were resuspended in 10 ml RFI Buffer and kept on ice for 30 minutes. The cells were centrifuged at 5000rpm for 10 minutes at 4°C and each pellet was resuspended in 3.2 ml RF2 Buffer. The tubes were kept on ice for 15 minutes. 100 µl aliquots were transferred to pre-cooled 1.5 ml microfuge tubes and the cells were stored at -70°C. The components of Buffer RF1 and RF2 are listed in Table 2.9.

Table 2.9. Components of buffers used in the preparation of competent *E. coli.*

BUFFER	COMPONENT	CONCENTRATION/ VOLUME ADDED	FINAL CONCENTRATION/ VOLUME
RF1	K-Acetate	1.47 g	30 mM
	$CaCl_2.2H_2O$ (dihydrate)	5 ml of a 1 M stock	10 mM
	Glycerol	7.5 ml	15%
	dH_2O		Adjusted to 450 ml
	Adjusted to pH 5.92 with 0.2 M acetic acid (Sigma). (0.2 M = 3 g in 250 ml dH_2O)		
	RbCl	6 g	100 mM
	$MnCl_2.4H_2O$ (tetrahydrate)	4.95 g	50 mM
	dH_2O		Adjusted to 500 ml
RF2	RbCl	5 ml of a 1 M stock	10 mM
	$CaCl_2.2H_2O$	5.5 g	75 mM
	H_2O		Adjusted to 500 ml

All chemicals and solutions were added in consecutive order from top to bottom, as illustrated in the table. Both RF1 and RF2 buffers were filter sterilised and stored at 4^oC prior to use. All chemicals were purchased from Sigma.

2.10.3 Transformation of plasmid DNA into *E. coli* (long method)

1-20 μl (approximately 1 μg DNA) of plasmid DNA was mixed into 100 μl competent *E. coli* on ice and left to incubate for 30 minutes. The cells were subjected to 42^{o}C for 1 minute on a digital dry bath. The cells were recovered immediately by adding 1 ml of liquid LB to each 1.5 ml microfuge tube. Each tube was incubated at 37^{o}C shaking for 1 hour and plated onto LB-amp agar. The plates were incubated overnight at 37^{o}C.

2.10.4 Transformation of plasmid DNA into *E. coli* (5 minute method)

LB-amp plates were pre-heated to 37ºC in an incubator for approximately 1 hour. 50 μl of competent *E. coli* were defrosted on ice. 1 μl of plasmid DNA was added to 50 μl *E. coli* immediately after defrosting. The cells were kept on ice for 5 minutes and selected onto warm LB-amp plates and incubated overnight at 37ºC.

2.10.5 Transformation of plasmid DNA into *E. coli* by electroporation

Mixtures of DNA and water (30 μl total volume) were prepared and transferred into pre-chilled polystyrol cuvettes (Starstedt, Numbrecht, Germany). The plasmid DNA was often too concentrated and had to be diluted with water to allow electroporation to work. The volumes of DNA to water in the mixtures depended upon the exact plasmid DNA concentration being used. The cuvettes were placed on ice and 20 μl of defrosted electro-competent *E. coli* were added and mixed with the DNA. The mixtures were incubated on ice for 10-20 minutes and then electroporated (0.9ms) in a Micropulser electroporator (BIORAD). The cells were recovered by adding 1 ml of LB to each

cuvette and transferring to sterile 1.5 ml microfuge tubes. The microfuge tubes were incubated for 1 h shaking at 37°C and the cells were selected on LB-amp plates to incubate overnight at 37^{o}C.

2.11 Yeast DNA isolation

2.11.1 Yeast genomic DNA isolation

Materials

(a) 1 M sorbitol/100 mM EDTA (Sigma) solutions were prepared by dissolving 18.2 g of sorbitol in 20 ml warm dH_2O and adding 2.92 g of EDTA. The solutions were adjusted to 100 ml with dH_2O, autoclaved and stored at room temperature.

(b) Zymolase stocks were prepared by adding 500 mg of zymolase (Sigma) to 100 ml dH_2O and filter sterilising. The stocks were aliquoted into 1 ml volumes and stored at -20^{o}C.

(c) 1 M Tris/100 mM EDTA solutions were prepared by dissolving 2.92 g of EDTA and 12.1 g Tris in 20 ml dH_2O and adjusting the final volume to 100 ml with dH_2O. The solutions were autoclaved and stored at room temperature.

(d) 10% SDS solutions were prepared by dissolving 10 g SDS in 20 ml dH_2O and adjusting the final volume to 100 ml with dH_2O. The solutions were autoclaved and stored at room temperature.

(e) 5 M potassium acetate (KAc) solutions were prepared by dissolving 49 g KAc in 20 ml dH_2O and adjusting the final volume to 100 ml with dH_2O. The solutions were autoclaved and stored at room temperature.

Method

To isolate genomic DNA from a desired strain, yeast were inoculated in 1.5 ml YPD and incubated overnight shaking at 30°C. The cells were centrifuged at 2000rpm for 5 minutes and the pellets were resuspended in 150 µl of 1 M sorbitol/100 mM EDTA in 1.5 ml microfuge tubes. 12 µl of 5 mg/ml zymolase was added to each set of cells and the tubes were incubated for 1 hour at 37°C. The mixtures were centrifuged at 13000rpm for 5 seconds and pellets resupended in 150 µl of 1 M Tris/100 mM EDTA. 15 µl of 10% SDS was mixed with the cell suspensions and incubated at 65°C for 30 minutes. 60 µl of 5 M KAc was added to each tube and left on ice for 1 hour. The resulting mixtures were centrifuged at 13000rpm for 5 minutes and the supernatants were retained. 195 µl of Isopropanol (Sigma) was added to each supernatant and allowed to sit for 5 minutes at room temperature. The DNA pellets were centrifuged at 13000rpm for ten seconds and allowed to air dry. The DNA was dissolved in 45 µl dH_2O and stored at -20°C.

2.11.2 Yeast plasmid DNA isolation

To isolate plasmid DNA from yeast, cells were inoculated overnight in 5 ml selective media at 30^oC 200rpm. The cells were harvested by centrifugation at 2000rpm for 5 minutes. All buffers used in this procedure were purchased in a plasmid miniprep kit from QIAGEN. The cell pellets were resuspended in 250 µl Resuspension Buffer in 1.5 ml microfuge tubes and approximately 200 µl of 0.5 mm soda lime glass beads (Biospec products Inc.) were added to the cell suspensions. The cells were vortexed (Vortex-2 Gene, Scientific Industries) for 5 minutes at maximum speed. At this stage the glass beads were at the bottom of the microfuge tubes and the liquid cell mixtures were

carefully removed. 250 µl of Lysis Buffer followed by 350 µl of Neutralising Buffer were added to the cells, mixed well and centrifuged for 10 minutes at 13000rpm. The supernatants were then removed and transferred to DNA binding columns (QIAGEN) where they were centrifuged for 1 minute at 13000rpm. Flow-through into the catchment tubes were discarded and 750 µl of Wash Buffer was added to each column, this was followed by centrifugation for 1 minute at 13000rpm. Flow-through was discarded and columns were centrifuged for an additional 1 minute to remove any residual buffer from the binding column. DNA was eluted by adding 50 µl of Elution Buffer directly into the binding columns and allowing them to sit for 1-2 minutes. The binding columns were transferred to fresh 1.5 ml microfuge tubes and plasmid DNA was isolated by a final 1 minute centrifugation at 13000rpm.

To ensure plasmid DNA was at an ideal concentration for further experimentation (ideal amount is 100-500 ng/µl), 17 µl of each DNA elution was transformed into *E. coli* by the 'long' method of transformation (section 2.10.3). Plasmid DNA was finally isolated by additional steps that will be discussed in section 2.12.

2.12 Isolation of plasmid DNA from *E. coli*

Following transformation of plasmid DNA into *E. coli*, individual bacterial colonies were isolated from the LB-amp plates. Each bacterial colony should contain hundreds-thousands of copies of the same plasmid. To isolate this DNA, a single colony was inoculated in 5 ml of LB-amp liquid and grown overnight at 37°C 200rpm. The cells were harvested by centrifugation for 5 minutes at 4000rpm. All buffers used in this procedure were purchased in a plasmid miniprep kit from QIAGEN. The cell pellets were

resuspended in 250 μl Resuspension Buffer. 250 μl of Lysis Buffer followed by 350 μl of Neutralising Buffer were added to the cells, mixed well and centrifuged for 10 minutes at 13000rpm. The supernatants were then removed and transferred to DNA binding columns where they were centrifuged for 1 minute at 13000rpm. Flow-through in catchment tubes was discarded and 750 μl of Wash Buffer was added to each column, this was followed by centrifugation for 1 minute at 13000rpm. Flow-through was discarded and columns were centrifuged for an additional 1 minute to remove any residual buffer from the binding column. DNA was eluted by adding 50 μl of Elution Buffer directly into the binding columns and allowing it sit for 1-2 minutes. The binding columns were transferred to fresh 1.5 ml microfuge tubes and plasmid DNA was isolated by a 1 minute centrifugation at 13000rpm. Plasmid DNA was stored at -20°C.

2.13 Measuring [*PSI*$^+$] propagation in yeast

The presence of [*PSI*$^+$] can be monitored in yeast strains by a colour assay (Figure 2.1). Sup35 is an *S. cerevisiae* protein involved in translation termination. When Sup35 aggregates into a non-functional form it is called [*PSI*$^+$]. Laboratory yeast strains have an ochre mutation (*ade2.1*) in a gene responsible for adenine biosynthesis. When Sup35 is in its normal unaggregated state it halts translation at this premature stop codon which leads to the build-up of a red pigment in the cells. Cells which are [*psi*$^-$] are red when grown on limiting amounts of adenine. When Sup35 is in its aggregated [*PSI*$^+$] form, there is reduced translation termination of the *ade2* gene and cells appear white on limiting adenine media (Figure 2.1 and 2.2). A second way of monitoring the presence of [*PSI*$^+$] is by growth of yeast cells on medium lacking adenine. [*PSI*$^+$] cells grow on

medium lacking adenine whereas [*psi*$^-$] cells do not. This is because [*PSI*$^+$] cells produce a fully functional Ade2 protein which is involved in the adenine biosynthesis pathway. [*psi*$^-$] cells disrupt this pathway and require supplemented adenine for normal growth.

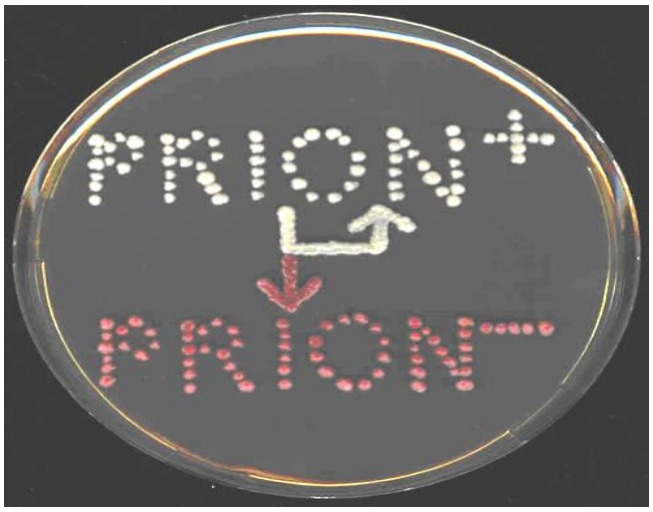

Figure 2.1. The presence of [*PSI*$^+$] is easily monitored by a colour assay.

2.14 Monitoring [*URE3*] propagation

[*URE3*] is the prion form of protein Ure2. Its activity was monitored by *ADE2* gene, under control of the *DAL5* promoter, in strain SB34. When Ure2 protein is active the *ADE2* gene is not translated and cells are red on media with limiting adenine. When Ure2 is in the aggregated [*URE3*] state *ADE2* is fully translated and colonies appear white or pink on media with limiting adenine (Schlumpberger *et al.*, 2001). [*URE3*] propagation is a lot more unstable than [*PSI*$^+$] propagation. Colonies often appear sectored after a few generations as the cell starts to lose [*URE3*]. In this study the effect of Sse1 mutants on the rate of [*URE3*] propagation was monitored. SB34 was prepared for transformation and WT Sse1 and thirteen Sse1 mutants were transformed into the

cells and selected on SC - leucine. The plates were incubated for 2 days at 30°C and colonies were marked as being red, white or sectored. The experiment was repeated in triplicate and [*URE3*] was measured as the average percentage of red, white and sectored colonies.

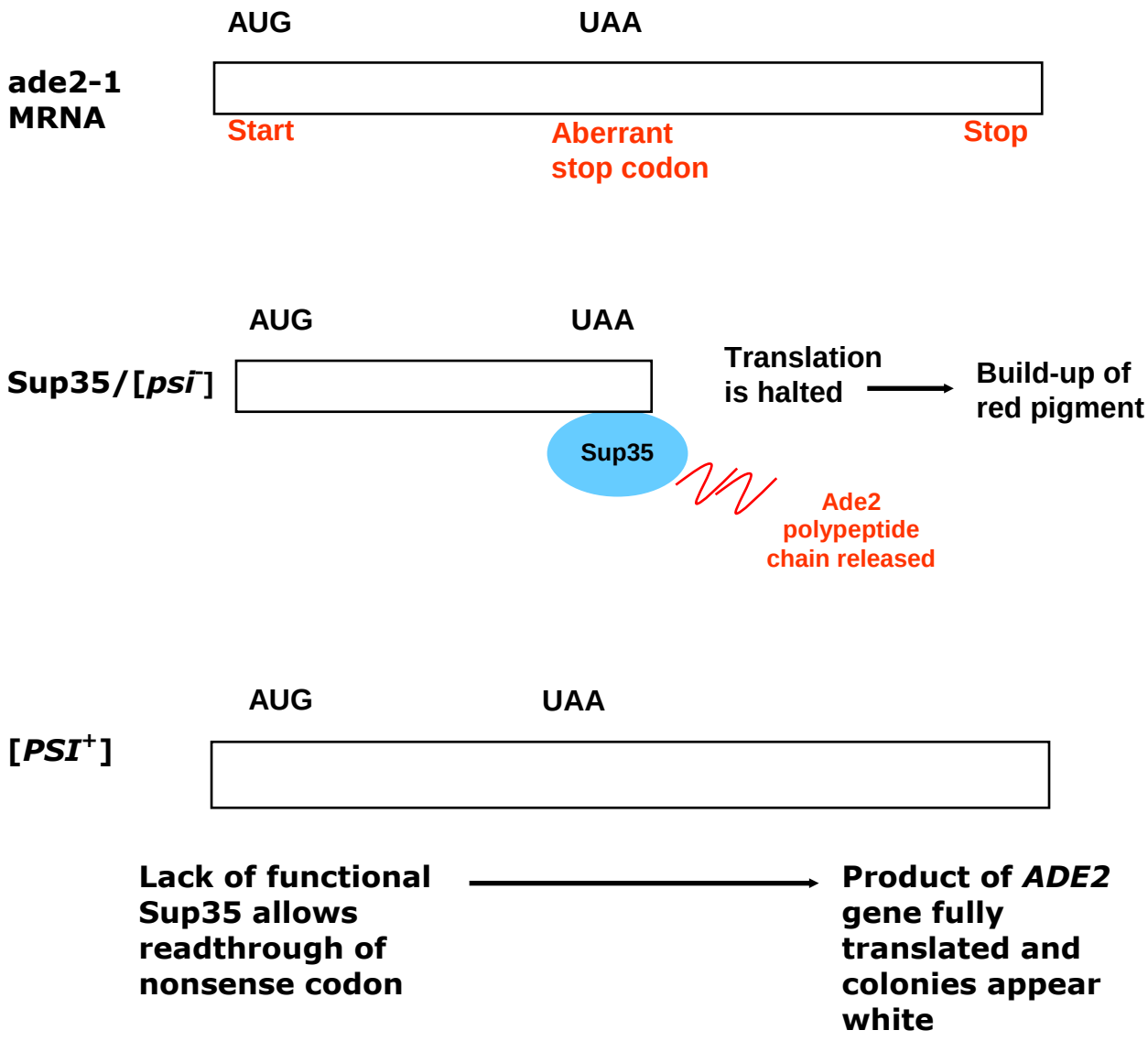

Figure 2.2. Sup35 translation termination efficiency when cells are [*PSI*$^+$] and [*psi*$^-$]. Laboratory yeast strains have an aberrant stop codon in *ade2-1* gene. [*psi*-] cells halt translation due to functional Sup35 and cells appear red. [*PSI*$^+$] cells allow readthrough of the stop codon and cells appear white.

2.15 Random mutagenesis of plasmid DNA using hydroxylamine

The method for random mutagenesis of plasmid DNA is derived from a protocol by Schatz *et al*. (1988). Hydroxylamine (Sigma) is the mutagen used but is made into a solution prior to mutagenesis (Table 2.10). Desired plasmid DNA was transformed into *E. coli* and extracted as described in sections 2.10.4 and 2.12. A DNA concentration of 5 μg was needed for this experiment. An accurate measurement of this was made on a Nanodrop 1000 Spectrophotometer (Mason Technology). 250 μl of hydroxylamine solution (Table 2.10) was added to 5 μg of DNA and incubated at 70^{o}C for 60 minutes. DNA was purified using a PCR purification kit (QIAGEN) and eluted in 50 μl Elution Buffer. Approximately 10 1.5 ml microfuge tubes were set-up, each containing 5 μl of the mutated DNA mixed with 25 μl of dH_2O. The DNA-dH_2O mixes were transformed into *E. coli* by electroporation (section 2.10.5). *E. coli* colonies were counted on LB-amp plates the following day. For DNA to be completely saturated with all possible mutations approximately 10,000 colonies were needed (1,000 colonies per plate). *E. coli* colonies were pooled together in 5 ml of LB-amp and incubated at 37^{o}C for 1 hour 200rpm. Plasmid DNA (mutant library) was extracted using methods in section 2.12. The mutant library DNA was stored at -20^{o}C until further use.

2.16 Isolating mutants by the plasmid shuffle technique

The mutant library was transformed into a desired yeast strain as described in section 2.9. 100 ng (0.2-1 μl) of mutant library was transformed into each set of yeast cells. Colonies were selected on SC – leucine, using sterile glass beads for an even spread, and subsequently replicated onto 5-FOA. 5-FOA plates were incubated for 2 days

Table 2.10. Components in hydroxylamine solution.

COMPONENT	AMOUNT
200 mM EDTA	20 μl
1 M NaCl	200 μl
Hydroxylamine	138.98 mg
Sodium Pyrophosphate	44.6 mg
dH_2O	1.78 ml

All components were purchased from Sigma.

at 30^{o}C. 5-FOA selects colonies that only contain a *LEU2* marker plasmid from the mutant library. Wild type gene is on a *URA3* marker plasmid which is toxic in the presence of 5-FOA. Colonies that appeared pink or red were selected and cultured onto fresh SC - leucine medium. The absence of *URA3* plasmid pRS316*SSE1* was re-confirmed by replicating colonies onto SC - uracil medium (no growth). The transformation was repeated if any mutant library DNA was still available. Plasmid DNA from each colony was extracted via methods described in section 2.11.2 and retransformed back into yeast to reconfirm the phenotype. Colonies that appeared red/pink were sent for sequencing as described in section 2.21.

When screening for new temperature-sensitive *sse1* mutants the same procedure was carried out with the exception that CM03 was used and the 5-FOA replicated plates were incubated at 37^{o}C. Any colonies that failed to grow at 37^{o}C were picked off from their corresponding SC - leucine plate. Secondary screening of potential mutants involved

extracting the plasmid DNA, retransforming it back into yeast and performing a comparative growth assay at 37^{o}C.

2.17 Isolating second-site suppressor mutants

Plasmid mutants Sse1^{G342D} and Sse1^{G616D} were used in this study to screen for second-site mutations that suppress their original temperature-sensitive (ts) and [*psi*$^{-}$] phenotypes. Plasmid DNA was prepared and mutagenised as described in section 2.15. DNA mutant libraries of G342D and G616D were transformed into CM02 along with WT Sse1, pRS315, Sse1^{G342D} and Sse1^{G616D}. The transformants were selected on SC -leucine medium, using glass beads to get an even lawn of cells, and incubated for 2 days at 30^{o}C. There were approximately twenty mutant library plates and one for each control. The plates were subsequently left at room temperature for a day before replicating them onto 5-FOA. The 5-FOA plates were incubated overnight at 37^{o}C or for 2 days at 30^{o}C. For ts reverting mutant analysis WT Sse1 was the only plate with complete cell growth as pRS315 control and ts mutants G342D and G616D were non-viable. Colonies were screened for potential growth at 37^{o}C and individual colonies were picked (primary screen). Plasmid DNA from each isolate was extracted and re-transformed into CM02. Comparative growth analysis at 37^{o}C confirmed which isolates were potential second-site suppressors (sss) (secondary screen). Any G342D/G616D mutant isolates that survived at 37^{o}C were sent for DNA sequencing.

Analysing potential sss for reverting mutant [*psi*$^{-}$] phenotype involved screening the 5-FOA plates for any colonies that looked white at 30^{o}C. These colonies were

selected and plasmids retransformed back into CM02. Potential sss were analysed by streaking onto YPD medium alongside the Sse1 mutant of interest and WT Sse1.

2.18 Site-directed mutagenesis of plasmid DNA

Site-directed mutagenesis is an effective tool for generating mutants of interest at specific amino acid residues. The technique of inducing mutations using oligonucleotides was first described by Hutchison *et al*. (1978). Complementary primer pairs were designed to anneal to approximately 40-50 bp of *SSE1* or *SSE2* DNA with one or more of the base pairs being mismatched to the WT sequence. This resulted in a single amino acid change in the protein sequence. Plasmid DNA was prepared and PCRs were setup as described in Table 2.11 using primers listed in Table 2.12.c. The PCR product was treated with 1 µl *Dpn*1 (New England Biolabs) and incubated for 1 hour at 37^{o}C. This digested away any methylated parental plasmid DNA. Approximately 8 µl of each PCR product was transformed into competent *E. coli* using the long transformation method as decribed in section 2.10.3. Approximately four *E. coli* colonies from each transformation were isolated and the plasmid DNA extracted as described in section 2.12. The plasmid DNA was sent for sequencing as described in section 2.21 using primers listed in Table 2.13. If sequence analysis confirmed the presence of the desired mutation, the plasmid was transformed into yeast to observe any phenotypic changes.

2.19 Genomic DNA knockout by homologous recombination

Certain yeast knockout strains used in this study were purchased from EUROSCARF. All other strains were made in the laboratory. Yeast knockout strains

were made by applying a technique called homologous recombination. This involves creating a gene disruption cassette that encodes a selectable marker. Located at either side of the selectable marker are segments of DNA homologous to the gene being knocked out. The knockout cassette incorporates itself into the genome at the corresponding chromosomal locus by homologous recombination.

Genomic knockouts were created using either the selectable marker *kanMX* (kanamycin resistance gene) or *HIS5*. *kanMX* knockout constructs were available in EUROSCARF strain BY4741 for *AKL1*, *HSL1*, *KIN2* and *SSE2*. These knockouts were transferred into G600 yeast strains by homologous recombination (Figure 2.3). Genomic DNA was isolated from the purchased BY4741 strains and primers were designed to anneal ~ 250 bp upstream and downstream of the gene being knocked out. Table 2.12.d lists all primers used for creating knockout strains. The PCR resulted in the amplification of the *kanMX* gene with overhangs homologous to the gene of interest (Figure 2.3).

The *SWI6* gene was knocked out with *HIS5*. Primers were designed to anneal to vector pUG27 at regions upstream and downstream of *HIS5*. The primers also included ~50 base pairs homologous to *SWI6* which acted as overhangs in the resulting knockout construct.

Following PCR, the desired yeast strains were prepared for transformation as described in section 2.9. Four transformations took place for each knockout, one was a water control and the others had varying concentrations of PCR product (10 μl, 30 μl and 60 μl). Transformed yeast were incubated overnight in 1 ml YPD media at 30^{o}C shaking and selected on G418 or SC - histidine plates the following morning (section 2.3.1). The

(a) Primers were designed to anneal upstream and downstream of *kanMX* gene

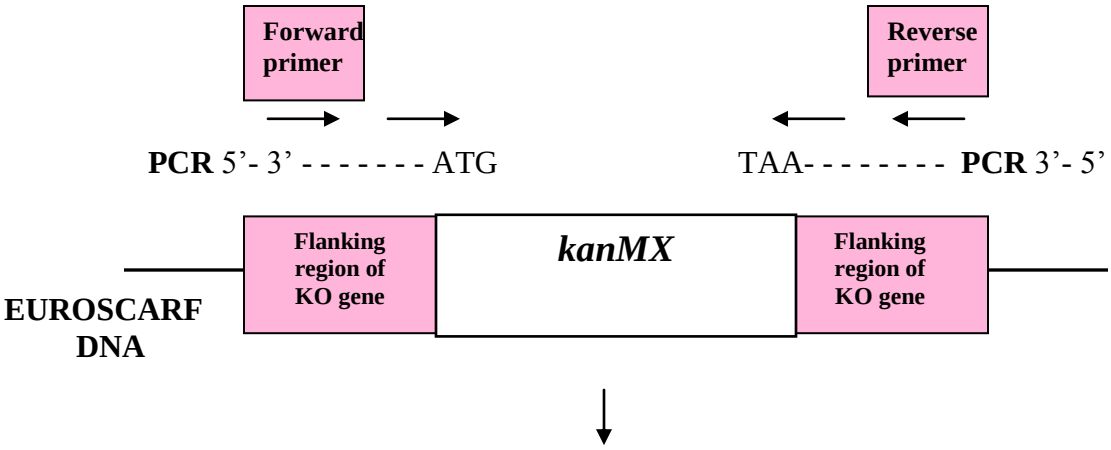

(b) DNA knockout cassette: primers amplify *kanMX* gene with the addition of overhangs that are homologous to the gene of interest.

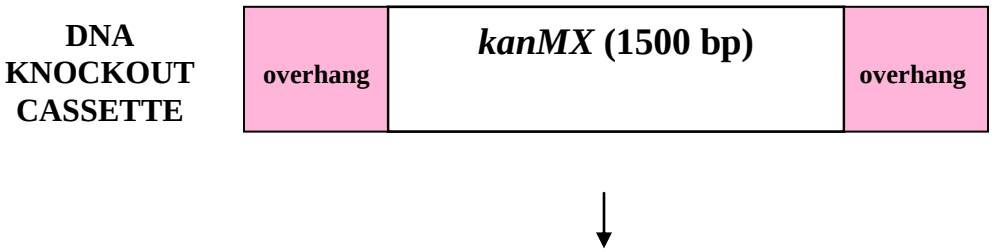

(c) Homologous recombination: knockout cassette was transformed into yeast and homologous overhangs enable *kanMX* to incorporate into genome at the desired site.

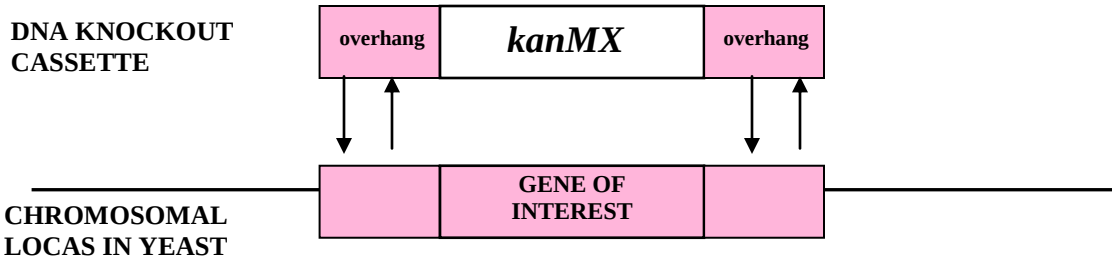

Figure 2.3. Creating *kanMX* DNA knockouts by homologous recombination. The kanamycin resistance gene replaces the gene of interest by homologous recombination.

plates were incubated for 2-3 days at 30^{o}C and colonies were tested for positive knockouts by diagnostic PCR. Diagnostic PCRs involved extracting genomic DNA (section 2.11.1) from each isolate and a WT control strain and performing the following PCR reactions on them;

(a) Forward and reverse primers that anneal outside the start and stop codon of the knocked out gene. If the gene was successfully knocked out the PCR product would correspond to the size of the *kanMX*/*HIS5* gene instead of wild type gene.

(b) Forward primer used in (a) with a reverse primer that anneals to the coding region of *kanMX*/*HIS5*. This PCR confirmed the gene was knocked out and the PCR product reflected the left flanking region of the knockout cassette.

(c) Reverse primer used in (a) with a forward primer that anneals internally in the coding region of *kanMX*/*HIS5*. This PCR confirmed the gene was knocked out and the PCR product reflected the right flanking region of the knockout cassette.

2.20 PCR analysis

2.20.1 PCR amplification

All primers were purchased from Sigma in the de-salted powder form. They were dissolved in molecular grade sterile water (Sigma) to produce 100 μM stock solutions. The volume of water added was indicated on the specific primer sticker, as provided by Sigma. They were further diluted 1/10 to produce 10 μM working samples. Stock and working primers were stored at -20^{o}C. PCRs were carried out using a Peltier Thermal cycler (MJ Research) in sterile PCR tubes (Starstedt). The dNTP mix was made using 2.5 mM each of dATP, dGTP, dTTP and dCTP (Sigma). Table 2.11 lists the

specific PCR reaction mixtures and cycles for the appropriate product. Table 2.12a-d lists the primers used for PCR.

2.20.2 Agarose gel electrophoresis

PCR products were resolved on 0.8% agarose gel at 90V for 45 minutes in a Biorad electrophoresis power-pack. 0.4 g agarose (Sigma) was dissolved in 50 ml of 1X TAE Buffer (Millipore), boiled and allowed to cool. Once cooled, 1 μl of a 10 mg/ml ethidium bromide solution (Sigma) was added to make a final concentration of 0.2 μg/ml. Care was taken when handling the carcinogen ethidium bromide. All materials that were in contact with the agent were disposed of in a separate ethidium bromide waste container. The molten agarose was poured into a casting rig and allowed to set. PCR products (3 μl) were mixed with 1 μl of 6X Blue Loading Dye (NEB) and 2 μl of dH_2O. The gel was submerged in 1X TAE Buffer and the PCR products were added to the wells alongside a 1kb molecular grade marker (NEB).

Table 2.11. PCR reaction mixtures and PCR cycles.

PCR	PCR MIXTURE (25 μl)	PCR CYCLE (TIME IN MINUTES)
1. PCR FOR GENOMIC KNOCKOUTS & DIAGNOSTIC TESTS	2.5 μl *Taq* Buffer (New England Biolabs, (NEB)) 1 μl dNTP mix (Sigma) 0.5 μl forward primer (Sigma) 0.5 μl reverse primer (Sigma)	95°C 5:00 95°C 0:30 55°C 0:30 72°C 1:00 per kb Go to 2 30 times 72°C 6:00

	1 µl $MgCl_2$ (NEB) 0.5 µl template DNA 0.5 µl *Taq* Polymerase (NEB) 18.5 µl molecular grade water	4°C overnight
2. PCR OF TEMPLATE DNA FOR CLONING	2.5 µl High Fidelity (HF) *Taq* Buffer (Invitrogen) 0.5 µl dNTP mix 0.5 µl forward primer 0.5 µl reverse primer 1 µl $MgSO_4$ (Invitrogen) 0.5 µl template DNA 0.2 µl HF *Taq* Polymerase (Invitrogen) 19.3 µl molecular grade water	94°C 2:00 94°C 0:30 62°C 0:30 62°C 1:00 per kb Go to 2 30 times 72°C 6:00 4°C overnight
3. SITE-DIRECTED MUTAGENESIS	2.5 µl PFU ULTRA Buffer (Starstedt) 0.5 µl dNTP mix 1 µl forward primer 1 µl reverse primer 0.5 µl template DNA 0.5 µl HF PFU ULTRA (Starstedt) 19 µl molecular grade water	95°C 1:00 95°C 0:30 55°C 1:00 62°C 2:00 per kb Go to 2 12 times 68°C 7:00 4°C overnight

Table 2.12.a PCR primers used to confirm knockout strains CM02 and CM03.

PRIMER	OLIGONUCLEOTIDE	FRAGMENT SIZE (BP)
SSE04F	ACGAAGATGATTCTAGAAG	2496 (WT *SSE1*)
SSE03R	TTAGGAGACTAATGCGTG	1943 (*kanMX* KO)
KAN02F	TTGATGACGAGCGTAATGG	
SSE03R	TTAGGAGACTAATGCGTG	772
SSE04F	ACGAAGATGATTCTAGAAG	
KAN01R	TGCGCACGTCAAGACTGTC	277
SSE05F	ATCACATCATACGAGGAG	2519 (WT *SSE2*)
SSE06R	TACTTTGAAACATAGGAC	1948 (*kanMX* KO)
KAN02F	TTGATGACGAGCGTAATGG	
SSE06R	TACTTTGAAACATAGGAC	861
SSE05F	ATCACATCATACGAGGAG	
KAN01R	TGCGCACGTCAAGACTGTC	293

Primers were used to perform diagnostic tests on CM02 and CM03 strains**.**
*Primers sse04, sse03, sse05 and sse06 all sequence regions of *SSE1* and *SSE2* genes. When *SSE1* and *SSE2* were genomically replaced by *kanMX* the primers amplified the knockout construct which resulted in a different size DNA band.

Table 2.12.b PCR primers used to clone segments of DNA into a vector.

PRIMER	OLIGONUCLEOTIDE	FRAGMENT SIZE (BP)
HSPH1F	CAAGCAGATTTTATACAGAAATATTTATACA TATGTCGGTGGTGGGGTTGGACGTGGC	2640
HSPH1R	CTTCCTGATTAAACAGGAAGACAAAGCATG CCTAGTCCAAGTCCATATTAACAGAA	
SSE2CLONEF	ACCGCGGTGGCGGCCGCTCTAGAACTAGTG GATCCAATCACATCATACGAGGAGTTTTAAGG	2365
SSE2CLONER	AAGCTTGATATCGAATTCCTGCAGCCCGGG GGATCCTTAATCAAGGTCCATGTTTTCATCAT TGT	
Q458pC210F	CAAGCAGATTTTATACAGAAATATTTATACA TATG ATGAGTACTCCATTTGGTTT	1445
Q458pC210R	GCGACTTCCTGATTAAACAGGAAGACAAA GCATGC TTATTCTGGAGTGTTTGGTG	

Table 2.12.c PCR primers used to amplify DNA for site-directed mutagenesis.

PRIMER	OLIGONUCLEOTIDE
SSE2G616DF	GTGGTTATACGATGAAGATTTCGATTCCATCAAAG
SSE2G616DR	CTTTGATGGAATCGAAATCTTCATCGTATAACCAC
SSE2Q504EF	CGGAAGATATTACGGTTGAAGAGCCAGTGCCTTTAC
SSE2Q504ER	GTAAAGGCACTGGCTCTTCAACCGTAATATCTTCCG
SSE2S384AF	GCTTTCATATGTGCCATTCACGCTCCAACTTTAAGGGTCAGG
SSE2S384AR	CCTGACCCTTAAAGTTGGAGCGTGAATGGCACATATGAAAGC
SSE2S384EF	GCTTTCATATGTGCCATTCACGAACCAACTTTAAGGGTCAGG
SSE2S384ER	CCTGACCCTTAAAGTTGGTTCGTGAATGGCACATATGAAAGC
SSE2S679AF	CAAAGAAGGGCACGCGCTGCAGCTGATGATAGCGATGACAACAA
SSE2S679AR	TTGTTGTCATCGCTATCATCAGCTGCAGCGCGTGCCCTTCTTTG
SSE2S679EF	CAAAGAAGGGCACGCGCTGCAGAAGATGATAGCGATGACAACAA
SSE2S679ER	TTGTTGTCATCGCTATCATCTTCTGCAGCGCGTGCCCTTCTTTG
SSE2S682AF	GCACGCGCTGCAAGTGATGATGCCGATGACAACAATGATGAAAAC
SSE2S682AR	GTTTTCATCATTGTTGTCATCGGCATCATCACTTGCAGCGCGTGC
SSE2S682EF	GCACGCGCTGCAAGTGATGATGAGGATGACAACAATGATGAAAAC
SSE2S682ER	GTTTTCATCATTGTTGTCATCCTCATCATCACTTGCAGCGCGTGC

SSE1S85AF	CCAGATTTCGAGCAAGAAGCTAAGCACTTCACCTCTAAGTTG
SSE1S85AR	CAACTTAGAGGTGAAGTGCTTAGCTTCTTGCTCGAAATCTGG
SSE1S85EF	CCAGATTTCGAGCAAGAAGAAAAGCACTTCACCTCTAAGTTG
SSE1S85ER	CAACTTAGAGGTGAAGTGCTTTTCTTCTTGCTCGAAATCTGG
SSE1S384AF	CTTTATTTGCGCCATTCACGCTCCAACTCTAAGAGTTAG
SSE1S384AR	CTAACTCTTAGAGTTGGAGCGTGAATGGCGCAAATAAAG
SSE1S384EF	CTTTATTTGCGCCATTCACGAACCAACTCTAAGAGTTAG
SSE1S384ER	CTAACTCTTAGAGTTGGTTCGTGAATGGCGCAAATAAAG

Table 2.12.d. PCR primers used to create genomic DNA knockouts.

PRIMER	OLIGONUCLEOTIDE	FRAGMENT SIZE (BP)
AKL1F	GGTGAACCCCGCCATTCTG	3809 (WT *AKL1*)
AKL1R	CTGTCAAATTGCGAGCAC	1989 (*kanMX* KO)
AKL1F	GGTGAACCCCGCCATTCTG	
KAN01R	TGCGCACGTCAAGACTGTC	353
AKL1R	CTGTCAAATTGCGAGCAC	
KAN02F	TTGATGACGAGCGTAATGG	742
HSL1F	CGTAAATTGGACAGCGAGAGG	5045 (WT *HSL1*)
HSL1R	GGATGACGAATCTTCTTGAGC	1995 (*kanMX* KO)

HSL1F	CGTAAATTGGACAGCGAGAGG	331
KAN01R	TGCGCACGTCAAGACTGTC	
HSL1R	GGATGACGAATCTTCTTGAGC	770
KAN02F	TTGATGACGAGCGTAATGG	
KIN2F	GACCTAGAAGTCCTGCTTTGC	3949 (WT *KIN2*)
KIN2R	GGGAATGCATCTAACTGTTCG	2012 (*kanMX* KO)
KIN2F	GACCTAGAAGTCCTGCTTTGC	
KAN01R	TGCGCACGTCAAGACTGTC	317
KIN2R	GGGAATGCATCTAACTGTTCG	
KAN02F	TTGATGACGAGCGTAATGG	801
SWI6KOF	GCTAAAAAAAAAAGAATAATAAAGGGGAA CACAGTATAATTCTCGAGAGGATGCAGCTG AAGCTTCG	1562
SWI6KOR	TAACTTCAAATAAAGTCATAAAAGTTAATG CAATGAAATCACATGCCCTCAGCATAGGCC ACTAGTGGATCTG	
SWI6F	CCTTGCAGCGTTACTAGCCATAG	3048 (WT *SWI6*)
SWI6R	GGCAAACCATTGGACGAAGAG	2167 (*HIS5* KO)
HIS5F	GAGGGTATATTGCTAGACGCC	971
HIS5R	CCGGAACAGCCTAATTCGTTAC	
SWI6F	CCTTGCAGCGTTACTAGCCATAG	1741
HIS5R	CCGGAACAGCCTAATTCGTTAC	

SWI6R	GGCAAACCATTGGACGAAGAG	
HIS5F	GAGGGTATATTGCTAGACGCC	1684

2.21 DNA sequence analysis

Yeast genomic or plasmid DNA was prepared as described in section 2.11. Approximately 1 μg of DNA was mixed in 1.5 ml microfuge tubes with 20 pmol of an appropriate primer to a final volume of 14 μl. Microfuge tubes were tagged with a prepaid barcode and samples were sent to Agowa Sequencing Services Berlin, Germany. DNA was sequenced by dye-terminator sequencing and results were available on the Agowa website. Sequencing results were compared to the gene of interest by BLAST analysis on NCBI. A list of the sequencing primers used to screen for *sse1* and *sse2* mutants are listed in Table 2.13. These primers were also used in addition to those listed in Tables 2.12a,b and d to confirm knockouts and clones.

Table 2.13. DNA sequencing primers.

PRIMER	OLIGONUCLEOTIDE
SSE04F	ACGAAGATGATTCTAGAAG
SSE07F	TACACCGAAGAACAACG
SSE08F	ACCAAGATGAAGCCATCG

SSE03R	TTAGGAGACTAATGCGTG
SSE07R	CGTTGTTCTTCGGTGTA
SSE08R	CGATGGCTTCATCTTGGTTC
SSE05F	ATCACATCATACGAGGAG
SSE2AF	CAGCTACTCAACTGACTGC
SSE2BF	CCGTGAAGAGCTGGAAG
SSE2CF	GATGCGATCCTTCCGGCTTG
SSE2DF	GGCACGCGCTGCAAGTGATGATAG
SSE06R	TACTTTGAAACATAGGAC
SSE2AR	GCAGTCAGTTGAGTAGCTG
SSE2BR	CTTCCAGCTCTTCACGG
SSE2CR	CAAGCCGGAAGGATCGCATC

2.22 Mating yeast strains to select for specific genotypes

The mating type of a haploid strain is determined by the *MAT* locus whereby yeast are either *MAT***a** or *MAT*α. Haploid cells mate with other haploid cells of the opposite mating type to produce a diploid. By a process called sporulation, diploids undergo a single meiotic event whereby they produce an ascus containing four haploid spores. Subsequent random spore analysis is useful for constructing strains necessary for genetic experiments.

2.22.1 Mating haploid yeast strains

Two yeast haploid strains containing desired genotypes were grown on selective nutrient media for two days at 30^{o}C. Using a wooden dowel, one strain was streaked through the other on a separate agar plate and incubated at 30^{o}C for two days. Mating occured where the two strains meet. The plates were replicated onto SD agar that was also supplemented with one or more amino acids. This supplementation depended upon the genotype of both strains as the agar was made specifically so that only diploids would survive. For example Y02146 (*MAT***a** *his3Δ1 leu2Δ0 met15Δ0 ura3Δ0 sse1::kanMX*) was mated with Y17167 (*MAT*α *his3Δ1 leu2Δ0 lys2Δ0 ura3Δ0 sse2*::*kanMX*) to create strain CM03. They were replicated onto medium whereby the haploid parents died and the diploids survived. The medium was supplemented with histidine, leucine and uracil as the absence of lysine and methionine is lethal to haploids. The replicated SD plates were incubated for 2 days at 30^{o}C.

2.22.2 Sporulation and random spore analysis

Diploid strains were patched onto sporulation medium and minimal sporulation medium (+ amino acids) using a wooden dowel. The components of sporulation media is outlined in section 2.3.1. The plates were incubated at 30^{o}C for 2 days and then left at room temperature for 2-5 days. Diploids undergo meiosis and sporulate into asci after 4-7 days due to the limited carbon source in the growth medium. The presence of asci or tetrads can be observed by light microscopy.

The cells were mixed with 200 µl of dH_2O in 1.5 ml sterile microfuge tubes. 5 µl β-glucuronidase (500 units) (Sigma) was added to cells and incubated on a rotor for 1 h at

room temperature. 100 µl of 0.5 mm glass beads were added to the cells and incubated on a rotor at room temperature for an additional 1 hour. 1 ml of dH_2O was added and the mixtures were vortexed for 2-3 minutes to disrupt the asci. The cell mixtures were centrifuged for 10 seconds at 13000rpm and the supernatants removed and placed into 15 ml falcon tubes. 4 ml of dH_2O was added to the cells and a serial dilution of 10^{-1} to 10^{-4} was made in fresh 1.5 ml microfuge tubes. 200 µl of each serial dilution was plated onto selective medium and incubated at 30^{o}C for 2 days.

Individual colonies on each plate represented a single spore segregated from the tetrad, or in some cases an unsporulated diploid. These colonies were analysed to see if they had the desired genotype (Figure 2.4.). For example, in the case of making CM03 the serial dilution was performed on SC - uracil as a pRS316*SSE1* plasmid was transformed in at the diploid stage. Plates were subsequently replicated onto 5-FOA and any colonies that died were taken as potential Δ*sse1*Δ*sse2* haploids. After phenotypic analysis, the DNA was extracted from individual colonies using methods described in section 2.11.1 and diagnostic PCRs were performed using PCR cycles in Table 2.11 and primers listed in Table 2.12 a and d.

2.23 Cloning DNA into plasmid vector by homologous recombination

2.23.1 Creating DNA fragment for cloning

In this study three plasmid clones were created by homologous recombination**.** These were pC210*HSPH1,* pC210Q458trunc and pRS315*SSE2*. The first step was to PCR template DNA using specifically designed primers listed in Table 2.12.b. These primers annealed to approximately 30 bp of the gene of interests coding region but also

incorporated approximately 30-40bp of DNA sequence from the plasmid vector as overhangs. The PCR cycle used is described in Table 2.11. HF *Taq* has better proof-reading than *Taq* so was used for cloning. The PCR product size was confirmed by gel electrophoresis.

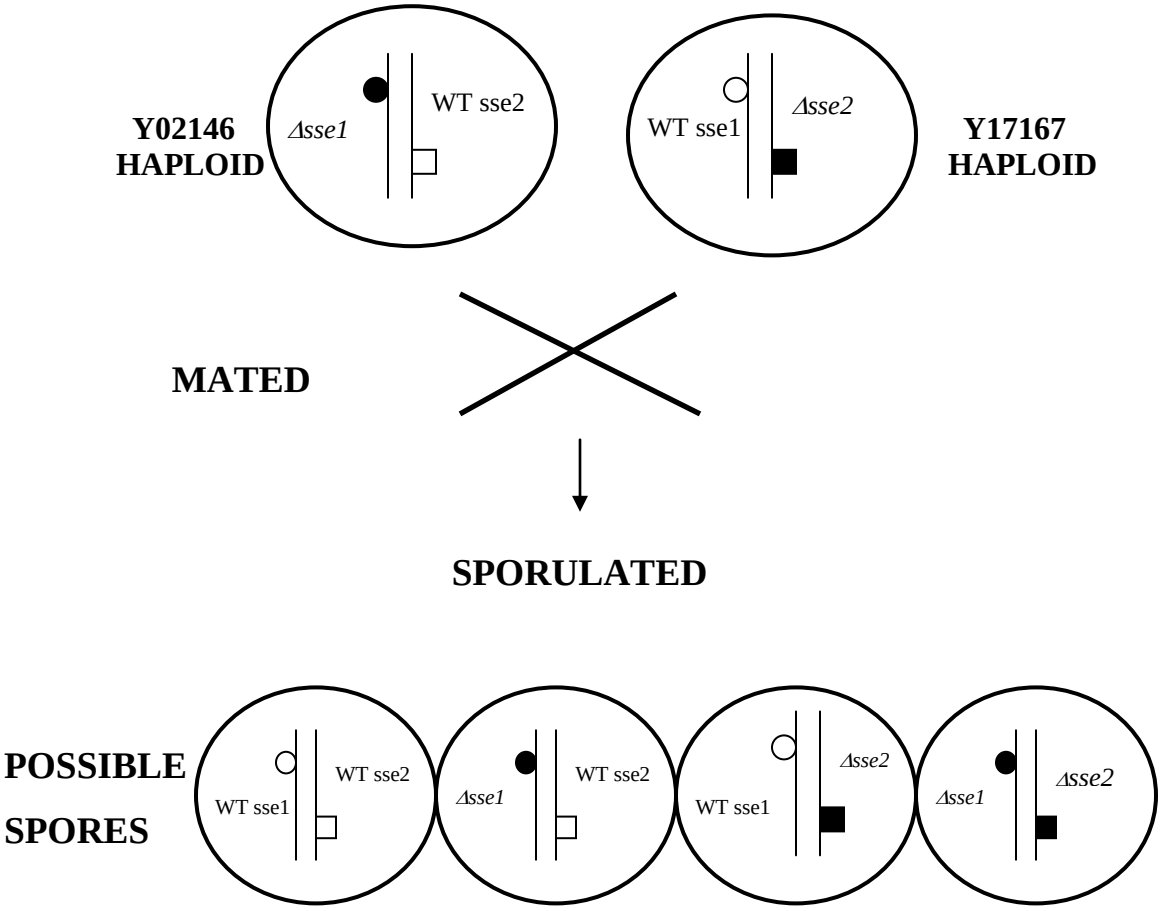

Figure 2.4. Creating yeast strain CM03 by mating and random spore analysis.

2.23.2 PCR purification of DNA fragment

100 µl PCR products were purified using a QIAGEN PCR purification kit. 500 µl of Buffer PB was added to each PCR product and transferred to QIAquick columns. The columns were centrifuged at 13000rpm for 1 minute, flow-through discarded and the columns were subsequently washed with 750 µl Buffer PE. The columns were centrifuged for 1 minute, flow-through discarded and centrifuged again for 1 minute to remove residual buffer. The binding columns were placed in fresh 1.5 ml microfuge tubes and DNA was eluted by adding 50 µl Buffer EB. The microfuge tubes were left to stand for 1 minute followed by centrifugation for 1 minute.

2.23.3 Restriction digest of plasmid DNA

Plasmid DNA pRS315 or pC210 was prepared as described in sections 2.10.4 and 2.12. pC210 vector DNA was digested with enzymes *Nde*1 and *Sph*1 in order to linearise the DNA and remove the *SSA1* gene. The reactions were as follows: 4 µg plasmid DNA, 5 µl Buffer 4 (NEB), 2U *Nde*1 (NEB), 2U *Sph*1 (NEB) and adjusted to 50 µl with molecular grade water. pRS315 vector DNA was digested with *Bam*H1 and the reactions were as follows: 4 µg plasmid DNA, 5 µl Buffer 2 (NEB), 2U *Bam*H1 (NEB) and adjusted to 50 µl with molecular grade water. The reactions were mixed in 1.5 ml microfuge tubes and incubated at 37^{o}C for 1 hour to allow digestion to occur. Following incubation, the mixtures were treated with 10U of Cip (NEB) per 1 mg of DNA and Buffer 3 (NEB) at a 10X concentration. The tubes were then incubated at 37^{o}C for 1 hour. Cip removes the phosphate groups at the ends of linear DNA. This prevents the plasmids from re-annealing.

2.23.4 Gel extraction and purification of plasmid DNA

Digested and Cip-treated vectors were analysed by agarose gel electrophoresis. This confirmed the size of the linearised vector and, in the case of pC210, that *SSA1* had been removed. The plasmids were excised from the gel under UV light using a clean scalpel. The pieces of gel were added to 1.5 ml microfuge tubes and weighed on a fine balance. If the agarose gel weighed more than 400 mg then it was split into two 1.5 ml microfuge tubes. Using a QIAGEN gel extraction kit, QG Buffer was added to the gels at a concentration of 100 µl per 100 mg of gel. The gels were then dissolved in the QG Buffer at 50^{o}C for 10 minutes. The dissolved samples were applied to QIAquick spin columns and centrifuged for 1 minute at 13000rpm. The flow-through was discarded and 750 µl Buffer PE was added to each column. The columns were centrifuged for 1 minute, flow-through discarded and centrifuged for an additional 1 minute. 50 µl of Buffer EB was added to the columns and left to stand for 1 minute. DNA was eluted by centrifugation for 1 minute. 3 µl of sample was analysed by agarose gel electrophoresis to confirm the presence of DNA.

2.23.5 Homologous recombination of vector and DNA fragment.

Prior to cloning, the exact DNA concentration of both vector and insert was calculated on a Nanodrop Spectrophotometer. Yeast cells were prepared for transformation as described in section 2.9. The cells acted as carriers for the cloning to occur. Four DNA samples were prepared as follows: (a) 700 ng insert/500 ng digested vector (b) 700 ng insert/500 ng undigested vector (c) 700 ng insert/H_2O (d) H_2O/500 ng digested vector. Each DNA mix was transformed into separate yeast cells as described in

section 2.9. The cells were selected on SC - leucine. Any colonies that grew on SC - leucine should have had an intact plasmid being expressed. For transformant (c) there were no colonies as it had no intact vector. Colony numbers were counted on transformants (a), (b) and (d). Sample (d) had digested vector so colonies were noted as being the amount of digested plasmids that had re-annealed. Sample (b) represented the number of colonies when 500 ng of intact vector was expressed. Colonies from cloning plate (a) were selected and plasmids extracted as described in section 2.11.2. Each plasmid was enzyme digested as described in section 2.23.3 and examined by agarose gel electrophoresis. Potential clones should have at least two DNA bands, one corresponding to the linearised vector and the other the size of the gene cloned. This depends on where and how often the enzyme cuts. Plasmids were sent to Agowa for sequencing to confirm the presence of the gene of interest. Figure 2.5 illustrates the methodology behind cloning by homologous recombination.

2.24 Western blot analysis

2.24.1 Preparing protein lysates

Yeast strains were grown overnight in 5 ml YPD at 30^{o}C shaking. They were diluted to an equal concentration of OD_{600nm} 0.1-0.2 in 25 ml YPD the following morning. The yeast cultures were incubated at 30^{o}C shaking until OD = 0.5-0.6 and centrifuged for 5 minutes at 2000rpm. 2 ml screw cap tubes (Starstedt) were ¾ filled with 0.5 mm glass beads and put on ice to chill. Each cell pellet was resuspended in 500 µl of Cell Lysis Buffer (Sigma) and transferred to the 2 ml tubes. The tubes were inverted to

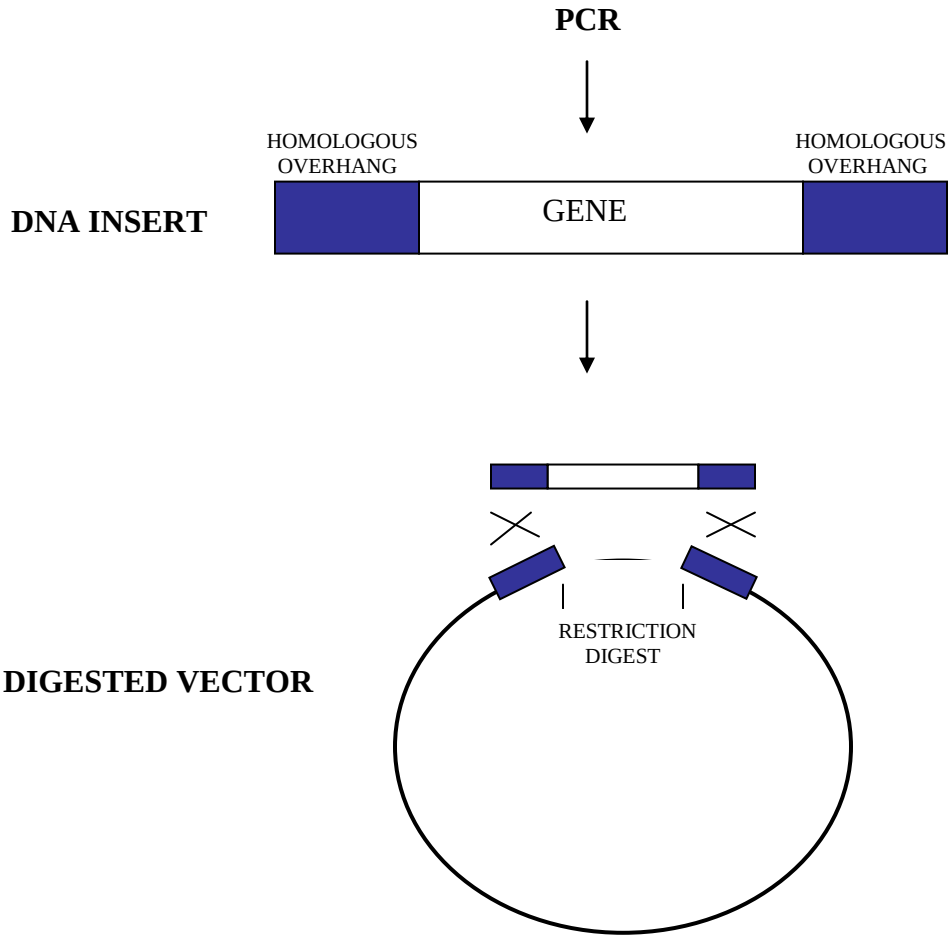

Figure 2.5. Schematic diagram of steps involved in cloning plasmid DNA by homologous recombination. DNA insert is created by PCR and contains overhangs homologous to plasmid vector DNA. Recombination occurs at the homologous regions and gene of interest is now expressed by the plasmid vector.

remove air bubbles and extra lysis buffer was added to fill the tubes. The cells were vortexed using a mini-bead beater for 20 seconds and incubated on ice for thirty seconds. This was repeated twice more to ensure that the cells were disrupted. The cells were centrifuged for 5 minutes at 7000rpm and the supernatants were transferred to sterile 1.5 ml microfuge tubes. The samples were either stored at -20^{o}C until further use or prepared

for gel electrophoresis. For running samples on polyacrylamide gels 60 µl of sample was mixed with 20 µl 4X Sample Buffer (Table 2.14) and incubated at 100^{o}C for 5 minutes.

2.24.2 Protein concentration determination

Protein concentration standard curves were prepared on a Nanodrop Spectrophotometer (nanodrop 1000, Mason) at OD_{595nm} by using several dilutions (0.125 µg-4000 µg/ml) of BSA (New England Biolabs). The BSA standard curves were saved and used to determine the protein concentration of various cell lysates.

The protein concentrations of cell lysates were quantified using the Bradford assay. This assay was originally developed by Marion Bradford (Bradford, 1976). Quickstart Bradford dye solution (Biorad) was allowed to warm at room temperature for 15 minutes and 1 ml was added to 1.5 ml microfuge tubes. 10 µl of lysate samples were added to Bradford reagent mixed well and incubated at room temperature for 5-30 minutes. Protein concentrations were read on the Nanodrop Spectrophotometer at OD_{595nm}. Bradford protein concentrations were determined against the BSA standard graphs.

2.24.3 Gel electrophoresis

Acrylamide gels were prepared using 1 mm BioRad glass plates with 15 well combs and 20 µl sample capacity. The components of the running gel and stacking gel are listed in Tables 2.15 and 2.16. The running gels were prepared first by mixing all the components in 15 ml falcon tubes. Polyacrylamide is a neurotoxin and was handled with care. While still liquid they were gently pipetted between two clean glass plates to

roughly a 70% capacity. The glass plates were sealed in a Biorad Gel Cassette and a Casting Frame. A few drops of 100% Isopropanol (Sigma) were added on top of the gels to allow them set smoothly. After 20-30 minutes the Isopropanol was removed, washed away with distilled water and the stacking gels were added between the two plates to 100% capacity. A comb was inserted between the glass plates and the gels were left to set for 30 minutes. The casting frames were assembled so that the short plates faced inward into the gel box and the clamping frames were sealed. The samples for electrophoresis were prepared by mixing the lysates with the Sample Buffer as described in section 2.24.1 and loaded directly into the gel at a concentration of 10 μg protein. 5 μl of prestained protein marker (NEB) was added alongside the samples. The gels were resolved in 1X Protein Gel Buffer (Table 2.19) at 100V per gel for 1.5 hours in a Biorad Mini-Protean3 Electrophoresis Module.

Table 2.14. Components in 4X Sample Buffer for Western blot analysis.

Buffer components	Final concentration/volume
Tris pH6.8	0.25 M
DTT	0.755 g
SDS	10%
Glycerol	50%
Bromophenol Blue	5 mg
Deionised water	adjusted to 10 ml

All components were purchased from Sigma.

Table 2.15. Volume of Buffers required for creation of one Resolving Gel.

Buffer components	12.75% Gel
Polyacrylamide (Invitrogen)	4.15 ml
10% Ammonium persulphate (Sigma)	100 µl
4X Gel Running Buffer	2.5 ml
TEMED (Sigma) (added last)	10 µl
Deionised water	3.3 ml

10% = 10 g Ammonium persulphate in final volume of 100 ml dH_2O.
Polyacrylamide is a carcinogen and needs to be handled with care.

Table 2.16. Volume of Buffers required for creation of one Stacking Gel.

Buffer components	12.75%
Polyacrylamide	0.4 ml
10% Ammonium persulphate	25 µl
2X Stacking Buffer	1.25 ml
TEMED (added last)	2.5 µl
Deionised water	0.825 ml

Table 2.17. Components of 10X Gel Running Buffer.

Buffer components	concentration
Tris	15 g
Glycine	72 g
SDS	5 g
Deionised water	adjusted to 500 ml

Table 2.18. Components of 2X Stacking Gel Buffer.

Buffer components	concentration
Tris	15 g
SDS	0.2 g
Deionised water	adjusted to 500 ml
pH 6.8	

Table 2.19. Components of 10X Protein Gel Buffer.

Buffer components	concentration
Tris	30.2 g
Glycine	18.8 g
10% SDS	100 ml
Deionised water	adjusted to 1000 ml

A 1X dilution of Protein Gel Buffer was made for resolving gels.

2.24.4 Gel transfer and blotting

After gel electrophoresis the plates were separated and the stacking gels removed. The gels were equilibrated in Transfer Buffer for 15 minutes (Transfer Buffer components in Table 2.20). PVDF transfer membrane paper (PerkinElmer) was cut at approximately the size of the gel (8cm x 5cm) and soaked in 100% Methanol (Sigma) for 5 seconds. The membranes were washed for 1 minute in water and 5 minutes in Transfer Buffer (Table 2.20). Whatmann paper (Schleicher and Schuell) was cut into 4 pieces approximately the same size as the gels and then soaked along with transfer sponges in Transfer Buffer. The Biorad gel Transfer system was assembled with sponges on the outside, two pieces of Whatmann paper either side, PVDF membrane on clear side of cassette (positive pole) and gel on top (negative pole). The system was locked, air bubbles removed and inserted into the blot chamber. The proteins that were separated in electrophoresis were transferred onto PVDF in Transfer Buffer at 100V for one hour.

PVDF blots were washed twice with TBS-t (Table 2.21) and 'blocked' in blocking solution (40 ml TBS-t with 2 g Marvel) for 1-2 hours at room temperature. The primary antibody was added to the blots in 5 ml TBS-t at a dilution of 1/2,000 for Hsp110 (Jeff Brodsky, University of Pittsburgh, USA) and Hsp70 (SPA-822) (Stressgen, Victoria, BC, Canada) antibodies and 1/150,000 for Hsp104 antibody (John Glover, University of Toronto). The blots were incubated with the primary antibody on a rocker (MSC) at room temperature overnight. The primary antibodies were washed off 3 times with TBS-t and the blots were incubated with a secondary antibody for 2 hours. The secondary antibodies were both alkaline phosphatase-conjugated and purchased from Sigma. They were goat anti-rabbit (Hsp104/Hsp110) or goat anti-mouse (Hsp70). They

were added to the blot in 5 ml of TBS-t at a 1/2000 dilution. The blots were washed 3 times with TBS-t prior to development.

Table 2.20. Components of 1X Transfer Buffer.

Buffer components	concentration
Tris	3.03 g (25 mM)
Glycine	14.4 g (192 mM)
Methanol	200 ml
Deionised water	adjusted to 1 litre

Table 2.21. Components of 10X TBS Buffer and 1X TBS-t.

Buffer components	concentration
10X TBS stock:	
Tris pH 7.5	12.14 g (100 mM)
NaCl	58.44 g (1 M)
Deionised water	adjusted to 1 litre
TBS-t :	
10X TBS Buffer	100 ml
Tween (Sigma)	1 ml
Deionised water	899 ml

2.24.5 Chemiluminescence and Western blot development

PVDF membranes were incubated with 2 ml CDP-Star Chemiluminescence reagent (Perkin Elmer) for 5 minutes. The membranes were transferred onto plastic overhead film and a piece of overhead was placed on top of each blot and bubbles or grooves were smoothed out. In a dark room the membranes were exposed to X-ray film (Kodak Biomax Ms) in an X-ray cassette for 30-60 seconds depending on the antibody used. The films were placed in 1/5 diluted Kodak Developer solution (Sigma) for 10 seconds, washed shortly with water and put in 1/5 diluted Kodak Fixer solution (Sigma) for 30 seconds. The films were washed thoroughly with water and allowed to dry.

2.24.6 Stripping membrane

Used PVDF membranes can be stripped of their antibodies and blotted again. This was performed if the development did not work sufficiently or if the same blot needed to be probed with a different antibody. The membranes were washed in water for 5 minutes and incubated in 200 mM NaOH (4 g NaOH in 500 ml dH_2O) (Sigma) for 5 minutes. The membranes were washed in water for 5 minutes and in TBS-t for 5 minutes. They were then blocked in blocking solution for 1 hour before incubating with primary antibody and following steps in section 2.24.4.

2.24.7 Staining membrane

To check for even protein loading the membranes were stained for 1 minute with amido black (0.1% naphthol blue black in 2% acetic acid and 45% MeOH) and destained for 1 hour in 2% acetic acid with 45% MeOH.

2.24.8 Staining gel

A gel replicate of each Western blot was stained after gel electrophoresis to show an even loading of protein. The staining solution was 0.1% Coomassie Brilliant Blue R250 in 25% EtOH /10% acetic acid and was left on the gels for 30-60 minutes. The gels were destained with 25% EtOH/10% acetic acid.

2.25 Sse1 3D crystal structure analysis

The Sse1 mutants were modeled onto the 3D crystal structure using the programme iMOL. Changing amino acid residues to examine their structural implications was done using MOE-Homology. MOE-Homology creates full-atom, energy-minimised 3D models of amino acid sequences. The underlying methodology is based on a combination of the segment-matching procedure of Levitt (1992) and an approach on the modeling of *indels* based on that of Fechteler *et al*. (1995).

2.26 G600 genome sequencing

2.26.1 Illumina library construction and sequencing

Genomic DNA was isolated from strain G600 using the standard protocol described in section 2.11.1. DNA libraries were generated using 1.5 μg of genomic DNA following the Illumina Genomic DNA sample preparation protocol with the exception that the samples were sheared using a bioruptor (Diagenode) instead of nebulisation. The samples were sonicated on high for 30 seconds and off for 30 seconds for a total 30 minutes with addition of ice after every 10 minutes to keep the samples cool. 16 pM of

the sequencing library was loaded onto a flowcell and single reads of 40 bases were generated using an Illumina GAII.

The images were processed into sequence data and aligned to the *S. cerevisiae* genome using the Illumina GA Pipeline v1.4. SNP detection and the generation of data to determine sequence coverage across the genome was performed with MAQ using the default settings. The Illumina quality scores were converted to the standard phred scores required by MAQ by using a modified version of the fq_all2std.pl script supplied with MAQ.

CHAPTER 3
ISOLATION AND CHARACTERISATION OF *sse1* MUTANTS THAT IMPAIR PRION PROPAGATION

3.0 Introduction

The aim of this Chapter was to gain insight into Hsp110's role in yeast prion propagation. A group of Hsp110 mutants were created, which were impaired in [*PSI*$^{+}$] propagation.

Yeast prions exploit cellular chaperones in order to maintain and replicate their aggregated state (Perrett and Jones, 2008). Heat shock proteins (Hsps) are a class of chaperones that are induced in response to cellular stress. Their normal function is in protein folding and disaggregation. However, prions like [*PSI*$^{+}$] are not refolded into their correct conformation but instead use Hsps to aid their propagation (Jones and Tuite, 2005).

Hsp110 is represented by the proteins Sse1 and Sse2 in yeast. The Sse1 protein is constitutively expressed whereas Sse2 is stress induced (Polier *et al*., 2008). The Hsp110 chaperone plays a critical role in yeast cellular physiology. Deletion of Sse1 results in slow-growing, temperature-sensitive cells and deletion of both Sse1 and Sse2 is lethal (Mukai *et al*., 1993; Shiryama *et al*., 1993; Shaner *et al*., 2006). Recent studies have shown that Hsp110 plays a role in yeast prion propagation (Fan *et al*., 2007; Kryndushkin and Wickner, 2007; Sadlish *et al*., 2008). Sadlish *et al*. (2008) demonstrated that deletion of Sse1 results in an increased amount of soluble Sup35 and that the presence of cytosolic Sse1 stimulates initial nucleation of Sup35 fibers. Sse1 interacts with the aggregated [*PSI*$^{+}$] form of Sup35 to a much greater extent than the [*psi*$^{-}$] version (Bagriantsev *et al*., 2008). These findings suggest that Sse1 plays an active role in [*PSI*$^{+}$] propagation.

Sse1 acts as a 'holdase' by binding denatured proteins (Oh *et al*., 1999). It has also been suggested that Sse1 binds aggregated polypeptides in order to present them to Hsp70 (Dragovic *et al*., 2006). Sse1 is a divergent member of the Hsp70

superfamily and it physically associates with the Hsp70 protein Ssa1 *in vivo*. Together Hsp110 and Hsp70 play a major role in the peptide binding cycle (Fan *et al*., 2007). The ATPase activity of Ssa1 (Hsp70) governs the binding and release of misfolded proteins. Sse1 acts as a nucleotide exchange factor (NEF) by removing ADP from Ssa1. This results in an 'open' Ssa1 conformation that rapidly binds and releases aggregated substrates and promotes [*PSI*$^{+}$] propagation (Shaner *et al*., 2006). Crystal structure studies and mutational analysis indicate that Hsp70 and Sse1 interact mainly at the nucleotide binding domains, but the whole length of the Sse1 protein structure is required for complex formation (Shaner *et al*., 2004; Dragovic *et al*., 2006). Polier *et al*. (2008) demonstrated the importance of Sse1 NEF activity by creating mutations at known Hsp70 binding sites. Mutants with severe reduction in NEF activity could not complement a Δ*sse1*Δ*sse2* deleted strain, while other mutants displayed temperature-sensitive phenotypes.

The main objective was to isolate a group of Sse1 mutants that are impaired in their ability to propagate [*PSI*$^{+}$] prion. Once Sse1 mutants were identified they were characterised according to their effects on [*PSI*$^{+}$]. This study helped in understanding the complexity of Sse1 and its role in prion propagation. It also revealed the importance of particular amino acid residues and how altering them can have negative effects on the function of Sse1.

3.1 Strategy used to isolate *sse1* mutants that impair [*PSI*$^{+}$] propagation

The plasmid shuffle technique was used to isolate *sse1* mutants (Figure 3.1). This strategy was previously used by Loovers *et al*. (2007) and Jones and Masison (2003) in isolating *ssa1* mutants that affect [*PSI*$^{+}$] propagation. The method,

described in section 2.16, involves mutating *SSE1* plasmid DNA with hydroxylamine and screening for mutants in an appropriate Δ*sse1*Δ*sse2* strain. Impairment to [*PSI*$^+$] propagation was measured subjectively, by the red/white colour assay, on medium with limiting adenine. The method for this measurement is described in section 2.13. The mutant [*PSI*$^+$] phenotypes were subsequently confirmed by growth on medium lacking adenine and mating with a [*psi*$^-$] strain.

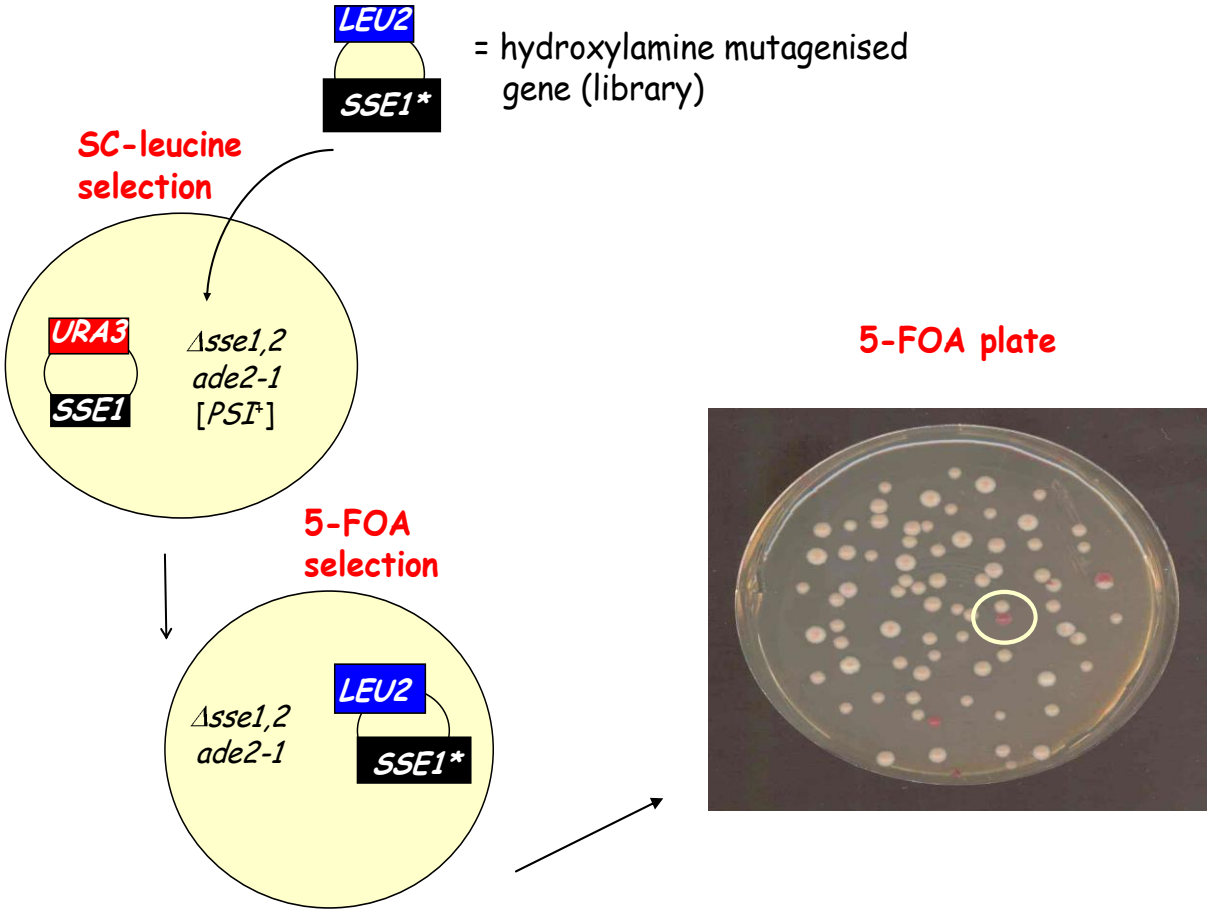

Figure 3.1. Proposed plasmid shuffle strategy to isolate *sse1* mutants that impair [*PSI*$^+$] propagation. pRS315*SSE1* was mutated with hydroxylamine and transformed into a Δ*sse1*Δ*sse2* strain. Medium containing 5-FOA selected for yeast with a *LEU2* marker plasmid and those with *URA3* plasmids were non-viable. *sse1* mutants were selected on rich medium with limiting adenine on the basis of their [*PSI*$^+$] colour phenotype.

3.2 Creating Δ*sse1*Δ*sse2* yeast strain CM02 for isolation of *sse1* mutants

Laboratory haploid yeast strains MYS101 (Δ*sse1*, *MAT***a**) and MYS105 (Δ*sse2*, *MAT*α) were mated on appropriate SD medium (strain genotypes available in Table 2.1). A copy of plasmid pRS316*SSE1* was transformed into the diploid strain. This enabled the selection of haploid Δ*sse1*Δ*sse2* cells after sporulation. The diploid cells were sporulated on minimal sporulation medium and random spore analysis was performed. Colonies were picked off and streaked onto SC - uracil medium (Figure 3.2.a) and replicated onto 5-FOA medium to select against any cells expressing pRS316*SSE1*. The colonies that were non-viable without pRS316*SSE1* were selected as potential Δ*sse1*Δ*sse2* haploid cells (Figure 3.2.b). Six potential Δ*sse1*Δ*sse2* strains were selected and their DNA isolated as described in section 2.11.1.

Diagnostic PCRs were performed using primers sse03, sse04, sse05, sse06, kan01 and kan02 (Table 2.12.a). The PCR cycles are described in Table 2.11. The PCR band sizes are annotated for the knockout constructs in Figure 3.3 for *sse1* and in Figure 3.5 for *sse2*. Figures 3.4 and 3.6 illustrate the diagnostic PCRs ran on 0.8% agarose gels. They represent PCRs performed on one isolated DNA sample GP2. The diagnostic gels illustrate that isolate GP2 had DNA bands equal in size to the kanamycin resistance gene, when primers that anneal upstream and downstream of *SSE1* and *SSE2* were used. The *sse1* and *sse2* knockouts were confirmed by PCR using primers that anneal internally to the *kanMX* gene and externally to the *SSE1*/*SSE2* gene. This strain was confirmed as haploid Δ*sse1*Δ*sse2* and designated CM02.

SC- uracil

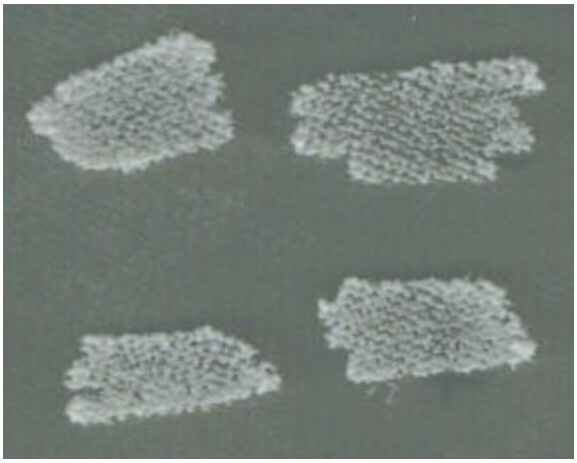

Figure 3.2.a. Growth of potential Δ*sse1*Δ*sse2* knockouts on SC - uracil. Random spore analysis results in haploid yeast cells with potential Δ*sse1*Δ*sse2* genotype. Colonies from random spore analysis were selected on SC - uracil medium, to maintain pRS316*SSE1* plasmid, and incubated at 30^{o}C for 2 days.

5-FOA

Figure 3.2.b. Replication onto 5-FOA resulted in colony lethality. Colonies from SC - uracil plate in Figure 3.2.a were replicated onto 5-FOA to select against pRS316*SSE1* plasmid. The plates were incubated at 30^{o}C for 2 days and colonies failed to grow. All four colonies were potential Δ*sse1*Δ*sse2* knockouts.

(1) Wild type

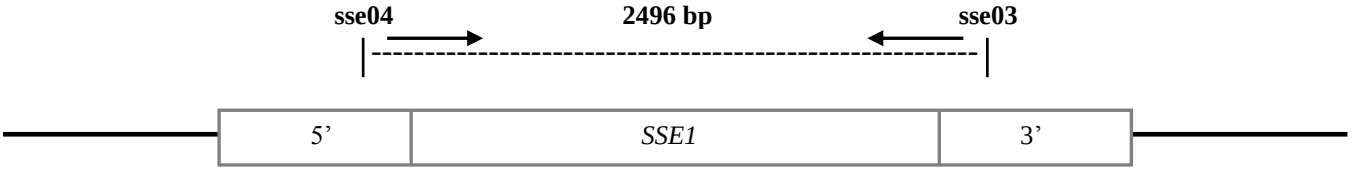

(2) Δ*sse1*

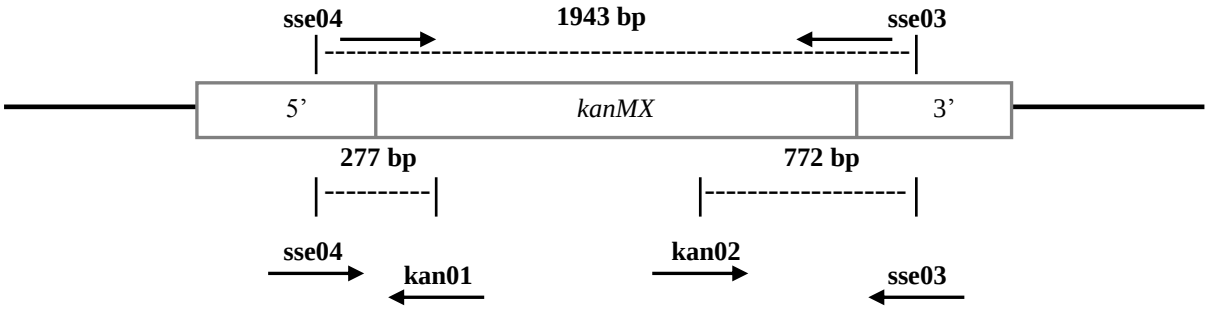

Figure 3.3. Illustration shows the expected wild type *SSE1* and Δ*sse1* PCR fragment sizes. (1) *SSE1* wild type DNA coding sequence is 2082 bp. Primers sse03R and sse04F are located upstream and downstream of the *SSE1* coding sequence. PCR using these primers should result in a DNA band of approximately 2496 bp. (2) illustrates an *sse1* knockout construct with *kanMX* gene replacing the coding sequence of *SSE1*. PCR using primers sse03R and sse04F should result in a band approximately 1943 bp in size. Internal kan01R and kan02F primers used with external sse03R and sse04F primers should result in two bands of 277 bp and 772 bp and confirms *SSE1* is replaced with *kanMX*.

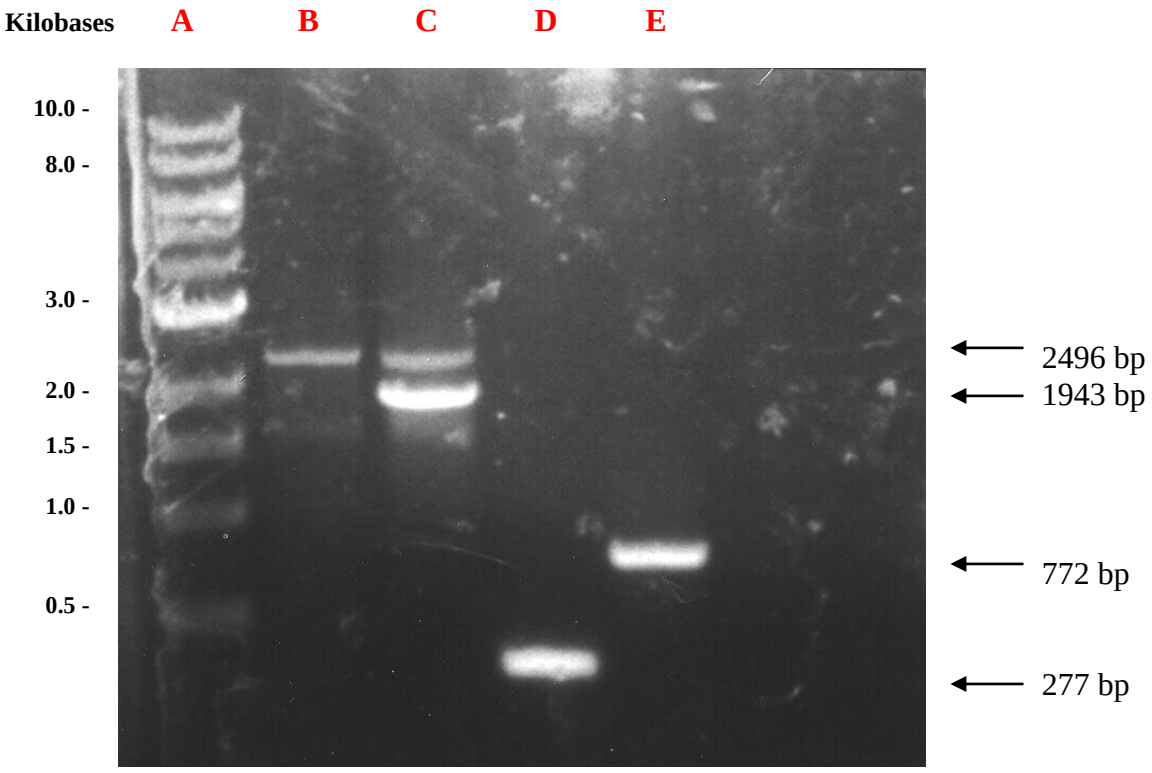

Figure 3.4. PCR confirmation of *sse1* knockout in strain CM02 by agarose gel electrophoresis. PCR represents DNA from sample GP2.

Lane A: 1kb molecular weight marker.

Lane B: G600 genomic DNA amplified with primers sse03 and sse04 results in a 2496 bp band for wild type *SSE1*.

Lane C: GP2 genomic DNA amplified with primers sse03 and sse04 results in two DNA bands. The 2496 bp band is wild type *SSE1* on pRS316 plasmid. The 1943 bp band is *kanMX* DNA replacing genomic *SSE1*.

Lane D: GP2 genomic DNA amplified with primers kan01 and sse04. The 277 bp band represents the left flanking region of *kanMX* knockout construct.

Lane E: GP2 genomic DNA amplified with primers kan02 and sse03. The 772 bp band represents the right flanking region of *kanMX* knockout construct.

(1) Wild type

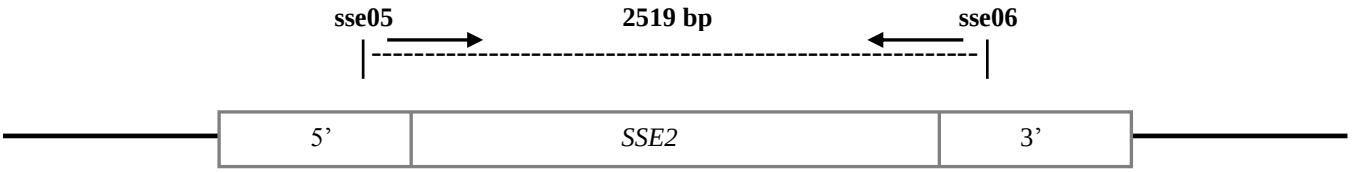

(2) Δ*sse2*

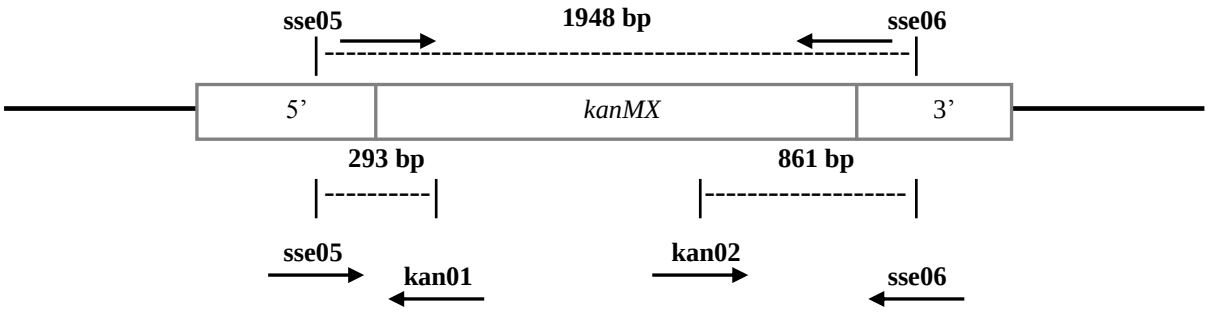

Figure 3.5. Illustration shows the expected wild type *SSE2* and Δ*sse2* PCR fragment sizes. (1) *SSE2* wild type DNA coding sequence is 2082 bp. Primers sse05F and sse06R are located upstream and downstream of the *SSE2* coding sequence. PCR using these primers should result in a DNA band of approximately 2519 bp. (2) illustrates an *sse2* knockout construct with *kanMX* gene replacing the coding sequence of *SSE2*. PCR using primers sse05F and sse06R should result in a band approximately 1948 bp in size. Internal kan01R and kan02F primers used with external sse05F and sse06R primers should result in two bands of 293 bp and 861 bp and confirms *SSE2* is replaced with *kanMX*.

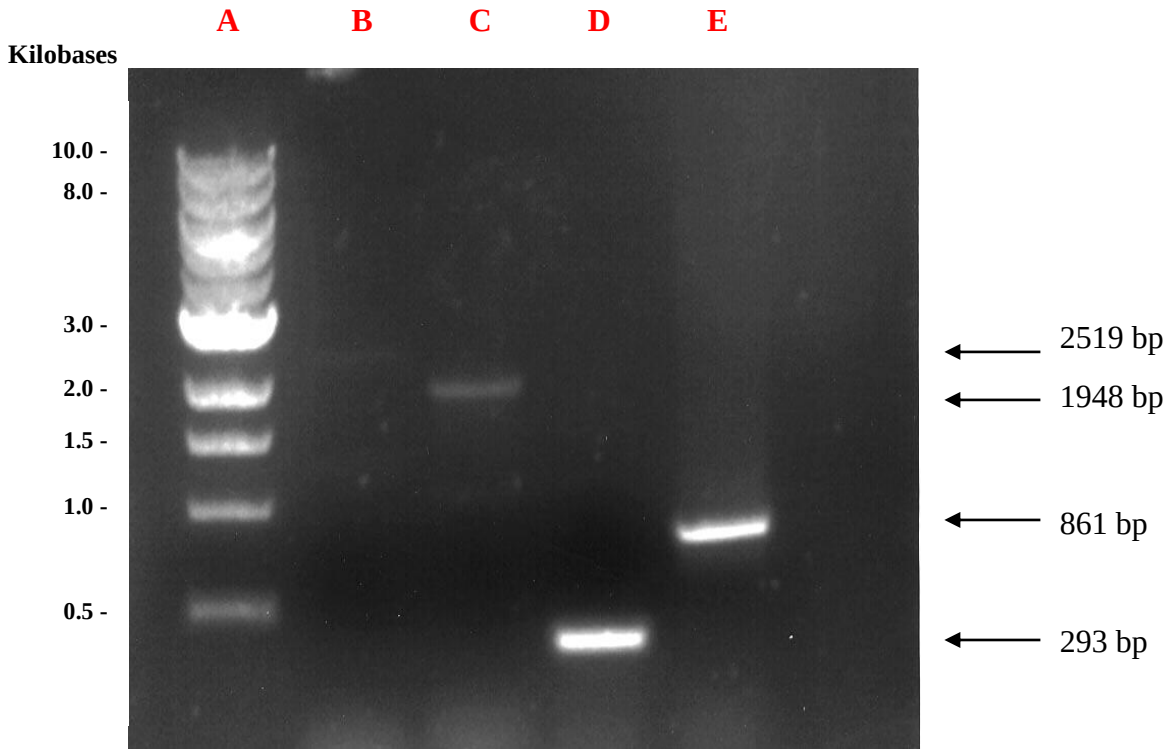

Figure 3.6. PCR confirmation of *sse2* knockout in strain CM02 by agarose gel electrophoresis. PCR represents DNA from sample GP2.

Lane A: 1kb molecular weight marker.

Lane B: G600 genomic DNA amplified with primers sseo5 and sse06 results in a 2519 bp band for wild type *SSE2*. Band is very faint but is there.

Lane C: GP2 genomic DNA amplified with primers sse05 and sse06 results in a 1948 bp band which is *kanMX* DNA replacing genomic *SSE2*.

Lane D: GP2 genomic DNA amplified with primers kan01 and sse05. The 293 bp band represents the left flanking region of *kanMX* knockout construct.

Lane E: GP2 genomic DNA amplified with primers kan02 and sse06. The 861 bp band represents the right flanking region of *kanMX* knockout construct.

3.3 Isolating *sse1* mutants with impaired [*PSI*$^{+}$] propagation

An *sse1* mutant library was created and transformed into CM02, along with positive and negative controls, as described in sections 2.15 and 2.16. Colonies that appeared dark pink or red on 5-FOA plates were selected as potential *sse1* mutants impaired in [*PSI*$^{+}$] propagation. From this primary screen eighty seven colonies were chosen (EP1-87). Subsequent plasmid isolation and transformation back into CM02 resulted in 30 plasmids exhibiting a reproducible phenotype. An example of this is in Figure 3.7.

3.4 Identifying amino acid changes in potential *sse1* mutants

Twenty nine potential *sse1* mutants were sent for sequencing after the secondary screen. *SSE1* sequencing primers used are listed in Table 2.13. The DNA sequencing results were compared to wild type *SSE1* DNA by BLAST analysis on NCBI. Seventeen *SSE1* plasmids had single amino acid changes and six plasmids had two amino acid changes. One *SSE1* plasmid came back having more than two mutations and five came back as wild type *SSE1*. Plasmids that were identified as WT *SSE1* but appeared [*psi*$^{-}$] may have mutations in the promoter or terminator sequence, but these plasmids were not analysed any further. The fact that some single mutations were isolated more than once suggests the screen was approaching saturation (Table 3.1 and 3.2). Figure 3.8 illustrates the position of thirteen single amino acid change mutants on the linear structure of Sse1.

CM02 + *SSE1*

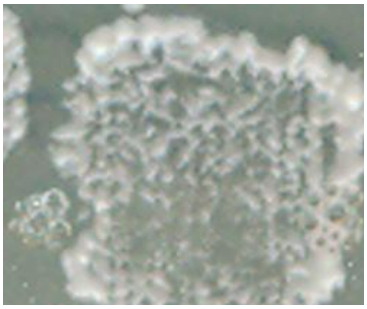

CM02 + pRS315

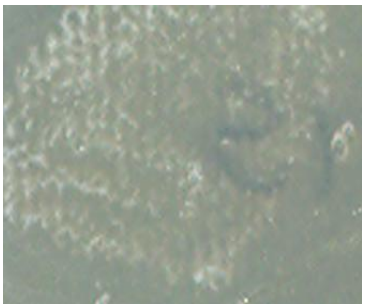

CM02 + EP56

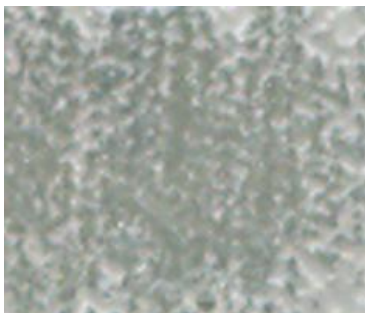

CM02 + EP57

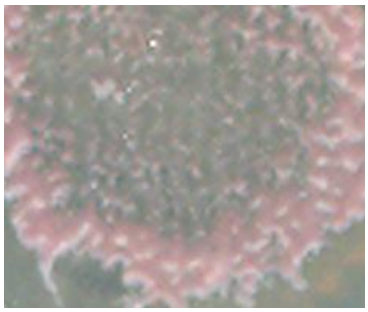

Figure 3.7. 5-FOA selection of *sse1* mutants in the secondary screen. Individual plasmids were isolated from selected colonies (EP1-87) in the primary screen and transformed back into CM02. Colony EP56 was picked in the first screen as [*psi*$^-$] however it appears [*PSI*$^+$] in the secondary screen. Colonies such as EP57 remained dark pink and were selected as potential [*psi*$^-$] mutants.

Table 3.1. *SSE1* plasmids isolated with single mutations.

PLASMID NAME	*SSE1* NUCLEOTIDE CHANGE	AMINO ACID CHANGE	TIMES ISOLATED
EP14	1028. G – A	G343D	1
EP25	1025. G – A	G342D	1
EP26	1108. G – A	E370K	1
EP33	706. G – A	D236N	1
EP39	1319. C – T	S440L	1
EP42	1372. C – T	Q458*	1
EP46	1094. C – T	T365I	1
EP49	122. G – A	G41D	3
EP50	122. G – A	G41D	3
EP51	110. C – T	P37L	1
EP55	1510. G – A	E504K	1
EP59	149. G – A	G50D	2
EP61	122. G – A	G41D	3
EP62	149. G – A	G50D	2
EP65	1660. G – A	E554K	1
EP68	1847. G – A	G616D	1
EP77	632. G - A	C211Y	1

This table illustrates their nucleotide change and corresponding amino acid change. Some mutants have appeared more than once indicating that the screen is approaching saturation.

Table 3.2. *SSE1* plasmids isolated with multiple mutations.

PLASMID NAME	*SSE1* NUCLEOTIDE CHANGE	AMINO ACID CHANGE	TIMES ISOLATED
EP3	88. G – A 1310. G – A	E30K G437D	1
EP54	149. G – A 151. G – A	G50D E51K	1
EP60	1025. G – A 1409. C – T	G342D P470L	1
EP66	809. G – T 1024. G – C	A270V G342R	2
EP67	1025. G – A 1411. G – A 1415. G – T	G342D E471K G472D	1
EP70	809. G – T 1024. G – C	A270V G342R	2
EP72	1372. C – T 1707. C – G	Q458* D569E	1

This table illustrates their nucleotide changes and corresponding amino acid changes. Some mutations from Table 3.1 appear in these isolates e.g. G50D, G342D and Q458*. It is difficult to determine which mutation is causing the [*psi*$^-$] phenotype when there is more than one present. Mutants found in this table were not included in any subsequent work.

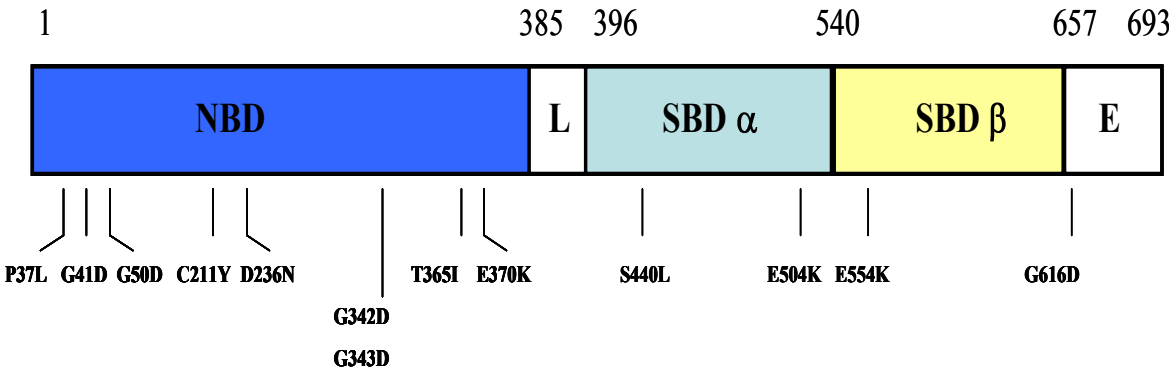

Figure 3.8. Thirteen single amino acid change mutants were identified in the screen. These mutants are located in various domains of Sse1. Sse1 is composed of a nucleotide binding domain (NBD), substrate binding domain (SBD), a linker (L) and a C-terminus extension (E).

3.5 Phenotypic analysis of Sse1 mutants

[*PSI*$^+$] phenotypes were assessed in each Sse1 mutant by their colour on limiting adenine medium and ability to grow on medium lacking adenine (as described in section 2.13). In Figure 3.9 the varying [*PSI*$^+$] phenotypes were observed after 2 days incubation at 30^{o}C, followed by 2 days at room temperature. WT Sse1 did appear [*PSI*$^+$] but had small hints of pink. However, all mutants had a weaker [*PSI*$^+$] phenotype than wild type as they were pink/red in colour. Mutants such as P37L and C211Y were pink on YPD so have some degree of [*PSI*$^+$] present. However, mutants G342D, D236N and G616D were completely [*psi*$^-$]. The position of the mutation and the specific amino acid change seems to have different effects on the ability of [*PSI*$^+$] to propagate.

In Figure 3.10 wild type Sse1 grows well on SC - adenine. However all the mutants struggled to grow after two days incubation at 30^{o}C. When mutants P37L, C211Y, G343D, and E504K were subsequently left at room temperature for 5 days they showed a small amount of growth. It was expected to see growth on SC – adenine for [*PSI*$^+$] weak mutants such as P37L and C211Y as they may contain some

non-functional Sup35 that allows readthrough of *ade2.1*. To further test their [*PSI*$^+$] phenotype the Sse1 mutants were mated with [*psi*$^-$] G621 and mutants P37L, C211Y, G343D, E504K and E554K all had some [*PSI*$^+$] present as the diploids demonstrated a white/pink colour (data not shown).

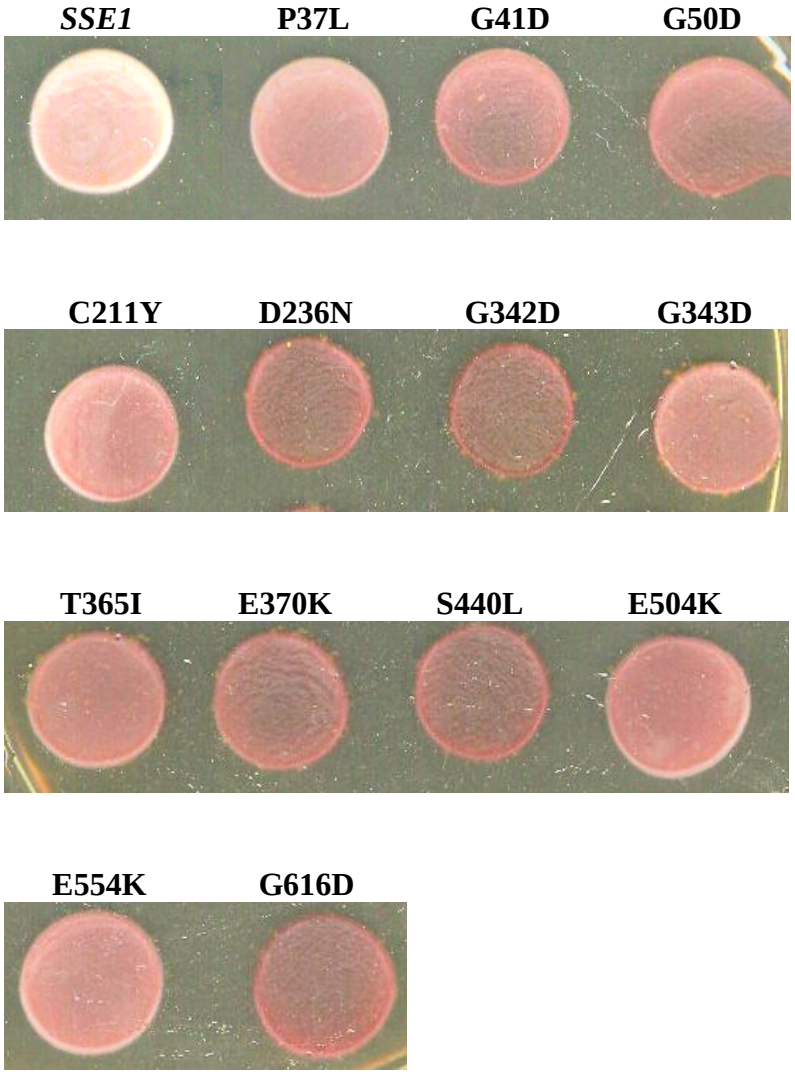

Figure 3.9. [*PSI*$^+$] colour phenotype of Sse1 mutants on YPD. 10 µl spots were placed onto YPD and incubated at 30^{o}C for 2 days. This was followed by an additional 2 days at room temperature.

Figure 3.10. Growth of Sse1 mutants on medium lacking adenine. 10 μl spots of each mutant was placed onto SC - adenine medium and incubated at 30^{o}C for 2 days. WT Sse1 grew well however the mutants struggled to grow. The plates were left at room temperature for another 5 days and some growth was visible for mutants P37L, C211Y, G343D, E504K and E554K.

In order to further characterise the Sse1 mutants they were subjectively scored by their red/white colours. This method has been used by others (Jones and Masison 2003; Loovers *et al*., 2007) and involves assigning each mutant a colour score according to a weak or strong [*PSI*$^{+}$] phenotype. All thirteen mutants were assessed in the presence of wild type *SSE1* (pre-FOA) and their expression alone in

the cell (post-FOA). This also helped confirm whether any of the mutants had a dominant effect over wild type *SSE1*. [*PSI*$^{+}$] (white) cells were scored as 0. Cells that were completely [*psi*$^{-}$] (dark red) were scored as 10. Any colour between white and red was scored subjectively between 0 and 10. Table 3.3 summarises the results of this assessment. The *sse1* mutants showed varying degrees of dominance as they all scored above 0 in pre-FOA analysis indicating that they have some ability to weaken [*PSI*$^{+}$] propagation in the presence of WT *SSE1*. The mutants which scored as 7-9 in post-FOA analysis were also considered [*psi*$^{-}$] as there were variations in the degree of shading.

3.6 Analysis of the effects of Sse1 mutants on [*URE3*] propagation

[*URE3*] is another well characterised yeast prion. It is the amyloid form of the Ure2 protein. Ure2 plays a role in regulating nitrogen metabolism (Lian *et al*., 2006). Like [*PSI*$^{+}$], the propagation of [*URE3*] is highly dependent on molecular chaperones. Recently, it was discovered that both over-expression and deletion of *SSE1* disrupts [*URE3*] propagation (Kryndushkin and Wickner, 2007).

In order to investigate whether the *sse1* mutants could alter the propagation of [*URE3*] the yeast strain SB34 (Bach *et al*., 2003) was transformed with each mutant, WT Sse1 and a negative control. At least 100 colonies were scored for each mutant as being white, red or sectored (Figure 3.11.a/b.). SB34 contains wild type Sse1 and Sse2 so any changes to [*URE3*] propagation came from a dominant effect exerted by the mutant (Loovers *et al*., 2007).

Table 3.3. Colour score for Sse1 mutants, according to their [*PSI*$^+$] phenotype.

SSE1 mutation	Times isolated	Colour pre-FOA	Colour post-FOA
None	-	0	0
P37L	1	3	5
G41D	3	4	8
G50D	3	5	8
C211Y	1	4	5
D236N	1	6	10
G342D	3	4	10
G343D	1	4	6
T365I	1	4	7
E370K	1	3	9
S440L	1	3	10
E504K	1	3	6
E554K	2	3	5
G616D	1	3	10

Assessment was carried out of mutants both in the presence of WT *SSE1* (pre-FOA) and mutants alone (post-FOA). Mutants G342D, E370K and G616D were scored as completely [*psi*$^-$]. Although WT Sse1 has shadings of pink it was assigned a 0 for comparative purposes.

Scale: 0 = white ([*PSI*$^+$])
10 = dark red ([*psi*$^-$])

(i) pRS315

(ii) pRS315*SSE1*

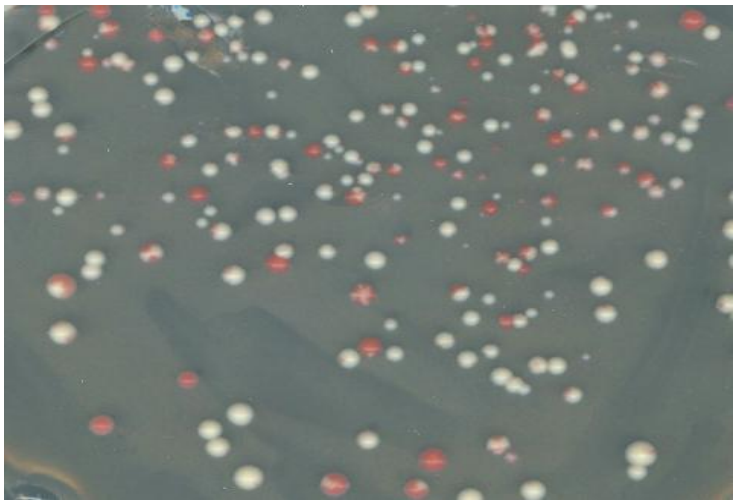

Figure 3.11.a. SB34 transformed with (i) pRS315 and (ii) pRS315*SSE1*. Transformants were selected on SC - leucine medium and incubated for 2 days at 30^{o}C. Each transformation was done in triplicate. The colonies were counted and scored as red, white or sectored. The presence of an extra copy of *SSE1* (ii) greatly inhibits [*URE3*] propagation compared to (i) SB34 with an empty vector.

(i) pRS315*SSE1*

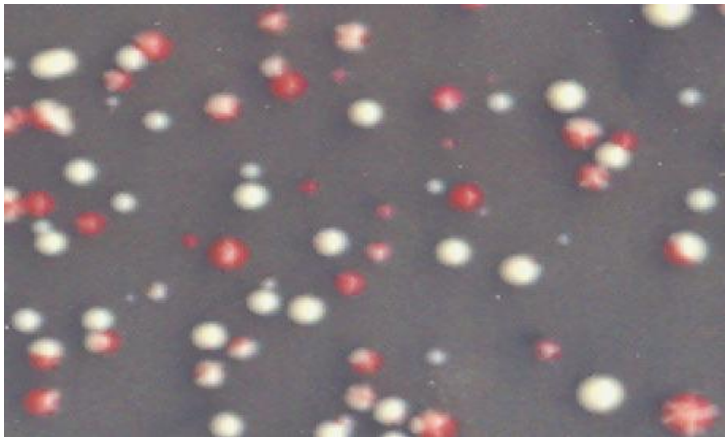

(ii) pRS315*SSE1*^{E370K}

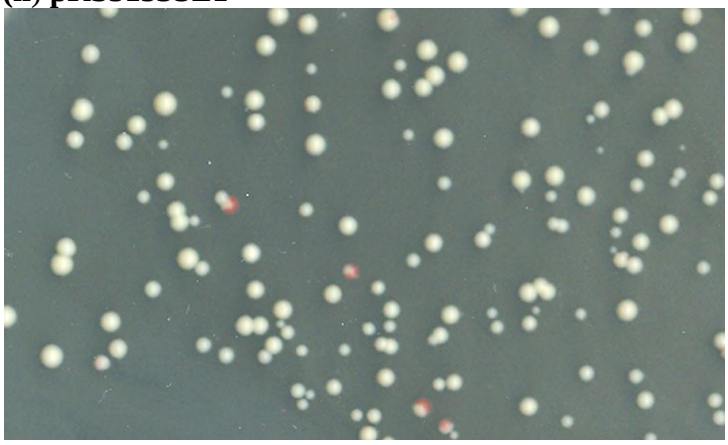

(iii) pRS315*SSE1*^{G616D}

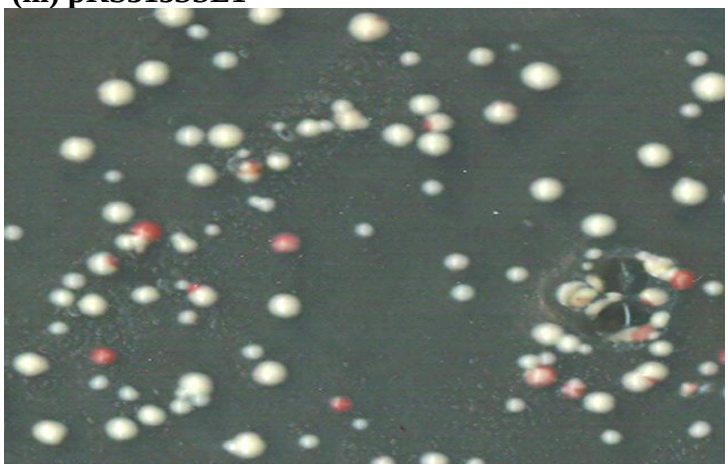

Figure 3.11.b. SB34 transformed with (i) pRS315*SSE1* (ii) pRS315*SSE1*^{E370K} and (iii) pRS315*SSE1*^{G616D}. Transformants were selected on SC - leucine medium and incubated at 30^{o}C for 2 days. Each transformation was repeated in triplicate. The colonies were counted and scored as red, white or sectored. Wild type *SSE1* over-expression inhibits [*URE3*] propagation greater than any of the mutants. The experiment was repeated for all thirteen mutants.

It was hypothesised that if the Sse1 mutants were fully functional, they would disrupt [*URE3*] propagation in a similar manner to wild type Sse1. However, in contrast to wild type Sse1 the mutants had no major effect on [*URE3*] stability (Table 3.4.). The Sse1 mutants with the least effect on [*URE3*] propagation were G41D, D236N and G342D. The Sse1 mutants were demonstrating a dominant negative expression over WT Sse1. They showed phenotypes similar to SB34 transformed with an empty vector control. [*URE3*] propagation is more unstable than [PSI^+] and wild type colonies tend to spontaneously lose [*URE3*] at a greater frequency.

3.7 Can over-expression of the protein Fes1 compensate for loss of Sse1 function in Δ*sse1*Δ*sse2* cells or *sse1* mutants?

Fes1 is a yeast cytosolic protein that shares functional similarity with Sse1. Fes1 was first characterised by Kabani *et al*. (2002). They discovered that Fes1 associates with the ADP-bound form of Ssa1 protein and promotes nucleotide release. Like Sse1, deletion of Fes1 weakens [PSI^+] propagation and the over-expression of Fes1 promotes [PSI^+] (Jones *et al*., 2004). Fes1 may also play a role in cellular thermostability as Δ*fes1* results in cells that are sensitive to high temperatures (Kabani *et al*., 2002). However differences do exist between these two nucleotide exchange factors (NEFs). In a genome-wide screen, Sse1 was found associated with many Hsp70-Hsp90-substrate complexes whereas Fes1 was notably absent (Zhao *et al*., 2005). Sse1 is more potent than Fes1 as a NEF as Sse1 accelerates ADP release from Ssa1 by 81 fold compared to only 8 fold by Fes1 (Raviol *et al*., 2006b; Sadlish *et al*., 2008). Since Fes1 and Sse1 share some functional characteristics it was aimed to see what influence Fes1 would have on growth and [PSI^+] propagation in the Sse1 strains.

Table 3.4. The relative effects of *sse1* mutants on [*URE3*] propagation.

MUTATION	% WHITE COLONIES	% RED COLONIES	% SECTORED[a]
WT	48	13	39
EMPTY VECTOR	96	2	2
P37L	90	3	7
G41D	96	1	3
G50D	94	4	2
C211Y	92	3	5
D236N	98	1	1
G342D	95	2	3
G343D	84	7	9
T365I	84	11	5
E370K	94	2	4
S440L	87	5	8
E504K	87	4	9
E554K	86	4	10
G616D	83	4	13

At least 100 colonies were counted and scored as red, white or sectored* for each mutant.

[a] Sectored colonies are colonies loosing [*URE3*] at various stages of development.

3.7.1 Fes1 overproduction cannot recover the Δ*sse1*Δ*sse2* non-viable phenotype in CM02

The deletion of both *sse1* and *sse2* renders cells non-viable and it is the loss of NEF activity responsible for this phenotype (Shaner *et al*., 2006; Polier *et al*., 2008). There is conflicting evidence as to whether Fes1 overproduction can compensate for the loss of both *sse1* and *sse2* (Raviol *et al*., 2006b; Sadlish *et al*., 2008). Raviol *et al*. (2006b) concluded that Fes1 only provides 'partial recovery' for Δ*sse1*Δ*sse2* cells, while Sadlish *et al*. (2008) found that incorporating an extra copy of *FES1* into the cell completely restores cell viability. This hypothesis was tested and resulted in no growth in strain CM02 Δ*sse1*Δ*sse2* transformed with plasmid pRS423*FES1* (Figure 3.12). Fes1 complementation is analysed further in Chapter 4 where it is over-expressed in a BY4741 background.

(a) pRS423 **(b) pRS423*FES1***

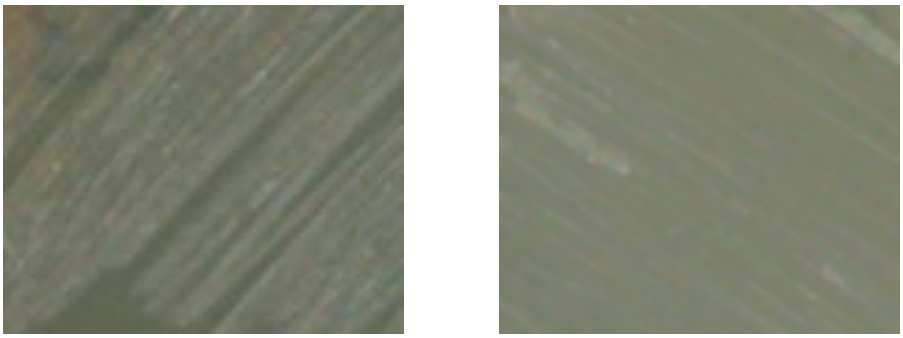

Figure 3.12. Analysis of Δ*sse1*Δ*sse2* growth recovery when *FES1* is over-expressed. Strain CM02 was transformed with (a) pRS423 and (b) pRS423*FES1*. The cells were selected on 5-FOA, to remove WT *SSE1*, and incubated at 30^{o}C for 2 days. (b) Over-expression of Fes1 does not recover a Δ*sse1*Δ*sse2* lethal phenotype in CM02.

3.7.2 Assessment of the effects of Fes1 over-expression on Sse1 mutant [*PSI*$^+$] phenotypes

It is unclear how the Sse1 mutants isolated in this screen are affecting [*PSI*$^+$] propagation. There is a possibility that some impair Sse1 NEF activity. Studies by Jones *et al*. (2004) showed that an Ssa1-21 mutant strain propagated [*PSI*$^+$] better when Fes1 protein was overproduced. The aim of this section was to investigate whether Fes1 could improve [*PSI*$^+$] in any of the Sse1 mutant strains.

CM02 was transformed with both pRS423 and pRS423*FES1* high copy plasmids, and selected on SC - histidine medium. Both strains were then transformed with WT *SSE1* and each of the thirteen *sse1* mutants and selected on SC - leucine - histidine medium. The cells were replicated onto 5-FOA to select against pRS316*SSE1*. Figure 3.13.a/b illustrates the phenotypic results of this test. The only Sse1 mutant with an improved [*PSI*$^+$] phenotype was G616D, as assessed by colour. There is a possibility that this mutant could disrupt Sse1 NEF activity, a function shared by both Sse1 and Fes1. The overall [*PSI*$^+$] phenotype of all the mutants appeared stronger in this experiment compared to in Figure 3.9.

Each strain was also grown on medium lacking adenine to determine if [*PSI*$^+$] was present (Figure 3.14). Sse1 mutant G616D showed only slight improved growth in the presence of pRS423*FES1* and some mutants seemed to grow better in the presence of control plasmid pRS423. The overall growth of the mutants on medium lacking adenine seemed greater than those observed in Figure 3.10.

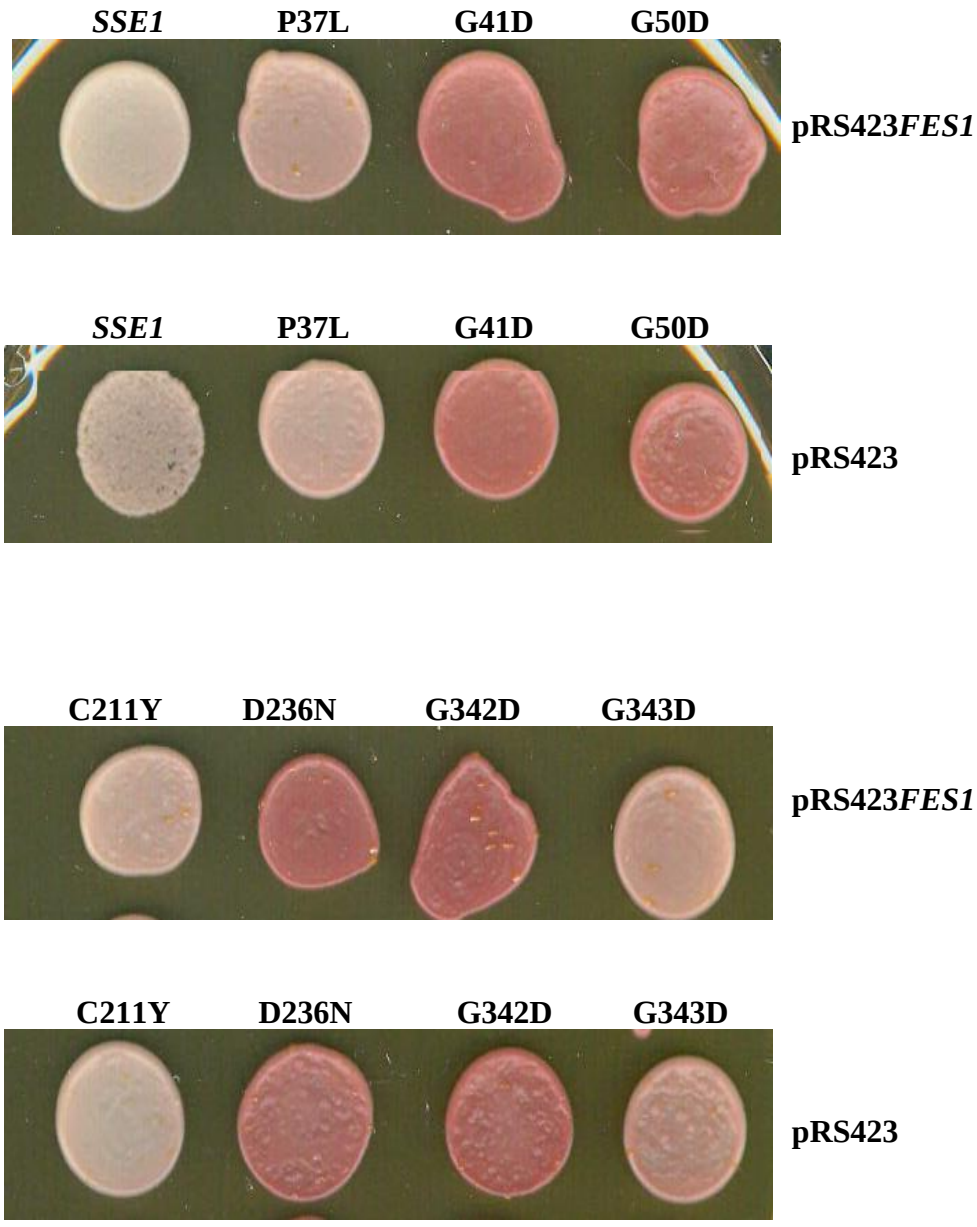

Figure 3.13.a. Analysis of *sse1* mutant [*PSI*$^{+}$] phenotypes when *FES1* is over-expressed. CM02 was first transformed with pRS423 and pRS423*FES1* followed by transformation of *sse1* mutants. Transformants were selected on SC - leucine - histidine medium and selected on 5-FOA to remove WT *SSE1*. 10 µl spots of each strain was placed onto YPD followed by 2 days incubation at 30^{o}C and 2 days at room temperature.

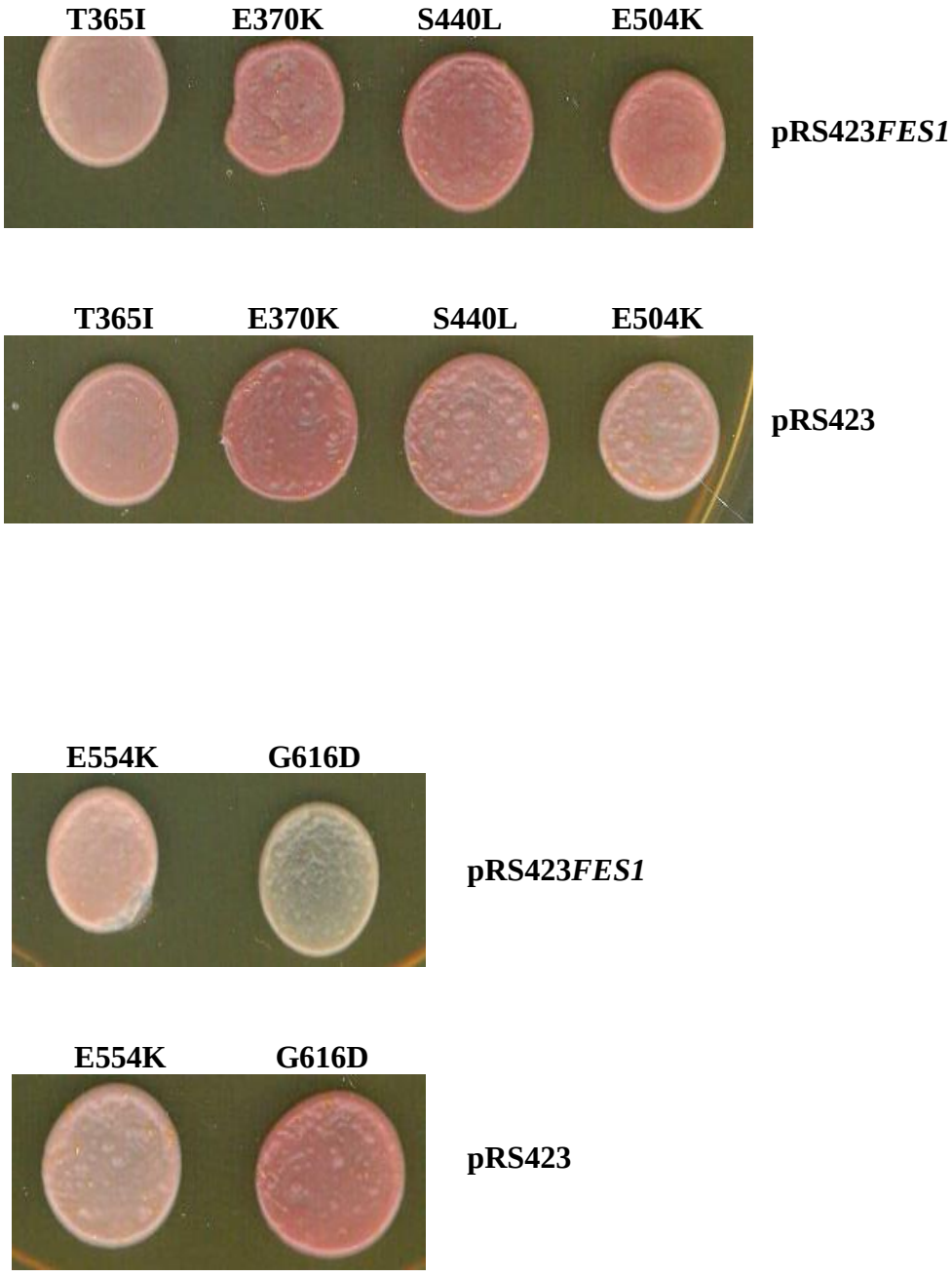

Figure 3.13.b. Analysis of *sse1* mutant [*PSI*$^+$] phenotypes when *FES1* is over-expressed. CM02 was first transformed with pRS423 and pRS423*FES1* followed by transformation of *sse1* mutants. Transformants were selected on SC - leucine - histidine medium and selected on 5-FOA to remove WT *SSE1*. 10 µl spots of each strain was placed onto YPD followed by 2 days incubation at 30^{o}C and 2 days at room temperature. Mutant G616D shows an improved [*PSI*$^+$] status in the presence of pRS423*FES1*.

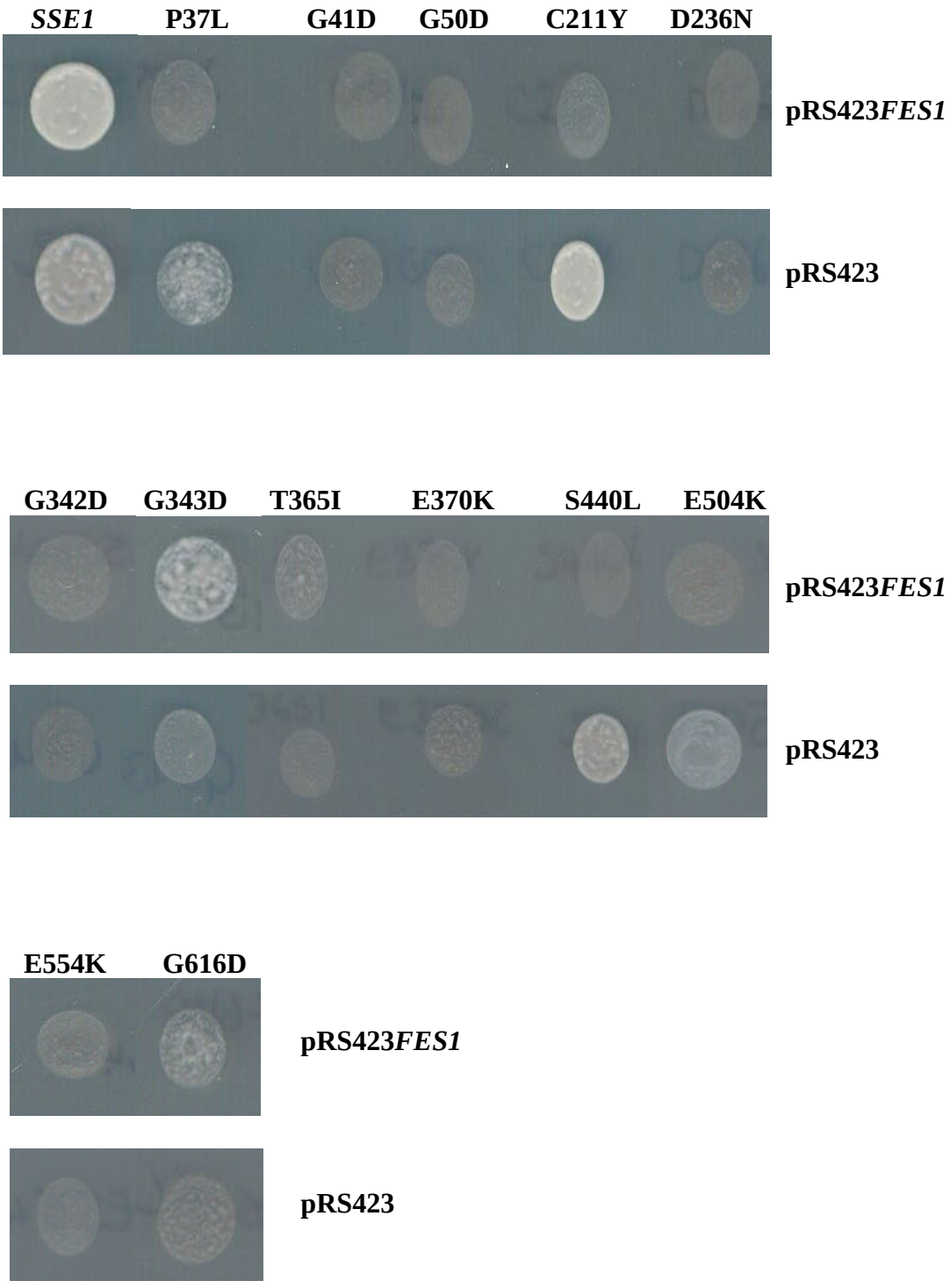

Figure 3.14. Analysis of *sse1* mutant growth on SC - adenine medium when *FES1* is over-expressed**.** Strains from Figure 3.13 were spotted (in 10 µl dH_2O) onto SC - adenine - histidine and incubated at 30^{o}C for 2 days. There was no great improvement in mutant [*PSI*$^{+}$] phenotypes in the presence of pRS423*FES1*. Slight improvement was seen for G343D and G616D.

3.8 Can a human Sse1 homolog complement deletion in a yeast strain?

The human genome contains four Hsp110 stress responsive genes designated *HSPH1* (Hsp110), *HSPH2* (APG-2), *HSPH3* (APG-1) and *HSPH4* (Grp170) (Vos *et al*., 2008; Kampinga *et al*., 2009). Mammalian HSPH1 and yeast Sse1 share general structural similarity and are both divergent members of the Hsp70 superfamily (Easton *et al*., 2000; Raviol *et al*., 2006a).

HSPH1, also known as Hsp110, has nucleotide exchange factor (NEF) function for mammalian Hsp70 and it is distantly related to yeast Sse1. NEF activity seems to be a conserved function amongst all Hsp110 homologs (Dragovic *et al*., 2006).

Studies by Oh *et al*. (1997) showed that the over-expression of mammalian Hsp110 in mammalian cell lines provided significant protection from heat stress. Hsp110 may also function as a protein disaggregase in mammals either by directly interacting with aggregates or indirectly through Hsp70 activity (Yamagishi *et al*., 2003). *In vitro* studies have shown that Hsp110 is very efficient at recognising and maintaining heat denatured proteins such as luciferase and presenting them to Hsp70 (Oh *et al*., 1997; Oh *et al*., 1999). This is why mammalian and yeast Hsp110 are often referred to as 'holdases' (Shaner *et al*., 2005).

Hsp110 is quite a heterogenous family of proteins since mammalian Hsp110 cannot compensate for Sse1 function *in vivo* (Shaner *et al*., 2004). Since HSPH1 and Sse1 share functional similarities it was aimed to see whether HSPH1 could compensate for loss of Sse1 and Sse2 in yeast strain CM02.

3.8.1 Cloning human *HSPH1* into vector pC210

HSPH1 (Hsp110) cDNA was purchased from ORIGENE and the coding sequence was amplified by PCR using primers HSPH1F/R listed in Table 2.12.b and PCR cycle 2 in Table 2.11. The PCR product was cloned into vector pC210, under the *SSA2* promoter, as described in section 2.23. Four potential clones were isolated for further analysis. A diagnostic digest using restriction enzyme *Nde*1 confirmed that one isolate was pC210*HSPH1* (Figure 3.15). The plasmid DNA was sent for sequence analysis to further verify that *HSPH1* was successfully cloned. Figure 3.16 illustrates the protein sequence similarities between yeast Sse1 and mammalian HSPH1 and Figure 3.17 illustrates the plasmid construct of pC210*HSPH1*.

3.8.2 Complementing CM02 Δ*sse1*Δ*sse2* with pC210*HSPH1*

HSPH1 did not complement Δ*sse1*Δ*sse2* in CM02 (Figure 3.18). This result concurs with Shaner *et al*. (2004) who stated that the mammalian Hsp110 isoform HSPH1 can not complement the deletion of both *sse1* and *sse2* in yeast. It can be speculated as to why it did not complement the loss of yeast Hsp110. Perhaps it can not provide yeast with essential Sse1 functions or HSPH1 may be too divergent to function in a yeast system. In Chapter 4 this plasmid construct is tested in a different strain background.

(i) pC210-*HSPH1* construct digested with *Nde*1 enzyme

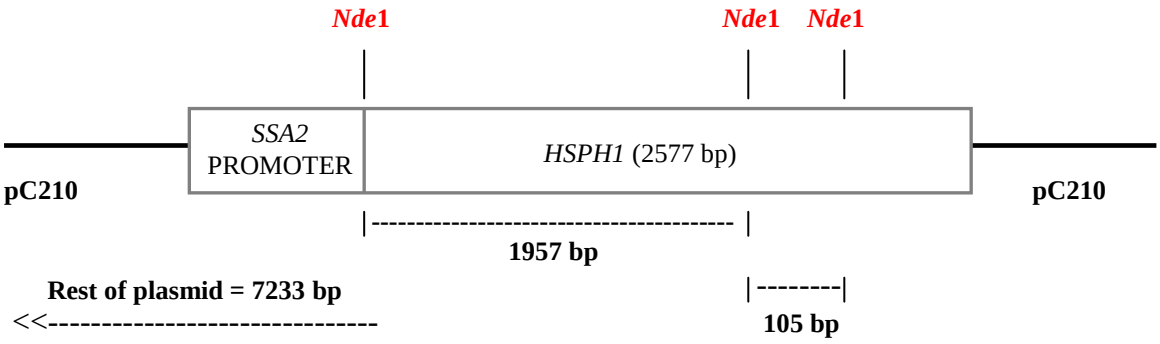

(ii) Agarose gel electrophoresis of digested vectors

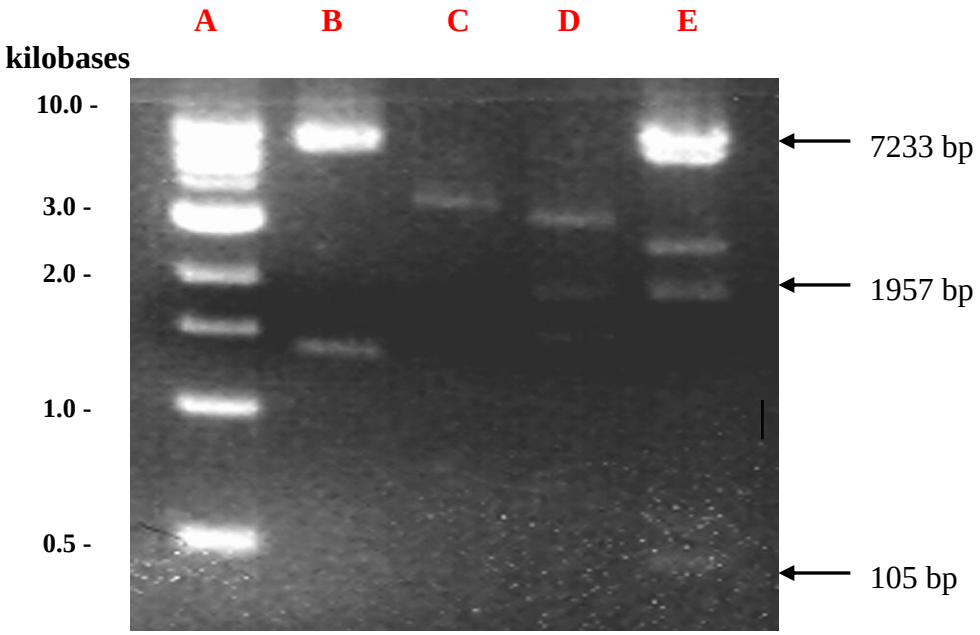

Figure 3.15. Diagnostic restriction digests of potential pC210-*HSPH1* constructs**.**

(i) pC210-*HSPH1* construct with expected base pair sizes after restriction digest with *Nde*1. *Nde*1 cuts *HSPH1* internally twice at position 1956 and 2061. *Nde*1 also cuts plasmid pC210 at end of the promoter region. These three cuts should result in three bands at 7233 bp, 1957 bp and 105 bp.

(ii) Agarose gel shows diagnostic restriction digest of four potential *HSPH1* clones.
Lane A: 1kb molecular weight marker.
Lane B-D: Potential clones 1-3 were digested with *Nde*1. Gel electrophoresis shows DNA bands that do not correspond to a *HSPH1* clone.
Lane E: Three DNA bands were visible for clone 4 that equate to the expected sizes. The extra band visible at approximately 2500 bp is unknown, it is possibly un-ligated vector. Clone 4 was sent for sequencing and confirmed that *HSPH1* was cloned in.

```
1   MSTPFGLDLGNNNSVLAVARNRGIDIVVNEVSNRSTPSVVGFGPKNRYLG
    ||. .|||:|:.:..:||||..||:.:.||.|:|.||||:.||.|||.:|
1   MSV-VGLDVGSQSCYIAVARAGGIETIANEFSDRCTPSVISFGSKNRTIG

51  ETGKNKQTSNIKNTVANLKRIIGLDYHHPDFEQESKHFTSKLVELDDKKT
    ...||:|.:::..|||:|.||..|..::.|..::|.::.:..||.|.:...
50  VAAKNQQITHANNTVSNFKRFHGRAFNDPFIQKEKENLSYDLVPLKNGGV

101 GAEVRFAGEKHVFSATQLAAMFIDKVKDTVKQDTKANITDVCIAVPPWYT
    |.:|.:.||:|:||..|:.||.:.|:|:|.:...|..:||..|:||.::|
100 GIKVMYMGEEHLFSVEQITAMLLTKLKETAENSLKKPVTDCVISVPSFFT

151 EEQRYNIADAARIAGLNPVRIVNDVTAAGVSYGIFKTDLPEGEEKPRIVA
    :.:|.::.|||:|.|||.:|::||:||..::|||:|.|||..:|||||.
150 DAERRSVLDAAQIVGLNCLRLMNDMTAVALNYGIYKQDLPSLDEKPRIVV

201 FVDIGHSSYTCSIMAFKKGQLKVLGTACDKHFGGRDFDLAITEHFADEFK
    |||:|||::..|..||.||:||||||.|...||::||..:.|||..|||
200 FVDMGHSAFQVSACAFNKGKLKVLGTAFDPFLGGKNFDEKLVEHFCAEFK

251 TKYKIDIRENPKAYNRILTAAEKLKKVLSAN-TNAPFSVESVMNDVDVSS
    ||||:|.:...:|..|:....|||||::|:| |:.|.::|..|||.|||.
250 TKYKLDAKSKIRALLRLYQECEKLKKLMSSNSTDLPLNIECFMNDKDVSG

300 QLSREELEELVKPLLERVTEPVTKALAQAKLSAEEVDFVEIIGGTTRIPT
    :::|.:.|||...||:::..|:...|.|..|..|:|..|||:||.||||.
300 KMNRSQFEELCAELLQKIEVPLYSLLEQTHLKVEDVSAVEIVGGATRIPA

350 LKQSISEAFGKPLSTTLNQDEAIAKGAAFICAIHSPTLRVRPFKFEDIHP
    :|:.|::.|||.:|||||.|||:|:|.|..|||.||..:||.|...|..|
350 VKERIAKFFGKDISTTLNADEAVARGCALQCAILSPAFKVREFSVTDAVP

400 YSVSYSWDKQVEDEDHM-EVFPAGSSFPSTKLITLNRTGDFSMAASYTDI
    :.:|..|:...||.:.: |||....:.|.:|::|..|.|.|.:.|.|:|.
400 FPISLIWNHDSEDTEGVHEVFSRNHAAPFSKVLTFLRRGPFELEAFYSDP

449 TQLPPNTPE-QIANWEITGVQLPEGQDSVPVKLKLRCDPSGLHTIEEAYT
    ..:|  .|| :|..:.:..|...:.:...||:|:|.:..|:.||..|..
450 QGVP--YPEAKIGRFVVQNVSAQKDGEKSRVKVKVRVNTHGIFTISTASM

498 IEDIEVEE----------------------------------------
    :|.:..||
498 VEKVPTEENEMSSEADMECLNQRPPENPDTDKNVQQDNSEAGTQPQVQTD
```

Figure 3.16. Protein alignment of Sse1 with HSPH1. Sse1 is the top sequence. The proteins are approximately 33% identical and 48% similar. The most highly conserved regions are in the ATPase domain. Nine out of the thirteen Sse1p residues identified as being important in prion propagation are conserved (mutant residues are in red).

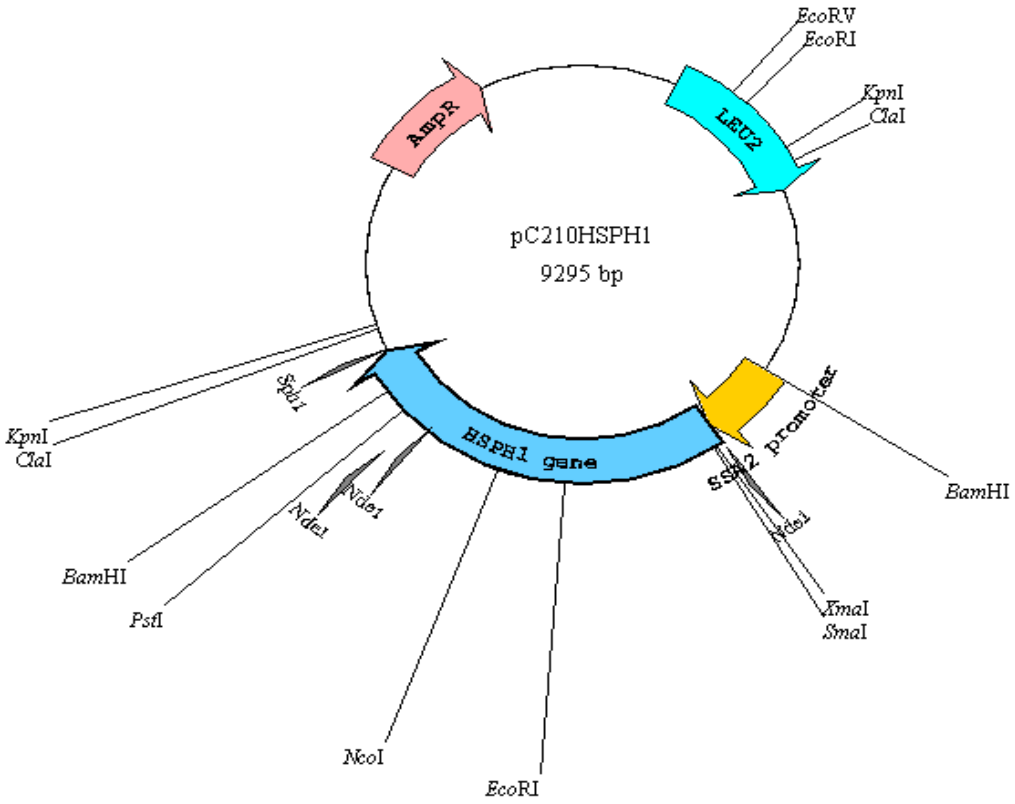

Figure 3.17. Construct of plasmid pC210 with cloned *HSPH1*.

Figure 3.18. HSPH1 does not restore viability in CM02 Δ*sse1*Δ*sse2*. CM02 was transformed with pC210*HSPH1*, pRS315 and pRS315*SSE1* and selected on SC - leucine plates. Transformants were replicated onto 5- FOA and incubated at 30^{o}C for 2 days.

3.9 Analysis of Sse1 mutant growth and rate of cell division

Hsp110 chaperones play a major role in cellular physiology. Deletion of Sse1 renders cells slow-growing (Shaner *et al*., 2006) and Sse1 is also involved in cell wall integrity signaling (Shaner *et al*., 2008). The aim in this section was to see whether any of the Sse1 mutants influence the rate of cell division at 30^{o}C. Cell doubling times were determined from growth curves which were carried out as described in section 2.7. Growth curves were repeated in triplicate. Generation Time (GT) is the amount of time it takes the parent yeast cell to replicate. Cell GT for each mutant was worked out as a percentage of wild type Sse1 GT (Table 3.5). The results from this experiment indicated that there were no major alterations in the rate of cell division for any of the strains carrying a mutant Sse1. Mutants D236N, G342D, E504K and G616D had the slowest generation time when compared to wild type Sse1.

3.10 Western blot analysis of chaperone protein abundance

Mutations to *sse1* may have an effect on the production of subsequent Sse1 protein or on other chaperone protein levels. [*PSI*$^{+}$] propagation can be influenced by the expression levels of molecular chaperones (Chernoff *et al*., 1995; Kushnirov *et al*., 2000).

Western blot analysis was performed to assess chaperone levels in yeast that harboured mutant alleles of *sse1*. Each of the thirteen mutants represented the sole Sse1 protein in the cell. 10 μg of each protein was loaded onto a polyacrylamide gel as described in section 2.24.3. The Sse1 mutants were probed with antibodies for Hsp110, Hsp104 and Hsp70. There was no considerable difference in the abundance of Hsp110, Hsp70 or Hsp104. This suggests that the effects of Sse1 mutants on [*PSI*$^{+}$]

propagation are not due to alterations in cellular chaperone levels. Figure 3.19 represents a Western blot with some alterations in the amount of protein. This Western blot was repeated on at least two more occasions and protein levels were consistent for all the Sse1 mutants.

Table 3.5. Generation Time (GT) of Sse1 mutants.

SSE1	**Generation Time (minutes)**
WT	100
P37L	96
G41D	100
G50D	101
C211Y	93
D236N	110
G342D	114
G343D	104
T365I	104
E370K	107
S440L	97
E504K	118
E554K	101
G616D	113

Generation times are represented as a percentage of wild type Sse1 GT. WT Sse1 had an average GT of 125 minutes. Some mutants were slightly faster at replicating than WT Sse1 i.e P37L, C211Y and S440L. The mutants with the slowest GT were G342D, E504K and G616D.

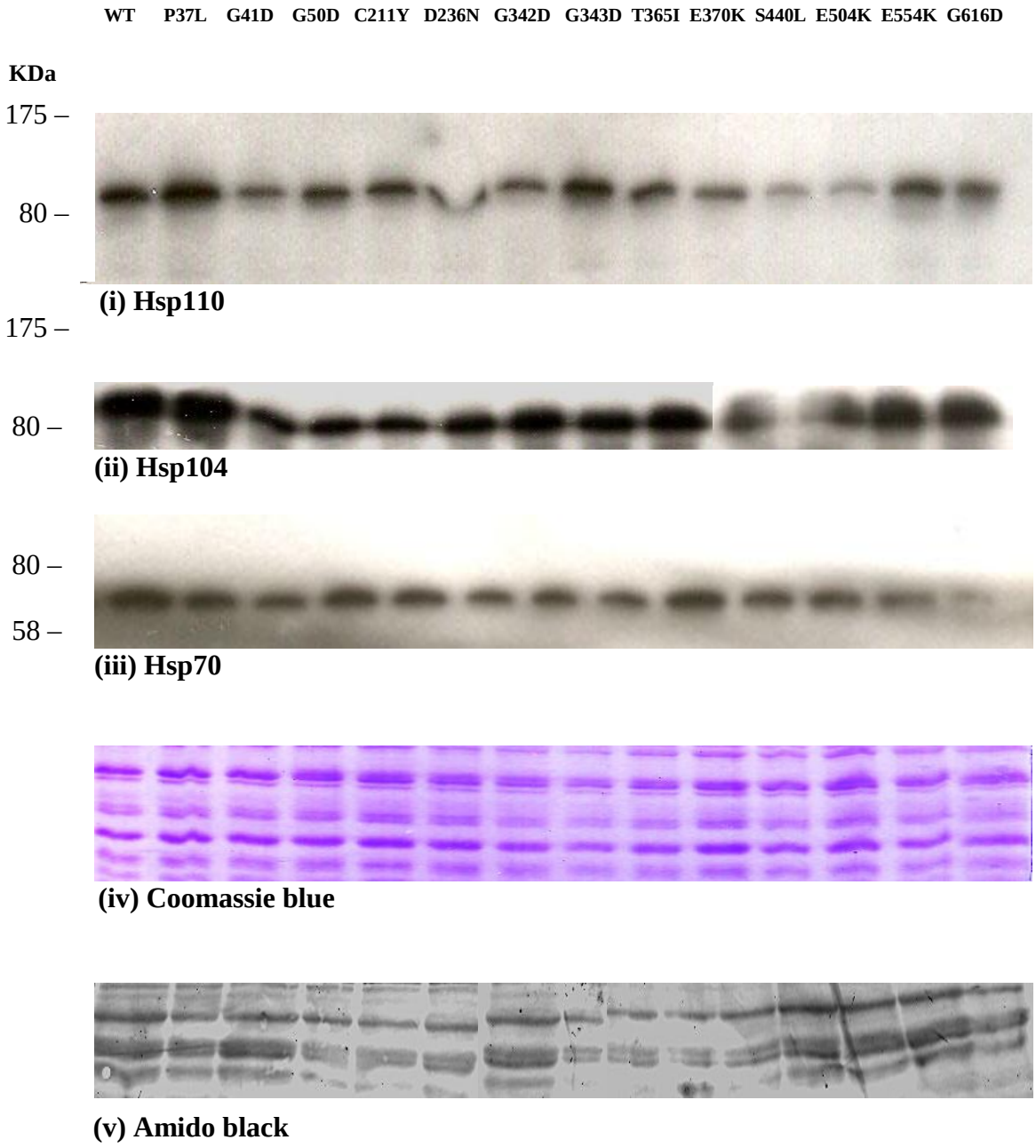

Figure 3.19. Protein abundance of (i) Hsp110 (ii) Hsp104 and (iii) Hsp70. Western blot shows chaperone levels in yeast with Sse1 mutations as indicated. 10 μg of protein from each mutant was loaded onto four gels. Three gels were probed with Hsp110, Hsp70 and Hsp104 antibodies and (iv) the fourth gel was stained with coomassie to show equal loading of samples. (v) Each blot was stained with amido black to show equal protein transfer. This Western blot reveals small chaperone alterations in Hsp70 for mutant G616D and Hsp110 for S440L/E504K. However this Western blot was repeated twice which confirmed that there were no changes to chaperone abundance.

3.11 Molecular modeling of Sse1 mutants

The crystal structure of Sse1 was determined by Liu and Hendrickson (2007). They hypothesised that although Hsp70 and Hsp110 are functionally divergent, Sse1 may retain some structural vestiges of Hsp70. The general structural organisation of Sse1 does reflect that of Hsp70, consisting of an N-terminal nucleotide binding domain (NBD), a β–sandwhich domain (SBD-β) and a three helical bundle domain (3HBD or SBD-α) in the C-terminus (Polier *et al*., 2008). Sse1 is larger than Hsp70 due to insertions in its substrate binding domain (SBD) and C-terminus extensions (Easton *et al*., 2000; Liu and Hendrickson, 2007). Sse1 interacts with Hsp70 (Yam *et al*., 2005; Shaner *et al*., 2005). The Hsp70 NBD co-elutes with the Sse1 protein in the presence of ATP (Andreasson *et al*., 2008). This binding characteristic is essential for Sse1 nucleotide exchange factor function. Sse1 crystal structure analysis and mutational analysis revealed that the NBD of Hsp70 embraces the NBD and 3HBD of Sse1. This leads to the opening of the Hsp70 binding cleft and subsequent nucleotide release. Almost the entire length of Sse1 is required for Sse1:Hsp70 complex formation (Shaner *et al*., 2004; Dragovic *et al*., 2006; Polier *et al*., 2008).

All thirteen Sse1 mutants have been modeled onto the Sse1 3D structure. The predicted structural implications of these amino acid changes on Sse1 have been examined. This analysis determined that certain mutants may be located at important Hsp70 interaction points and at sites of Sse1 interdomain communication. Other mutants had no obvious structural or functional implications. Gemma Kinsella from the Membrane Protein Lab in NUIM performed the molecular modeling of the Sse1 mutants.

3.11.1 The locations of the Sse1 mutants mapped onto the 3D crystal structure

The Sse1 mutants are dispersed across the structure of the Sse1 protein (Figure 3.20). Nine mutants are located in the NBD, three in the SBD-β and two in the SBD-α. In Figure 3.21 each Sse1 protein domain is highlighted and Hsp70 is bound to the NBD and 3HBD of Sse1.

The binding interface of Sse1:Hsp70 is mainly composed of hydrogen bonded water molecules that interact with both proteins. The most potent interaction is between the 3HBD of Sse1 and the α–helix9 of Hsp70 NBD (Polier *et al*., 2008). The extension region of Sse1 has not been fully crystalised. A 2D prediction of the extension region was performed using *Jnet* (Cuff and Barton, 2000) and it was predicted as being largely α-helical.

3.11.2 Possible structural implications of Sse1 mutants

The movement of proteins or 'protein dynamics' is important for protein function. Single amino acid substitutions can affect the dynamics of a protein (Wales and Engen, 2006). Possible structural changes caused by the mutations were analysed using MOE-Homology. MOE-Homology creates full-atom, energy-minimised 3D models of amino acid sequences. The underlying methodology is based on a combination of the segment-matching procedure of Levitt (1992) and an approach on the modeling of *indels* based on that of Fechteler *et al*. (1995). All thirteen mutants were analysed using this method but the figures only illustrate the results for five mutants (Figure 3.22.a-f).

Mutations can cause alterations to a protein by disrupting intramolecular interactions. Mutants can lose intramolecular bonds and interactions formed normally in wild type Sse1. Mutations can also disrupt amino acid polarity, charge and

hydrophobicity, which may ultimately lead to a loss of function. A summary of all the possible structural and interaction changes in each mutant is in Table 3.6.

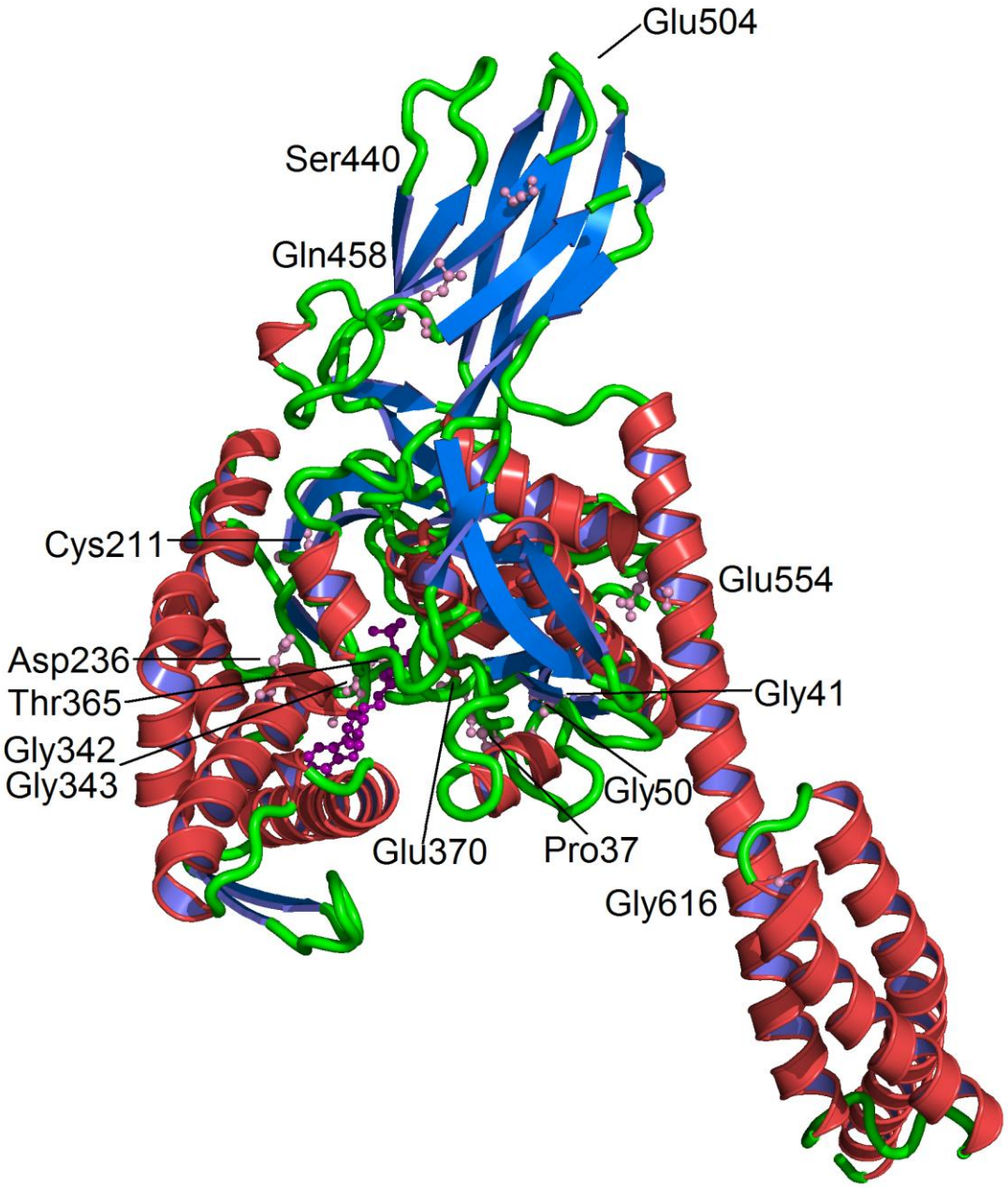

Figure 3.20. Sse1 crystal structure with mutant locations marked in pink and ATP in purple.

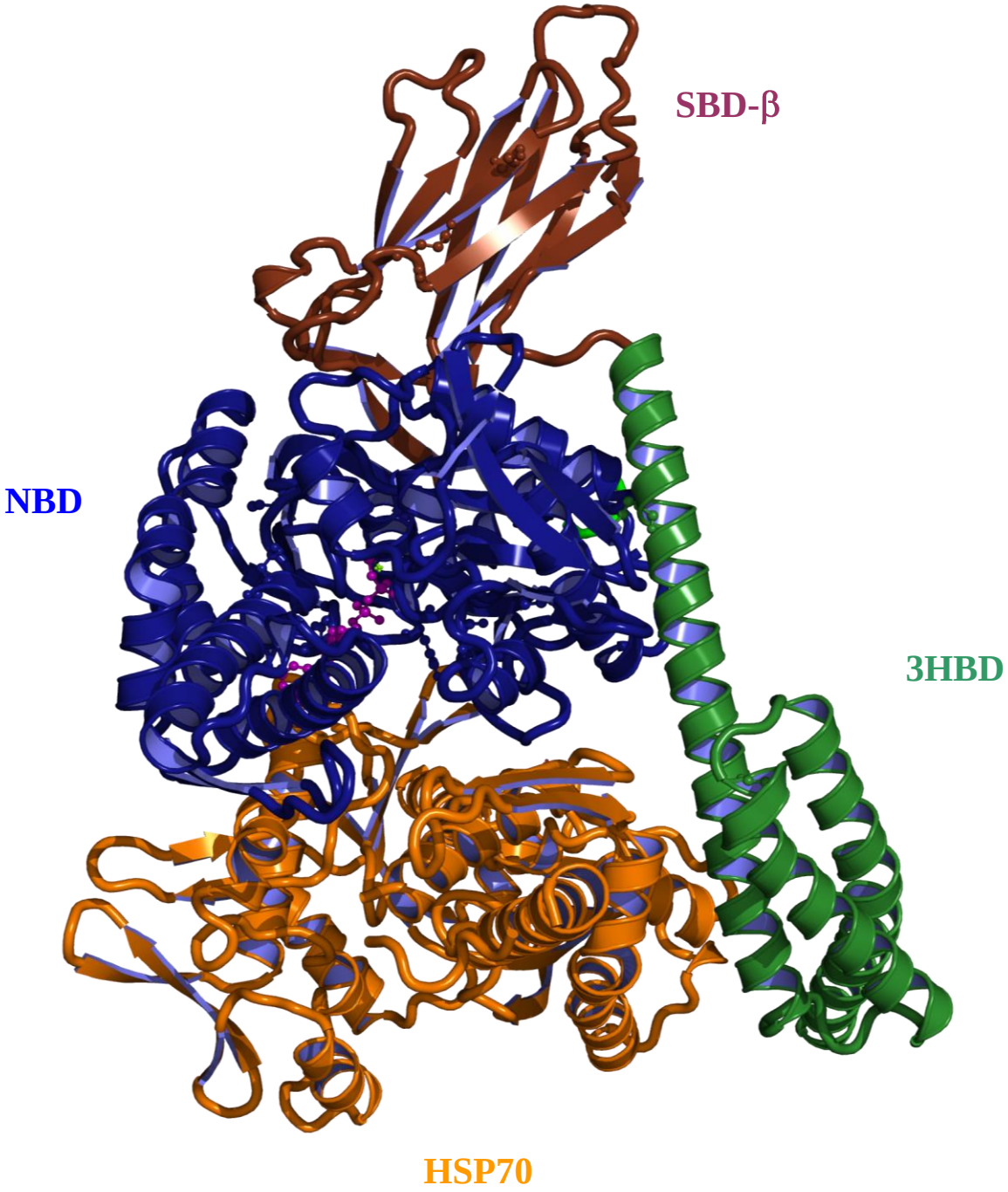

Figure 3.21. Sse1 crystal structure in complex with Hsp70. NBD is in blue, SBD-β in brown and 3HBD in green. Hsp70 (orange) physically interacts with the NBD and 3HBD of Sse1.

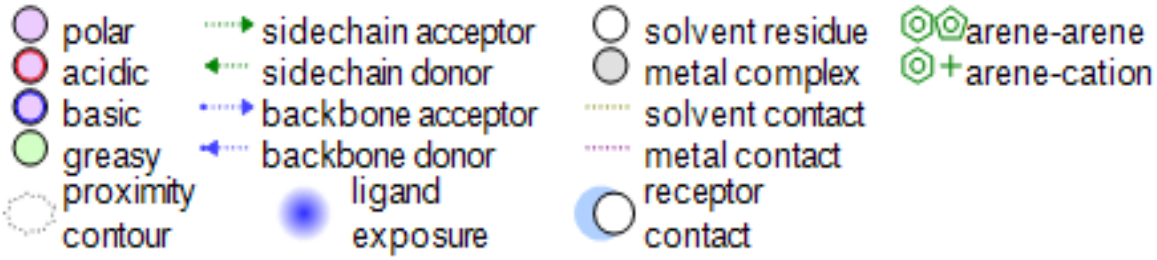

(i) G41

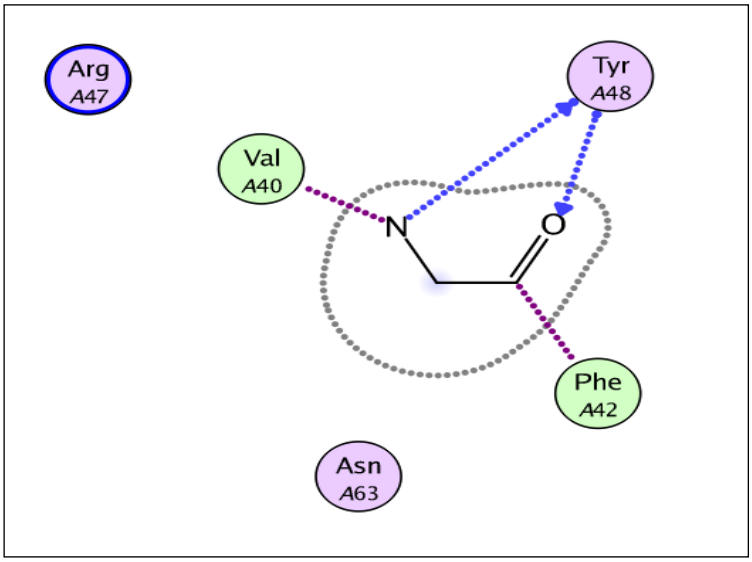

(ii) D41

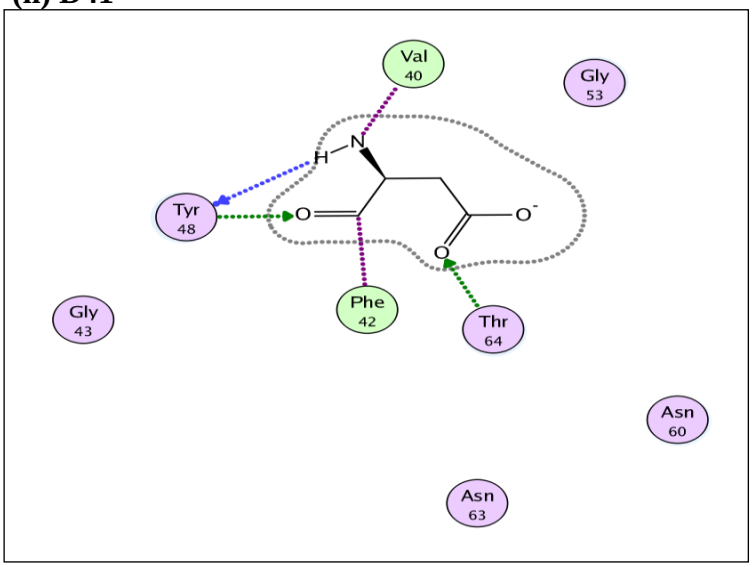

Figure 3.22.a. Amino acid alterations to Sse1 residue 41, from (i) glycine (G) to (ii) aspartic acid (D). This residue is on a β-strand in the NBD of Sse1. Change from a G41 to D41 makes a non-polar neutral residue polar acidic and it also introduces a new hydrogen bond with T64. This mutation could affect β-strand packing and perhaps affect a nearby helix that is involved in the Hp110:Hsp70 interface (A47).

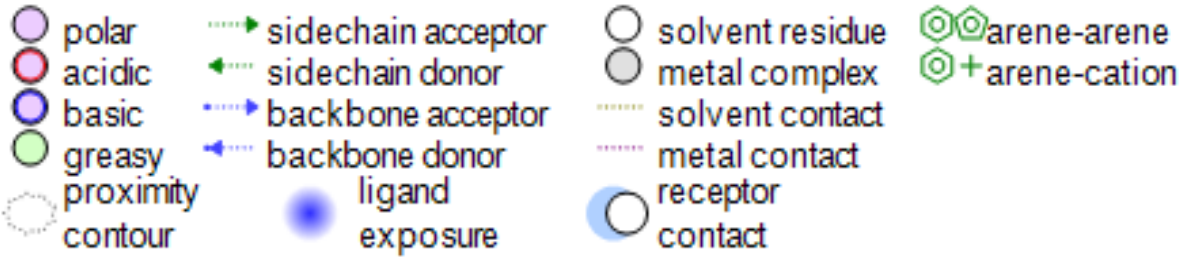

(i) G50

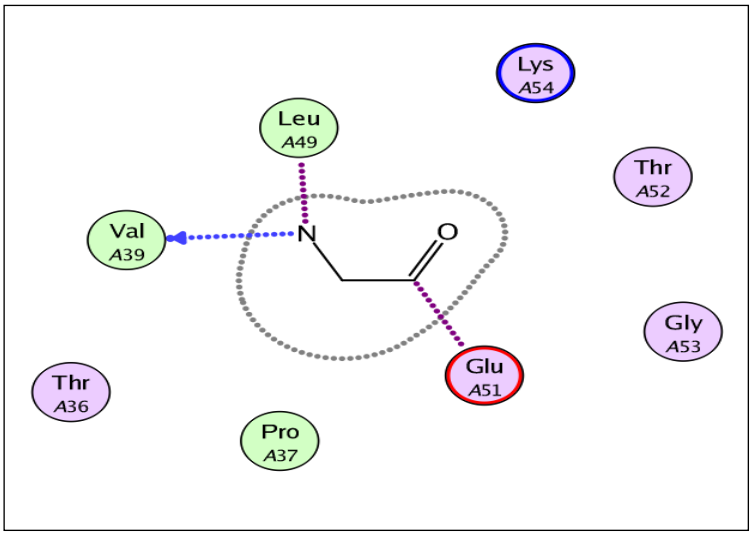

(ii) D50

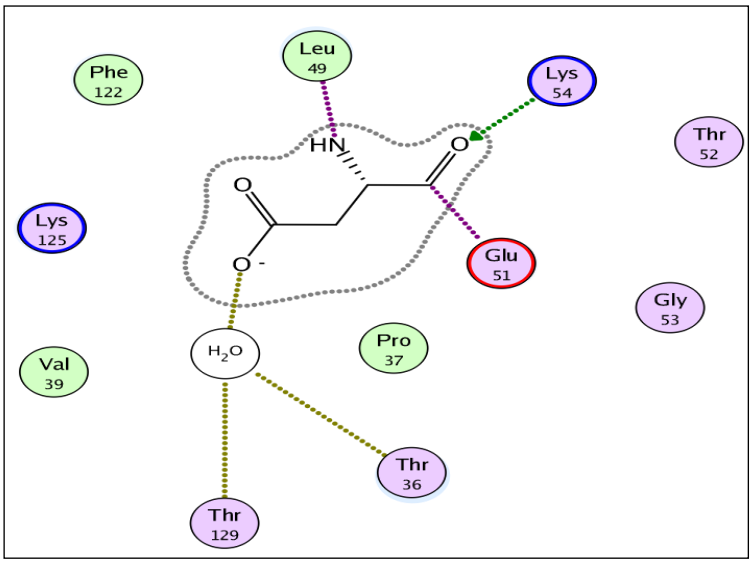

Figure 3.22.b. Amino acid alterations to Sse1 residue 50, from (i) glycine (G) to (ii) aspartic acid (D). This residue is at the start of a α-helix in the NBD of Sse1. Change from G50 to D50 makes a non-polar neutral residue polar acidic. D50 hydrogen bonds (HBs) with Sse1 K54 and forms water mediated interactions with T36 and T129. G50 HBs with V39. This mutation could affect β-strand packing and perhaps affect a nearby helix that is involved in the Hp110:Hsp70 interface.

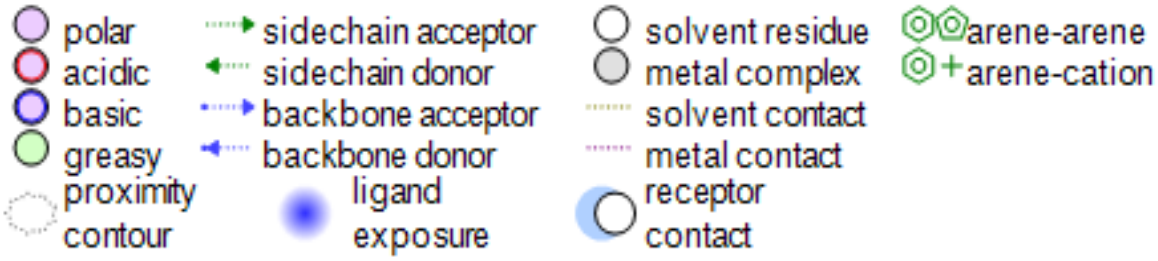

(i) D236

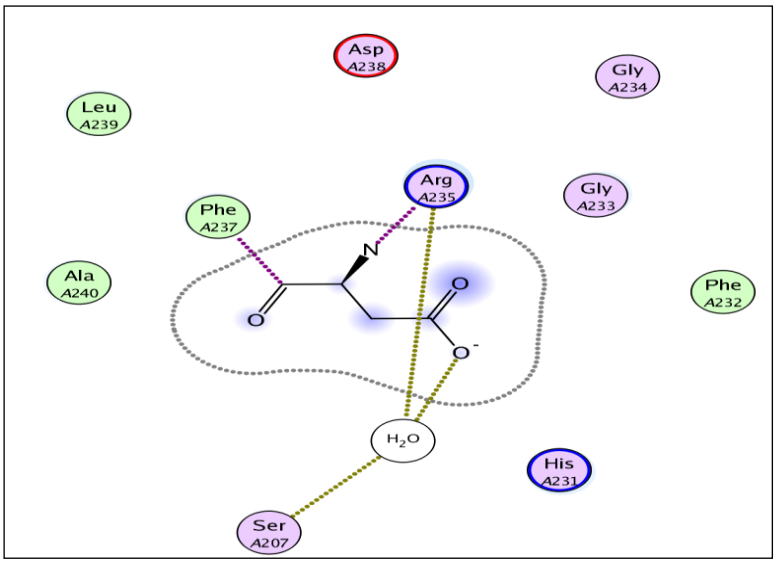

(ii) N236

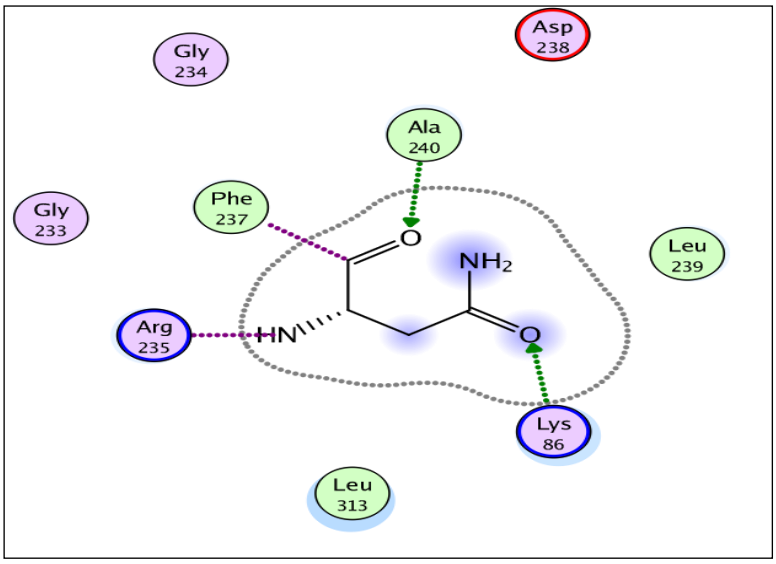

Figure 3.22.c. Amino acid alterations to Sse1 residue 236, from (i) aspartic acid (D) to (ii) asparagine (N). Change from D236 to N236 makes a polar acidic residue polar uncharged. (i) D236 forms water-mediated reactions with R235 and S207, Sse1 residues which interact with ATP. (ii) Mutation N236 loses interaction with S207 and forms HBs with K86 and A240.

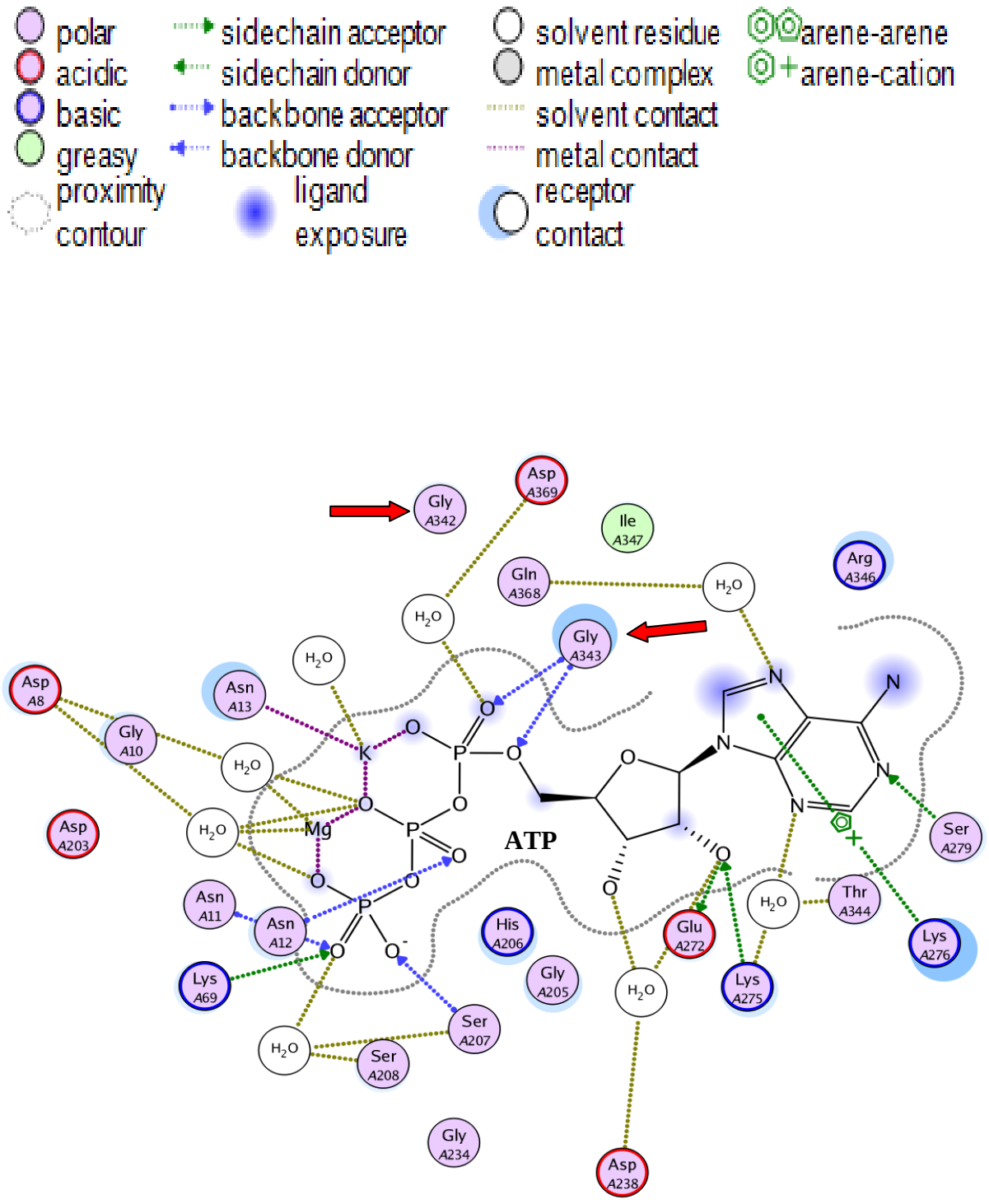

Figure 3.22.d. Schematic 2D diagram of Sse1 ATP binding pocket. Residues G342 and G343 are located in this binding cleft. A single mutation to a residue in the ATP binding pocket can affect its function and the orientation of other amino acids important for binding (MOE Chemical Computing Group, 2008).

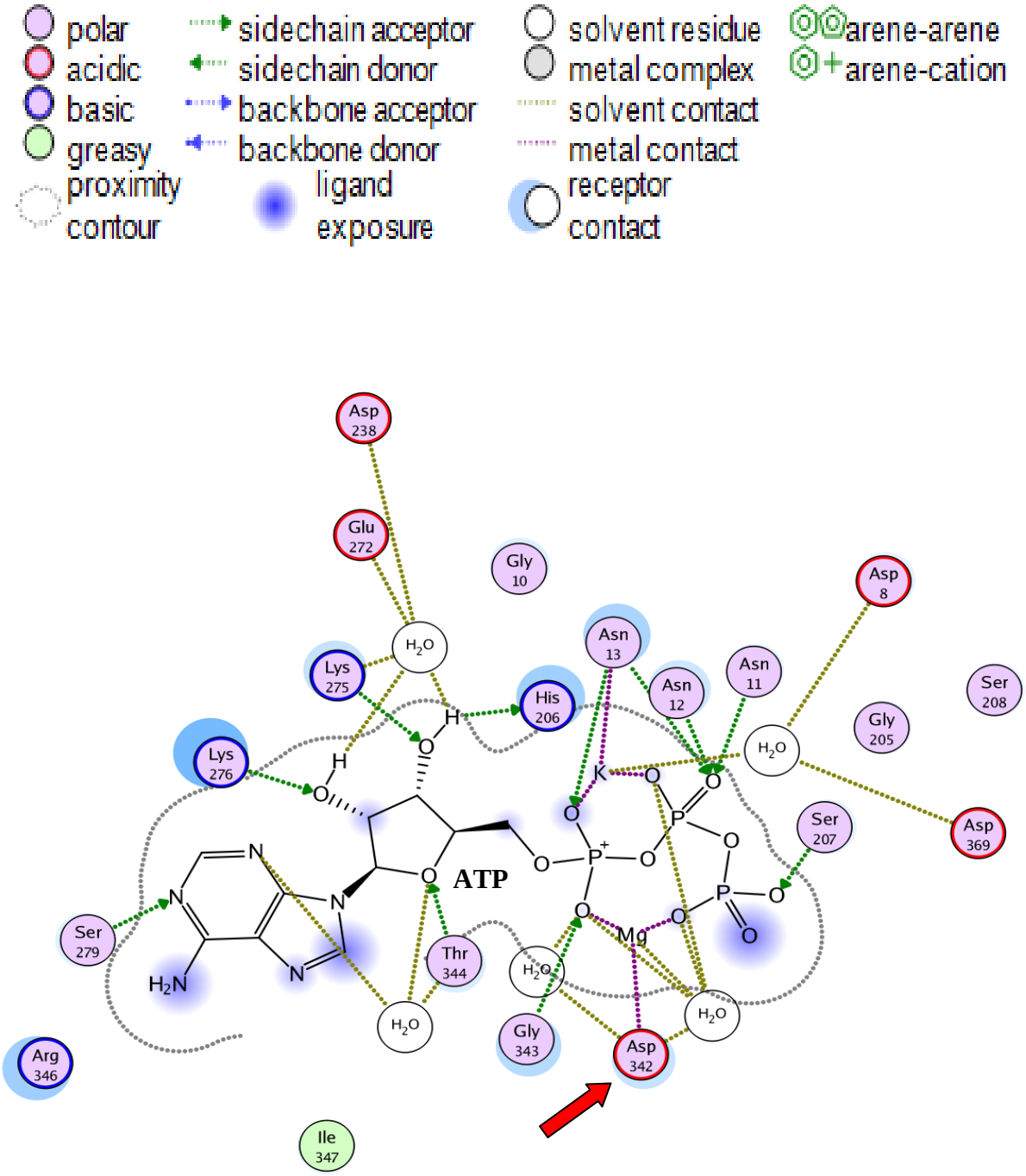

Figure 3.22.e. Schematic 2D diagram of Sse1 ATP binding pocket with residue G342 (glycine) changed to D342 (aspartic acid). In this mutation a non-polar neutral residue becomes polar acidic. G342 and D342 both HB with T345 and Q368 in Sse1. However D342 forms a water-mediated Mg bond. This mutation is likely to affect ATP binding.

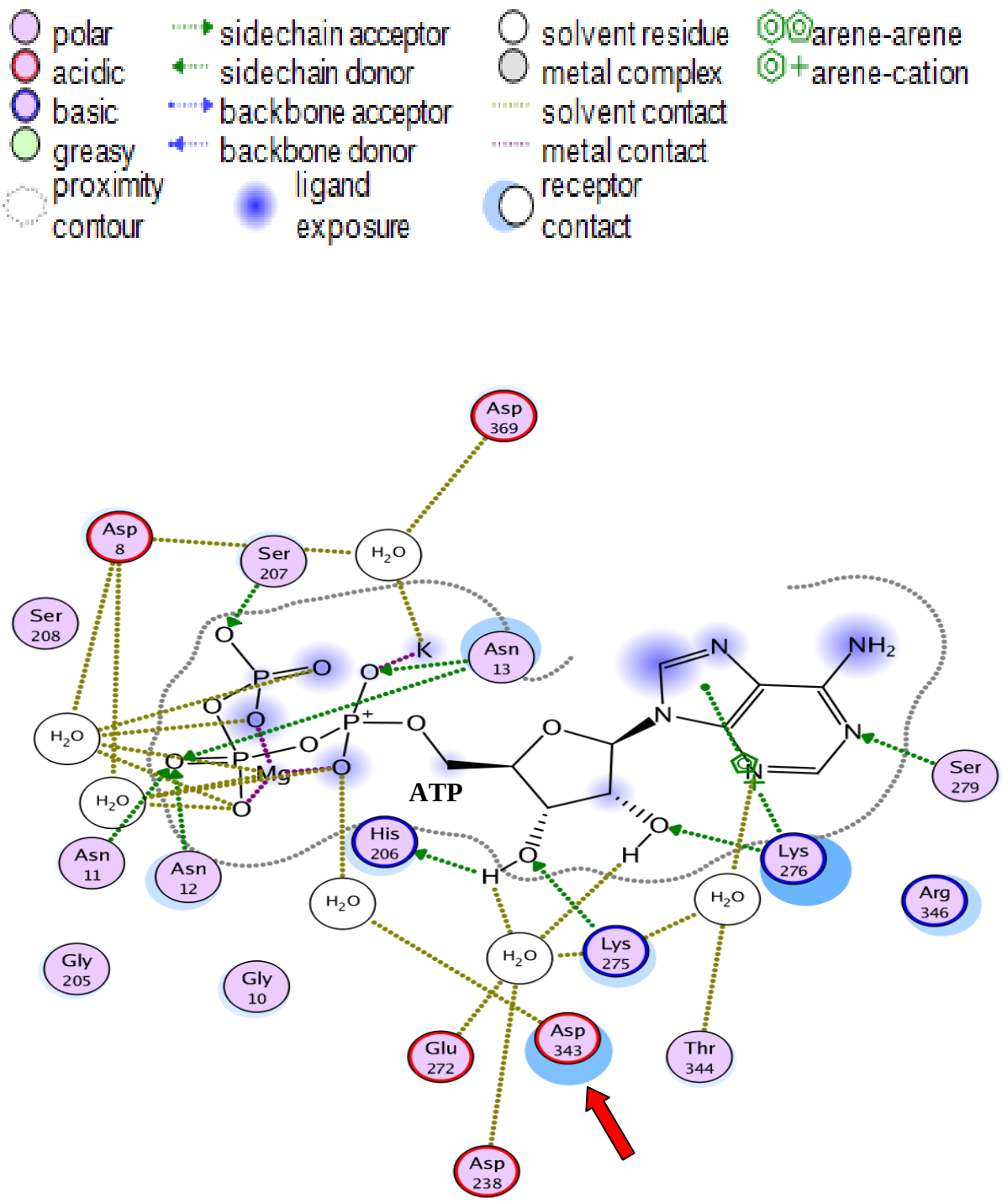

Figure 3.22.f. Schematic 2D diagram of Sse1 ATP binding pocket with residue G343 (glycine) changed to D343 (aspartic acid). In this mutation a non-polar neutral residue becomes polar acidic. G343 interacts with ATP but forms no other HBs. D343 HBs with T344 and R346 in Sse1. D343 also forms a water-mediated interaction to ATP instead of a hydrogen bond seen in G343. This mutation is likely to affect ATP binding.

Table 3.6. Summary of Sse1 mutants structural effects on the Sse1 3D model.

MUTATION	AMINO ACID AND INTERACTION CHANGES	LIKELY STRUCTURAL EFFECTS
P37L	Both WT and mutant non-polar hydrophobic.	Unclear. May disrupt ATP binding through different amino acid residue.
G41D	Non-polar neutral to polar acidic. HB with T64 introduced.	May impact Hsp70 binding site or β-strand packing
G50D	Non-polar neutral to polar acidic. HBs & water mediated bonds with K54, T36 and T129 introduced.	Unclear. May impact Hsp70:Hsp110 interface by disrupting a different amino acid residue
C211Y	Both WT and mutant polar uncharged residues. Both HB with A227.	Unclear
D236N	Polar acidic to polar uncharged. Loss of interaction with S207. Loss of S207 ATP binding.	Unclear Loss of ATP binding?
G342D	Non-polar neutral to polar acidic. Magnesium bond introduced. Both HB with T345 and Q368.	ATP binding
G343D	Non-polar neutral to polar acidic. Mutant HBs with T344 and R346.	ATP binding
T365I	Polar uncharged to non-polar hydrophobic. Residue 365 HBs to Hsp70.	Hsp70 binding
E370K	Polar acidic to polar basic. Mutant forms HBs with different region to WT interactions. E370 HBs to two Hsp70 residues.	Hsp70 binding
S440L	Polar uncharged to non-polar hydrophobic. S440 has no HBs. L440 HBs to D407.	Unclear
E504K	Polar acidic to polar basic. Loss of interaction with residue G505.	Unclear
E554K	Polar acidic to polar basic. Mutant loss of interaction with R47 but gains L550 and I551.	Hsp70 binding
G616D	Non-polar neutral to polar acidic. Mutant and WT Hsp70 surrounded by similar residues but HB different. Nearby residues contact Hsp70.	Hsp70 binding

From here some of the mutants were characterised according to their potential change of function. Residues 364-367 in Sse1 tightly contact the Hsp70 backbone. Thr365 in Sse1 shapes the Sse1 surface into a conformation that cradles Hsp70 residue Tyr134 (Polier *et al*., 2008). One of the mutants isolated in this screen was located at T365 (T365I).

Glu554 in Sse1 is found in a buried polar interaction with Arg47 of Sse1. This interaction is located at the core of the interface between Sse1 3HBD and NBD. This ensures correct positioning of the 3HBD and is probably critical for complex formation with Hsp70 (Polier *et al.*, 2008). One of the mutants was located at this point (E554K). However, E554K did not cause severe disruption to [*PSI*$^{+}$], compared to the other mutants. Polier *et al*. (2008) created E554A which showed significantly diminished complex formation with Hsp70. E554A also showed a growth defect at 37^{o}C by strongly impairing nucleotide exchange. However they discovered that it requires multiple mutations at the binding interface to completely disrupt the interaction. In this study the Sse1 mutants believed to affect Hsp70 binding include G41D, T365I, E370K, E554K and G616D.

Binding of ATP to Sse1 at the NBD is essential for Hsp70:Sse1 complex formation (Shaner *et al*., 2006). Two of the mutations are located in the nucleotide binding cleft (G342D and G343D). G343 was seen to make hydrogen bonds with ATP. Mutant G342D is [*psi*$^{-}$] and G343D is [*PSI*$^{+}$] weak, phenotypes which may be due to effects on ATP binding. Other mutants that may affect the ATP binding site include P37L and E370K.

3.12 Chapter discussion

Thirteen new mutations within the yeast molecular chaperone Sse1 have been generated. In order to study the effects the mutants have on [*PSI*$^{+}$], an

appropriate Δ*sse1*Δ*sse2* yeast strain CM02 was made. The thirteen mutants were characterised according to their [*PSI*$^+$] phenotypic effects. Mutant Q458* appeared [*psi*$^-$] in the initial screen but expressed a nonsense stop codon mutation (TAA), potentially creating a truncated protein. Mutant Q458* was not included in the phenotypic analysis and its possible disruption to [*PSI*$^+$] propagation is discussed in Chapter 4. All thirteen mutants demonstrated a weak [*PSI*$^+$] phenotype when compared with wild type Sse1. The mutants with the most severe loss of [*PSI*$^+$] were D236N, G342D, S440L and G616D (Table 3.3). The results presented in this Chapter suggest that the efficient propagation of [*PSI*$^+$] is dependent upon the chaperone Sse1. Although Sse1 binds aggregated proteins and acts as a 'holdase' (Oh *et al*., 1999), it can be speculated that the Sse1 mutants may affect [*PSI*$^+$] indirectly through its influence on Ssa function (Fan *et al*., 2007; Kryndushkina and Wickner, 2007). Both Fan *et al*. (2007) and Kryndushkin and Wickner (2007) performed tests on Sse1 mutants K69Q and G233D concluding that Ssa1 binding and ATP hydrolysis is necessary for efficient Sse1 function in prion propagation. It is also possible that Sse1 directly affects [*PSI*$^+$] propagation through interaction with Sup35 aggregates.

Sse1 mutants P37L, C211Y, G343D, E504K and E554K all appeared to retain some [*PSI*$^+$] but they failed to grow on SC – adenine after two days incubation (Figure 3.10). These results were surprising. Mutants such as P37L and C211Y scored low in their effects on [*PSI*$^+$] propagation and were expected to show partial growth on SC - adenine medium. Perhaps these [*PSI*$^+$] weak mutants were failing to grow on SC – adenine because they affect cellular processes other than [*PSI*$^+$] propagation? Or perhaps they need longer incubation times at 30^{o}C as they have less [*PSI*$^+$] present than WT Sse1? When mated with a [*psi*$^-$] strain, the [*PSI*$^+$] weak mutants did demonstrate [*PSI*$^+$] dominance confirming that the mutants do possess

some [*PSI*$^{+}$]. However, when the spot test was repeated on SC - adenine - histidine in the presence of pRS423 in Figure 3.14, [*PSI*$^{+}$] weak mutants such as C211Y did show some growth. The only difference in the two experiments was the presence of a histidine marker plasmid and that histidine was lacking from the medium. The overall [*PSI*$^{+}$] phenotype of the mutants also seemed improved on YPD in Figure 3.13. These results were unclear and suggested that perhaps something else is occurring and is affecting the results.

The Sse1 mutants were further characterised by whether or not they impaired [*URE3*] propagation. Previous studies have shown that the overproduction of Sse1 cures [*URE3*]. All thirteen Sse1 mutants failed to cure [*URE3*] to the same extent as wild type Sse1 (Table 3.4). The Sse1 mutants were exerting a dominant negative effect over WT Sse1, by disrupting Sse1's normal [*URE3*] curing ability. Kryndushkin and Wickner (2007) isolated two Sse1 mutants with different effects on [*URE3*] propagation. They isolated an Sse1^{G233D} mutant known to disrupt ATP binding and hydrolysis. This mutant was incapable of Ssa1 binding, lost its NEF function and when over-expressed it failed to cure [*URE3*]. In contrast Sse1^{K69M} binds ATP and retains Ssa1 binding and NEF activity. Overproduction of Sse1^{K69M} cured [*URE3*] which suggests that Sse1 may be affecting [*URE3*] indirectly through its Hsp70-related functions. This suggests that a combination of ATP binding, Ssa1 interaction and NEF activity are essential for Sse1 to efficiently cure [*URE3*]. However, NEF activity alone is not sufficient to inhibit propagation as Fes1 fails to cure [*URE3*] when overproduced (Kryndushkin and Wickner, 2007). One interesting observation was that the mutants with the least curing effect all lie in the nucleotide binding domain (NBD). The NBD is essential for binding of nucleotides such as ATP and in turn drives Ssa1 ATP hydrolysis. As all the Sse1 mutants failed to carry out

[*URE3*] curing functions to the same magnitude as WT Sse1 it can be speculated that the mutants affect either, or a combination of, ATP binding, substrate binding, Hsp70 interaction and NEF activity (section 3.11.2 for Sse1 mutant structural effects). All of the mutants had a collective response indicating that [*URE3*] function is lost through many Sse1 processes. It is unclear as to whether this is occurring directly through Sse1 or indirectly through interaction with other chaperones.

The Fes1 protein associates with ADP-bound Hsp70 and promotes nucleotide release in a similar manner to Sse1 (Kabani *et al*., 2002). There is conflicting evidence as to whether Fes1 overproduction can compensate for loss of Sse1 and Sse2. This theory was investigated and found that Fes1 could not support growth in Δ*sse1*Δ*sse2*. This suggested that Sse1 has critical cellular functions other than NEF activity. Both Sadlish *et al*. (2008) and Raviol *et al*. (2006b) found either full or partial recovery of cell viability when Fes1 was over-expressed. The reasons for differences in these results could be due to the varying strain backgrounds and expression vectors used by each group. Raviol *et al*. (2006b) and our experiment used pRS423*FES1* whereas Sadlish *et al*. (2008) used p425-GPD-*FES1*. All three background strains were also different which could account for the different results observed. This is examined further in Chapter 4 where Fes1 is over-expressed in a different (BY4741) background strain.

Investigations into the Sse1 mutant [PSI^{+}] phenotypes, in the presence of an extra copy of *FES1*, revealed that it only improved propagation in one mutant. Sse1 mutant G616D showed an improved [PSI^{+}] phenotype when *FES1* was over-expressed (Figure 3.13.b). This result suggested that G616D potentially disrupts the ability of Sse1 to function as a NEF. G616D is in the SBD and could impair Sse1-Hsp70 interaction and subsequent Hsp70 nucleotide exchange. The other Sse1

mutants showed no improvement in [*PSI*$^{+}$] in the presence of pRS423*FES1*. Perhaps the mutants affect other functions such as ATP or peptide binding. The overall [*PSI*$^{+}$] phenotype of the mutants appeared stronger in this experiment compared to in Figure 3.9. Perhaps the additional plasmid is having an effect on the colony colours? Each Fes1 + Sse1 mutant strain was also grown on medium lacking adenine (Figure 3.14). Mutant G616D showed only slight improved growth in the presence of pRS423*FES1* and mutant G343D also displayed growth, indicating that Fes1 over-expression had no great effect on the mutant's ability to propagate [*PSI*$^{+}$]. The overall growth pattern in Figure 3.14 was surprising and unclear. Certain mutants grew well in the presence of the control plasmid but not in the presence of *FES1* and the mutant growth patterns did not always reflect their [*PSI*$^{+}$] phenotype observed in Figure 3.13. The only difference between this growth analysis and that observed in Figure 3.9 was the presence of control plasmid pRS423 and the absence of histidine in the medium. The small alterations in nutrient growth medium or the presence of pRS423 could result in different cell growth abilities. These results may be highlighting the complexity of the adenine biosynthesis pathway and how it can be influenced by cross-talk from other metabolic activities. SC medium is quite nutrient deficient compared to YPD rich medium, this could affect the up-regulation or activation of cellular pathways which in turn could interfere with growth patterns.

Human Sse1 homolog HSPH1 could not recover cell viability in Δ*sse1*Δ*sse2*. This result is supported by Shaner *et al*. (2004) and Raviol *et al*. (2006a) who stated that mammalian Hsp110 cannot functionally compensate for yeast Sse1. Yeast and mammalian Hsp70 are structurally conserved and yeast Sse1 can form complexes with bovine and human Ssa1. 90% of the residues that form the Hsp70 interface are conserved between mammals and yeast. In comparison the human and yeast Hsp110

binding interface only share 61% identity (Polier *et al*., 2008; Schuermann *et al*., 2008). Perhaps Sse1 residues critical for interaction with Hsp70 are not conserved in human HSPH1. This is examined further in Chapter 4 by expressing HSPH1 in a different (BY4741) background strain.

Investigations into the growth rates of yeast harbouring mutant Sse1's revealed that the mutants had only small differences in cell generation time (GT), when compared to WT Sse1. These small alterations in growth rates may not be severe enough to disrupt [*PSI*$^{+}$]. Mutant S440L was [*psi*$^{-}$] but it grew at a slightly faster rate than WT. Western blot analysis suggested that the effects of Sse1 mutants on [*PSI*$^{+}$] propagation are not influenced by changes in chaperone abundance. All thirteen mutants had normal growth rates and protein chaperone levels irrespective of their effects on [*PSI*$^{+}$] propagation.

Finally, 3D crystal structure studies revealed possible structural and functional disruptions caused by the Sse1 mutations. Changes to amino acid residues caused by these mutations potentially alter the dynamics of Sse1 and possibly the subsequent function of the protein. ATP binding, Hsp70 binding and interdomain communication appears to be the main functions which the mutant Sse1's are disrupting. Mutants with potentially the most severe structural effects are those located at known intramolecular interaction sites e.g G343D, T365I, E370K and E554K. However, these structural disruptions are not reflected in all the mutants [*PSI*$^{+}$] phenotypes. T365I and E370K were considered [*psi*$^{-}$] but mutants G343D and E554K were only considered [*PSI*$^{+}$] weak with respect to their effects on [*PSI*$^{+}$] (Table 3.3). Perhaps the amino acid changes in these mutants were not severe enough to completely disrupt [*PSI*$^{+}$] propagation. Mutants predicted as having the least structural effects were P37L (both residues nonpolar hydrophobic) and C211Y (both

residues polar uncharged). Their lack of structural disruption is reflected by their [*PSI*$^{+}$] phenotype as they both scored quite low for their loss of [*PSI*$^{+}$], compared to other mutants (Table 3.3). Differences in the severity of structural effects caused by each mutant may account for the differences in [*PSI*$^{+}$] phenotypes observed in section 3.5.

From the results in this Chapter thirteen Sse1 mutants have been identified that impair *S. cerevisiae* prion propagation. Phenotypic analysis and structural modeling suggests that Sse1 plays an integral role in prion propagation in yeast.

CHAPTER 4
INVESTIGATION INTO THE TEMPERATURE-SENSITIVE EFFECTS OF *sse1* MUTANTS

4.0 Introduction

The aim of this Chapter was to investigate why certain Sse1 mutants displayed temperature-sensitive phenotypes. The initiative behind this Chapter was to see if the Sse1 mutants had any influence on cellular processes other than prion propagation.

The non-viable Δ*sse1*Δ*sse2* phenotype indicates that Hsp110 plays an important role in normal cellular homeostasis. It has been suggested that Sse1 plays a role in providing cellular thermostability, Hsp90 signaling and in cell wall integrity (CWI) signaling (Lee-Yoon *et al*., 1995; Liu *et al*., 1999; Shaner *et al*., 2008).

Changing environmental temperature is the most predominant stress that all organisms have to cope with. Microbes such as yeast have evolved mechanisms that allow them to adapt to temperature alterations (Strassburg *et al*., 2010). Hsp110 has been identified as a heat stress-induced protein in yeast and in a number of eukaryotes including *Arabidopsis thaliana, Caenorhabditis elegans* and mammals (Lee-Yoon *et al*., 1995). As well as having an abundance of heat shock proteins to protect the cell from the onslaught of protein denaturation, yeast also contain a resilient cell wall composed of thick polysaccharide layers (Parsell and Lindquist, 1993; Cabib *et al*., 1998).

Cell wall damage caused by heat stress results in the activation of the cell wall signaling pathways (Kamada *et al*., 1995). This involves signaling through kinase cascades resulting in the activation of transcription factors for genes involved in protection against temperature stress (Torres *et al*., 1991; Paravicini *et al*., 1992). Loss of function of any protein kinase in the signal cascade results in cell temperature sensitivity (ts) and cell lysis that can be recovered by support on highly osmotic substances such as 1 M Sorbitol (Levin, 2005).

Sse1 has been shown to physically interact with the molecular chaperone Hsp90 and is required for Hsp90-mediated signaling (Liu *et al*., 1999; Mandal *et al*., 2010). Client proteins such as transcription factors and protein kinases depend upon Hsp90 for effective signaling (Mayer and Bukau, 1999). Hsp90 has been implicated in playing a major role in the cell wall signaling pathway. Mutants defective in Hsp90 function are temperature-sensitive and remediated by osmotic support. The cell wall integrity (CWI) signaling kinase Slt2 is a client protein of Hsp90 and it requires proper Hsp90 chaperone functioning in order to be an active kinase protein (Millson *et al*., 2005; Piper *et al*., 2006; Truman *et al*., 2007).

Shaner *et al*. (2008) proposed that Sse1 signals through the CWI pathway in conjunction with Slt2. They discovered that deletion of Sse1 results in osmoremedial temperature sensitivity and sensitivity to cell wall antagonists, characteristics shared by mutants of the CWI pathway. Temperature-sensitive phenotypes caused by Δ*sse1* or *sse1* mutants may not be solely due to cellular protein aggregation (Truman *et al*., 2007; Wright *et al*., 2007) but caused by weakened cell walls as a result of improper CWI signaling (Shaner *et al*., 2008).

Sse1 has also been linked with PKA signaling and it has been shown that the temperature-sensitive effects of Δ*sse1* can be suppressed by decreasing PKA signaling (Trott *et al*., 2005). Trott *et al*. (2005) demonstrated that Δ*sse1* temperature sensitivity was alleviated by growth on non-fermentable carbon sources suggesting that Sse1 is a negative regulator of PKA signaling.

The work presented in this Chapter identified temperature-sensitive Sse1 mutants and the main objective was to investigate whether they are affecting CWI signaling, Hsp90 signaling, PKA signaling or another cellular process. Results from this investigation led to the generation of a new Δ*sse1*Δ*sse2* strain in a BY4741

background and subsequent analysis of Sse1 mutant characteristics in this new strain. This allowed a comparative analysis of G600 and BY4741 background strains to be carried out, concentrating on areas such as strain sensitivity and growth when expressing Sse1 and Sse1 mutants.

4.1 Sse1 mutants have increased temperature sensitivity

4.1.1 Temperature sensitivity testing of Sse1 mutants by comparative growth analysis

In Chapter 3 it was established that particular mutations in Sse1 affect the propagation of yeast prions [*PSI*$^{+}$] and [*URE3*]. As Sse1 is a heat shock protein and an important cellular chaperone one of the objectives was to assess whether the mutants have any effects on cellular thermostability. Comparative growth analysis was carried out on each mutant in strain CM02. The plates were incubated at 30^{o}C, 37^{o}C and 39^{o}C and growth was monitored over 2 days. After 48 hours it was evident that mutants G342D and G616D were temperature-sensitive (ts) at 37^{o}C and that all the remaining mutants grew relatively well at this temperature (Figure 4.1.a-e). At 39^{o}C treatment varying degrees of growth was seen for all thirteen mutants. Most mutants were growth deficient but some grew as well as WT Sse1 (P37L, E504K). Table 4.1 summarises a subjective analysis of mutant growth at 39^{o}C in comparison to WT Sse1 after 2 days.

As wild type (WT) Sse1 cells did not display complete growth at 39^{o}C after 2 days, the plates were incubated for an additional 24 hours. This resulted in improved growth for WT Sse1 but mutants G342D and G616D were still non-viable (data not shown). Mutants G41D, G50D, C211Y and D236N displayed partial growth after 3 days incubation at 39^{o}C but were still inhibited in comparison to WT Sse1

(Figure 4.2).

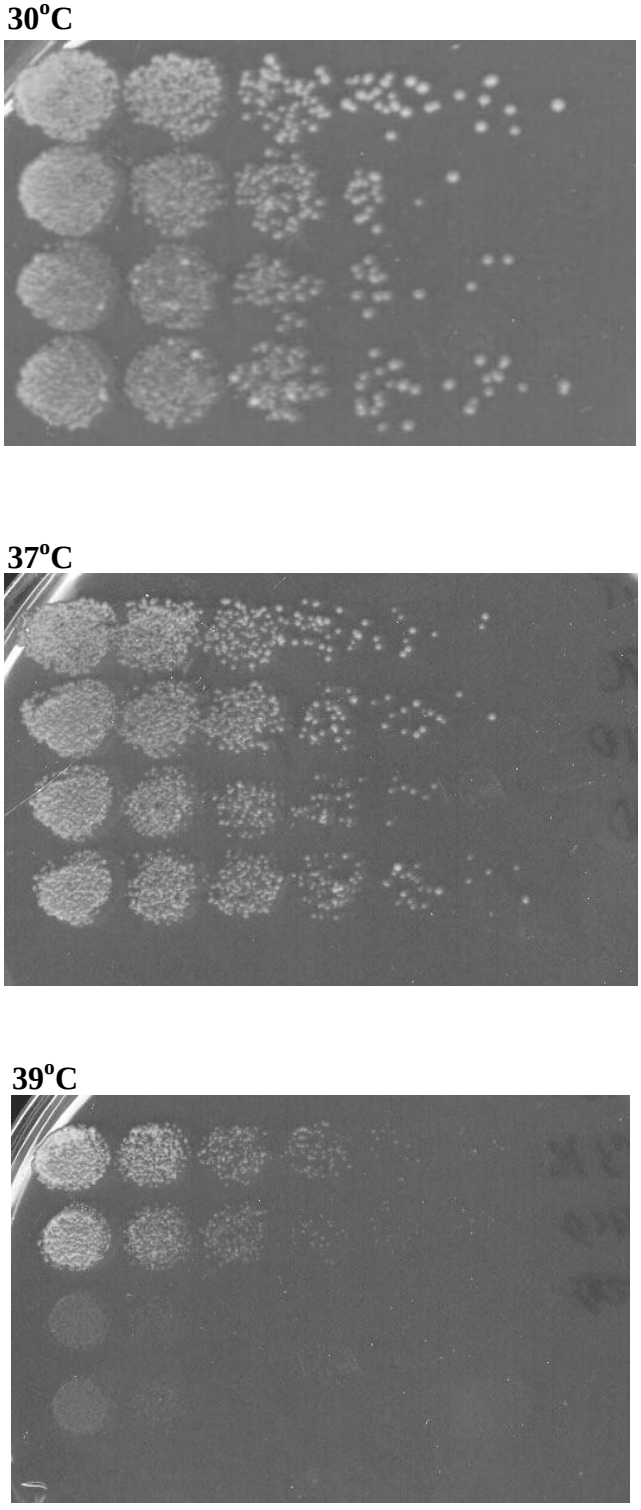

Figure 4.1.a. Comparative growth assay of Sse1 mutants P37L-G50D. The assay was performed as described in section 2.6 and selected on YPD plates. The plates were incubated at 30°C, 37°C and 39°C for 48 h. P37L grew as well as WT Sse1 at 39°C.

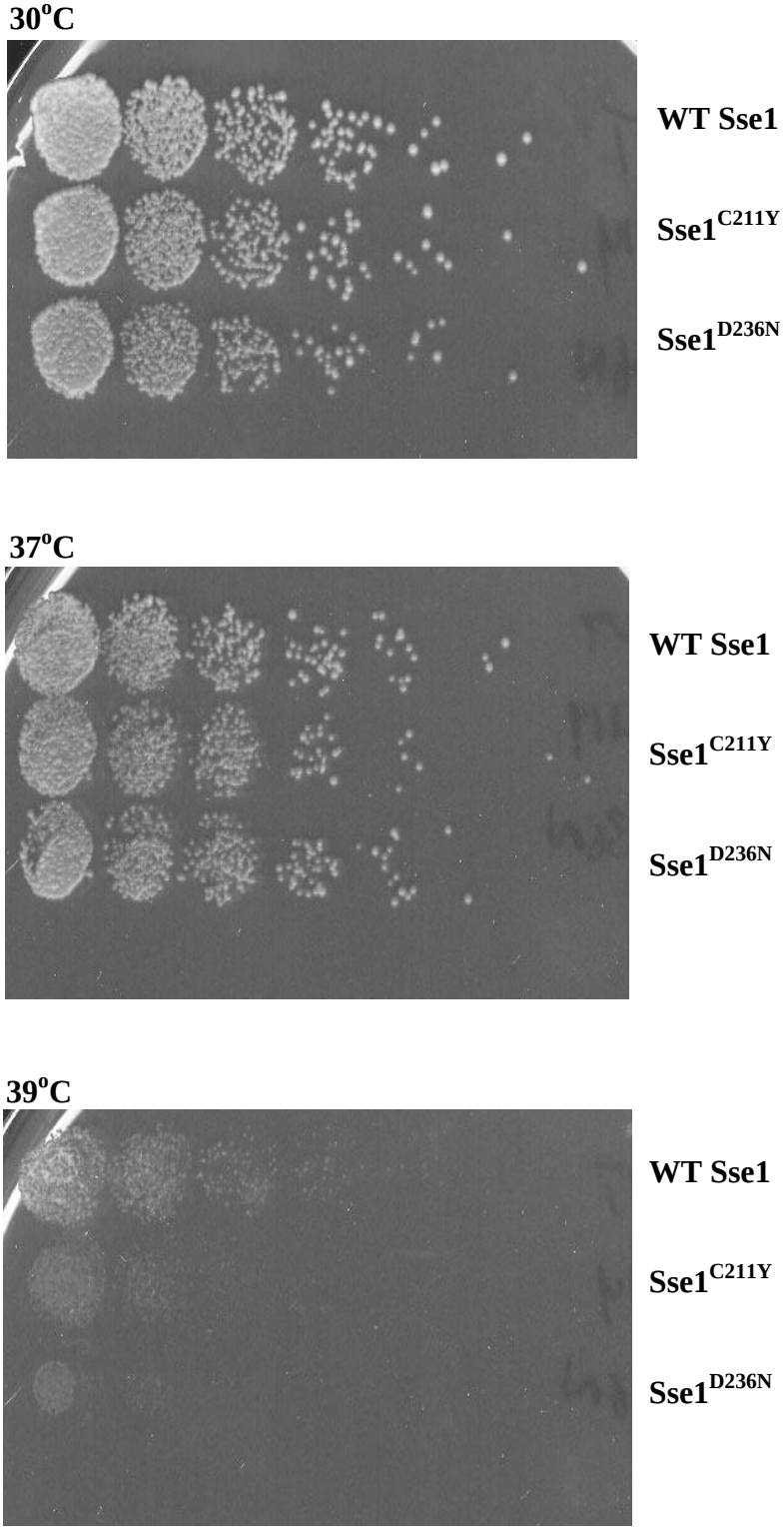

Figure 4.1.b. Comparative growth assay of Sse1 mutants C211Y-D236N. The assay was performed as described in section 2.6 and selected on YPD plates. The plates were incubated at 30°C, 37°C and 39°C for 48 h.

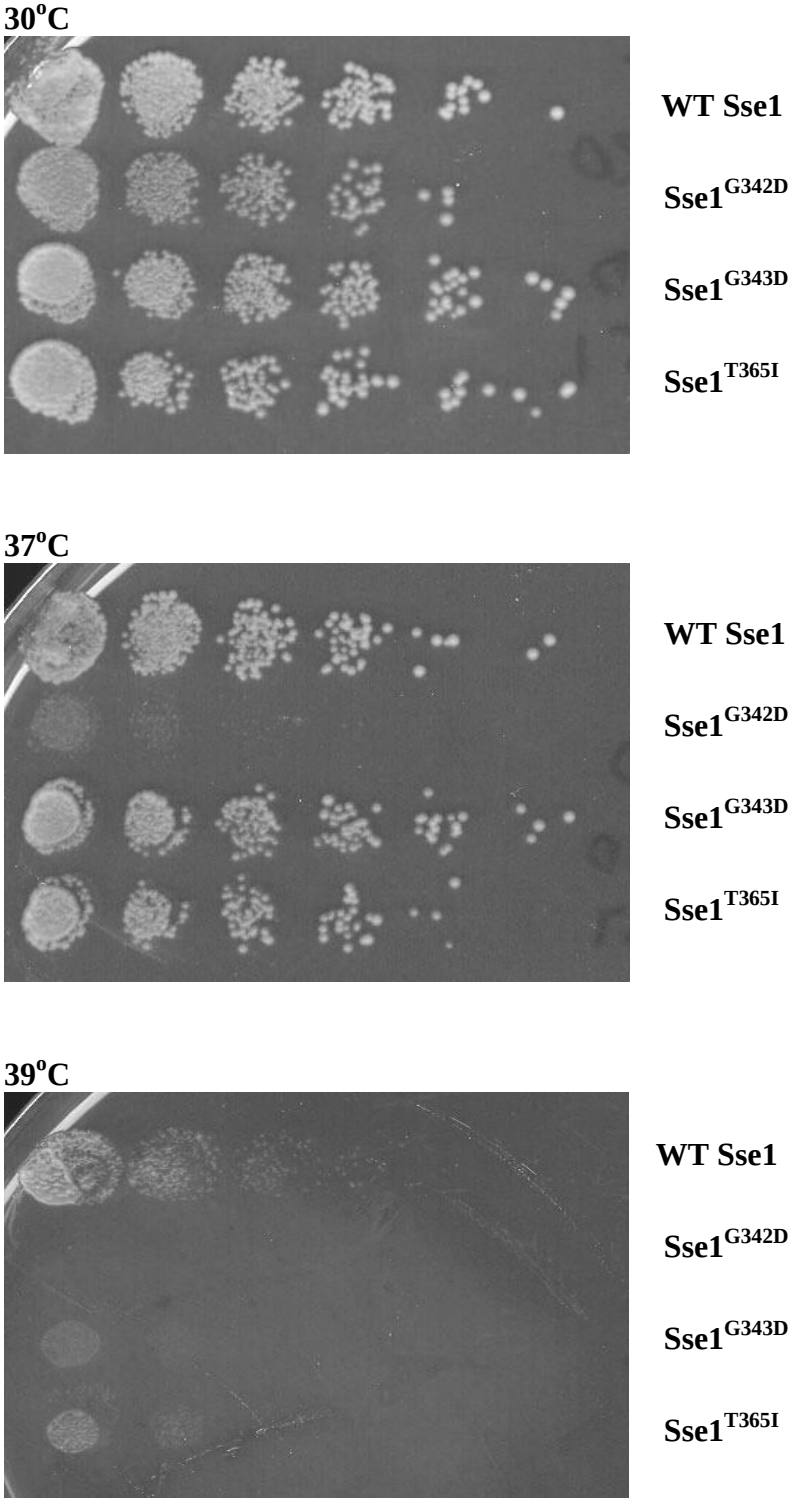

Figure 4.1.c. Comparative growth assay of Sse1 mutants G342D-T365I. The assay was performed as described in section 2.6 and selected on YPD plates. The plates were incubated at 30°C, 37°C and 39°C for 48 h. Mutant G342D was completely ts at 37°C and 39°C.

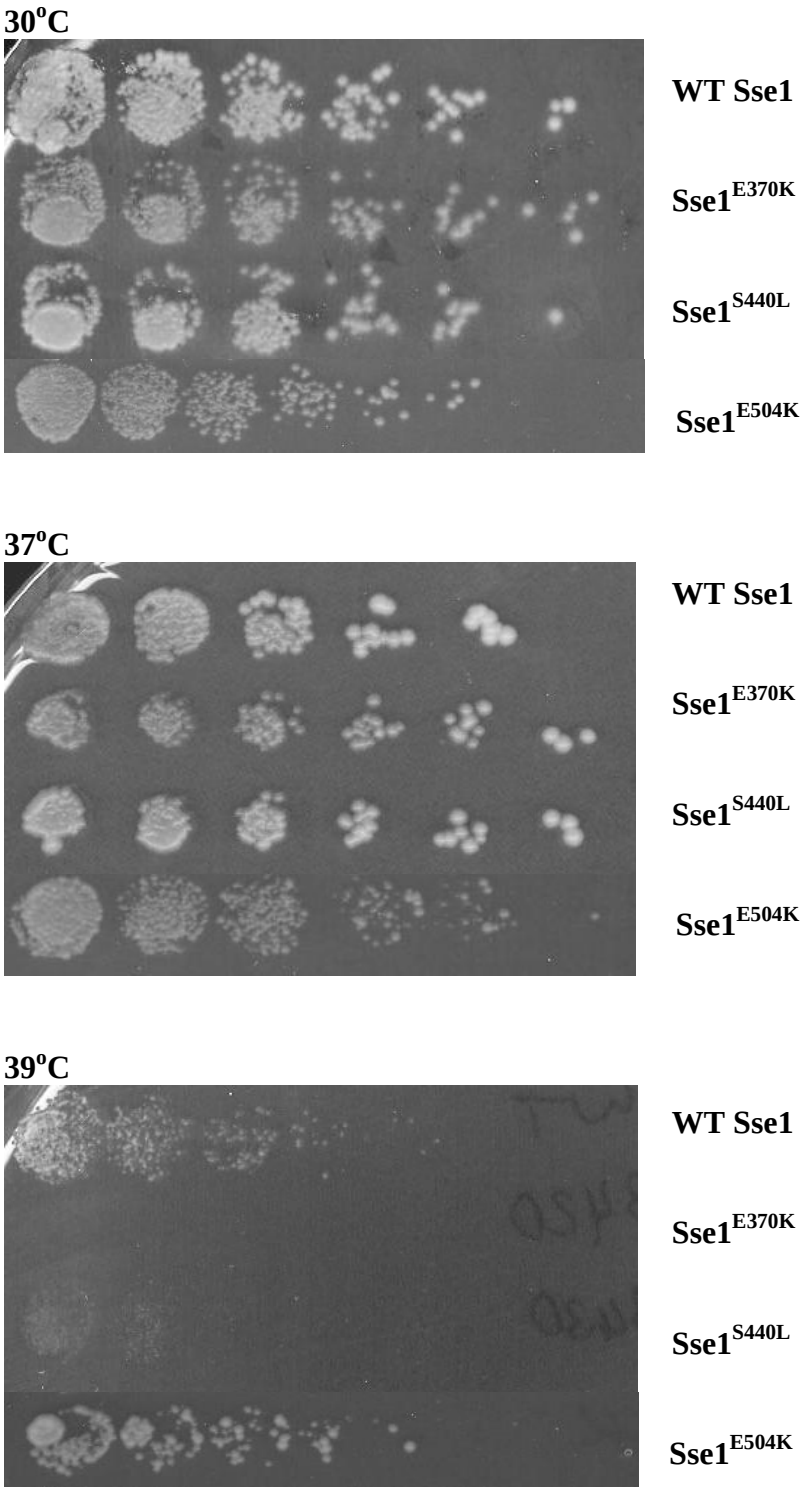

Figure 4.1.d. Comparative growth assay of Sse1 mutants E370K-E504K. The assay was performed as described in section 2.6 and selected on YPD plates. The plates were incubated at 30°C, 37°C and 39°C for 48 h. E504K grew as well as Sse1 at 39°C.

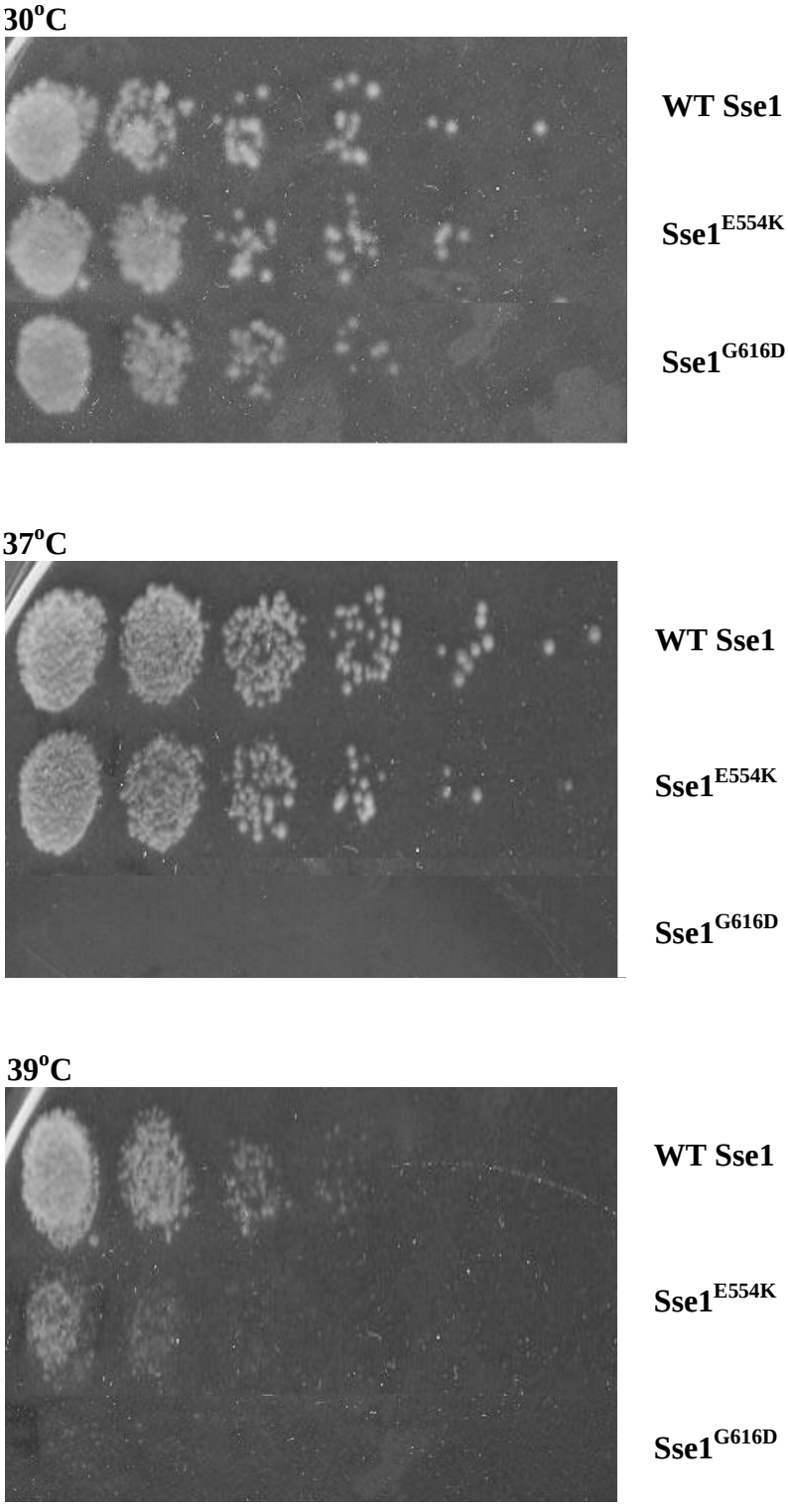

Figure 4.1.e. Comparative growth assay of Sse1 mutants E554K-G616D. The assay was performed as described in section 2.6 and selected on YPD plates. The plates were incubated at 30°C, 37°C and 39°C for 48 h. Mutant G616D was ts at 37°C and 39°C.

Table 4.1. Subjective growth score for mutants incubated at 39^{o}C for 2 days.

MUTATION	GROWTH SCORE
WT	10
P37L	9
G41D	1
G50D	1
C211Y	4
D236N	2
G342D	0
G343D	3
T365I	4
E370K	1
S440L	3
E504K	10
E554K	6
G616D	0

Mutants were compared to the WT Sse1 cell growth that was on the same plate. WT Sse1 did not demonstrate complete growth after 2 days but was given a score of 10 for comparative purposes.
Mutants G342D and G616D were completely non-viable and mutants P37L and E504K grew nearly as well as or as well as WT Sse1.

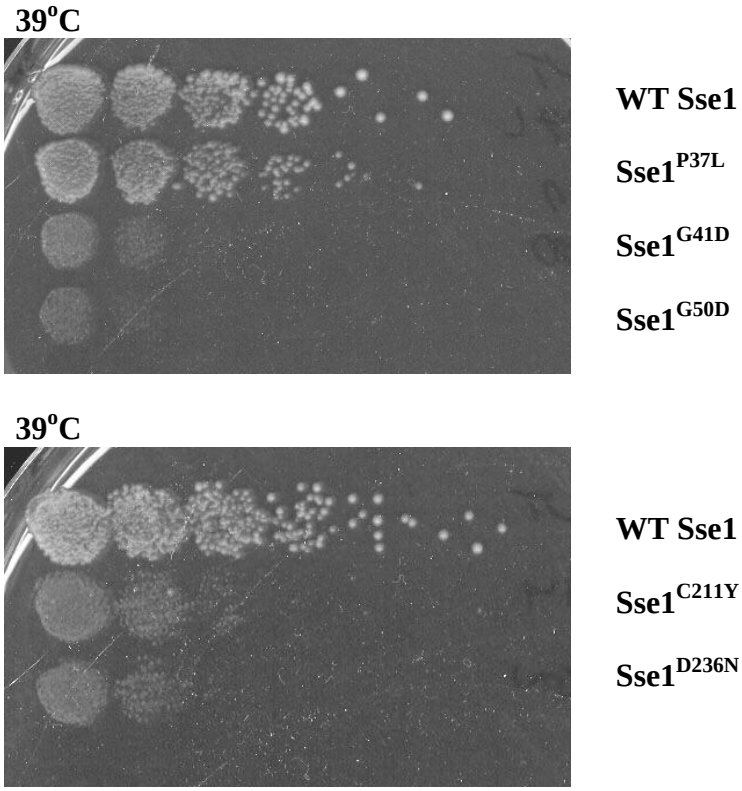

Figure 4.2. Comparative growth analysis of Sse1 temperature-sensitive mutants after 3 days incubation. The plates were incubated at 39°C for 3 days. WT had complete growth after 3 days and Sse1 mutants G41D, G50D, C211Y and D236N were slow-growing.

The results from these experiments indicated that normal Sse1 function is required for protecting the cell against extreme environmental temperatures. 39°C is an extreme temperature to which WT Sse1 is slightly sensitive after 2 days growth (possibly due to lack of Sse2) (Figure 4.1a-e). However, most of the mutants were very sensitive after 2 and 3 days growth. 39°C sensitive mutants could affect the stability and folding of Sse1 under extreme heat shock. If this temperature makes the mutant protein non-functional then the cell would ultimately be Δ*sse1*Δ*sse2*. Given the structural analysis data from Chapter 3, it was speculated that perhaps mutants G342D and G616D are affecting the protein dissagregation system. This could occur directly through Sse1 or indirectly through Hsp70 interaction.

4.1.2 Growth on high osmotic medium recovers temperature sensitivity in G342D and G616D

Mutants that cause cell lysis at increased temperatures are often located in genes involved in cell wall maintenance (Paravicini *et al*., 1992). G342D and G616D temperature sensitivity was suppressed by increasing the osmolarity of the growth medium with 1 M sorbitol (Figure 4.3). Paravicini *et al*. (1992) previously isolated 121 random temperature-sensitive mutants of which 12 were osmotically stabilised. Paravicini *et al*. (1992) and Shaner *et al*. (2008) both tested temperature-sensitive mutants for cell permeability and lysis at increased temperatures in a method first used in yeast by Cabib and Duran (1975). They found that certain osmoremedial temperature-sensitive mutants had substantial levels of 'leakage' (cellular contents leaking into external environment) indicating some sort of disruption to cell wall integrity (Paravicini *et al*., 1992; Shaner *et al*., 2008).

In yeast, environmental osmotic changes often initiate the cell wall integrity (CWI) pathway and HOG response pathway (Fuchs and Mylonakis, 2009). When yeast grow on hypoosmotic solutes such as YPD the MAP kinase CWI pathway is activated. Mutants which prevent MAP kinase signaling lyse in the absence of osmotic stabilisers such as 1 M sorbitol (Lee and Levin, 1992; Davenport *et al*., 1995).

It is possible that Sse1 mutants G342D and G616D have become more permeable at increased temperatures, due to alterations to MAP kinase signaling or some other signaling pathway, making growth on hypotonic medium (YPD) lethal compared to the support provided by 1 M sorbitol. This test was repeated on YPD medium containing 0.4 M NaCl and the results were similar confirming that it is an

increased osmolarity effect rather than a sorbitol-specific effect that was recovering cell growth (data not shown).

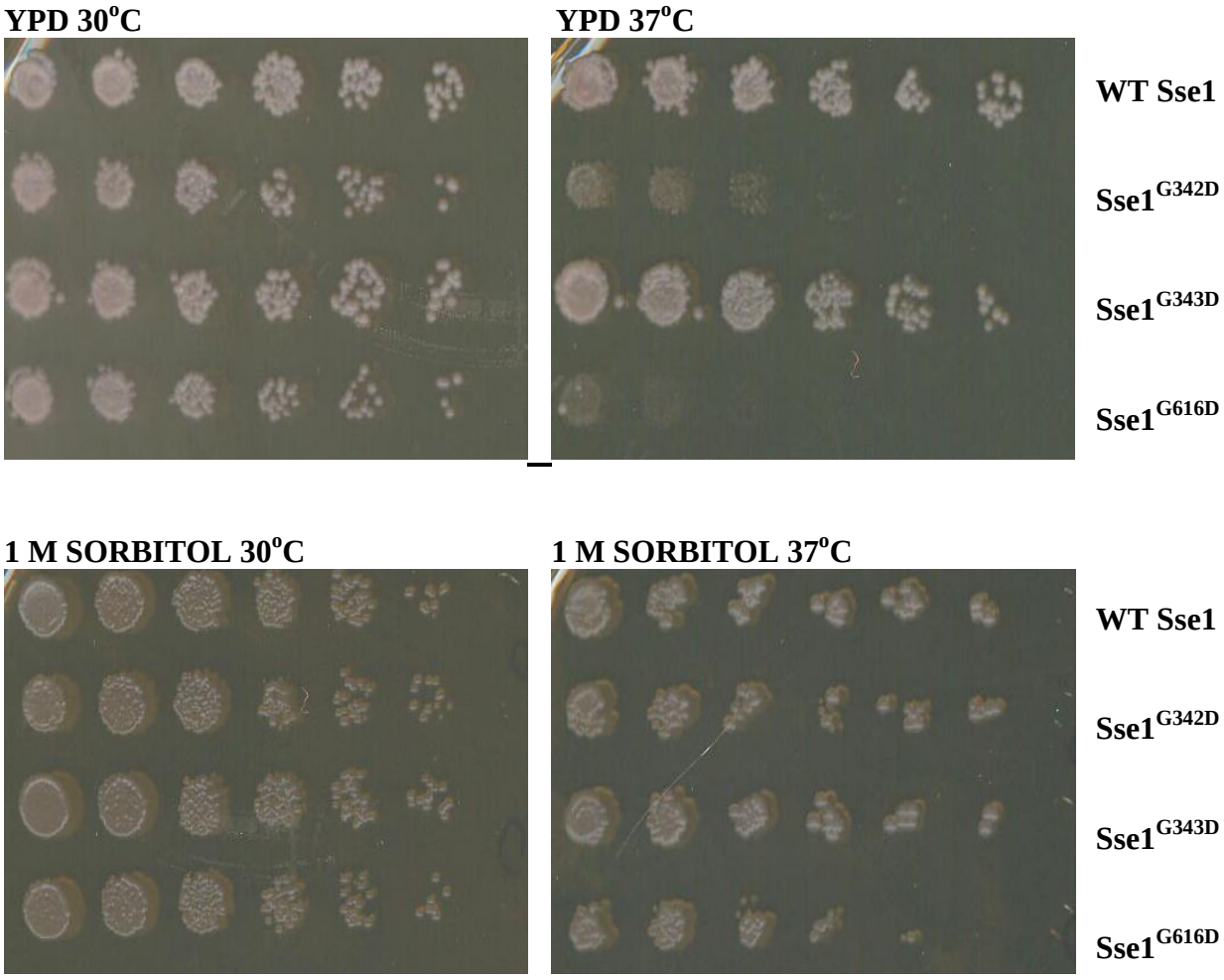

Figure 4.3. Comparative growth analysis performed on WT Sse1 and mutants G342D, G343D and G616D in strain CM02. The cells were serial diluted onto YPD and YPD + 1 M sorbitol and incubated at 30°C and 37°C for 2 days. 1 M sorbitol recovered normal growth in Sse1 mutants G342D and G616D.

4.2 Investigations into the role of Sse1 in cell wall integrity signaling

Exposure of *S. cerevisiae* to environmental stress such as heat and oxidative shock results in the activation of five separate mitogen-activated protein kinase (MAPK) cascades (Chen and Thorner, 2007). The cell wall integrity (CWI) signaling

pathway uses one of these MAP kinase cascades to mediate cell wall biosynthesis and maintenance (Levin, 2005). This cascade is initiated by cell wall stress sensors Mid2 and Wsc1 (Verna *et al*., 1997; Ketela *et al*., 1999) which ultimately leads to the activation of the kinase Pkc1 (Nonaka *et al*., 1995). Pkc1 activates a cascade of phosphorylation through MAP kinases which results in the activation of two transcription factors Rlm1 and SBF (Swi4/Swi6). These transcription factors trigger the expression of genes involved in cell wall synthesis (Madden *et al*., 1997; Jung *et al*., 2002). Figure 4.4 illustrates this cascade and the biological factors involved in its signaling.

Loss of function of any kinase or transcription factor in this cascade can lead to temperature-sensitive cell lysis that is remediated by osmotic support (Lee and Levin, 1992). Levin (2005) discusses in the review paper that other phenotypes seen by mutants of CWI signaling include sensitivity to cell wall damaging agents such as caffeine, calcofluor white and congo red (Martin *et al*., 2000; Errede *et al*., 1995).

A number of reports have linked protein chaperone function with CWI signaling (Millson *et al*., 2005; Piper *et al*., 2006). Shaner *et al*. (2008) proposed that Sse1 may be involved in CWI signaling. They performed co-immunoprecipitation assays and found that Sse1 co-purifies with the CWI signaling kinase Slt2. They also found that deletion of Sse1 results in osmoremedial temperature sensitivity and sensitivity to cell wall damaging agents, atypical characteristics of CWI signaling mutants. In this section the aim was to determine whether the temperature-sensitive (ts) mutants G342D and G616D were affecting this signaling cascade by performing a number of cell wall sensitivity tests.

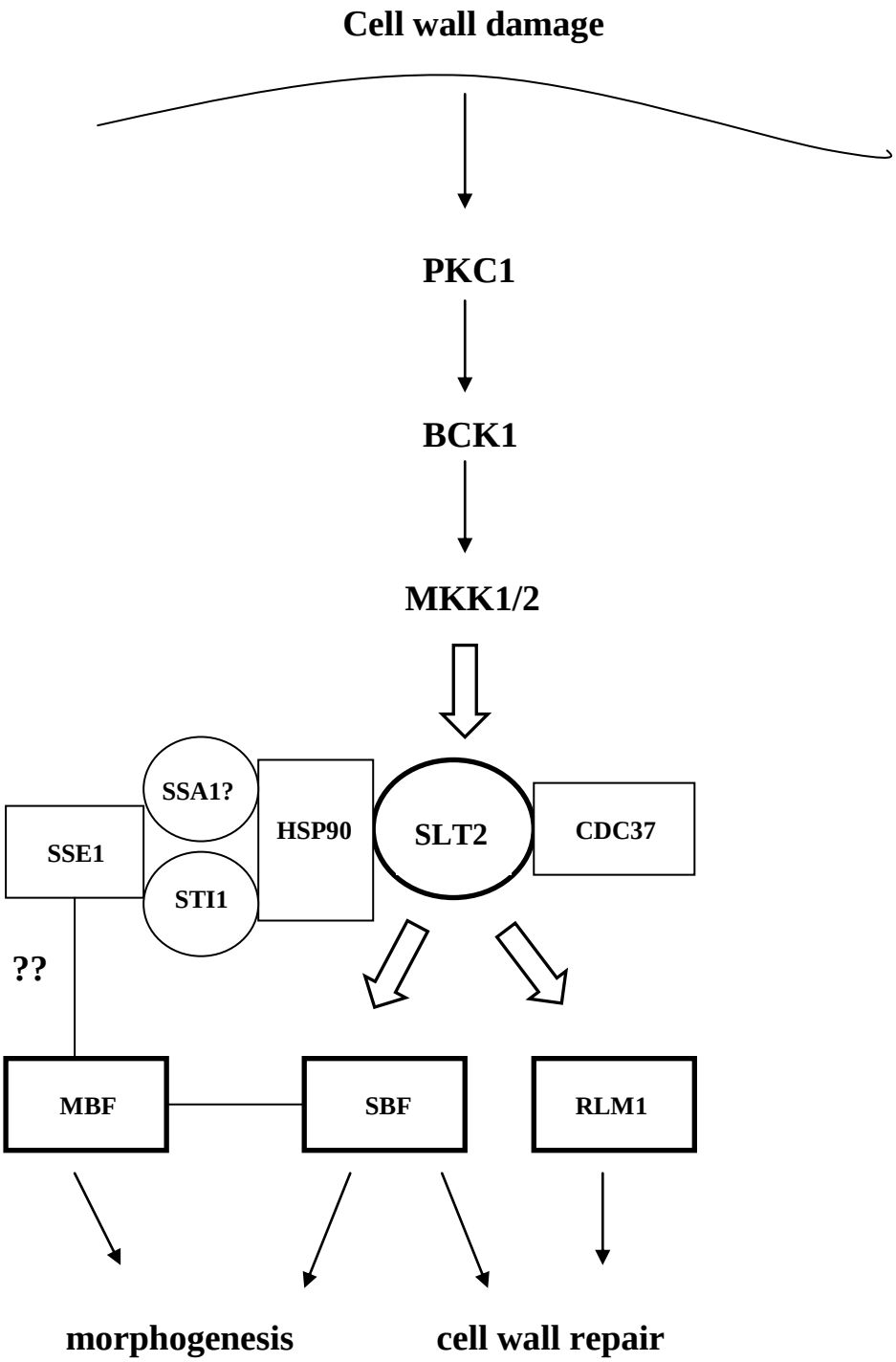

Figure 4.4. Cell wall integrity signaling pathway. The interaction of chaperones Hsp90, Sse1 and Sti1 with the terminal Slt2 Map kinase is believed to help signal through to transcription factors SBF and Rlm1. Chaperones may also play a role in the functions of MBF, a transcription factor that works alongside SBF in initiating cell morphogenesis. This figure is adapted from Shaner *et al*. (2008) and they also suggest a role for Ssa1 in this pathway.

4.2.1 Temperature-sensitive Sse1 mutants show sensitivity to cell wall damaging agents

Mutants of the MAP kinase cascade often display sensitivity to cell wall damaging agents. For example, deletion of the Rlm1 transcription factor renders cells caffeine sensitive (Watanabe *et al*., 1997). Shaner *et al*. (2008) showed that Δ*sse1* cells are sensitive to congo red and caffeine when compared to WT cells. Exposure of yeast cells to agents such as calcofluor white, caffeine and congo red leads to the disruption of the cell wall network and subsequent activation of the MAP kinase pathway (Ketela *et al*., 1999; De Nobel *et al*., 2000).

If the Sse1 temperature-sensitive mutants are defective in the CWI signaling pathway then they should show sensitivity to cell wall damaging agents. Comparative growth analysis was performed on CM02 with WT Sse1, $Sse1^{G342D}$ and $Sse1^{G616D}$. In some cases G600 WT strain and mutant $Sse1^{G343D}$ were also included as controls. The cells were selected on medium with varying concentrations of congo red, calcafluor white, caffeine and SDS and grown at 30^{o}C for 2 days (Figure 4.5 and 4.6). Interestingly, WT G600 was more resistant to chemical stress than CM02. This difference may be due to the absence of Sse2 in CM02. Mutants G342D and G616D were very sensitive to the chemical agents and looked slightly more sensitive than WT Sse1 when grown on SDS and calcafluor white. However, due to the varying degrees of sensitivity seen in all strains an accurate comparison could not be made. The temperature-sensitive mutants were sensitive to the cell wall damaging agents but strain CM02 also showed sensitivity. These results were suggestive but not conclusive that the Sse1 mutants may be affecting CWI signaling.

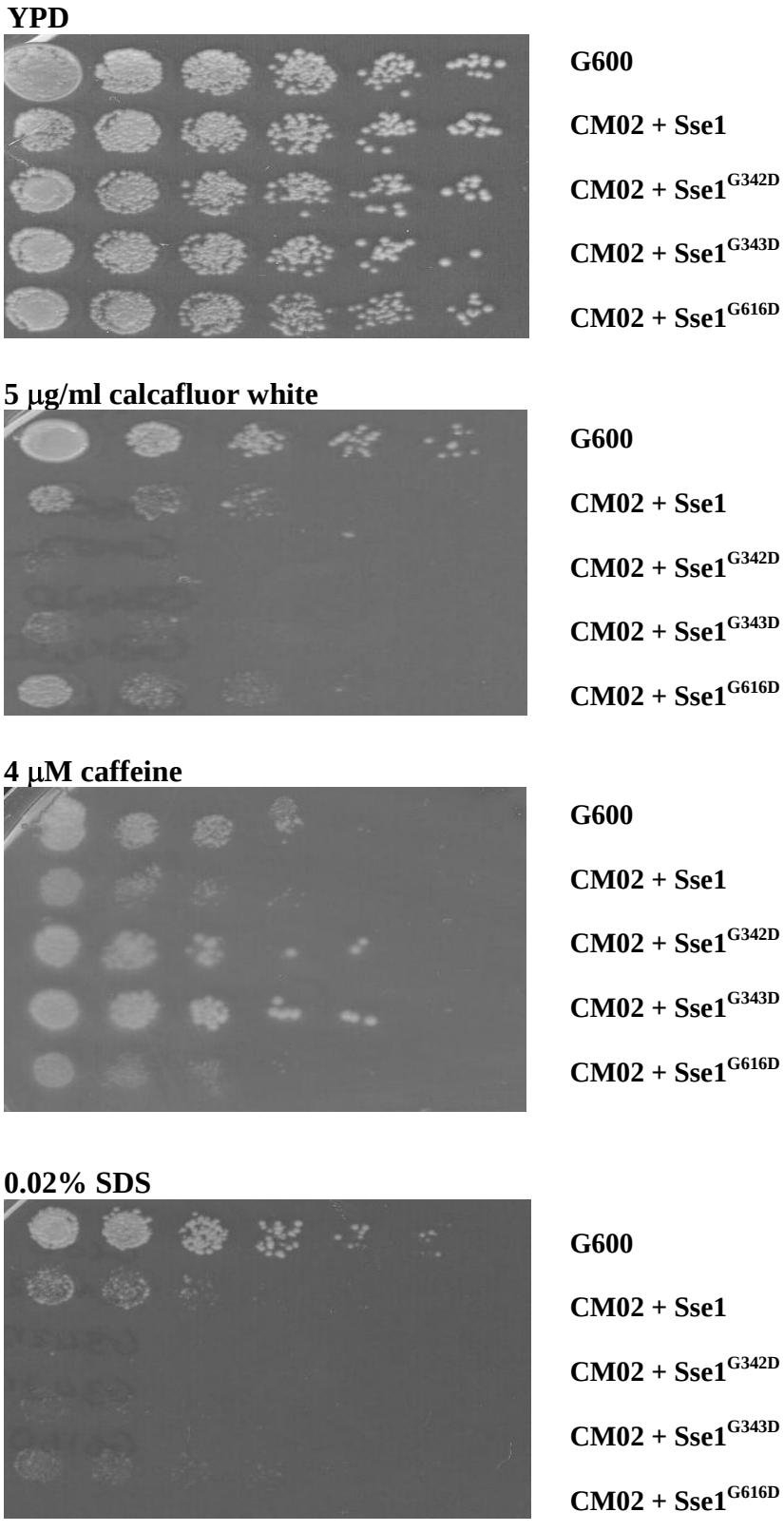

Figure 4.5. Comparative growth analysis of Sse1 mutants on cell wall damaging agents. Initial tests included WT G600 and mutant G343D as controls. The cells were spotted onto YPD plates that had varying concentrations of chemicals and incubated at 30^{o}C for 2 days. CM02 with WT Sse1 appears, in most cases, just as sensitive as all three Sse1 mutants.

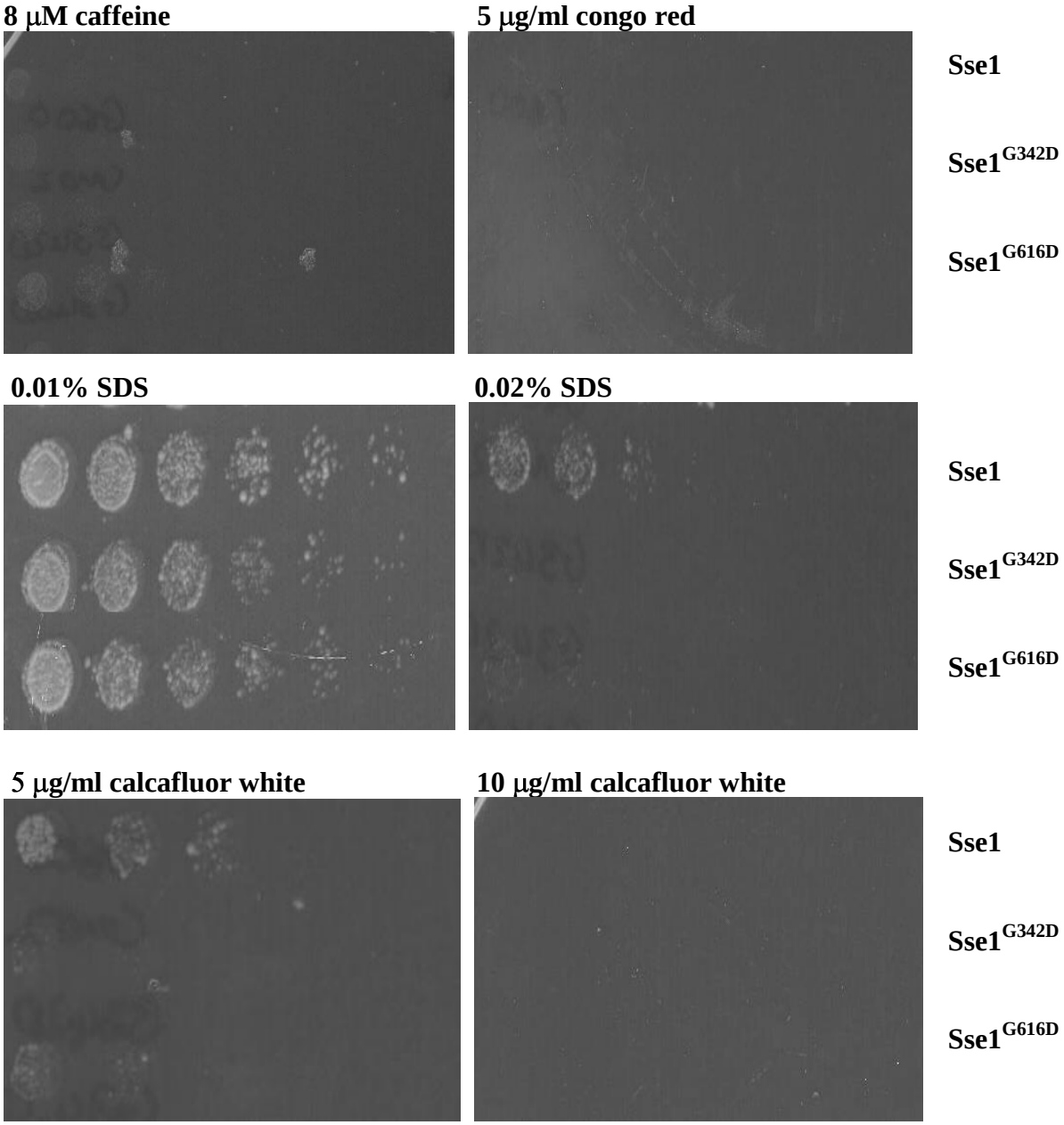

Figure 4.6. Comparative growth analysis of Sse1 mutants on cell wall damaging agents. The cells were spotted onto YPD medium that had varying concentrations of chemicals and incubated at 30^{o}C for 2 days. Strain CM02 was very sensitive to cell wall damaging agents even in the presence of WT Sse1. The lack of growth of mutants on SDS and calcafluor white suggests they could be affecting CWI but it is inconclusive due to strain sensitivity.

4.2.2 Can inducers of cell wall signaling recover growth in G342D and G616D?

Pkc1 and Bck1 are essential components of the CWI signaling pathway. Pkc1 (protein kinase C) transmits the first signal through the cascade in response to cell wall damage (Levin and Bartlett-Heukusch, 1992). Pkc1 phosphorylates Bck1 at several different sites (Levin *et al*., 1994). Bck1 (bypass of C kinase) phosphorylates Mkk1/2 which ultimately leads to the up-regulation of cell wall repair genes (Irie *et al*., 1993). Bck1 was first isolated as a suppressor of Pkc1 deletion (Lee and Levin, 1992).

The deletion of the *PKC1* gene results in the most severe growth defect shown by deletion of any of the members of the MAP kinase pathway. It is believed that Pkc1 regulates a multitude of biological pathways as it is the only protein kinase C isoform found in *S. cerevisiae* (Levin *et al*., 1990; Lee and Levin, 1992) compared to at least ten isoforms found in mammals (Mellor and Parker, 1998). Deletion of the *BCK1* gene also affects the growth and proliferation of yeast as it results in temperature-sensitive growth that is remediated by osmotically stabilising agents (Lee and Levin, 1992).

As Pkc1 and Bck1 are involved in the stimulation of cell wall repair the constitutively active forms of these proteins were expressed in the Sse1 temperature-sensitive mutants. This helped clarify whether or not the mutants were affecting the CWI pathway. Phosphorylated activated forms of Pkc1 and Bck1 were expressed on plasmids p241 and p636, respectively, and transformed into CM02 that expressed Sse1, G342D or G616D. Comparative growth analysis was performed and cells were incubated on SC - uracil medium for 2 days at 30^{o}C and 37^{o}C. *PKC1* and *BCK1* did appear to improve temperature-sensitive growth in mutants G342D and G616D at 37^{o}C, particularly in cells with p241*PKC1* (Figure 4.7.a/b).

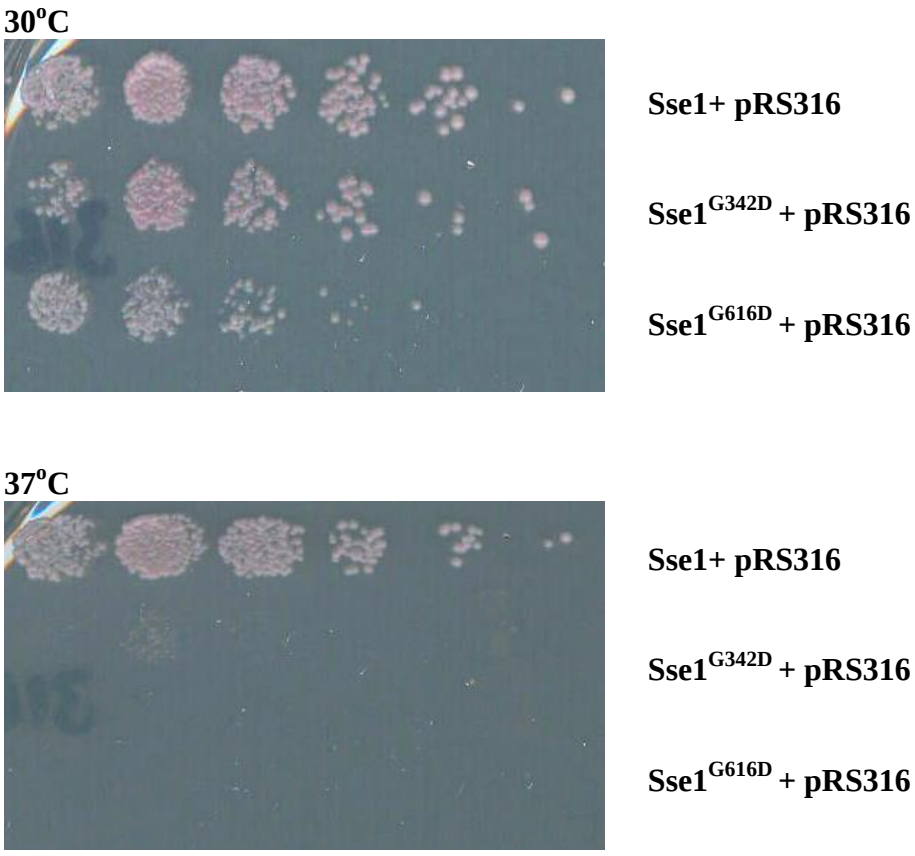

Figure 4.7.a. Comparative growth analysis of CM02 with WT Sse1 and temperature-sensitive mutants in the presence of pRS316 empty vector. The cells were selected on SC - uracil and incubated for 2 days at 30°C and 37°C. Mutants $Sse1^{G342D}$ and $Sse1^{G616D}$ both failed to grow at 37°C.

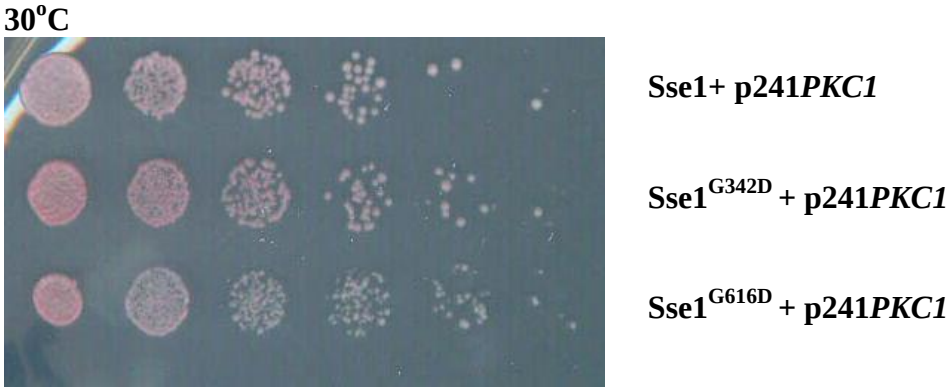

Figure 4.7.b. Comparative growth analysis of CM02 with WT Sse1 and temperature-sensitive mutants in the presence of plasmid p241*PKC1*. The cells were selected on SC - uracil and incubated for 2 days at 30°C and 37°C. Mutants Sse1^{G342D} and Sse1^{G616D} showed slightly enhanced growth at 37°C when p241*PKC1*was expressed.

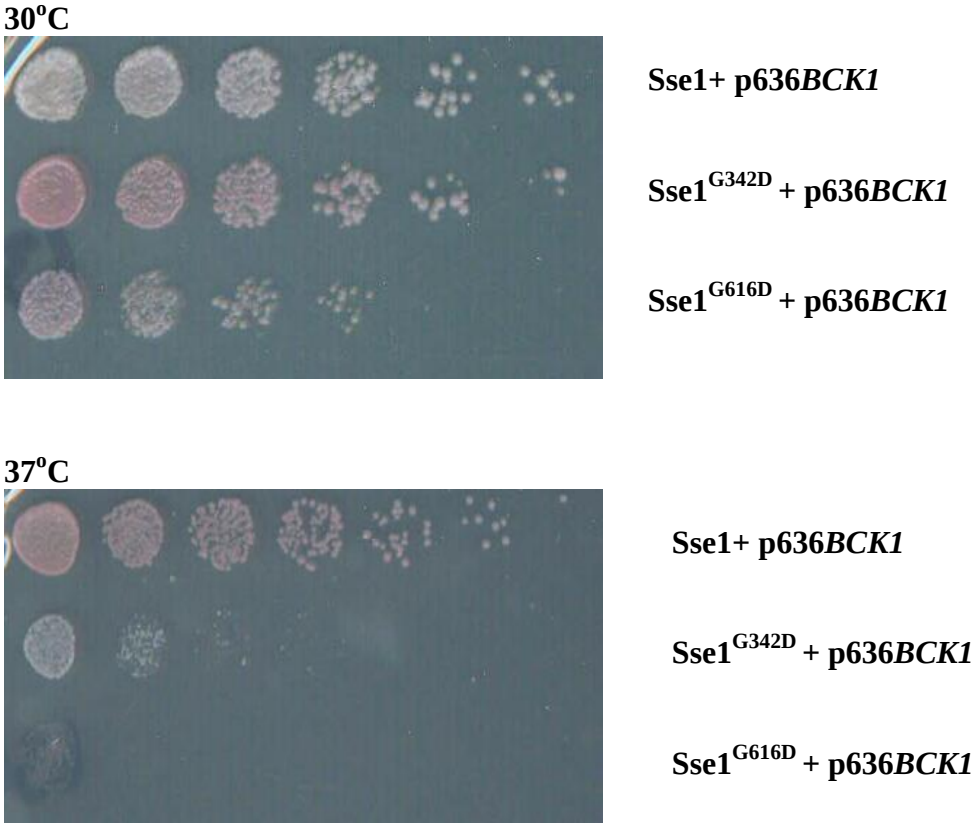

Figure 4.7.c. Comparative growth analysis of CM02 with WT Sse1 and temperature-sensitive mutants in the presence of plasmid p636*BCK1*. The cells were selected on SC - uracil and incubated for 2 days at 30°C and 37°C. Mutant Sse1^{G342D} showed slightly enhanced growth at 37°C when p636*BCK1* was expressed.

4.3 Isolation of second-site suppressor mutants that recover G342D and G616D temperature-sensitive phenotypes

Previous work in the laboratory has shown that the effects of a chaperone mutant on [*PSI*$^{+}$] propagation can be reversed by the addition of a second mutation to the protein structure (unpublished data). Isolating such mutants can help gain insight into the structural organisation of the protein and how altering particular residues affects intramolecular interactions. The aim was to isolate second-site suppressors (sss) of mutant G342D and G616D to restore Sse1 wild type phenotypes. The fact that G616D and G342D were ts and [*psi*$^{-}$] provided an opportunity to alter both these functions.

Second-site suppressors of a particular mutation can be isolated by treating the plasmid DNA with hydroxylamine as described in section 2.15. Once the mutant library was created it was transformed into CM02 along with WT Sse1, pRS315 and Sse1^{G342D} or Sse1^{G616D} and selected on SC - leucine medium. Approximately 4,000 colonies were screened for each library by replicating the plates onto 5-FOA. Two screens were carried out for each mutant library. One set of 5-FOA plates were incubated at 37^{o}C overnight and the other at 30^{o}C for 2 days. This enabled the isolation of ts revertants and [*psi*$^{-}$] revertants separately for both G342D and G616D. Isolation of potential sss is fully described in section 2.17.

The screen for sss which affect the mutant [*PSI*$^{+}$] phenotypes resulted in the isolation of pink colonies that, when restreaked, appeared [*psi*$^{-}$]. No white/[*PSI*$^{+}$] sss were isolated in this screen. No sss for G616D temperature sensitivity were isolated either, but potential G342D temperature-sensitive sss were isolated. Five potential G342D temperature-sensitive sss were isolated in the primary screen. These plasmids were isolated and transformed back into CM02 for further phenotypic analysis

(secondary screen). The potential sss were subsequently analysed by comparative growth analysis in order to assess whether they fully recovered temperature sensitivity at 37^{o}C (Figure 4.8). In the comparative growth analysis, isolate P9, P11 and P13 all showed a reproducible phenotype and were sent for sequencing. P9 returned as Sse1$^{G342D\ T100I}$ but P11 and P13 sequenced as WT Sse1 so perhaps hydroxylamine reverted them back to WT and they got through the screen as potential sss. Mutant T100I is located in the nucleotide binding domain of Sse1 and somehow altered Sse1^{G342D} in a way that modifies its temperature-sensitive phenotype. T100I also improved mutant G342D [*PSI*$^{+}$] phenotype slightly as it appeared pink on YPD at 30^{o}C. This means that this mutation may not be specific in its effects as it can improve G342D temperature-sensitive growth and possibly [*PSI*$^{+}$] propagation. This screen was not saturated as mutant T100I was only isolated once.

The difficulty in isolating Sse1 mutant sss could have been due to the low number of colonies screened. When transformed into yeast, the mutant library resulted in approximately 4,000 colonies per screen. Based on similar mutational studies on *SSA1* and Hsp104 plasmid DNA the rate of mutant generation is approximately 8%. The low number of colonies that went through the screen in this experiment would have only produced 320 mutants. It was disappointing that T100I was the only mutant to produce a desirable phenotype and this did not indicate much about the Sse1 structure. The fact that 2 mutants were WT reverts suggested that the screen was not worth pursuing.

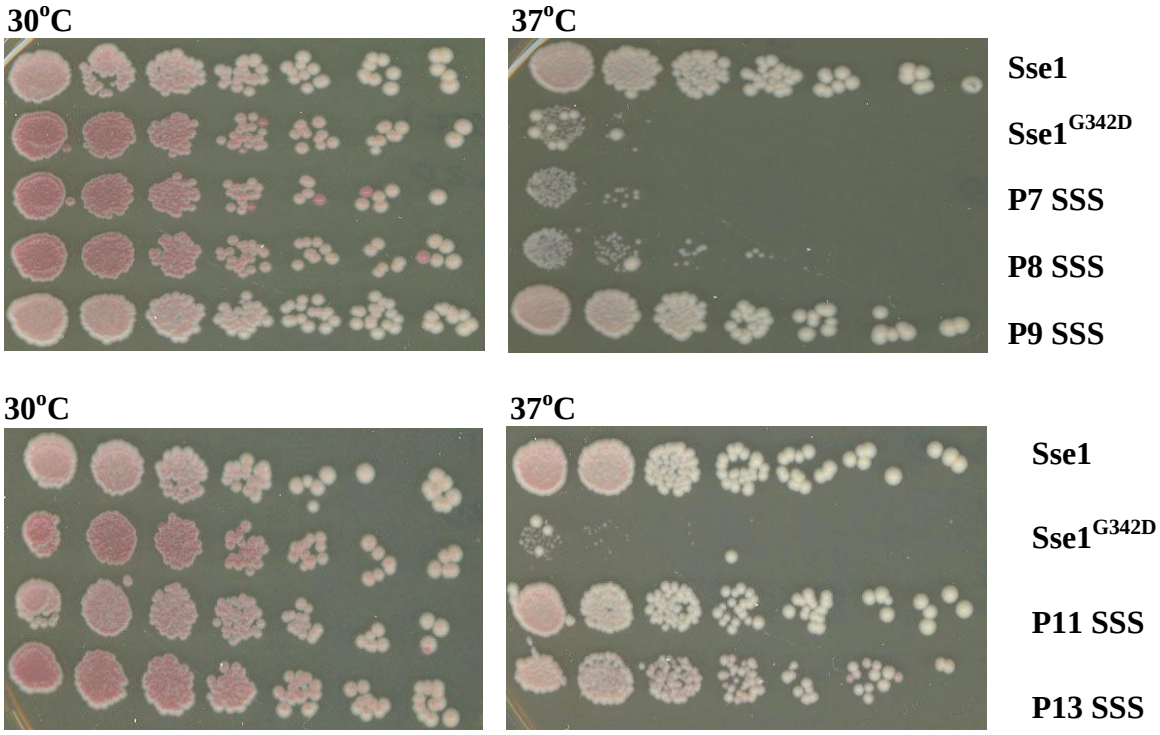

Figure 4.8. Recovery of Sse1^{G342D} mutant temperature sensitivity by second-site suppressor T100I. Comparative growth analysis was performed on YPD medium and grown for 3 days at 30°C and 37°C. Cells were grown for 3 days to allow colony colour to develop and to confirm definite ts recovery phenotypes. Plasmid P9, P11 and P13 all recovered growth at 37°C. Each plasmid was sent to Agowa for sequence analysis.

4.4 Creating a BY4741 Δ*sse1*Δ*sse2* strain to compare growth and sensitivity with CM02

4.4.1 Reasoning behind making BY4741 Δ*sse1*Δ*sse2*

The results from tests carried out in section 4.2.1 prompted the creation of a new Hsp110 deletion strain. CM02 with WT Sse1 was non-viable on YPD containing 5 μg/ml of congo red, 10 μg/ml calcofluor white and non-viable on high concentrations of caffeine. These results can be compared to those found by Shaner *et al*. (2008). They expressed Sse1 in a BY4741 Δ*sse1*Δ*sse2* strain and found that cells were sensitive but survived on media containing up to 30 μg/ml calcofluor white and 10 μM caffeine.

CM02 appeared to have strain background effects which disrupted sensitivity tests. Strain BY4741 is more widely used for CWI signaling analysis so a new strain was generated. This would help to compare our results to those from other studies. Euroscarf strains Y02146 (*MAT***a***his3Δ1leu2Δ0 met15Δ0 ura3Δ0 sse1::kanMX)* and Y17167 (*MAT*α *his3Δ1leu2Δ0 lys2Δ0 ura3Δ0 sse2*::*kanMX)* were purchased, in order to create BY4741 Δ*sse1*Δ*sse2* double knockout. BY4741 has no *ade2.1* ochre mutation so [PSI^{+}] phenotypes could not be monitored.

4.4.2 Confirmation of BY4741 Δ*sse1*Δ*sse2* knockout strain

Euroscarf strains Y02146 and Y17167 were mated on SD + histidine, leucine and uracil medium. The diploids were selected as being able to grow without supplemented methionine or lysine. A copy of plasmid pRS316*SSE1* was transformed into the diploid strain. This enabled the selection of haploid Δ*sse1*Δ*sse2* cells after sporulation. Diploid cells were sporulated on minimal sporulation medium and random spore analysis was performed. The cells were selected on SC - uracil medium and colonies were replicated onto 5-FOA medium (Figure 4.9) to select against any cells expressing pRS316*SSE1*. Colonies that were non-viable without pRS316*SSE1* were selected as potential Δ*sse1*Δ*sse2* haploid cells. Figure 4.10 represents the test carried out to determine the genotype of the knockout strains. Single BY4741 *sse1* and *sse2* mutants had either a *lys2* or *met15* mutation but each of the four potential double knockouts had wild type genomic variants of these mutations. This was proven by strain growth on medium lacking lysine or methionine (Figure 4.10).

Four potential Δ*sse1*Δ*sse2* strains were selected and their DNA isolated as described in section 2.11.1. Diagnostic PCRs were performed using primers sse03, sse04, sse05, sse06, kan01 and kan02 (Table 2.12.a). PCR cycles are described in

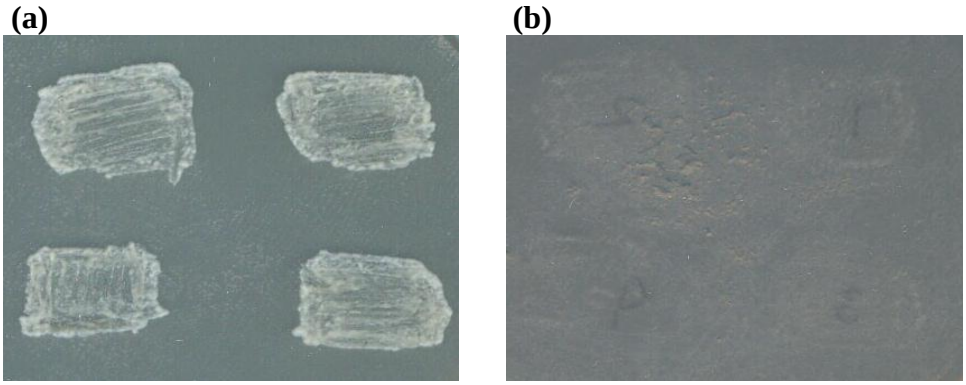

Figure 4.9. Confirming *sse1* and *sse2* knockout in BY4741. After diagnostic PCR analysis four haploid BY4741 yeast strains had a Δ*sse1*Δ*sse2* genotype. (a) They were selected on SC - uracil and (b) replicated onto 5-FOA to confirm that the removal of pRS316*SSE1* results in cell death.

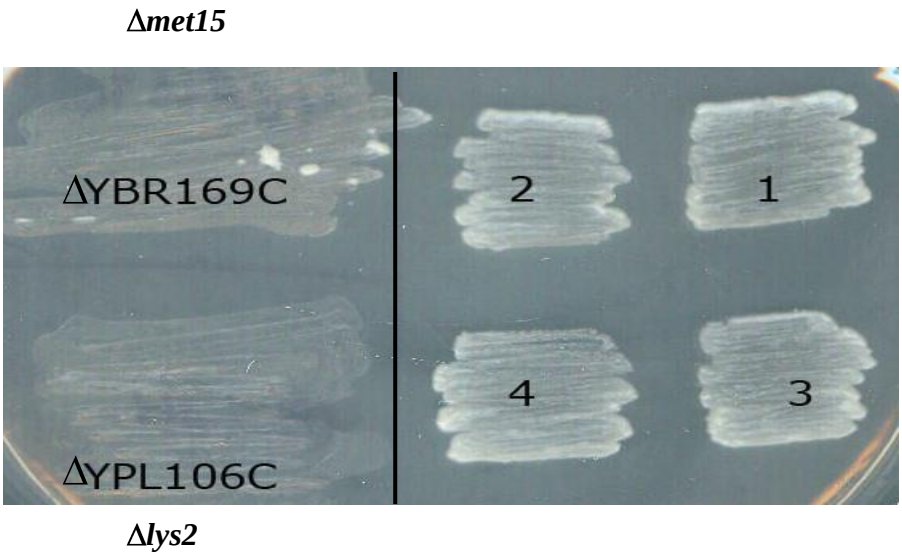

Figure 4.10. Determining the *lys2*/*met15* genotype of BY4741 Δ*sse1*Δ*sse2*. Euroscarf strains ΔYBR169C (*his3*Δ*1 leu2*Δ*0 met15*Δ*0 ura3*Δ*0 sse1::kanMX*) and ΔYPL106C (*his3*Δ*1 leu2*Δ*0 lys2*Δ*0 ura3*Δ*0 sse2*::*kanMX*) were selected on SD + histidine + leucine alongside four double knockouts of Δ*sse1*Δ*sse2*. Each double mutant survived in the absence of methionine and lysine. CM03 isolate 1 genotype is *MAT***a** *his3*Δ*1 leu2*Δ*0 ura3*Δ*0 sse1*::*kanMX sse2*::*kanMX* pRS316*SSE1*.

Table 2.11. Figures 4.12 and 4.14 illustrate the diagnostic PCRs ran on 0.8% agarose gels and Figures 4.11 and 4.13 annotate these band fragment sizes. Figures 4.12 and 4.14 represent PCRs performed on isolated DNA samples GP1-4. All four strains

were confirmed as Δ*sse1*Δ*sse2* haploid cells but the gels illustrate the presence of knockout construct flanking regions for GP1 only (Figure 4.12 and 4.14). The strain was designated CM03 and had the following genotype; *MAT***a** *his3*Δ*1 leu2*Δ*0 ura3*Δ*0 sse1*::*kanMX sse2*::*kanMX* pRS316*SSE1*.

(1) Wild type

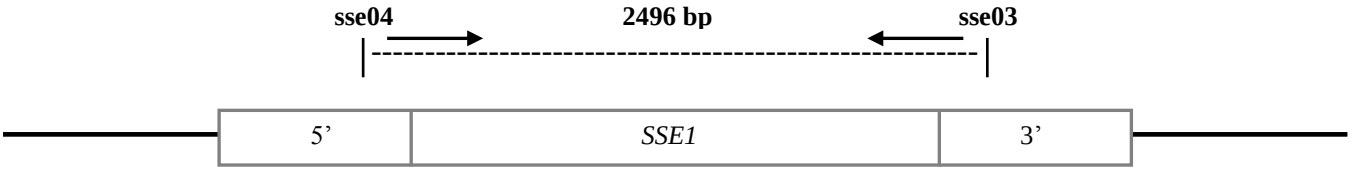

(2) Δ*sse1*

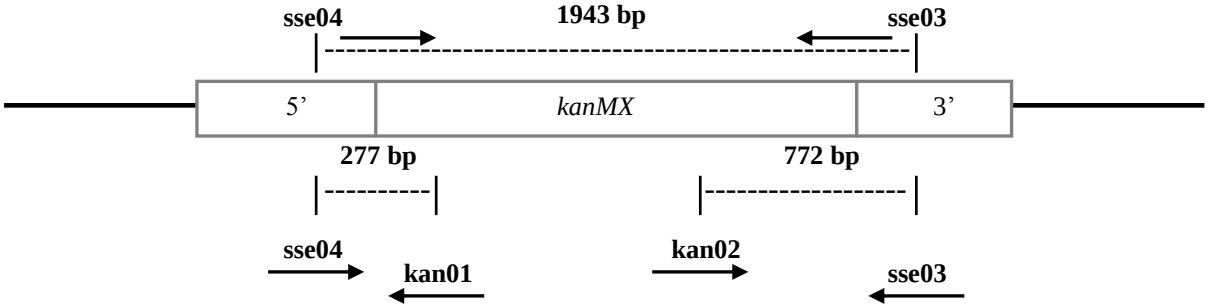

Figure 4.11. Illustration shows the expected wild type *SSE1* and Δ*sse1* PCR fragment sizes. (1) *SSE1* wild type DNA coding sequence is 2082 bp. Primers sse03R and sse04F are located upstream and downstream of the *SSE1* coding sequence. PCR using these primers should result in a DNA band of approximately 2496 bp. (2) illustrates an *sse1* knockout construct with *kanMX* gene replacing the coding sequence of *SSE1*. PCR using primers sse03R and sse04F should result in a band approximately 1943 bp in size. Internal kan01R and kan02F primers used with external sse03R and sse04F primers should result in two bands of 277 bp and 772 bp and confirms *SSE1* is replaced with *kanMX*.

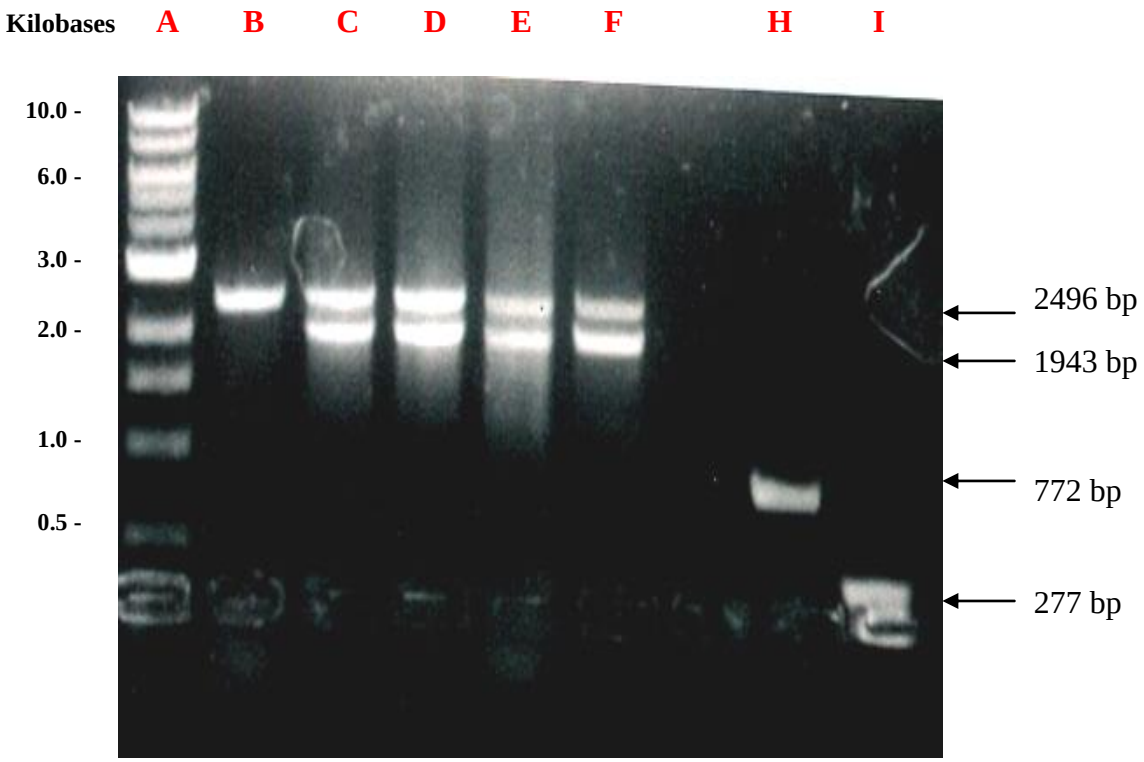

Figure 4.12. PCR confirmation of *sse1* knockout in strain CM03 by agarose gel electrophoresis. PCR is represented by GP1 DNA isolate.

Lane A: 1kb molecular weight marker

Lane B: G600 genomic DNA amplified with primers sse03 and sse04 results in a 2496 bp band for wild type *SSE1*.

Lane C-F: Four potential *sse1* knockouts (GP1-4). Genomic DNA amplified with primers sse03 and sse04 results in two DNA bands. The 2496 bp band is wild type *SSE1* on pRS316 plasmid. The 1943 bp band is *kanMX* DNA replacing genomic *SSE1*.

Lane H: GP1 genomic DNA amplified with primers kan02 and sse03. The 772 bp band represents the right flanking region of *kanMX* knockout construct.

Lane I: GP1 genomic DNA amplified with primers kan01 and sse04. The 277 bp band represents the left flanking region of *kanMX* knockout construct.

(1) Wild type

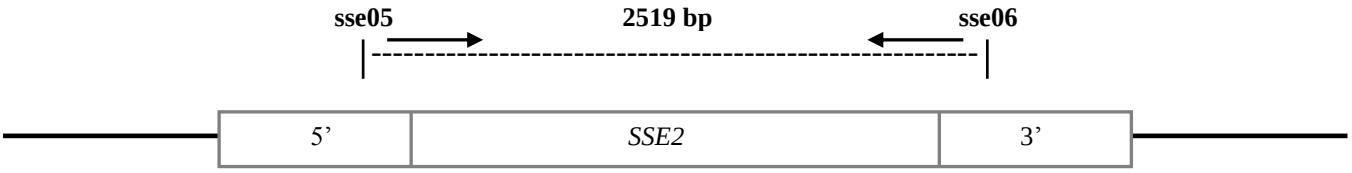

(2) Δ*sse2*

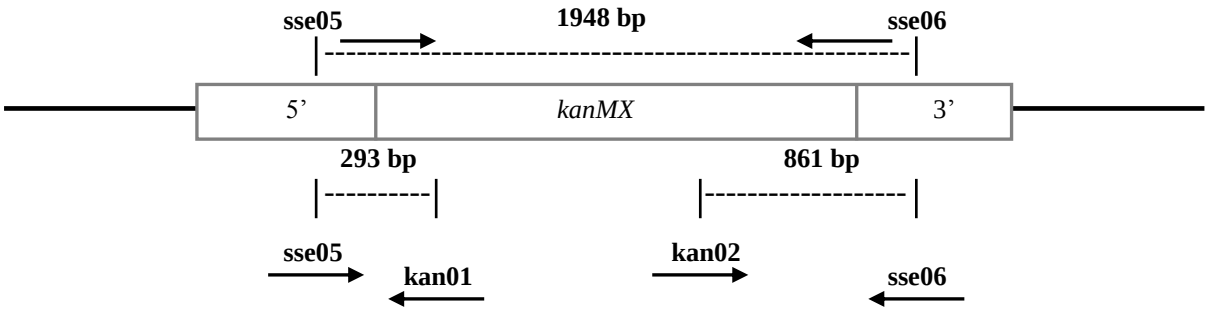

Figure 4.13. Illustration shows the expected wild type *SSE2* and Δ*sse2* PCR fragment sizes. (1) *SSE2* wild type DNA coding sequence is 2082 bp. Primers sse05F and sse06R are located upstream and downstream of the *SSE2* coding sequence. PCR using these primers should result in a DNA band of approximately 2519 bp. (2) illustrates an *sse2* knockout construct with *kanMX* gene replacing the coding sequence of *SSE2*. PCR using primers sse05F and sse06R should result in a band approximately 1948 bp in size. Internal kan01R and kan02F primers used with external sse05F and sse06R primers should result in two bands of 293 bp and 861 bp and confirms *SSE2* is replaced with *kanMX*.

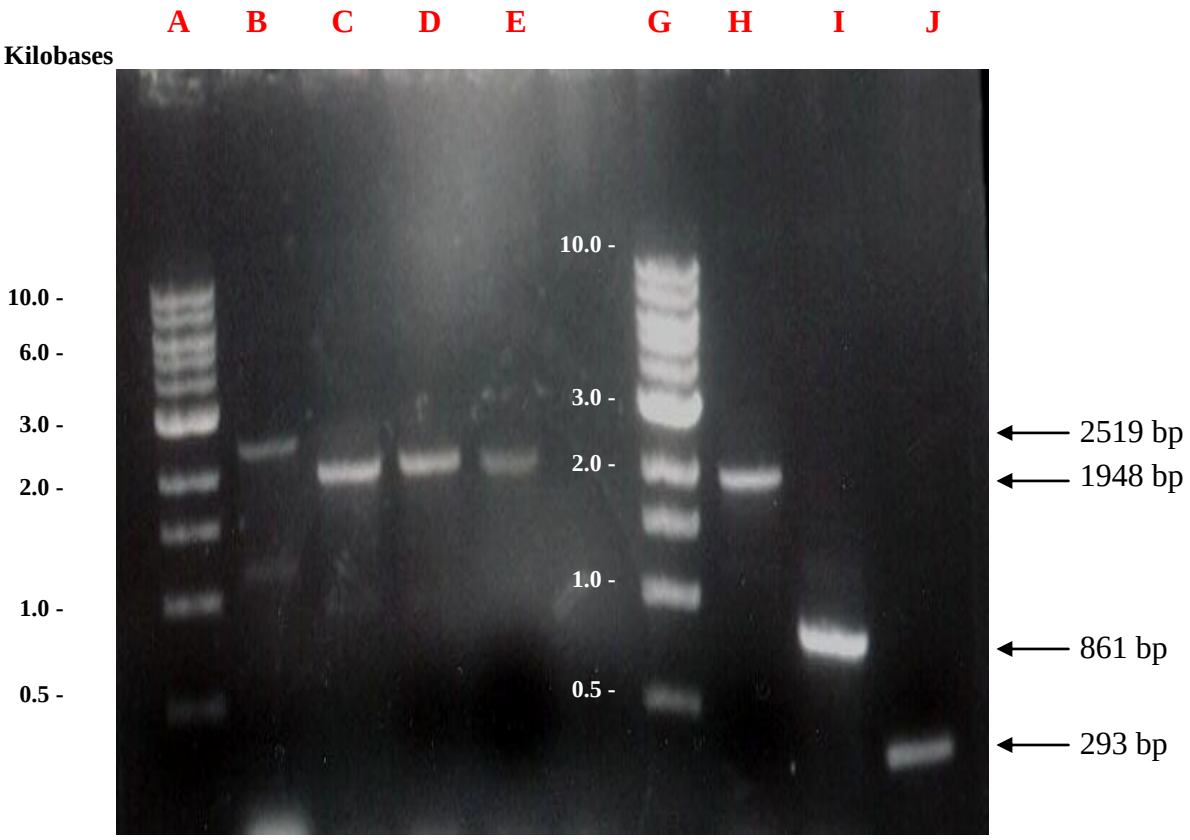

Figure 4.14. PCR confirmation of *sse2* knockout in strain CM03 by agarose gel electrophoresis.

Lane A: 1kb molecular weight marker.

Lane B: G600 genomic DNA amplified with primers sseo5 and sse06 results in a 2519 bp band for wild type *SSE2*.

Lane C-E: GP1-3 genomic DNA amplified with primers sse05 and sse06 results in a 1948 bp band which is *kanMX* DNA replacing genomic *SSE2*.

Lane G: 1kb molecular weight marker.

Lane H: GP1 genomic DNA amplified with primers sse05 and sse06 results in a 1948 bp band.

Lane I: GP1 genomic DNA amplified with primers kan02 and sse06. The 861 bp band represents the right flanking region of *kanMX* knockout construct.

Lane J: GP1 genomic DNA amplified with primers kan01 and sse05. The 293 bp band represents the left flanking region of *kanMX* knockout construct.

4.5 Testing temperature sensitivity of Sse1^{G342D} and Sse1^{G616D} in strain CM03

Sse1 mutants G342D and G616D displayed temperature-sensitive growth in strain CM02 at 37^{o}C. In order to confirm their temperature-sensitive phenotype they were expressed in the new BY4741 strain CM03. Mutants were transformed into CM03 and replicated onto 5-FOA to remove pRS316*SSE1* (Figure 4.15). Comparative growth analysis was performed on YPD, including wild type Sse1 and Sse1^{G343D} as controls, and plates were incubated at 30^{o}C and 37^{o}C for 2 days. The results from this experiment suggested that G616D is a temperature-sensitive mutant and that G342D is only slightly sensitive at 37^{o}C (Figure 4.16). Growth at 37^{o}C on 1 M sorbitol also fully restored the growth of both ts mutants (Figure 4.16). Plasmids p241*PKC1,* p636*BCK1* and pRS316 control were transformed into each strain and comparative growth analysis was performed on SC - uracil medium. The plates were incubated at 37^{o}C for 2 days and the results confirmed that G342D is not a non-viable mutant in CM03 but slow-growing and that the activation of Pkc1 or Bck1 cannot recover growth in mutant G616D (Figure 4.17). This suggested that the Pkc1 and Bck1 recovery phenotype observed in CM02 was strain specific and that these mutants may not be disrupting CWI signaling.

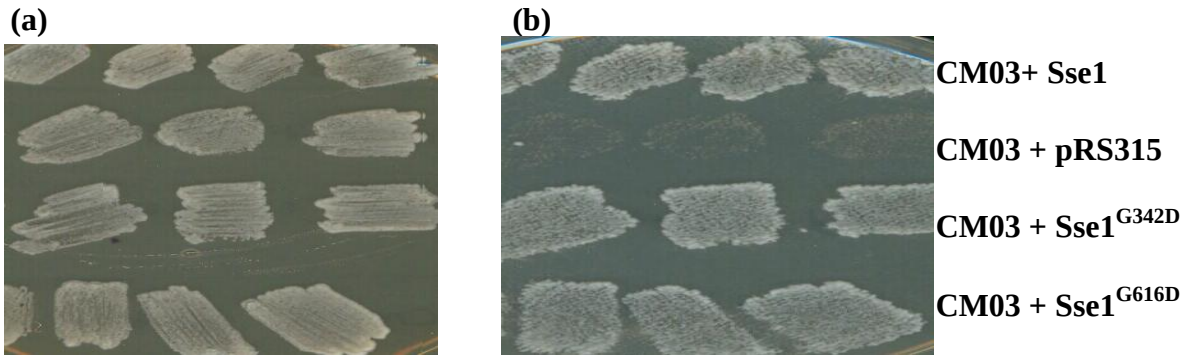

Figure 4.15. Transformation of Sse1 mutants into strain CM03. (a) Each transformant was selected on SC - leucine followed by (b) replication onto 5-FOA to select against pRS316*SSE1*.

(a) YPD 30°C

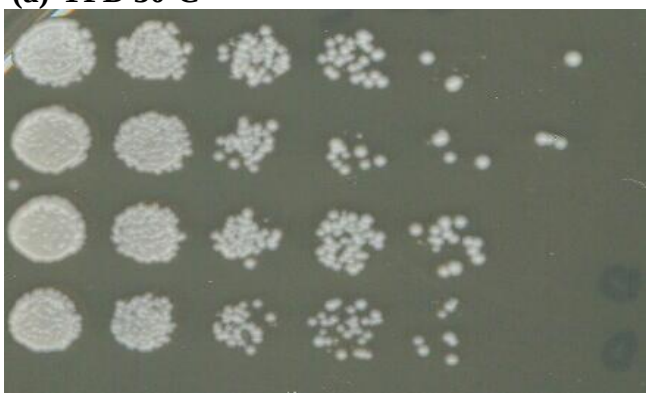

CM03+ Sse1

CM03 + Sse1^{G342D}

CM03 + Sse1^{G343D}

CM03 + Sse1^{G616D}

(b) YPD 37°C

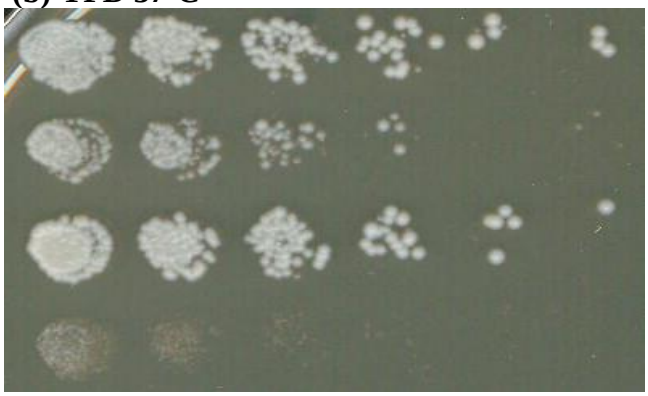

CM03+ Sse1

CM03 + Sse1^{G342D}

CM03 + Sse1^{G343D}

CM03 + Sse1^{G616D}

(c) YPD + 1 M sorbitol 37°C

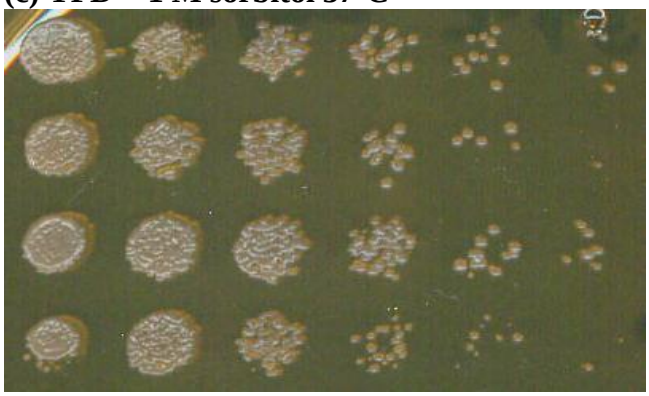

CM03+ Sse1

CM03 + Sse1^{G342D}

CM03 + Sse1^{G343D}

CM03 + Sse1^{G616D}

Figure 4.16. Analysis of temperature-sensitive status of Sse1 mutants in CM03. Mutants G342D, G343D and G616D were subjected to comparative growth analysis on YPD medium and YPD + 1 M sorbitol medium and incubated at 30°C and 37°C. (b) This confirmed that G616D is a ts mutant as it was non-viable at 37°C, however G342D did show some growth at 37°C. (c) 1 M sorbitol fully recovered G616D at 37°C. This suggested that G616D may still impair CWI signaling.

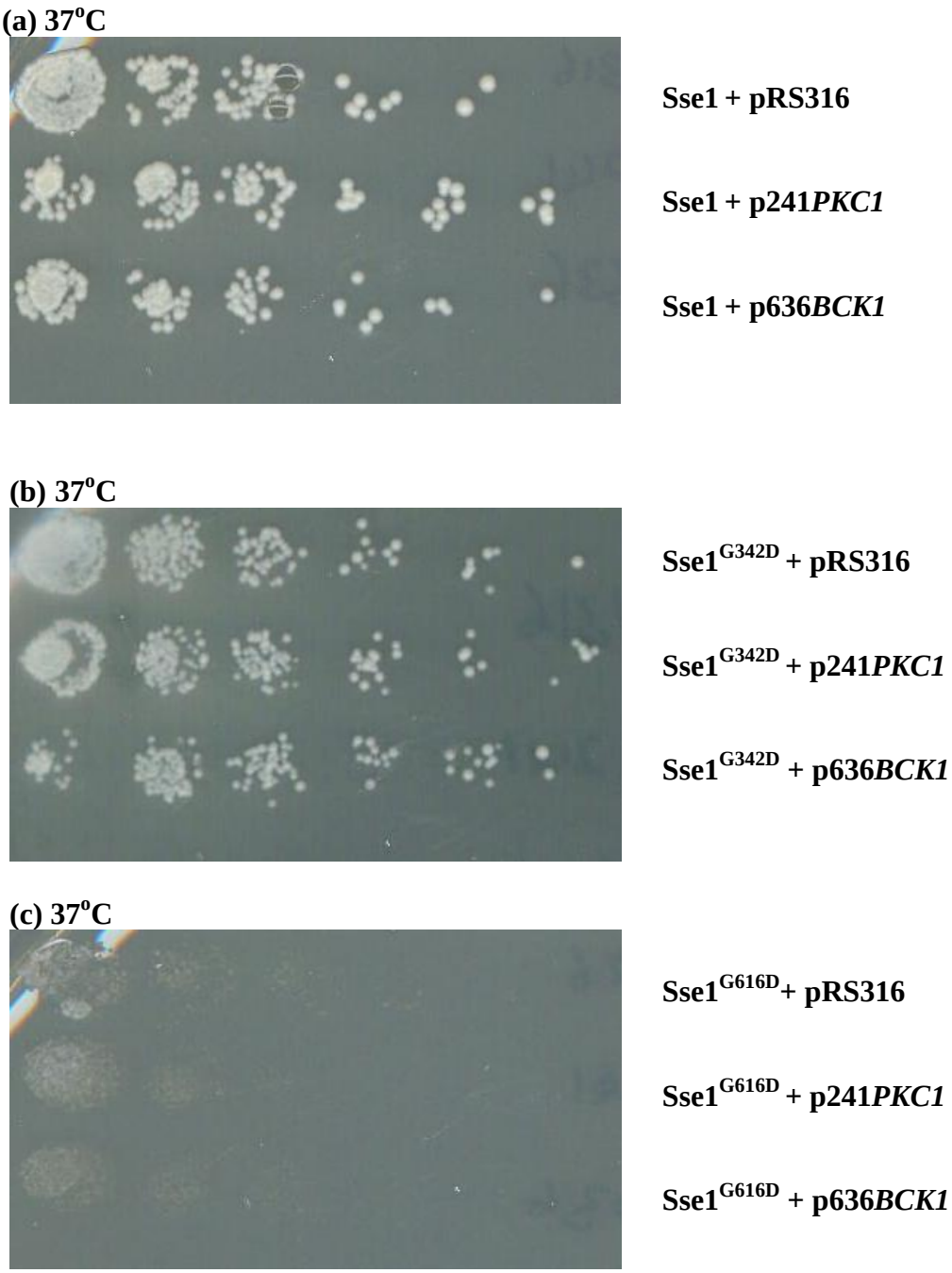

Figure 4.17. Analysis of the effects of Pkc1 and Bck1 over-expression in CM03. CM03 + Sse1, Sse1^{G342D} and Sse1^{G616D} were transformed with p241*PKC1*, p636*BCK1* and pRS316. Comparative growth analysis was performed on SC - uracil medium and plates were incubated for 2 days at 37^{o}C. (c) Pkc1 and Bck1 activation failed to recover G616D ts in strain CM03. (b) G342D control did not show any temperature sensitivity.

4.6 Analysis of CM03 sensitivity to cell wall damaging agents in the presence of WT Sse1 and Sse1 mutants

Sse1 temperature-sensitive mutants were transformed into strain CM03 for comparative growth analysis on YPD, caffeine, congo red, calcofluor white and SDS. A BY4741 Δ*slt2* strain was used as a control as it represents a mutant of CWI signaling.

Slt2 (Mpk1) is activated in response to cell wall perturbations. Treatment of WT cells with congo red and calcofluor white has been shown to strongly induce Slt2 phosphorylation (De Nobel *et al*., 2000). Stimulation of Slt2/Mpk1 results in phosphorylation of Rlm1 and SBF, transcription factors that induce the expression of cell wall synthesis genes (Madden *et al*., 1997; Dodou and Treisman, 1997). A Δ*slt2* strain was included in this study as a control that should show sensitivity to cell wall damaging agents.

The first thing noticed from the results of this experiment was that CM03 grew better on the chemical agents than CM02 did (Figure 4.18.a/b). However there was no difference in sensitivity between WT Sse1 and Sse1 mutants which indicated that the ts mutants may not affect CWI signaling after all. Δ*slt2* was selective in the agents it was sensitive to. It showed no sensitivity to SDS and grew relatively well on low concentrations of caffeine. Δ*slt2* was particularly sensitive to congo red even at concentrations of only 5 μg/ml which is substantial when the Sse1 ts mutants survived on concentrations up to 25 μg/ml. Δ*slt2* and CM03 were both very sensitive to calcofluor white but Sse1 did grow better as Δ*slt2* was non-viable at concentrations of 30 μg/ml (Figure 4.18.a/b).

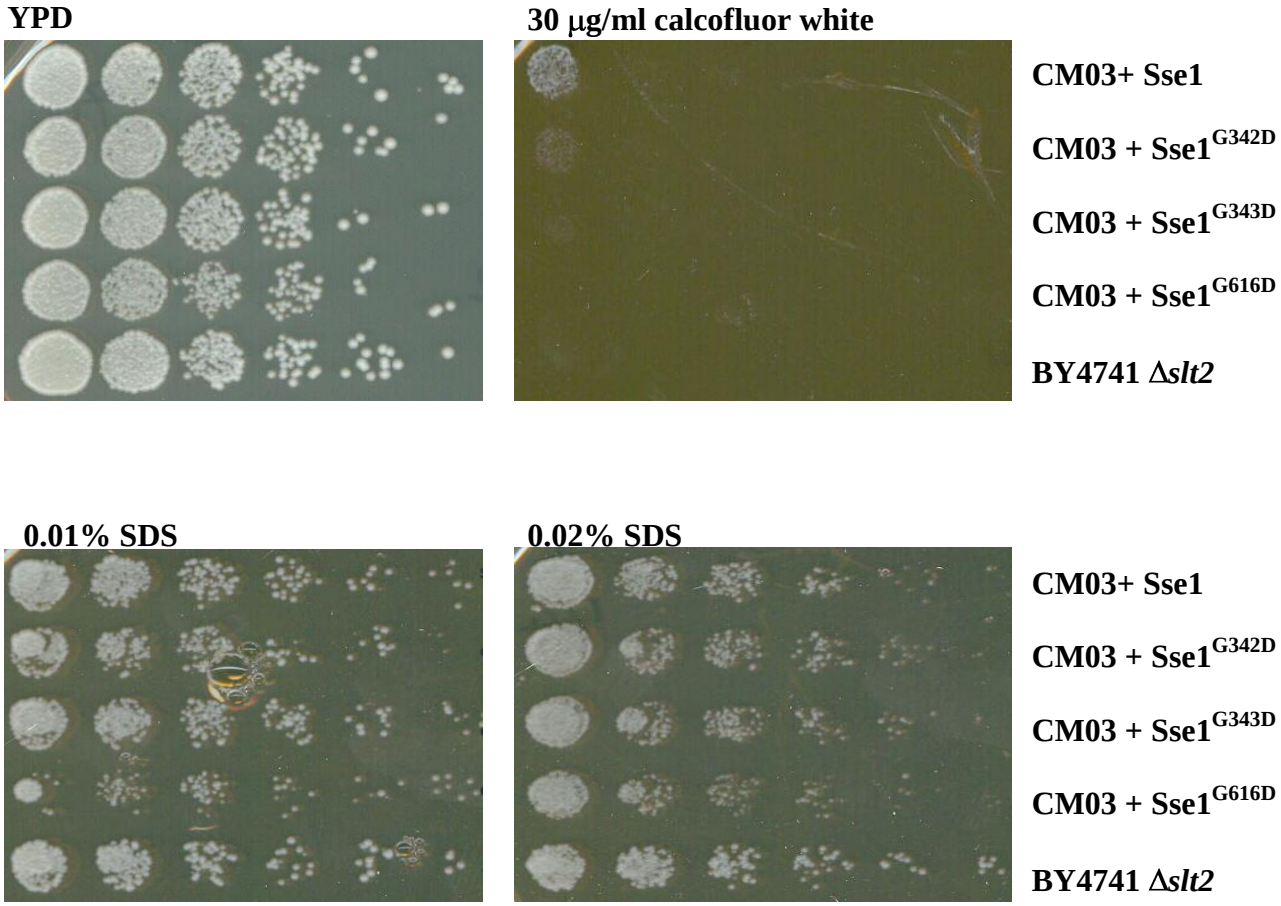

Figure 4.18.a. Testing the sensitivity of strain CM03 to SDS and calcofluor white. Comparative growth analysis was performed on WT Sse1, Sse1^{G342D}, Sse1^{G343D}, Sse1^{G616D} and BY4741Δ*slt2*. The cells were selected on YPD or YPD with varying concentrations of cell wall damaging agents. CM03 was sensitive to calcofluor white and all strains were non-viable at concentrations above 30 μg/ml. For SDS, strains grew relatively well with G616D being slightly more sensitive. Δ*slt2* grew well on SDS but failed to grow on calcofluor white.

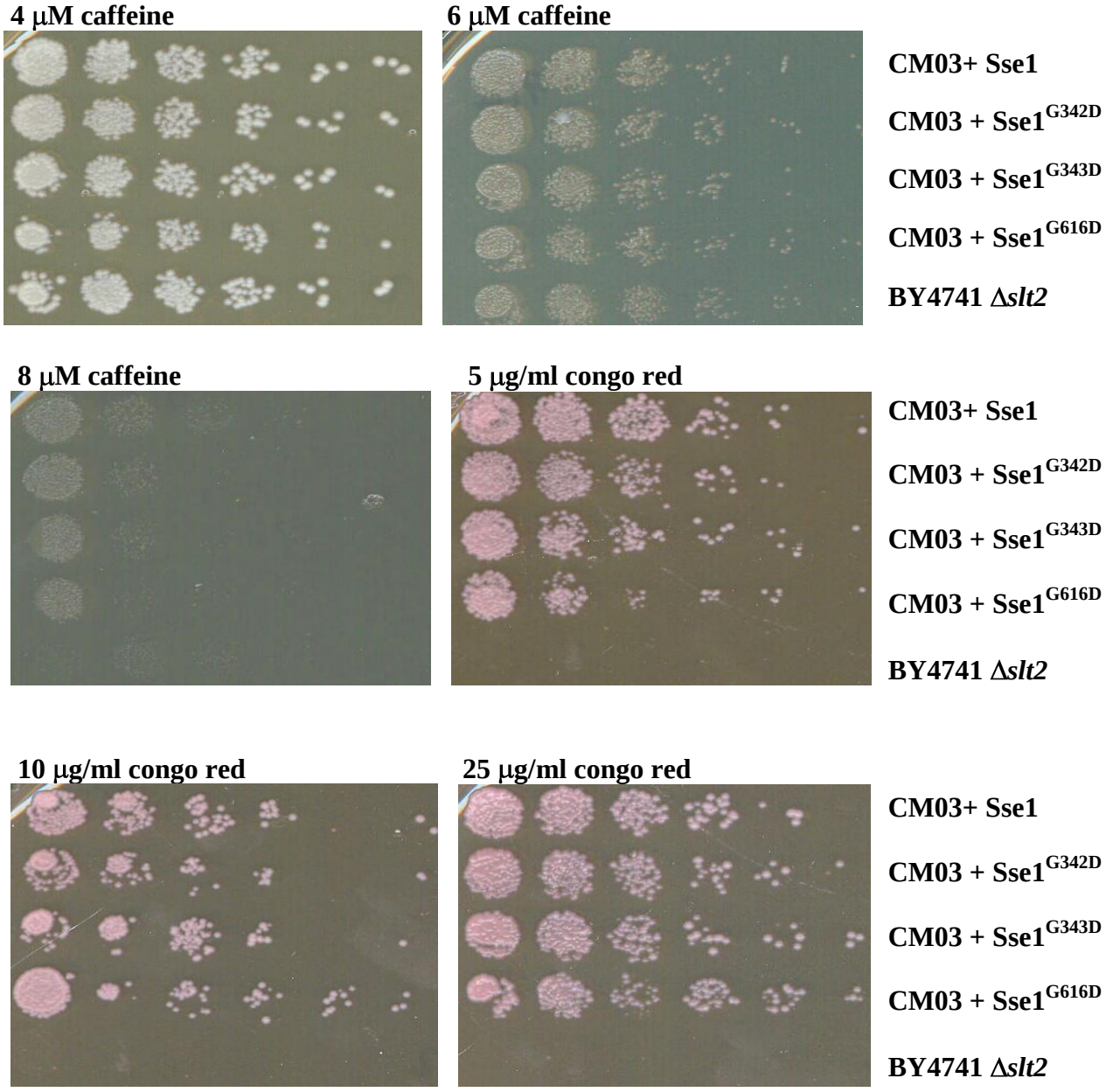

Figure 4.18.b. Testing the sensitivity of strain CM03 to caffeine and congo red. Comparative growth analysis was performed on WT Sse1, Sse1^{G342D}, Sse1^{G343D}, Sse1^{G616D} and BY4741Δ*slt2*. The cells were selected on YPD or YPD with varying concentrations of cell wall damaging agents. CM03 was sensitive to high concentrations of caffeine but there was no distinguishable difference between WT and mutant growth. Δ*slt2* was non-viable even at 5 μg/ml congo red but was not sensitive to low concentrations of caffeine.

4.7 Analysis of the effects of Sse1 temperature-sensitive mutants on Hsp90 signaling

Hsp90 is an essential cytosolic yeast chaperone that was first isolated as a regulator of steroid hormone receptors (Pratt, 1998). Hsp90 is one of the most abundant eukaryotic cytosol proteins which has stress-related and cellular house-keeping functions (Mayer and Bukau, 1999). It has since been elucidated that Hsp90 forms the core of a large macromolecular complex that includes other co-chaperones, co-factors and substrates (Zhao *et al*., 2005). It plays a central role in cell signaling by maintaining the activity of protein kinases and it is also functionally required at a higher level in response to cell thermal stress (Nathan *et al*., 1997; Zhao *et al*., 2005).

Sse1 interacts with the Hsp90 complex (Liu *et al*., 1999). Sse1 has been shown to be involved in the development and activity of Hsp90 substrates by regulating the transfer of client proteins to and from Hsp90, in the early stages of the chaperone cycle (Liu *et al*., 1999; Goeckeler *et al*., 2002; Lee *et al*., 2004). Like Sse1, Hsp90 mutants exhibit osmoremedial temperature sensitivity (Piper *et al*., 2006; Truman *et al*., 2007). Given that Sse1 is required for Hsp90 signaling and chaperone activity it was an objective to determine if the Sse1 temperature-sensitive mutants affected Hsp90 signaling. Δ*sse1* strains are known to be hypersensitive to Hsp90 inhibitors (Liu *et al*., 1999).

Figure 4.19 illustrates the results of Sse1 mutant comparative growth analysis on medium containing geldanamycin, which at 80 μM normally inhibits the growth of Hsp90 mutants and Hsp90 co-chaperone mutants. If Sse1 mutants are affecting Hsp90 signaling then they should show sensitivity to geldanamycin. This inhibitor targets Hsp90 by binding to its ATP binding domain, a region essential for client protein activation (Pearl and Prodromou, 2000). The result of this experiment

was that the Sse1 mutants showed no sensitivity to geldanamycin therefore they are not disrupting Hsp90 signaling (Figure 4.19).

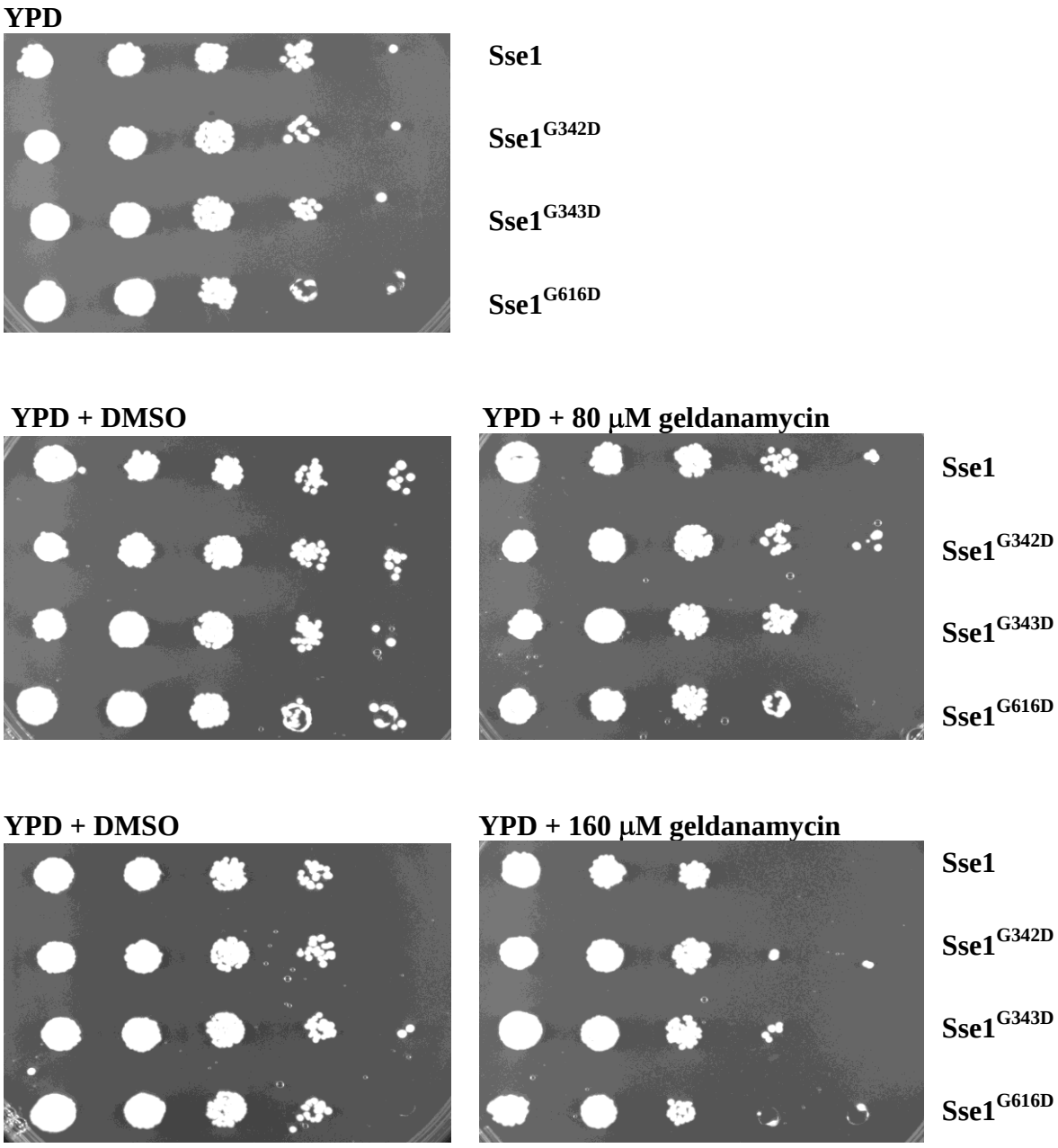

Figure 4.19. Comparative growth analysis of Sse1 mutant sensitivity to geldanamycin. CM03 + Sse1, Sse1^{G342D}, Sse1^{G343D} and Sse1^{G616D} were serial diluted onto YPD medium containing 80/160 μM geldanamycin or DMSO control. The plates were incubated at 30^{o}C for 2 days and analysed for differences in growth. Hsp90 and Hsp90 co-chaperone mutants are usually sensitive to 80 μM geldanamycin. Hsp90 signaling appeared normal in these Sse1 mutants. Zhai Chao from Dr Panaratou's laboratory Kings College London carried out these experiments.

A v-src assay was also performed. Sse1 mutant strains were transformed with a plasmid containing v-src under the control of a GAL promoter. V-src (viral sarcoma) is a non-receptor tyrosine kinase protein and Hsp90 plays a major role in tyrosine phosphorylation mediated by v-src (Xu and Lindquist, 1993). Xu and Lindquist (1993) found that a reduction in cellular Hsp90 levels has a major impact on v-src activity and that v-src regulates the phosphorylation activity and cellular localisation of Hsp90.

The theory behind this experiment was that if the Sse1 mutants affect Hsp90 signaling then v-src levels would also diminish and the cells would be viable and grow better than WT Sse1. V-src is toxic to yeast and its activity can be monitored by cell viability. This occurs in a cell cycle dependent manner (in M phase). However the plates were monitored over 24 h and all strains grew at the same rate (Figure 4.20). These results led to the conclusion that Sse1 temperature-sensitive mutants are not affecting Hsp90 activity.

4.8 Analysis of the effects of Sse1 temperature-sensitive mutants on protein kinase (PKA) signaling

Yeast readily ferment glucose and fructose in order to generate energy and cellular carbon metabolites (Johnston and Carlson, 1992). Glucose is detected by signal transduction components that transfer the signal into the cell nucleus where adjustments to gene expression are made (Santangelo, 2006). Glucose stimulates the cAMP/PKA signaling pathway by activating GTPase or G protein-coupled receptors on the cell surface. Efficient PKA signaling promotes protein synthesis, cell division and down-regulates stress response genes (Schneper *et al*., 2004; Santangelo, 2006). PKA signaling is responsible for inducing >90% of all genes regulated by glucose

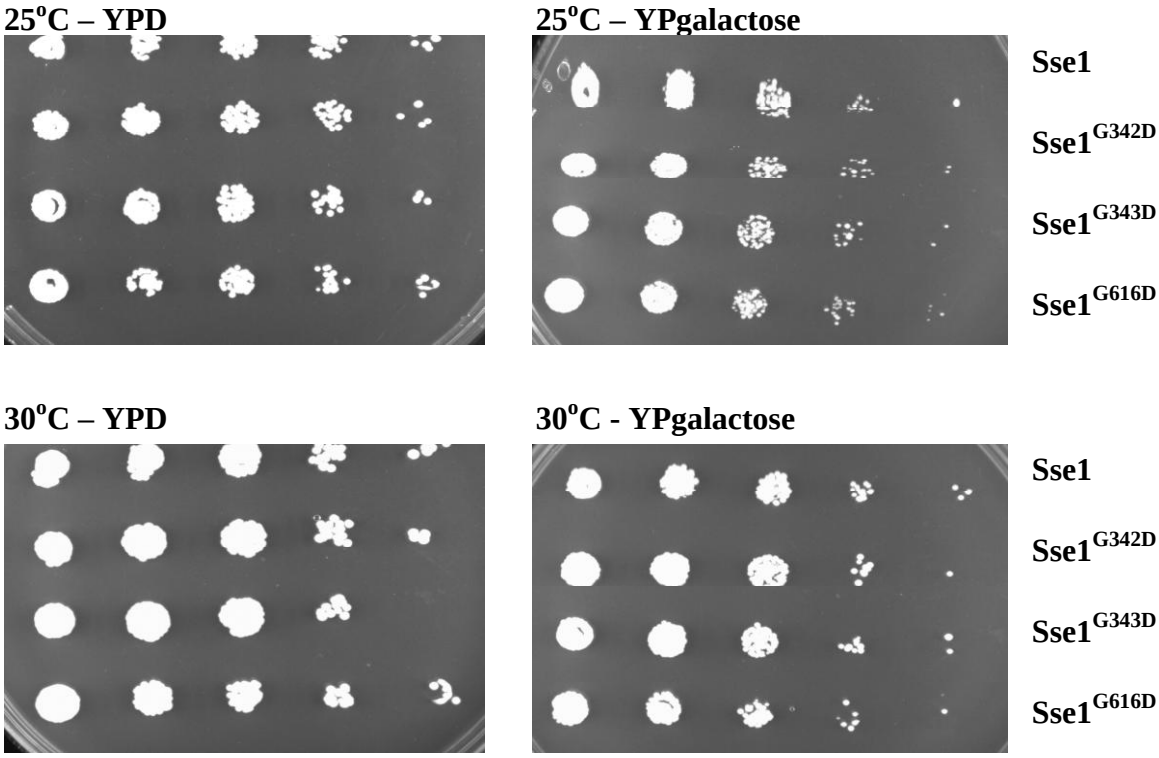

Figure 4.20. V-src assay on Sse1 mutants by comparative growth analysis. Strain CM03 was transformed with WT Sse1, $Sse1^{G342D}$ $Sse1^{G343D}$ and $Sse1^{G616D}$ and strains were transformed with plasmid vector containing v-src DNA. Strains were maintained on YPD-glucose before comparative growth analysis on YP-gal medium. The plates were incubated at 30°C for 2 days and monitored over this period. No difference in growth pattern was observed between WT Sse1 and Sse1 mutants. Zhai Chao from Dr Panaratou's laboratory Kings College London carried out these experiments.

and it responds to changes in glucose concentration by changing the magnitude and direction of gene transcription (Broach and Deschenes, 1990; Wang *et al*., 2004; Zaman *et al*., 2009). The external carbon supply available to yeast affects cell division and morphology. Yeast cells grown on glucose are larger than those grown on a non-fermentable carbon source such as ethanol (Johnston *et al*., 1979). Cells starved of adequate fermentable carbon depend on signaling through both a MAP kinase cascade and a cAMP dependent PKA (Lengeler *et al*., 2000; Pan *et al*., 2000;

Truckses *et al*., 2004). PKA deleted strains are non-viable (Zaman *et al*., 2009) and mutants that affect PKA signaling are sensitive to growth on non-fermentable carbon.

It has been suggested that the cAMP/PKA signaling cascade may also play a role in thermotolerance (Zhu *et al*., 2000). Sse1 has been linked with PKA signaling and it has been shown that the temperature-sensitive effects of Δ*sse1* can be suppressed by decreasing PKA signaling (Trott *et al*., 2005). Growth on ethanol and glycerol decreases PKA signaling (Thevelein and De Winde, 1999). Trott *et al*. (2005) demonstrated that Δ*sse1* temperature sensitivity was alleviated by growth on non-fermentable carbon sources suggesting that Sse1 is a negative regulator of PKA signaling.

As the growth of Sse1 mutants $Sse1^{G342D}$ and $Sse1^{G616D}$ was sensitive at 37^{o}C (both in CM02), they may be mimicking a Δ*sse1* loss of function effect and could be alleviated by decreasing PKA activity. The theory was that if they are affecting the role of Sse1 in regulating PKA activity then they should show growth at 37^{o}C on non-fermentable carbon sources. Mutant G342D was included in this analysis before it was confirmed non-ts.

Yeast strains CM02 and CM03 were transformed with ts mutants and analysed by comparative growth analysis on YP-ethanol and YP-glycerol. After 2 days growth at 30^{o}C and 37^{o}C the plates were analysed. It appeared that CM02 and CM03 with Sse1 mutants were very sensitive to ethanol even at 30^{o}C and no growth recovery was observed at 37^{o}C for either mutant (Figure 4.21). CM02 + $Sse1^{G616D}$ did appear a lot more sensitive to ethanol than WT Sse1 at 30^{o}C and 37^{o}C but this result was not reflected in CM03. Interestingly Sse1 mutants G342D and G616D grew as well as WT Sse1 at 37^{o}C when spotted onto YP-glycerol (Figure 4.21). This indicated that perhaps the ts Sse1 mutants are not functioning properly as PKA regulators and

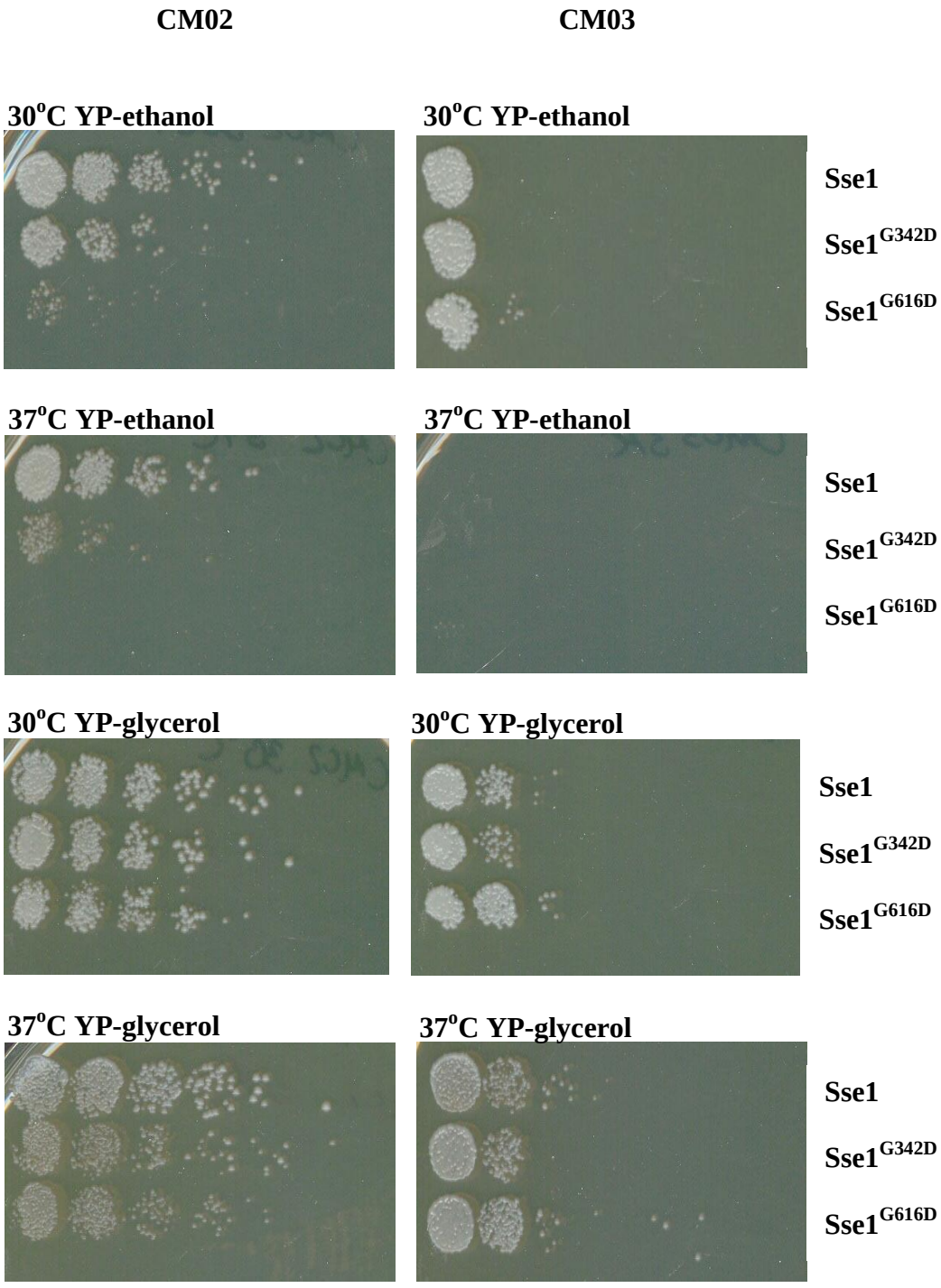

Figure 4.21. Analysis of Sse1 mutant growth on non-fermentable carbon sources. CM02 and CM03 were transformed with WT Sse1, Sse1^{G342D} and Sse1^{G616D}. Comparative growth analysis was performed on YP-glycerol and YP-ethanol and plates were incubated at 30^{o}C and 37^{o}C. Yeast were sensitive to growth on ethanol, particularly in CM03. Ts mutant Sse1^{G616D} is normally non-viable at 37^{o}C on glucose medium however its growth was restored on YP-glycerol. This indicates that Sse1 is a negative regulator of PKA signaling and perhaps G616D is affecting this function. Mutant G342D showed similar growth but as it is not a definite ts mutant a conclusion could not be made.

down-regulation of this pathway can completely restore a wild type phenotype.

4.9 A phenotypic and genetic comparison of strains CM02 and CM03

4.9.1 Comparing growth and sensitivity to chemicals reveals that these strains are very different

Because of the differences observed between CM02 and CM03 a comparative analysis study was performed on the two strains. Figure 4.22 is a summary of CM02 and CM03 growth on a variety of cell wall damaging agents. These comparative growth assays were performed previously and are comprised in this figure in way that emphasises the differences in sensitivity between the strains. CM02 is clearly more sensitive to cell wall damage than CM03 indicating a possible strain background difference (Figure 4.22). This strain sensitivity difference appears to be specific for these chemical agents as CM02 grew better on non-fermentable carbon in Figure 4.21.

Both strains were transformed with mutant G342D, which appeared non-viable in CM02 but only slow-growing in CM03 (Figure 4.23). It appears that the effects of mutant G342D are over-emphasised in CM02, possibly due to strain background differences.

4.9.2 Fes1 complements a Δ*sse1*Δ*sse2* deletion in strain CM03

As discussed previously in Chapter 3, Fes1 is a nucleotide exchange factor that works alongside Sse1 in the Hsp70 peptide binding cycle (Kabani *et al*., 2002). As it shares functional similarity with Sse1 it was an aim to see if it could compensate yeast for the loss of Sse1 and Sse2. In Chapter 3 it was concluded that pRS423*FES1* could not compensate for CM02Δ*sse1*Δ*sse2* non-viable phenotype. In contrast,

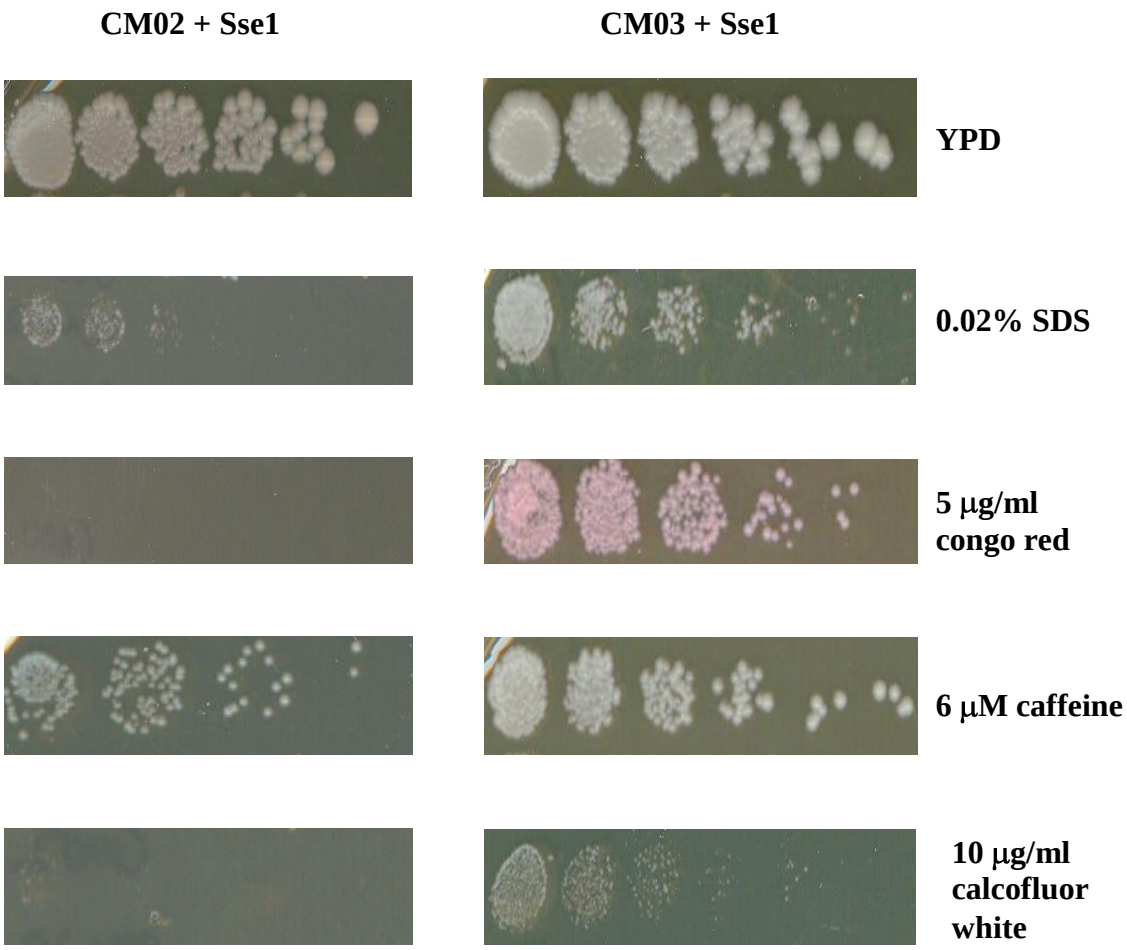

Figure 4.22. A summary of CM02 and CM03 growth and their sensitivity to cell wall damaging agents. Comparative growth analysis was performed on CM02Δ*sse1*Δ*sse2* + pRS315*SSE1* and CM03Δ*sse1*Δ*sse2* + pRS315*SSE1* in previous sections. This summary illustrates how CM02 is more sensitive than CM03 to cell wall damaging agents.

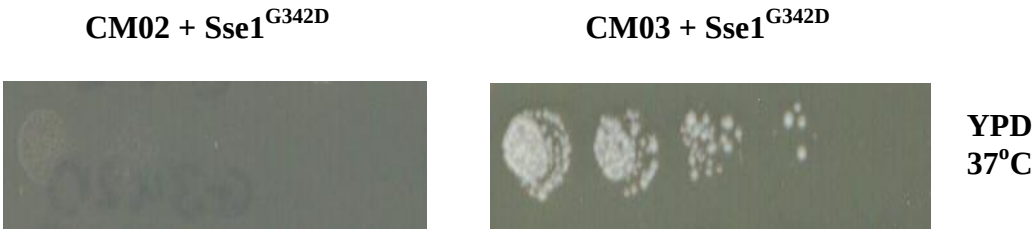

Figure 4.23. Comparative growth analysis of CM02 + Sse1^{G342D} and CM03 + Sse1^{G342D} at 37°C. Sse1 mutant G342D was temperature-sensitive at 37°C in CM02 but not in CM03.

previous work by Raviol *et al*. (2006b) and Sadlish *et al*. (2008) suggested that Fes1 could partially/fully complement Δ*sse1*Δ*sse2*. Therefore pRS423*FES1* was transformed into CM03 to see if the previous result may be due to CM02 strain background effects.

Figure 4.24 illustrates the result of transforming pRS423*FES1* and pRS423 into both CM02 and CM03. WT Sse1 was removed from each strain by replication onto 5-FOA. Surprisingly Fes1 did compensate for loss of Sse1 and Sse2 in strain CM03 but not in CM02. In conclusion, Fes1 can complement Δ*sse1*Δ*sse2* and previous negative results in CM02 could be related to strain background differences.

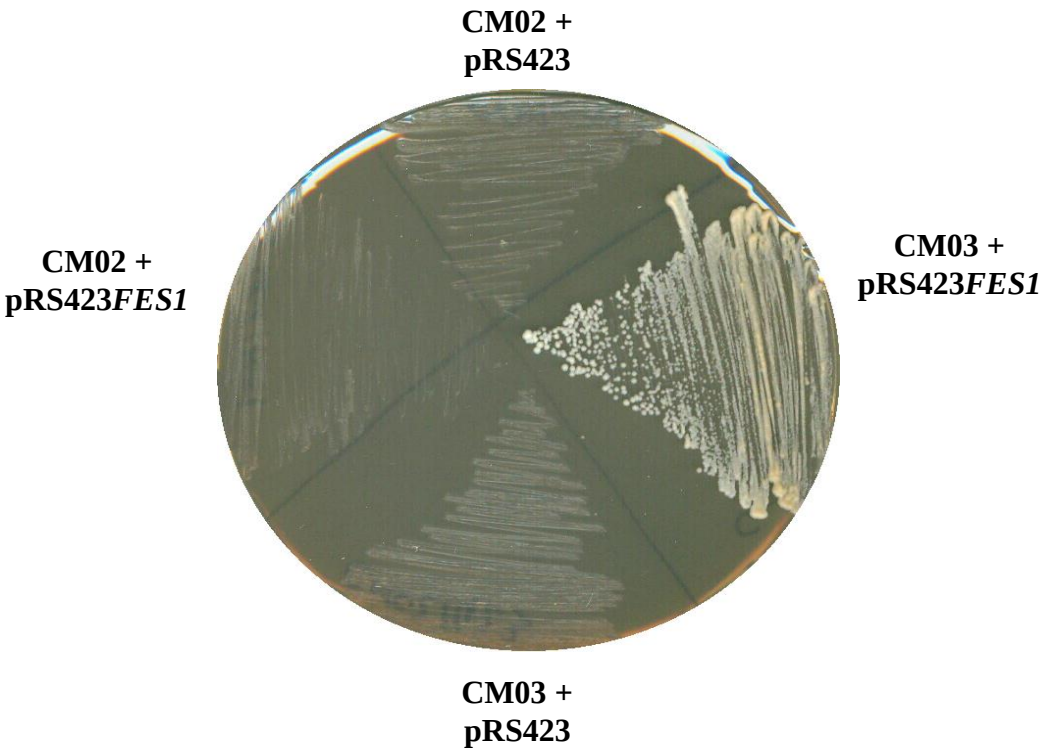

Figure 4.24. Fes1 complementation in CM02 and CM03. pRS423 and pRS423*FES1* were transformed into CM02 and CM03, selected on SC - histidine and incubated for 2 days at 30°C. Colonies were patched onto fresh SC - histidine medium and replicated onto 5-FOA to select against pRS316*SSE1*. 5-FOA plates were incubated for 2 days at 30°C. Cell growth for CM03 + pRS423*FES1* was slow on 5-FOA but the strain grew well when restreaked onto fresh SC – histidine medium.

4.9.3 HSPH1 complements a Δ*sse1*Δ*sse2* deletion in strain CM03

As discussed previously in Chapter 3, HSPH1 is the yeast Hsp110 human homolog. It functions as a nucleotide exchange factor for mammalian Hsp70 and is distantly related to yeast Sse1 (Dragovic *et al*., 2006). HSPH1 has functional and general structural similarities to yeast Sse1 which prompted us to see if HSPH1 could compensate for loss of Hsp110 in yeast. *HSPH1* was cloned under control of the *SSA2* promoter into pC210 vector as described in section 2.23. To test whether pC210*HSPH1* could complement Δ*sse1*Δ*sse2* the plasmid was transformed it into CM02 and CM03 along with positive and negative controls. Following 5-FOA selection HSPH1 was able to provide essential function in CM03 but not CM02 (Figure 4.25). From this figure it is clear that the results are comparable to those found in Figure 4.24 where Fes1 could also complement Δ*sse1*Δ*sse2* in CM03. This highlights again the possible genotypic differences between the strain backgrounds.

4.9.4 Analysis of the Sse1 mutant Q458* in CM02 and CM03

Sse1 mutant Q458* was isolated as a [*psi*$^-$] mutant, as described in Chapter 3. The amino acid change is from a glutamine (Q) to a TAA stop codon. It was unclear whether this mutation created a truncated Sse1 protein and for this reason it was not included in the Sse1 mutant phenotypic analysis in Chapter 3. The fact that Sse1^{Q458*} point mutation allowed for the growth of a fully functional yeast strain led to the speculation that this premature stop codon may be subjected to a high level of readthrough. To investigate this theory further truncated Sse1 was cloned, under the control of the *SSA2* promoter, into pC210. Primers were designed to anneal to the ATG start codon of Sse1 and the reverse primer annealed to amino acid position 458.

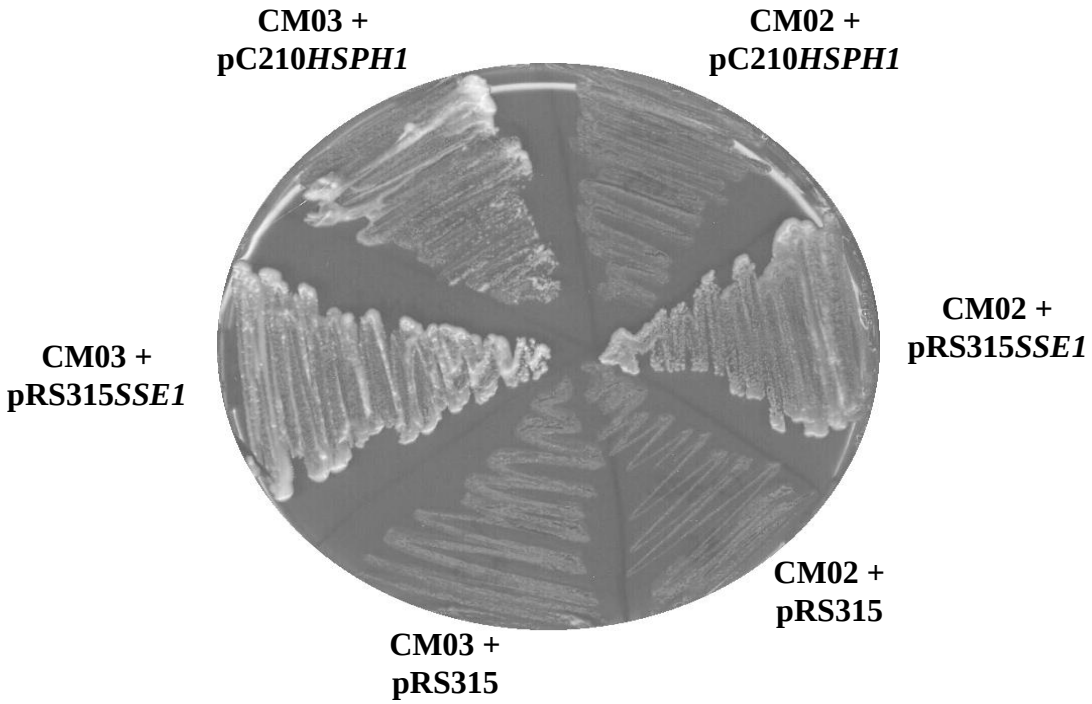

Figure 4.25. HSPH1 complementation in CM02 and CM03. pRS315, pRS315*SSE1* and pC210*HSPH1* were transformed into CM02 and CM03, selected on SC - leucine and incubated for 2 days at 30^{o}C. Transformants were patched onto fresh SC - leucine medium and replicated onto 5-FOA to select against pRS316*SSE1*. 5-FOA plates were incubated for 2 days at 30^{o}C. Cell growth for CM03 + pC210*HSPH1* was slower than growth for pRS315*SSE1* on 5-FOA but the strain grew well when restreaked onto fresh SC - leucine.

The PCR product contained overhangs homologous to pC210 and it was cloned as described in section 2.23 using primers and PCR cycles described in Table 2.11 and 2.12.b. Four potential clones were tested by diagnostic PCR (Figure 4.26) and one isolate was sent for sequence analysis. The confirmed pC210*SSE1*Q458 vector (Figure 4.27) was transformed into both CM02 and CM03 along with pRS315*SSE1*^{Q458*} point mutation vector and positive/negative controls.

Interestingly, the Sse1 truncated protein could not support growth in either CM02 or CM03 (Figure 4.28 and 4.29) indicating that Sse1 may not be able to form a fully functional protein when truncated by over 200 amino acids. However, the point mutation mutant *SSE1*^{Q458*} did support growth in CM02 but not in CM03. It seems that there may be a high level of readthrough in CM02 compared to CM03.

(i) pC210-Q458 construct digested with *Nde*1 and *Sph*1 enzymes

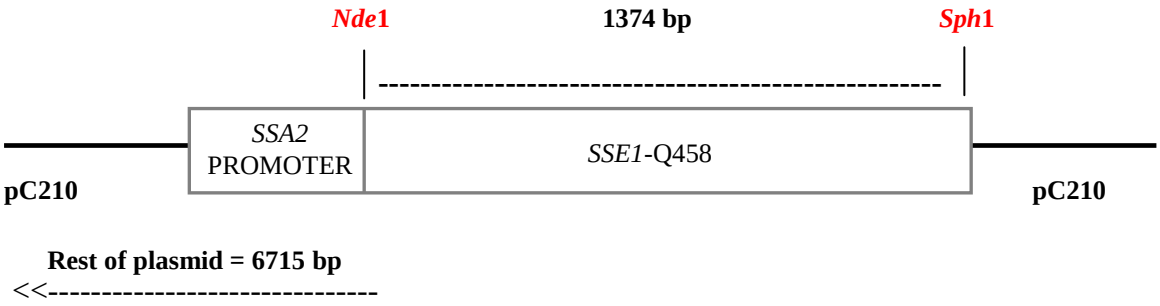

(ii) Agarose gel electrophoresis of digested vectors

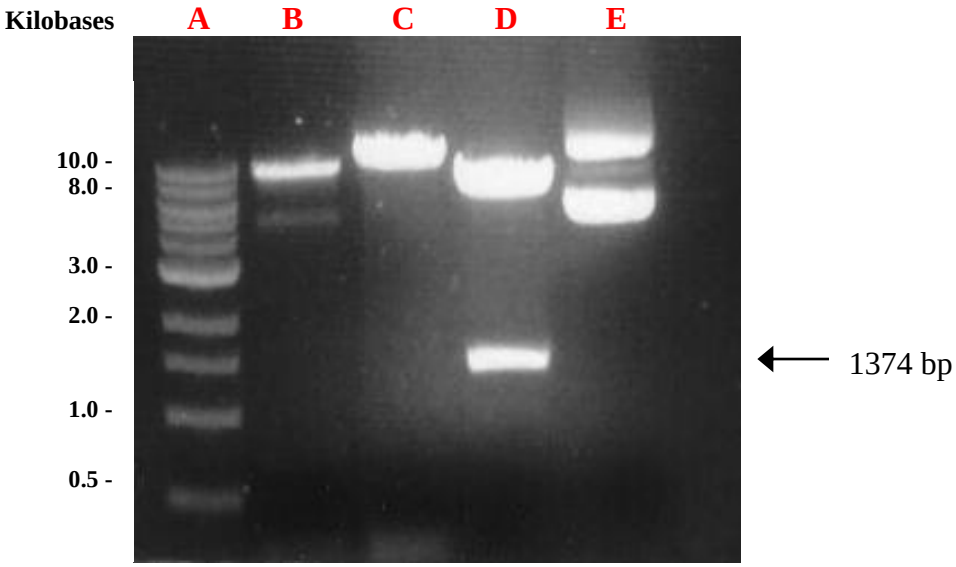

Figure 4.26. Diagnostic restriction digest of potential pC210-Q458trunc clones.

(i) pC210-*SSE1*Q458trunc construct with expected bp sizes after restriction digest with *Nde*1 and *Sph*1. *Nde*1 cuts plasmid pC210 at end of the promoter region and *Sph*1 cuts at the end of the cloned *SSE1*Q458 sequence. This should result in two bands of 6715 bp and 1374 bp.
(ii) Agarose gel electrophoresis of four potential Q458trunc plasmid clones. Each isolate was digested with restriction enzymes *Nde*1 and *Sph*1.
Lane A: Molecular weight marker
Lane B-C: Potential pC210-Q458trunc clones. DNA bands did not correspond to a successful clone.
Lane D: Potential pC210-Q458trunc clone 3. The large top band was very concentrated and hard to determine exact size. The smaller band was approximately 1374 bp. This clone was sent for sequencing and confirmed as a pC210-Q458trunc clone.
Lane E: Potential pC210-Q458trunc clone 4. DNA bands did not correspond to a successful clone.

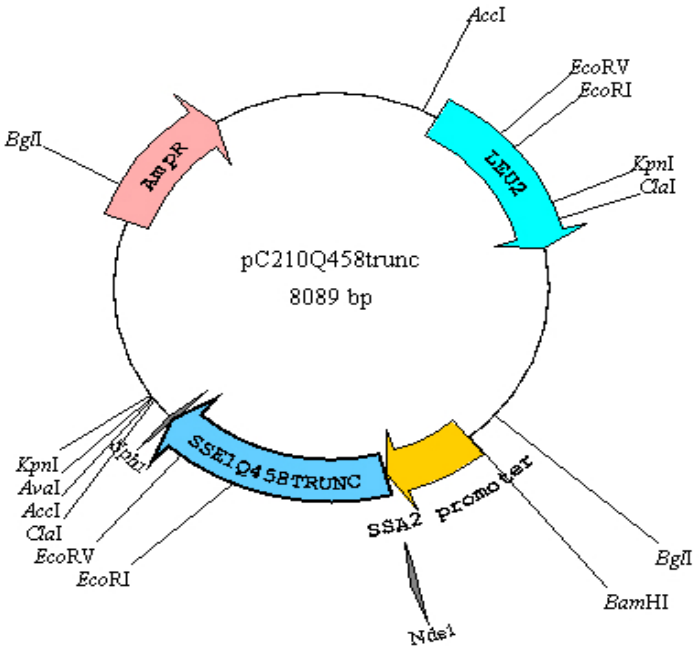

Figure 4.27. Construct of plasmid pC210 with Sse1 protein truncation at position 458.

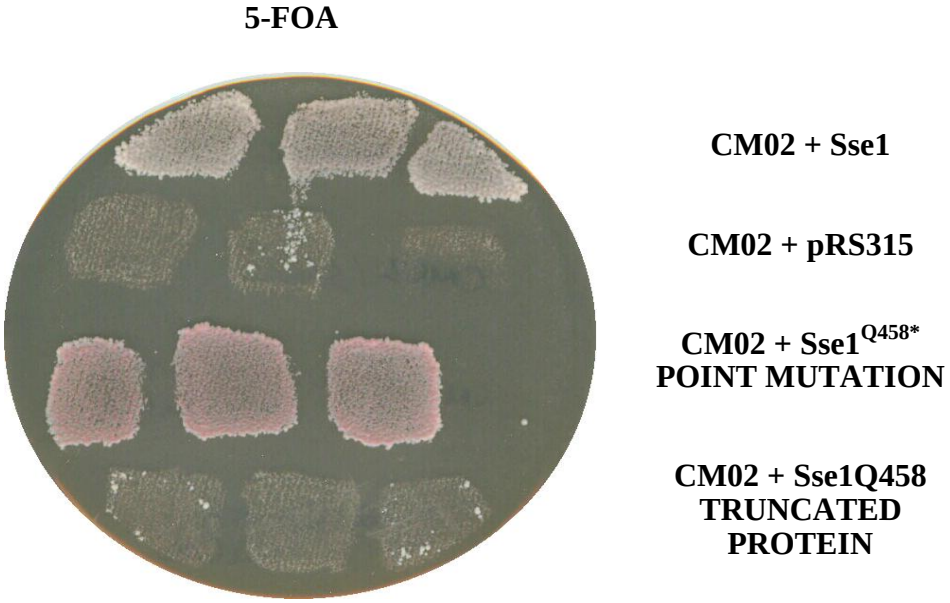

Figure 4.28. Growth status of CM02 cells expressing the Sse1 point mutation Q458* and Sse1 Q458 truncation protein. WT Sse1, pRS315, Sse1^{Q458*} and Sse1Q458 truncation protein were transformed into CM02, selected on SC - leucine and incubated for 2 days at 30^{o}C. All strains grew on SC - leucine and were replicated onto 5-FOA to select against pRS316*SSE1*. This figure illustrates how Q458* can support growth and the Q458 truncated protein cannot.

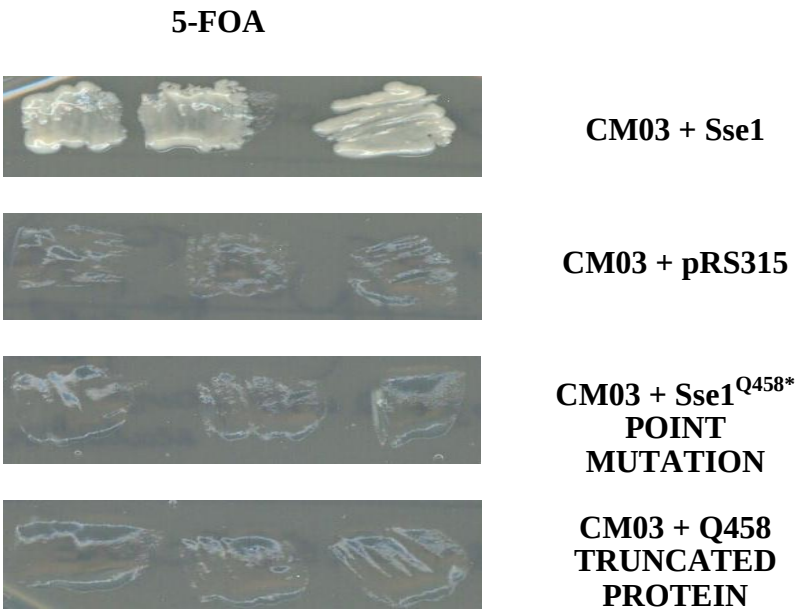

Figure 4.29. Growth status of CM03 cells expressing the Sse1 point mutation Q458* and Sse1 Q458 truncation protein. WT Sse1, pRS315, $Sse1^{Q458*}$ and Sse1Q458 truncation protein were transformed into CM03, selected on SC - leucine and incubated for 2 days at 30^{o}C. All strains grew on SC - leucine and were replicated onto 5-FOA to select against pRS316*SSE1*. This figure illustrates how both Q458* or the Q458 truncated protein cannot support growth.

4.10 Yeast strain G600 genome sequencing

4.10.1 Identification of SNPs in G600 strain

To further investigate the differences between CM02 and CM03 next generation sequencing was used to analyse G600 genomic DNA. This resulted in the identification of approximately 6,500 high quality SNPs (Single Nucleotide Polymorphisms) in G600 genomic DNA compared to reference strain S288C (BY4741). Using an Illumina GAII approximately 40X genome coverage was obtained. Isolated SNPs equated to approximately 1,500 non-synonymous amino acid changes. DNA sequencing was carried out in St James hospital in conjunction with Trinity College. A summary of the SNP data is presented in Table 4.2. Detailed

Table 4.2. SNPs present in G600 compared to reference strain S288C.

Chromosome	Size(bp)[a]	ORFs[a]	Total number of SNPs	SNPs in ORFs	Non-synonymous amino acid changes
I	230,208	117	157	126	59
II	813,178	456	885	516	211
III	316,616	183	228	157	65
IV	1,531,919	836	38	28	22
V	576,869	324	47	34	23
VI	270,148	141	32	14	7
VII	1,090,947	583	625	340	120
VIII	562,643	321	10	5	2
IX	439,885	241	505	304	98
X	745,741	398	380	270	94
XI	666,454	348	515	312	117
XII	1,078,175	578	652	461	150
XIII	924,429	505	655	380	138
XIV	784,333	435	673	396	177
XV	1,091,289	598	983	618	228
XVI	948,062	511	79	54	34
mito	85,779	19	87	62	4
Totals	12,070,898	6,602	6,551	4,077	1,549

[a]The information was obtained from the *Saccharomyces* Genome Database.

sequence analysis data is supplemented as a hard copy (CD) and located in Tables S3 and S4.

SNPs were located in three kinase proteins known to interact and phosphorylate Sse1 and Sse2. They are Hsl1, Kin2 and Akl1. These SNPs equated to five non-synonymous amino acid changes in Hsl1 (P1136R, V1308I, V1400I, N1439D and S1482T) and four in Akl1 (S176P, F812L, S997P, S1090G) (supplemented Tables S3/S4). Such changes could affect Sse1 and Sse2 protein phosphorylation and subsequent functions. Four non-synonymous amino acid changes were identified in the protein Pkc1 (supplemented Table X). This protein kinase is the first signaling kinase in CWI pathway and perhaps these mutations in G600 are responsible for the strains sensitivity to chemical compounds. A single non-synonymous change (P2005L) was identified in G600 Ira2 protein. This protein plays a role in PKA signaling which could impact the sensitivity of strain CM02 or the functionality of Sse1.

Some ORFs had altered natural stop codons. Nat4 is an acetyltransferase protein responsible for acetylation of histones H4 and H2A (Song *et al*., 2003). In G600 a Nat4 stop codon, at 286aa, was identified as an arginine (R) mutation resulting in the addition of 53 amino acids to the C-terminus of the protein (supplemented Tables S3/S4). This could potentially alter yeast molecular and biological processes. However Song *et al*. (2003) also concluded that *nat4* delete mutants displayed no obvious phenotypes. Other ORFs with altered natural stop codons included MFT1 (involved in transcription elongation and telomere maintenance), YNR066C, CRS5 (copper resistantance gene) and YGR067C (supplemented Tables S3/S4).

4.10.2 Analysis of G600 ISCMs

In addition to non-synonymous amino acid changes ISCMs (Inactivating Stop Codon Mutations) were also identified in a variety of genes (Table 4.3). The fact that the sequence data correctly identified the *ade2* nonsense mutation in strain G600 (Table 4.3) provided confidence that the other identified ISCMs would also be correct. The presence of ISCMs and SNPs in G600 could have major implications on the interpretation of [*PSI*$^{+}$] associated phenotypes. Increased translation read-through of aberrant stop codons in a [*PSI*$^{+}$] expressing strain may lead to accumulation of ISCMs as there is less selective pressure against them.

Figure 4.30 illustrates the phylogenetic distribution of yeast strains that have been generated by the *Saccharomyces* Genome Resequencing project. Analysis of this phylogeny was carried out by Dr David Fitzpatrick (NUI Maynooth). This shows that strain G600 is more related to the reference strain S288c.

Figure 4.31 illustrates sequencing chromatogram results for chromosome V and XII. The large peaks in the graph represent repetitive sequences that appear more than once in the chromosome e.g. origins of replication (ORFs) or transposable elements. Ribosomal DNA copies also come off as large broad peaks. A copy of all chromosomal sequencing chromatograms is available in supplementary Figure Y.

Table 4.3. ORFs in G600 containing single internal nonsense mutations.

Systematic name[a]	Gene name[a]	Biological function[a]	Chromosomal SNP position	Nonsense change and consequence
YBR074W	-	Putative metalloprotease	387,247	Q323TAA 653 amino acid truncation
YNL106C	*INP52*	Polyphosphatidylinositol phosphatase, dephosphorylates a number of phosphatidylinositols (PIs) to PI	422,546	W651TAG 532 amino acid truncation
YOR128C	*ADE2*	Adenine biosynthesis	566,003	E64TAA 507 amino acid truncation
YOR129C	*AFI1*	Arf3p polarisation-specific docking factor, required for polarised distribution of the ADP-ribosylation factor Arf3p	566,901	E887TAA 6 amino acid truncation

[a]Information obtained from the *Saccharomyces* Genome Database.

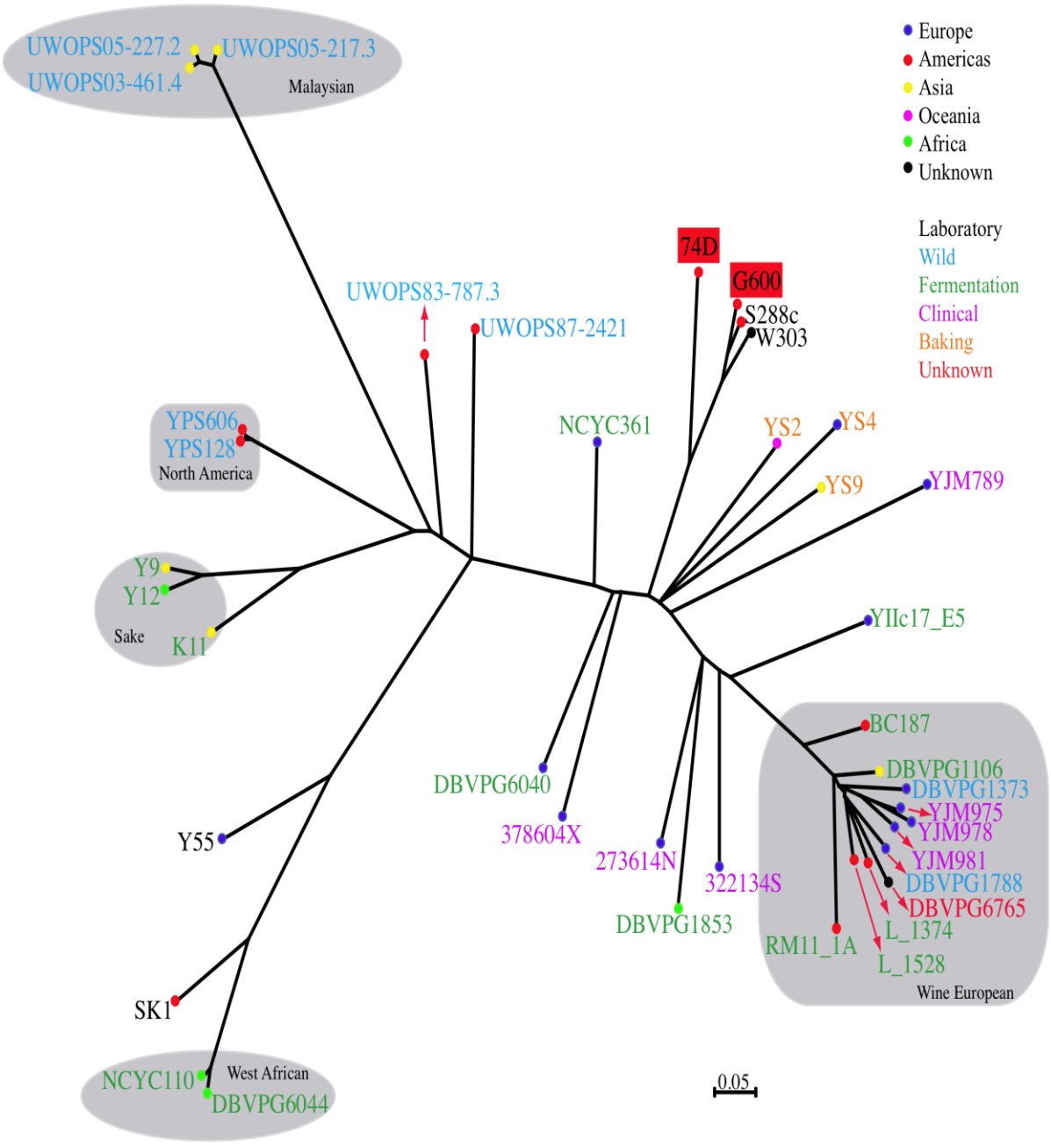

F**igure 4.30.** Phylogenetic distribution of yeast species. 74D is another commonly used yeast strain in prion research laboratories. This phylogeny was generated by Liti *et al*. (2009).

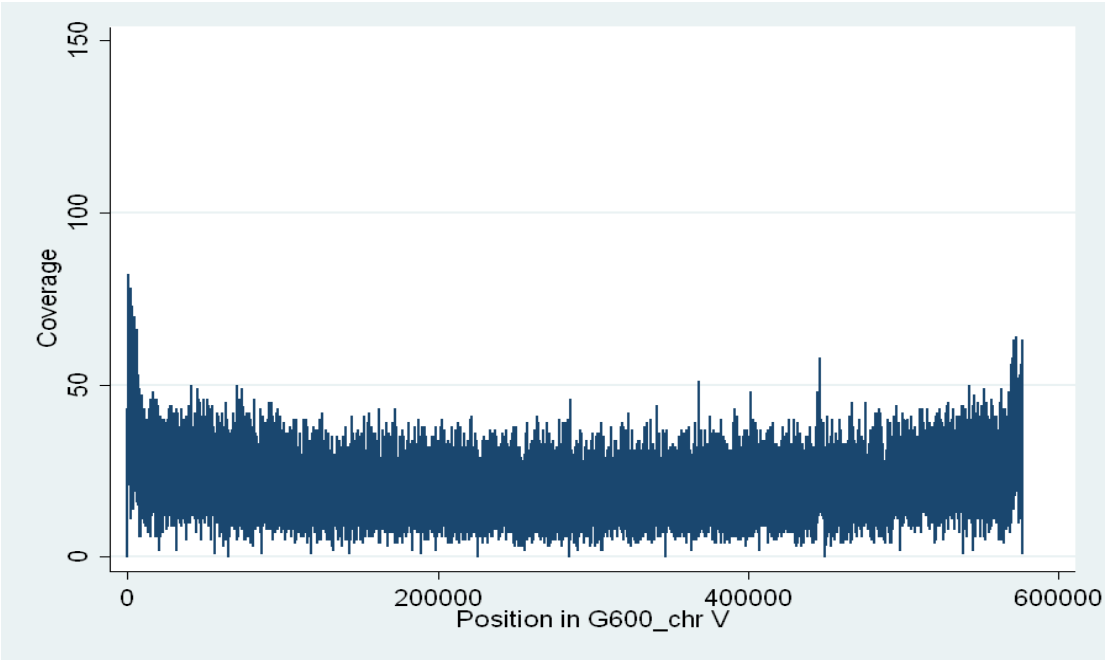

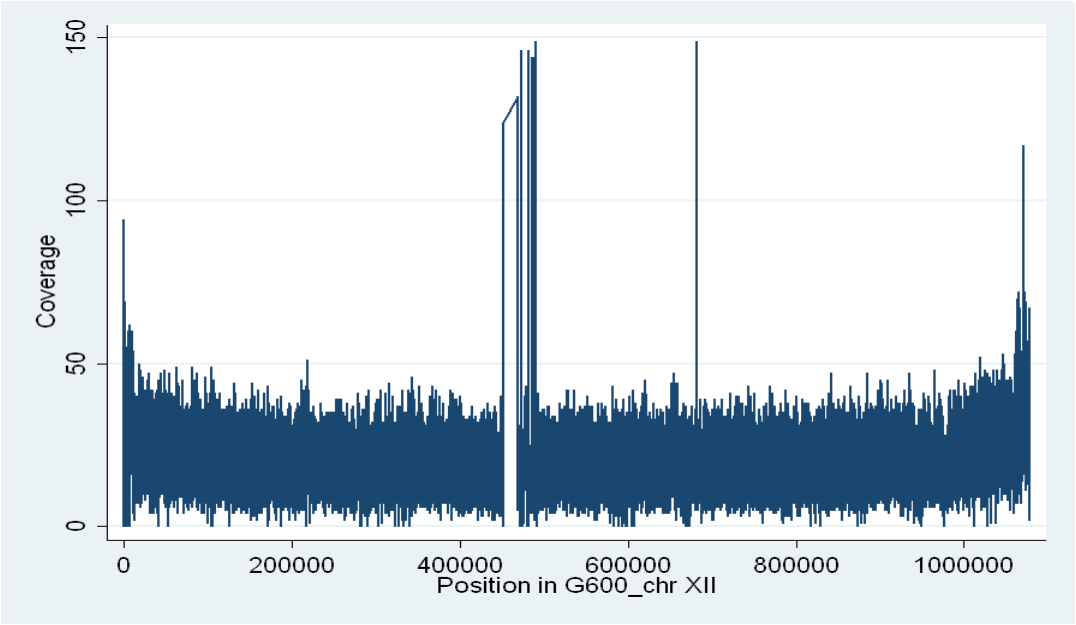

Figure 4.31. Chromatogram showing chromosomal coverage from DNA sequencing. Graphs represent full 40X coverage of chromosome V and XII. Chromosome XII has more repetitive sequence and more ribosomal DNA copies than chromosome V. Repetitive sequence and ribosomal DNA have a higher coverage as they overlap and map onto each other, resulting in larger peaks.

4.10.3 Analysis of G600 sensitivity to cell wall damaging agents in the presence of a plasmid expressing gene YBR074W

The identification of nonsense mutations in YBR074W, YOR129C and YNL106C in G600 may have implications for cellular homeostasis in this strain. As seen in section 4.9 G600 strain CM02 showed a higher level of sensitivity to cell wall damaging agents than BY4741 strain CM03. CM03 was also able to complement Δ*sse1*Δ*sse2* growth by the over-expression of Fes1 and HSPH1 and CM02 was not. Of the three identified ISCMs YBR074W and YNL106C were concentrated on as YOR129C only had a 6 amino acid truncation.

YNL106C or INP52 is a member of a conserved family of phosphoinositide phosphatases. It is a 136 kDa membrane protein and its deletion is viable (Stolz *et al*., 1998). The phosphoinositides are regulators of the actin cytoskeleton and membrane trafficking (Corvera *et al*., 1999) and it has been suggested that YNL106C (INP52) may play a role in actin cytoskeleton re-organisation following osmotic stress (Ooms *et al*., 2000). YBR074W is a less well characterised gene but it does form a putative protease which may act as a vacuolar proteolytic enzyme (Wiederhold *et al*., 2009).

YBR074W ISCM creates a 653 amino acid truncated protein at Q323 and YNL106C ISCM creates a 532 amino acid truncated protein at W651. To determine whether ISCMs to genes YBR074W and YNL106C were causing strain sensitivity plasmid vectors containing these genes were purchased from Euroscarf. At the time only plasmid pYCGYBR074W was available from Euroscarf and an attempt to clone YNL106C into a vector was unsuccessful. Plasmids pRS316 and pYCGYBR074W were transformed into G600 [PSI^{+}] and G600 [psi^{-}] (previously cured on 3 mM GdnHCl). Yeast were cultured in SC - uracil media to maintain plasmid expression and comparative growth analysis was performed on YPD and YPD supplemented

with cell stress chemicals. The plates were incubated for 2 days at 30^{o}C. Interestingly, [*psi*$^{-}$] versions of G600 were more sensitive to chemical cell wall stress than [*PSI*$^{+}$] strains (Figure 4.32. a-c). When G600 [*psi*$^{-}$] yeast were exposed to 0.005% SDS, 0.01% SDS and 10 μg/ml congo red the expression of pYCGYBR074W did improve cell growth compared to the control. This suggests that the incomplete translation of YBR074W in G600 [*psi*$^{-}$] may affect the cells ability to withstand chemical stress. This result was significant as Inactivating Stop Codon Mutations (ISCMs), such as the one identified in YBR074W, may be responsible for G600 strain sensitivity.

4.11 Random mutagenesis screen for the isolation of new Sse1 temperature-sensitive mutants

The rationale behind this screen was to isolate ts mutants that affect Sse1 residues important for cell wall signaling through PKA or CWI. This could help gain insight into important amino acid residues that are structurally and functionally involved in Sse1 interactions and signaling processes. pRS315*SSE1* mutant library was created as described in section 2.15 and transformed into CM03 along with WT pRS315*SSE1* and pRS315. Plasmid shuffle was performed on transformants by selecting colonies on 5-FOA and incubating plates at 37^{o}C for two days (Figure 4.33). Approximately 10,000 colonies went through the primary screen. Twenty five potential temperature-sensitive mutants were isolated from 5-FOA and the corresponding colonies were picked from SC - leucine replication plates. The secondary screen involved isolating these plasmids as described in section 2.11.2 and transforming them back into CM03. Each potential ts mutant was analysed by

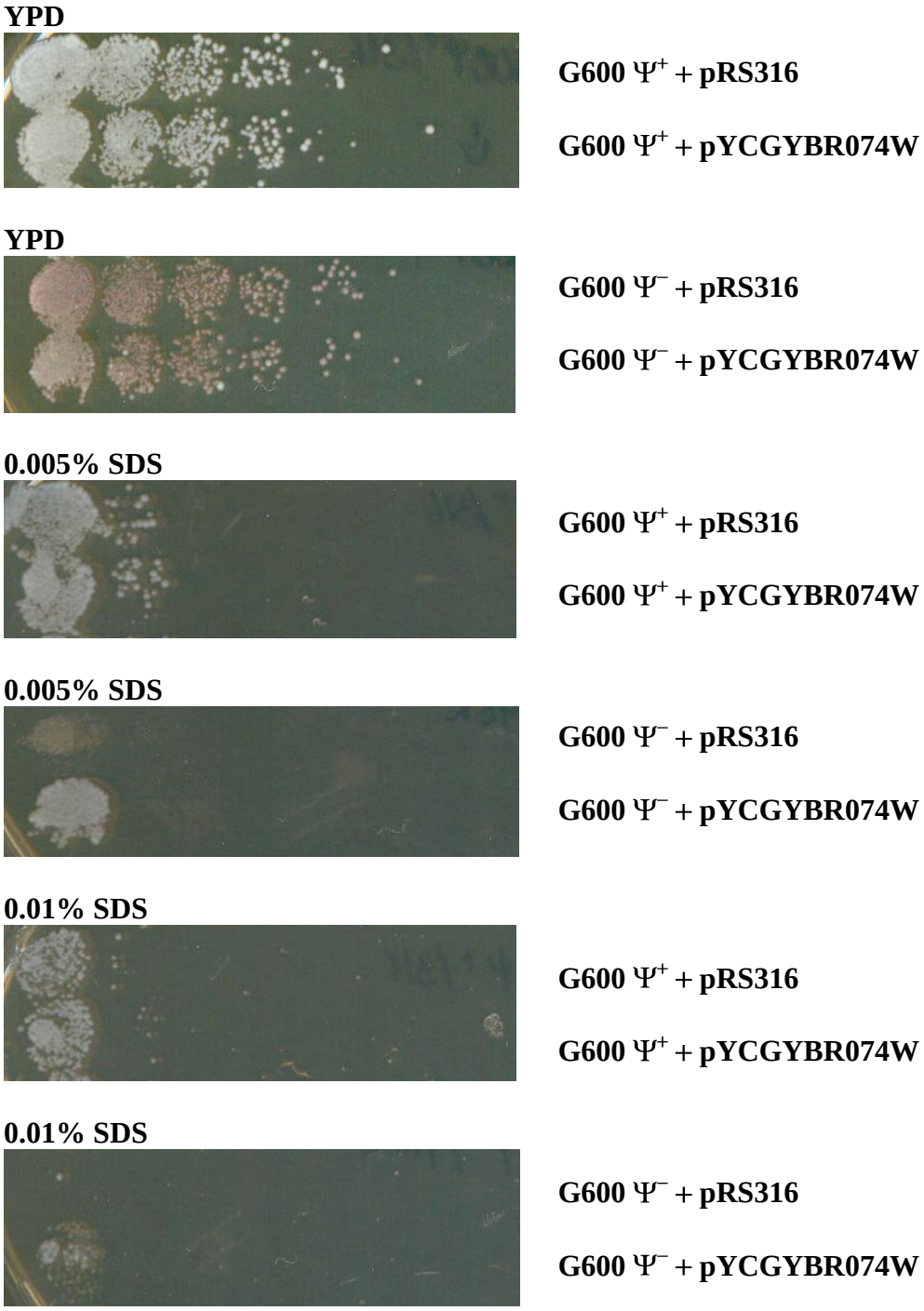

Ψ^+ = [*PSI*$^+$]
Ψ^- = [*psi*$^-$]

Figure 4.32.a. Comparative growth analysis of G600 sensitivity to cell wall damaging agents. G600 [*PSI*$^+$] and [*psi*$^-$] were transformed with pRS316 and pYCGYBR074W. Transformants were grown in SC - uracil media before being serial diluted onto YPD and medium containing varying concentrations of SDS. The plates were incubated for 2 days at 30^{o}C. G600 [*psi*$^-$] control was non-viable on SDS medium, however the expression of pYCGYBR074W restored some cellular growth. G600 [*psi*$^-$] appeared more sensitive to the cell wall damaging agent SDS than G600 [*PSI*$^+$].

10 μg/ml congo red

G600 Ψ$^+$ + pRS316

G600 Ψ$^+$ + pYCGYBR074W

10 μg/ml congo red

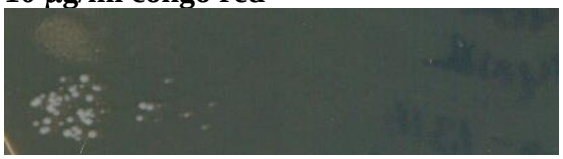

G600 Ψ$^-$ + pRS316

G600 Ψ$^-$ + pYCGYBR074W

10 μM caffeine

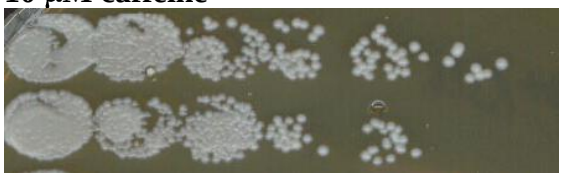

G600 Ψ$^+$ + pRS316

G600 Ψ$^+$ + pYCGYBR074W

10 μM caffeine

G600 Ψ$^-$ + pRS316

G600 Ψ$^-$ + pYCGYBR074W

3 mM H_2O_2

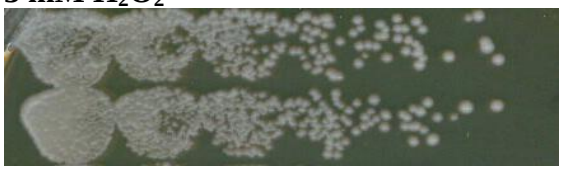

G600 Ψ$^+$ + pRS316

G600 Ψ$^+$ + pYCGYBR074W

3 mM H_2O_2

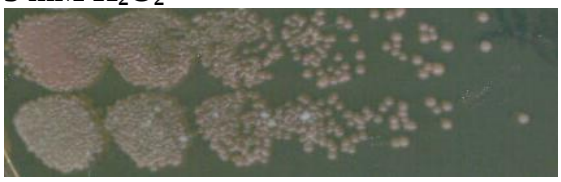

G600 Ψ$^-$ + pRS316

G600 Ψ$^-$ + pYCGYBR074W

Ψ$^+$ = [*PSI*$^+$]
Ψ$^-$ = [*psi*$^-$]

Figure 4.32.b. Comparative growth analysis of G600 sensitivity to cell wall damaging agents. G600 [*PSI*$^+$] and [*psi*$^-$] were transformed with pRS316 and pYCGYBR074W. Transformants were grown in SC - uracil media before being serial diluted onto YPD medium containing varying concentrations of chemical agents. The plates were incubated for 2 days at 30^{o}C. G600 [*psi*$^-$] control was non-viable on congo red medium, however the expression of pYCGYBR074W restored some cellular growth. 3 mM H_2O_2 and caffeine treatment had no effect on any of the strains. G600 [*psi*$^-$] appeared more sensitive to cell wall damaging agent congo red than G600 [*PSI*$^+$].

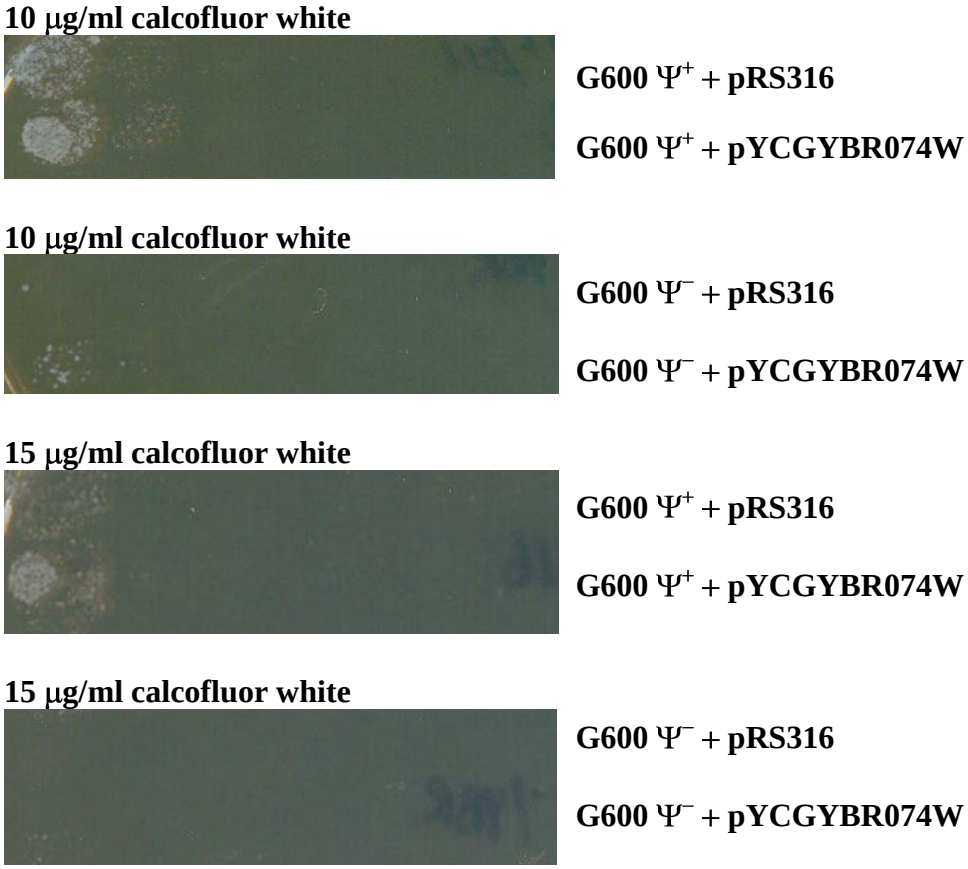

$\Psi^+ = [PSI^+]$
$\Psi^- = [psi^-]$

Figure 4.32.c. Comparative growth analysis of G600 sensitivity to cell wall damaging agents. G600 [*PSI*$^+$] and [*psi*$^-$] were transformed with pRS316 and pYCGYBR074W. Transformants were grown in SC - uracil media before being serial diluted onto YPD medium containing varying concentrations of calcofluor white. The plates were incubated for 2 days at 30^{o}C. G600 [*psi*$^-$] and [*PSI*$^+$] were sensitive to calcoflour white medium, however the expression of pYCGYBR074W did restore some growth in G600 [*psi*$^-$]. G600 [*psi*$^-$] appeared more sensitive to cell wall damaging agent calcofluor white than G600 [*PSI*$^+$].

comparative growth at 30^{o}C and 37^{o}C which led to four isolates (EP10, 11, 21, 22) having a reproducible ts phenotype (Figure 4.34). Each isolate was sent for sequence analysis and they all returned as Sse1^{G616D}. This mutant was isolated in previous screens as a ts mutant in CM02. Given that this was the only mutant obtained and was isolated four times suggests that the screen was saturated. The results from this screen

indicate that it may be difficult to isolate 37°C ts mutants in Sse1. Perhaps more mutants could have been isolated if the screen was performed at 39°C. The reason why the screen was carried out at 37°C rather than 39°C was to identify specific cell wall signaling mutants rather than general ts mutants.

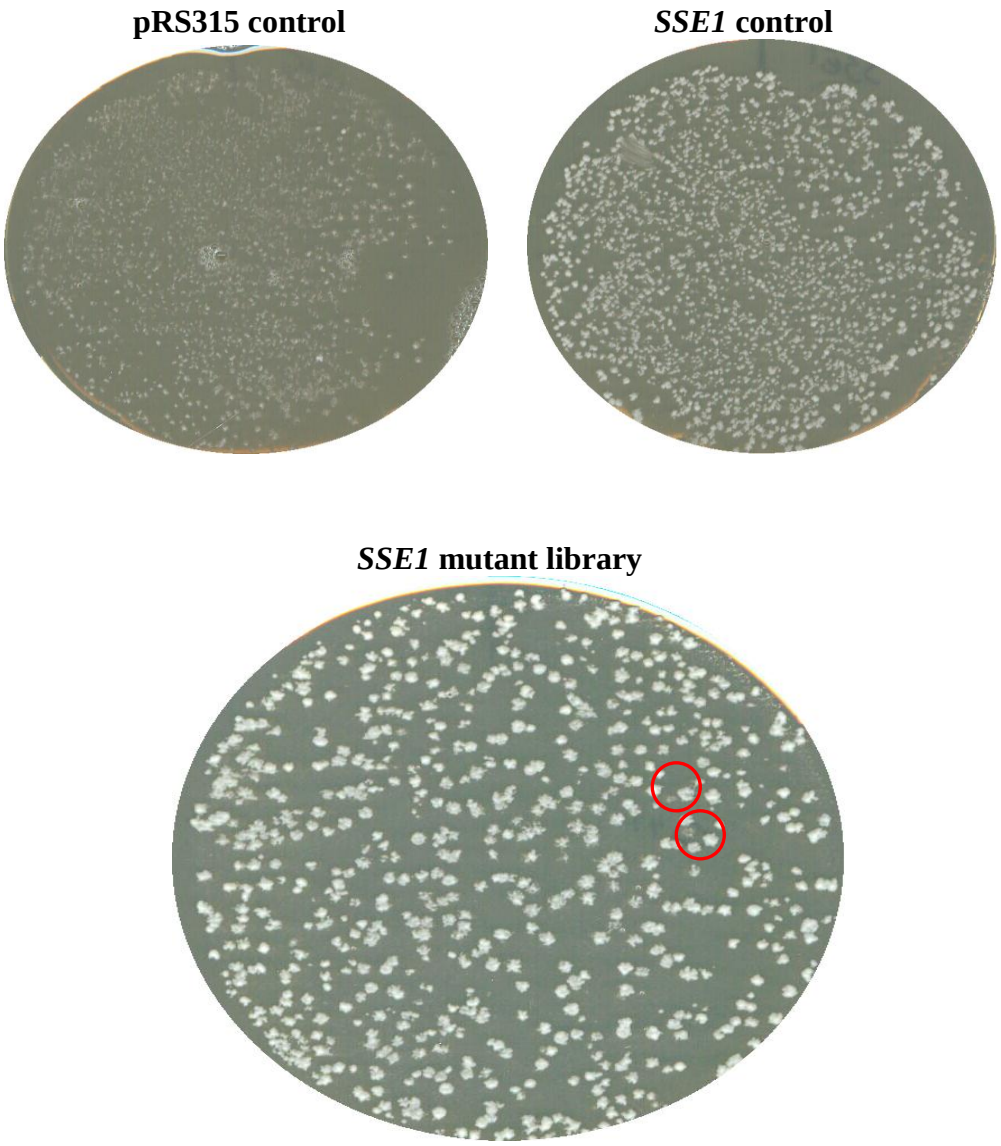

Figure 4.33. Primary screen for the isolation of Sse1 temperature-sensitive mutants. Strain CM03 was transformed with *SSE1* mutant library, WT *SSE1* and empty vector controls. 5-FOA replication and 24 hour incubation at 37°C resulted in a number of potential temperature-sensitive plasmids. Examples of colonies that were selected as potential ts mutants are highlighted (red circles).

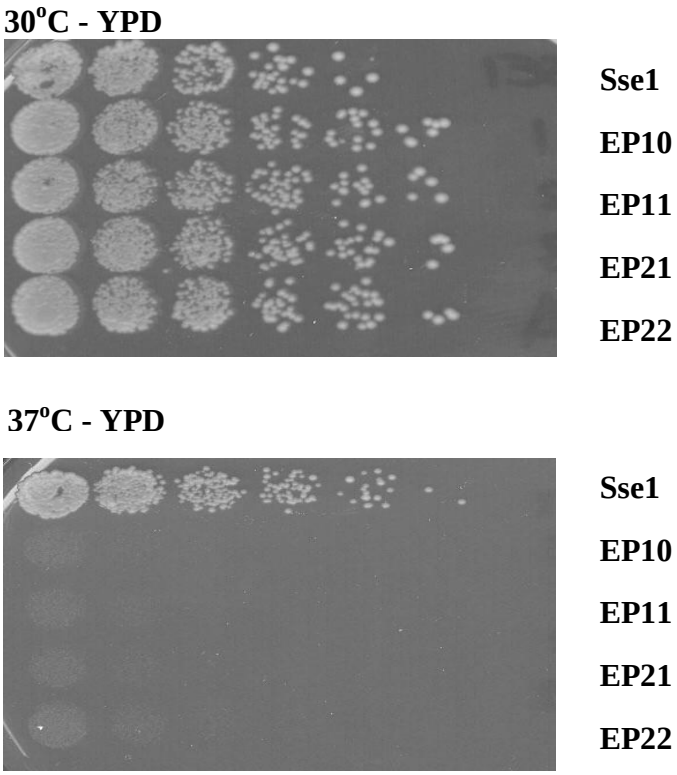

Figure 4.34. Secondary screen for the isolation of potential Sse1 temperature-sensitive mutants. Comparative growth analysis was performed on twenty five potential ts mutants. Yeast were serial diluted onto YPD and incubated at 30°C and 37°C for 2 days. Four isolates were confirmed as ts. Sequence analysis revealed that they were all $Sse1^{G616D}$.

4.12 Investigation into the effects of *SWI6* deletion on Sse1 mutant growth and cellular morphology

SBF and MBF are transcription factors which mediate transcription in late G_1 phase of cell cycle progression (Koch and Nasmyth, 1994; Breeden, 1996). They function as heterodimers composed of the regulatory protein Swi6 (Breeden and Nasmyth, 1987) and DNA binding protein Swi4 or Mbp1 (Andrews and Herskowitz, 1989; Koch *et al*., 1993). SBF (Swi6-Swi4) plays a role in CWI signaling as a Mpk1 target. Δ*swi4* and Δ*swi6* mutants are sensitive to calcofluor white and Swi6 is

phosphorylated by Mpk1 (Slt2) in response to cell wall stress (Igual *et al*., 1996; Madden *et al*., 1997).

It has been suggested that Sse1 may genetically interact with the transcription factor SBF in a manner that supports cell growth and proliferation (Shaner *et al*., 2008). In this investigation a combination of Swi6 and Hsp110 mutant strains were generated that have abnormal growth and cell morphology indicating that these components do interplay in similar cellular mechanisms.

4.12.1 Knocking out *SWI* genes in CM03

SWI6 was replaced by a *HIS5* marker in strain CM03. This was performed by knockout by homologous recombination using methods described in section 2.19. A PCR product of the *SWI6* knockout cassette (Figure 4.35) was transformed into CM03 and colonies were replicated onto SC - histidine. Colonies were picked off to confirm the presence of a knockout. Diagnostic PCRs were carried out on approximately six potential knockouts using primers listed in Table 2.12.d and PCR cycle listed in Table 2.11. The expected PCR product sizes are annotated in Figure 4.36. Three isolates were confirmed as Δ*swi6* and Figure 4.37 illustrates the PCR results for one of these strains.

Shaner *et al*. (2008) successfully created a BY4741 Δ*swi6*Δ*swi4* strain, a combination of deletions previously believed to be non-viable. One of the aims in this study was to make this double deletion in CM03. In order to knockout *SWI4* with the same *HIS5* gene *HIS5* was successfully removed from CM03Δ*swi6* by a method known as 'Cre lox'. This was performed by transforming vector pSH47 into CM03Δ*swi6*. This vector expresses a cre-recombinase that recognises *loxP* sites. The *HIS5* knockout construct from vector pUG27 contains *loxP* sites which have been

incorporated into CM03Δ*swi6* either side of the *HIS5* gene. The cre-recombinase loops out the internal *HIS5* gene and the strands recombine. *SWI4* deletions were attempted on three separate occasions and were unsuccessful each time.

(i) PCR annotation for *HIS5* knockout cassette

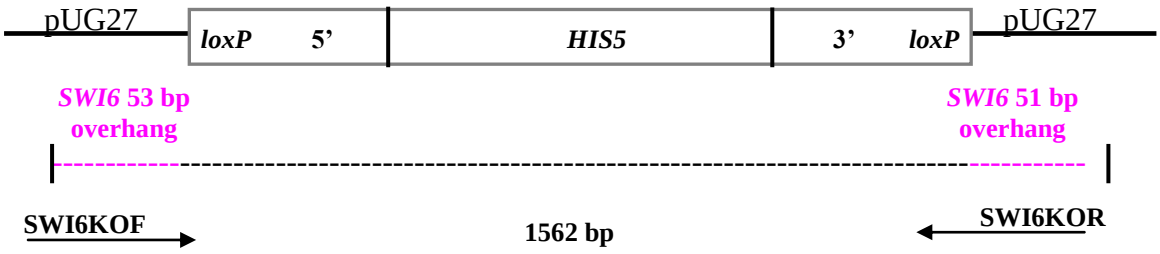

(ii) Agarose gel electrophoresis of PCR product

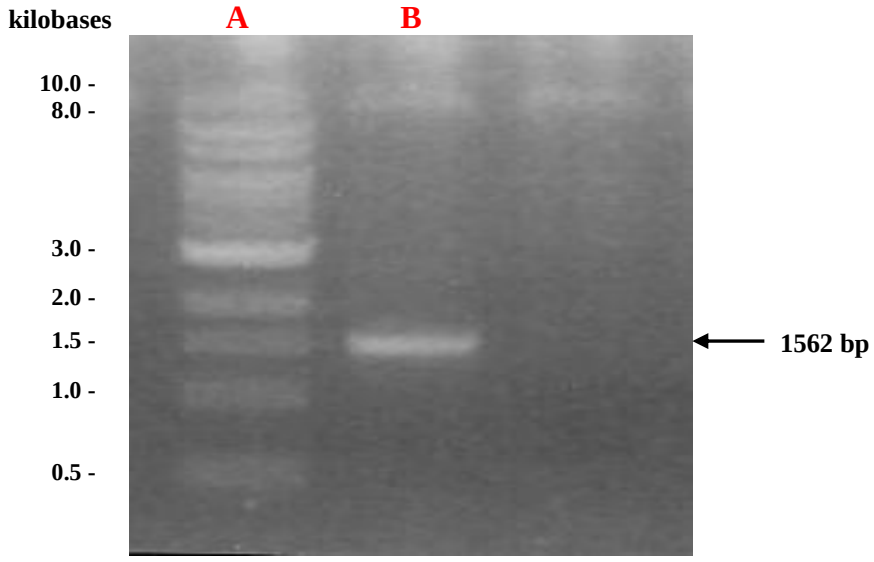

Figure 4.35. PCR product of Δ*swi6 HIS5* knockout cassette.
(i) Illustration of the expected band size for the Δ*swi6 HIS5* knockout cassette. Primers SWI6KO F/R were designed with sequence overhangs homologous to upstream and downstream of *SWI6* coding sequence. The primers also annealed to DNA upstream and downstream of the *HIS5* promoter and terminator sequence, in plasmid pUG27. The total PCR product was expected to be approximately 1562 bp.
(ii) Primers SWI6KO F/R were used on plasmid pUG27 which resulted in a product size of 1562 bp. This PCR product was used to knockout *SWI6* in CM03 by homologous recombination. Lane A illustrates 1kb DNA ladder and lane B is the knockout cassette PCR product.

(1) wild type *SWI6*

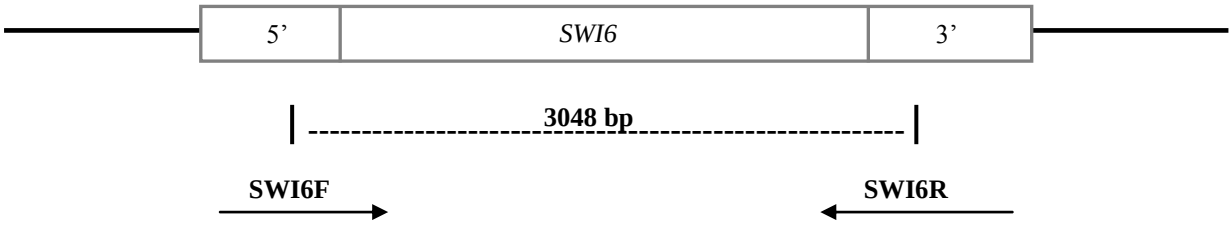

(2) Δ*swi6*

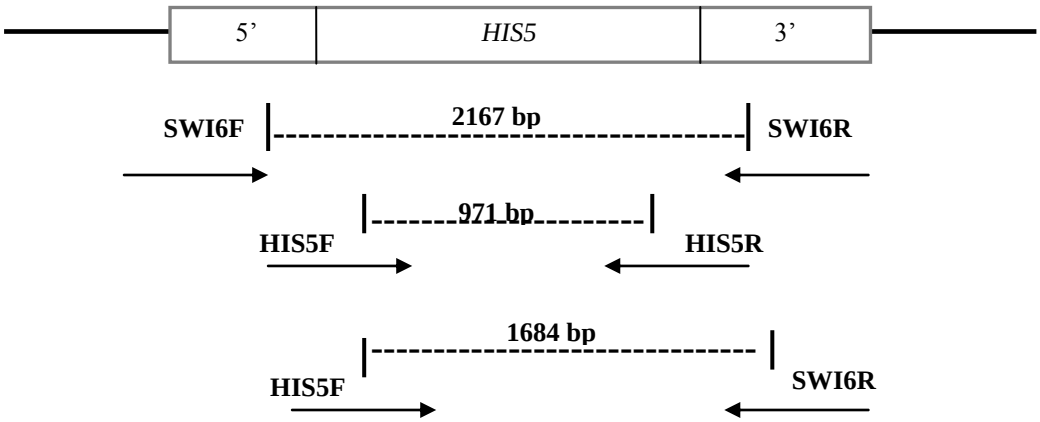

Figure 4.36. Illustration shows the expected wild type *SWI6* and Δ*swi6* constructs and PCR fragment sizes. (1) *SWI6* wild type DNA coding sequence is 2412 bp. Primers SWI6F and SWI6R are located upstream and downstream of *SWI6* coding sequence. PCR using these primers should result in a DNA band of approximately 3048 bp for wild type *SWI6*. (2) illustrates a *swi6* knockout construct with *HIS5* gene replacing the coding sequence of *SWI6*. The *HIS5* DNA used was from vector pUG27. PCR of the knockout construct, using primers SWI6F and SWI6R, should result in a band approximately 2167 bp in size. HIS5 F/R primers anneal internally to the *HIS5* DNA sequence and should result in a DNA band of 971 bp. PCR of the knockout construct, using primers SWI6R and HIS5F, should result in a DNA band approximately 1684 bp in size and corresponds to the right flanking region of the Δ*swi6* knockout construct.

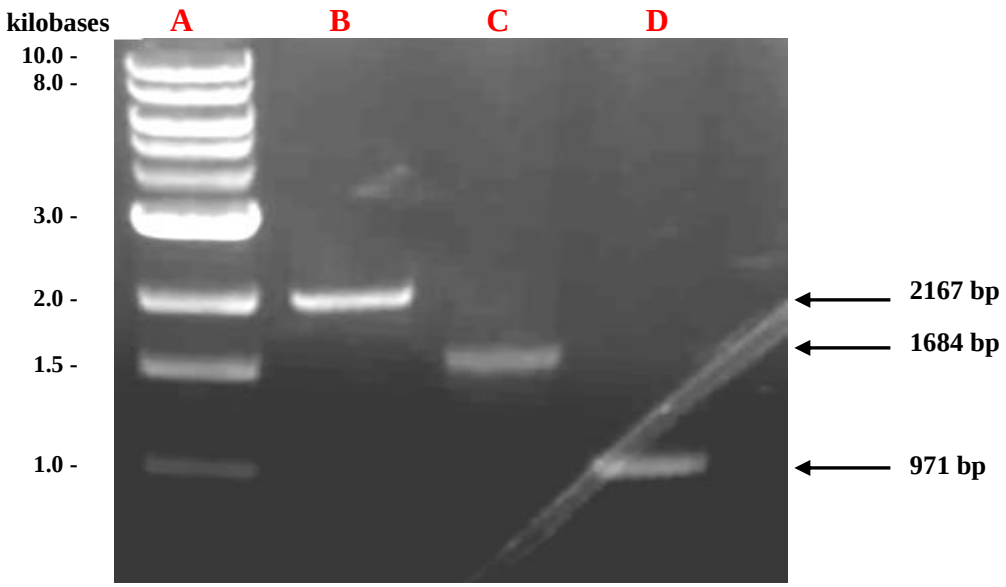

Figure 4.37. Diagnostic PCR of *swi6* knockout in strain CM03.

Lane A: 1kb molecular weight marker.

Lane B: PCR product from potential Δ*swi6* genomic DNA using primers SWI6F/R. This resulted in a DNA band approximately 2167 bp in size and corresponds to *HIS5* gene replacement. WT *SWI6* would result in a 3048 bp band.

Lane C: PCR product from potential Δ*swi6* genomic DNA using primers SWI6R and HIS5F. This resulted in a DNA band approximately 1684 bp in size and corresponds to the right flanking region of the CM03 Δ*swi6* knockout construct.

Lane D: PCR product from potential Δ*swi6* genomic DNA using primers HIS5F/R. This resulted in a DNA band approximately 971 bp in size and confirms that *HIS5* gene has been successfully incorporated into the CM03 genome. All primers are listed in Table 2.12.d.

4.12.2 Comparative growth analysis of CM03Δ*swi6* expressing WT Sse1, Sse2 and Sse1 mutants

To further investigate the relationship between Sse1 and SBF components strains were constructed with various mutations and deletions in Sse1, Sse2 and Swi6. The aim was to see what effect a Swi6 deletion would have on Sse mutant growth at

restrictive temperatures. In section 4.1 the temperature-sensitive effects of Sse1 mutants in strain CM02 were tested. This led to the conclusion that particular Sse1 mutants are ts to varying degrees at 39^{o}C. These mutants may have similar effects in CM03 and CM03Δ*swi6*. [*psi*$^{-}$] mutants were used in this study because they may have the biggest phenotypic and functional alterations although [*PSI*$^{+}$] phenotypic effects could not be analysed in CM03.

Sse1 mutants G41D, G50D, G342D and T365I were selected and their growth compared to WT Sse1 and Sse2 by comparative growth analysis (Figure 4.38). One major difference observed was that G41D, G50D and T365I grew well at 39^{o}C when these mutants were nearly completely non-viable in CM02 at this temperature. In CM03 mutant G342D was non-viable at 39^{o}C but grew well at 37^{o}C (Figure 4.38) suggesting that this mutant is ts but at a higher temperature of 39^{o}C.

Δ*swi6*Δ*sse1*Δ*sse2* + Sse1 grew relatively well and was the only strain to survive at 39^{o}C (Figure 4.39). However, in agreement with observations made by Shaner *et al*. (2008), Δ*swi6*Δ*sse1*Δ*sse2* + Sse2 growth was sensitive even at 30^{o}C (Figure 4.39). They tested Δ*swi6* growth alone at 30^{o}C and 37^{o}C and found that it grew normally and Δ*sse1* alone was slightly slow-growing, so it must be the combined effect of Sse1 and Swi6 deletion making the strain sick. Shaner *et al*. (2008) concluded that this phenotype may be caused by disruption to CWI pathway.

Four Sse1 mutants G41D, G50D, G342D and T365I were also expressed in CM03Δ*sse1*Δ*sse2*Δ*swi6* and analysed by comparative growth analysis. All Sse1 mutants were non-viable at 39^{o}C indicating that their particular mutation to Sse1 was incapable of providing a function to keep the cell alive in the presence of Δ*sse2* and Δ*swi6* (Figure 4.39). However the mutations to Sse1 did not have as severe of an

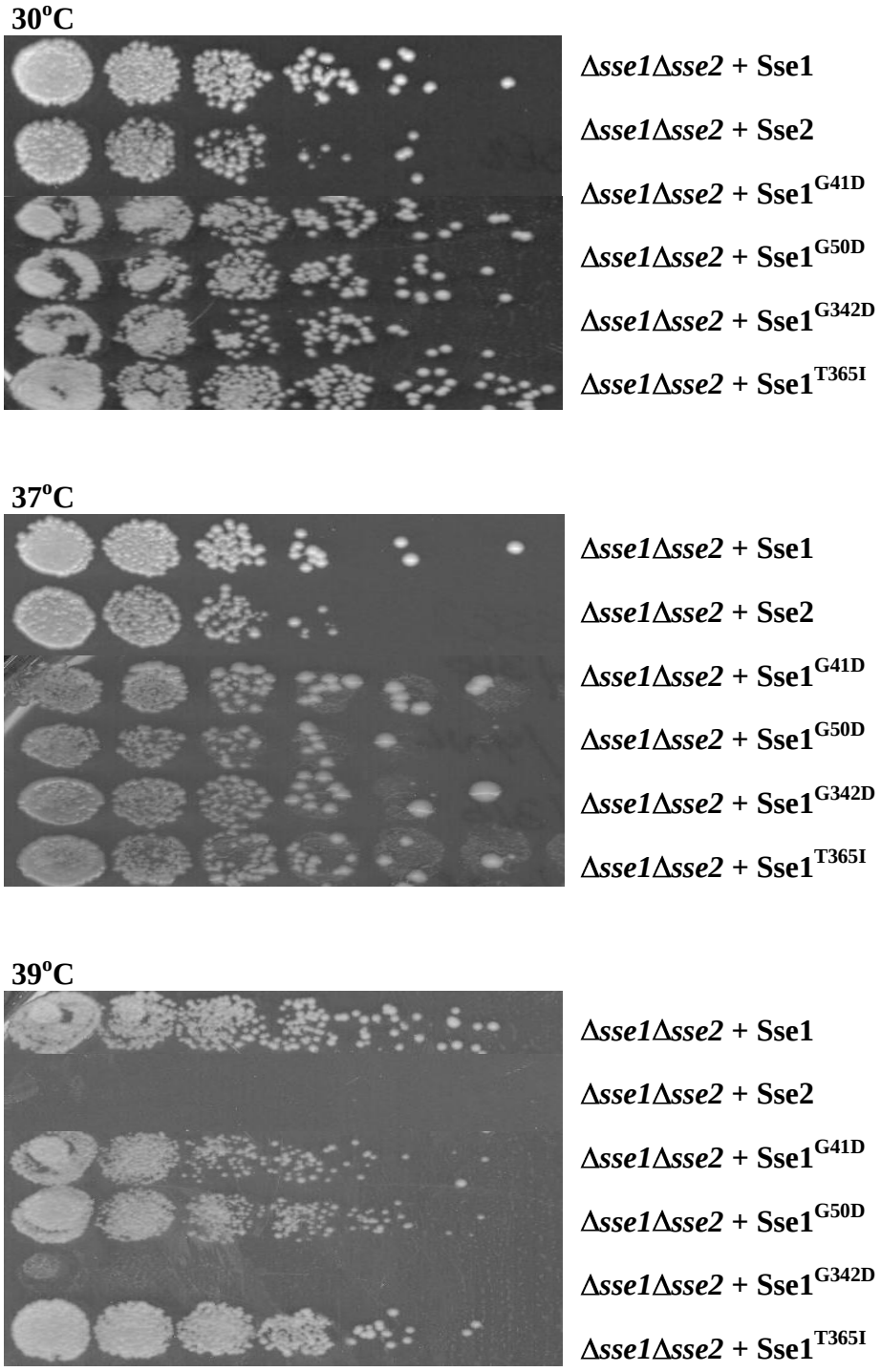

Figure 4.38. Comparative growth analysis of CM03 expressing Sse1 and Sse2 mutants. CM03Δ*sse1*Δ*sse2* was transformed with either Sse1, Sse2 or a selection of Sse1 mutants. Cells were selected on SC - leucine, incubated at 30°C for 2 days and replicated onto 5-FOA. Comparative growth analysis was performed on YPD and plates were incubated at 30°C, 37°C and 39°C for 2 days. All strains grew well at 30°C and 37°C however mutant G342D was completely non-viable at 39°C. All mutants grew much better at 39°C in strain CM03 compared to strain CM02.

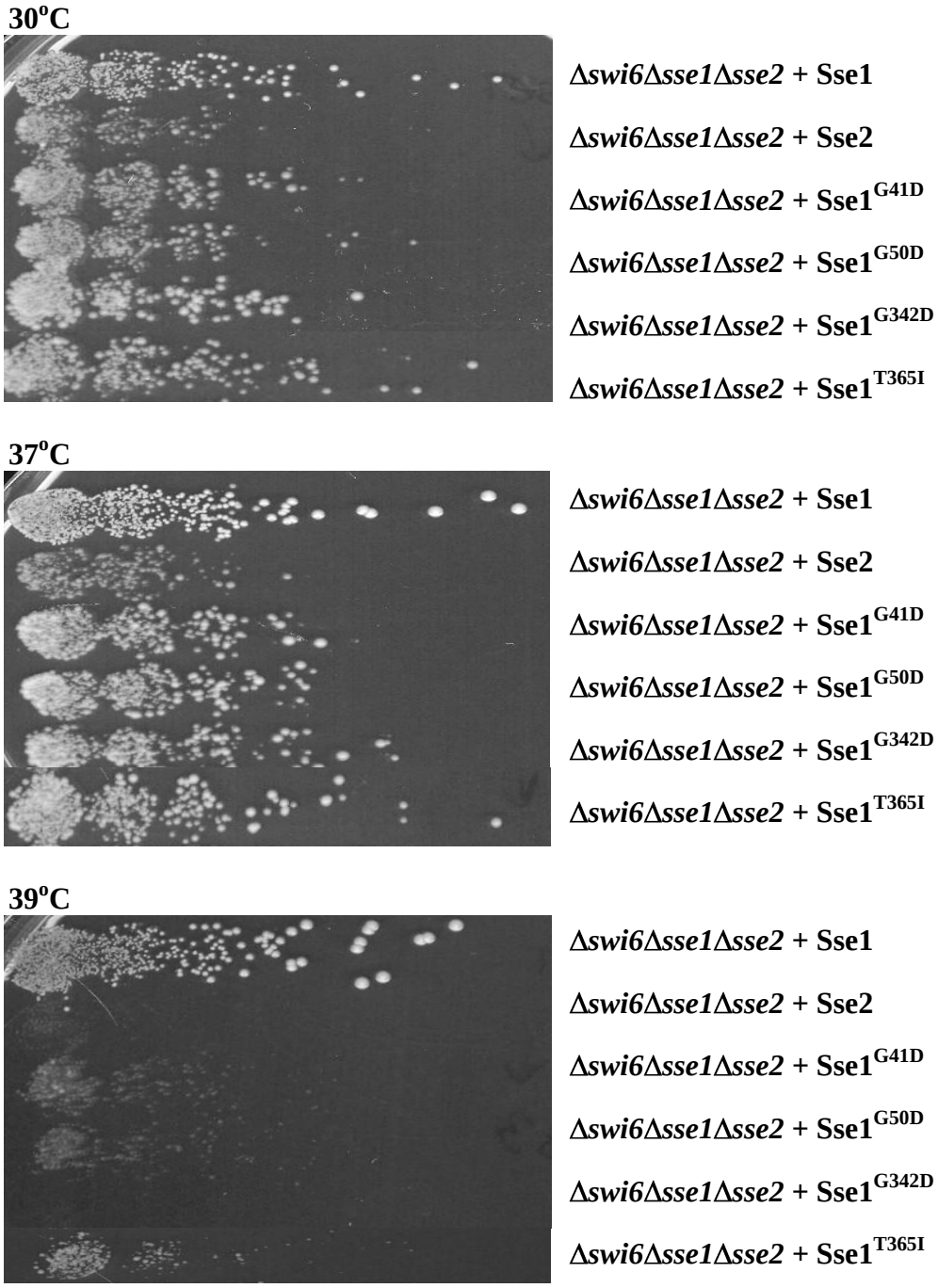

Figure 4.39. Comparative growth analysis of CM03Δ*swi6* expressing Sse1 and Sse2 mutants. CM03Δ*sse1*Δ*sse2*Δ*swi6* was transformed with either Sse1, Sse2 or a selection of Sse1 mutants. Cells were selected on SC - leucine, incubated for 2 days at 30°C and replicated onto 5-FOA. Comparative growth analysis was performed on YPD and plates were incubated at 30°C, 37°C and 39°C for 2 days. CM03Δ*swi6*Δ*sse1*Δ*sse2* + Sse2 struggled to grow even at 30°C. These results can be compared to the mutants in Figure 4.38 where they were in the presence of WT Swi6. The deletion of Swi6 made Δ*sse1* and Sse1 mutant strains non-viable at 39°C.

effect as complete deletion of Sse1, which when combined with Δ*swi6* demonstrated incomplete growth even at 30^{o}C. These results can also be compared to those found in Figure 4.38 when Sse1 and mutants were expressed alone. It appears that the deletion of *SWI6* does impair the ability of Sse1 and Sse1 mutants to grow at normal and restrictive temperatures.

4.12.3 Analysis of the effect of *swi6* deletion on cellular morphology

Yeast strains from section 4.12.2 were further classified according to their cellular morphology. Cell morphology is a good indicator for how 'healthy' a particular yeast strain is. Yeast normally have a small oblong shape which results from maintenance through cell cycle control, gene expression, cell wall synthesis and various signaling interactions (Blacketer *et al*., 1995). Swi4 and Swi6 transcription factors are known to control the expression of many cell cycle regulating proteins and their deletion has been implicated in abnormal bud elongation morphology (Nasmyth and Dirick, 1991; Andrews and Moore, 1992; Blacketer *et al*., 1995).

As Swi6 and Sse1 play a role in CWI signaling, and deletion of both genes has an effect on yeast growth (as seen in section 4.12.2), the next step taken was to determine whether a combination of these mutations disrupts cell structure. Cell morphology was examined by light microscopy at 40X magnification. Cells in Δ*swi6*Δ*sse1*Δ*sse2* + Sse2, Δ*swi6*Δ*sse1*Δ*sse2* + Sse1 and Δ*swi6*Δ*sse1*Δ*sse2* + Sse1 mutants were large, elongated and amorphous and were similar to those found by Shaner *et al*. (2008). In comparison, Sse1/2 deletion or Sse1 mutants alone produced circular shaped budding cells and seemed to have little obvious impact to cell morphology (Figure 4.40.a/b). However, Shaner *et al*. (2008) also discovered that Δ*swi6* alone results in approximately 30% of cells being elongated and the rest

normal so Swi6 deletion alone has some impact on cellular morphology. However, when BY4741Δ*swi6* cells were observed by light microscopy there was no alteration to cell morphology (Figure 4.40.c).

The additional deletion of *swi6* in Sse1 mutants had a huge impact on cell structure resulting in cells with disrupted structure, size and bud formation. The most severe abnormalities was seen for Δ*swi6*Δ*sse1*Δ*sse2* + Sse2, Δ*swi6*Δ*sse1*Δ*sse2* + $Sse1^{G50D}$ and Δ*swi6*Δ*sse1*Δ*sse2* + $Sse1^{T365I}$ where approximately 80% of cells were amorphous or elongated, indicative of defects to cell cycle regulation (Shaner *et al*., 2008). The least effect observed was for Δ*swi6*Δ*sse1*Δ*sse2* + Sse1 and Δ*swi6*Δ*sse1*Δ*sse2* + $Sse1^{G342D}$ which only produced approximately 30-40% elongated cells and the rest appeared normal. This was interesting since $Sse1^{G342D}$ alone is ts at 39^{o}C and was expected to have quite a severe affect on cellular homeostasis. Somehow the functions for Sse1 in temperature stability and cell morphology must be distinct and unrelated. It was not surprising that Δ*swi6*Δ*sse1*Δ*sse2* + Sse1 had one of the least effects as it still expressed WT Sse1 which probably plays a bigger role than Sse2 in cellular homeostasis.

4.13 Chapter discussion

This Chapter further classified thirteen Sse1 mutants according to their growth, sensitivity and involvement in cellular signaling processes. The understanding of Sse1 as a molecular chaperone and as a regulator of cell signaling and thermostability has been extended. Analysis of the strain CM02 led to the creation of a new background strain in BY4741 (CM03) in which the Sse1 mutant phenotypes could be compared. This allowed the creation of a comparative profile of these two yeast strains on a genetic and phenotypic level.

(a) CM03Δ*sse1*Δ*sse2* + Sse1

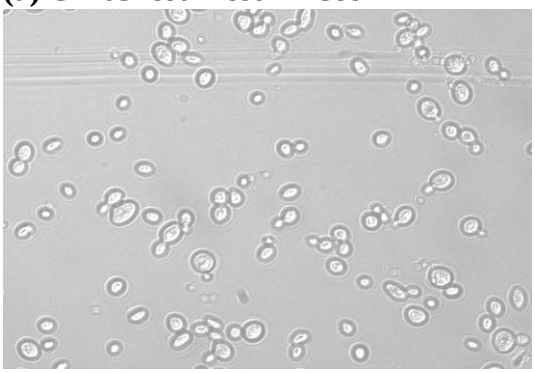

(b) CM03Δ*sse1*Δ*sse2*Δ*swi6* + Sse1

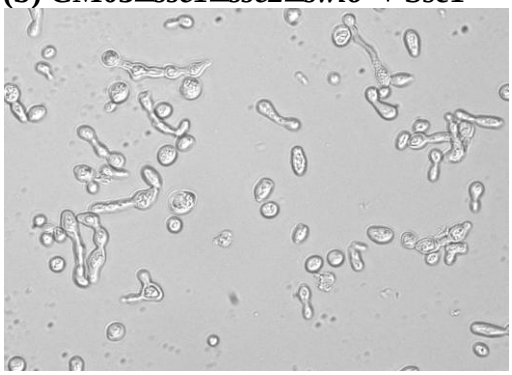

(c) CM03Δ*sse1*Δ*sse2* + Sse2

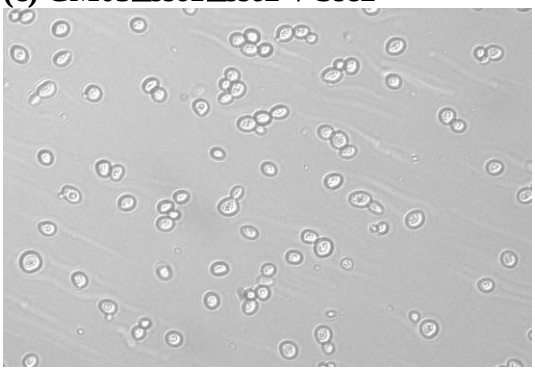

(d) CM03Δ*sse1*Δ*sse2*Δ*swi6* + Sse2

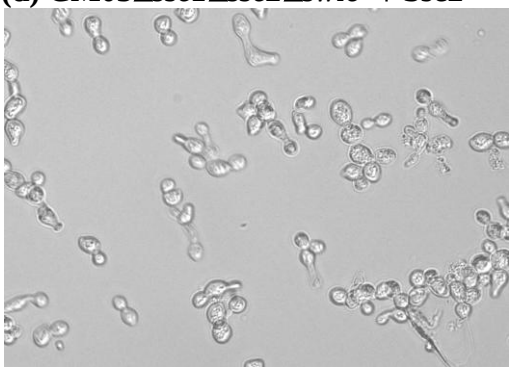

(e) CM03Δ*sse1*Δ*sse2* + Sse1^{G41D}

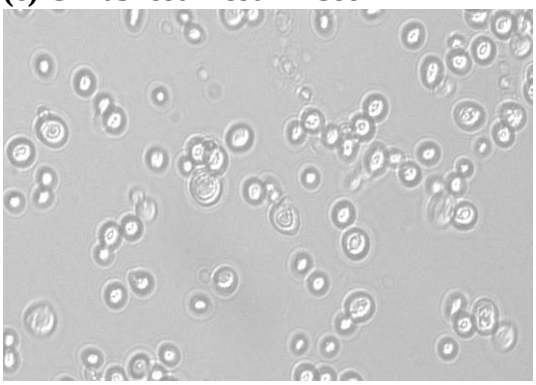

(f) CM03Δ*sse1*Δ*sse2*Δ*swi6* + Sse1^{G41D}

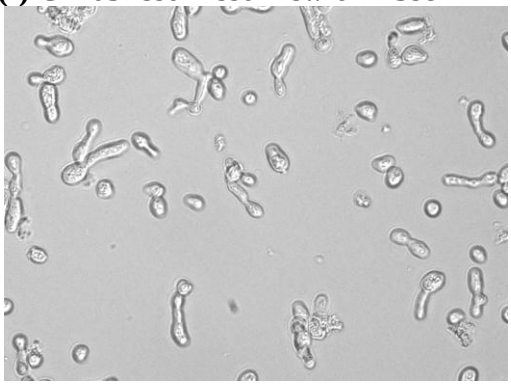

40X magnification

Figure 4.40.a. Analysis of yeast cellular morphology changes when *swi6* is deleted. CM03Δ*sse1*Δ*sse2* and CM03Δ*sse1*Δ*sse2*Δ*swi6* were transformed with Sse1, Sse2 and four Sse1 mutants. Cells were selected on SC - leucine, incubated at 30^{o}C for 2 days and replicated onto 5-FOA. Strains were maintained on SC-leucine and prepared by streaking on glass slides with 20 μl dH_2O. Cells were analysed at 40X under light microscopy.

(g) CM03Δ*sse1*Δ*sse2* + Sse1^{G50D}

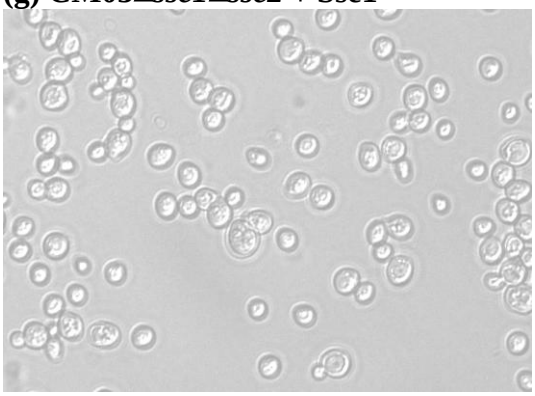

(h) CM03Δ*sse1*Δ*sse2*Δ*swi6*+ Sse1^{G50D}

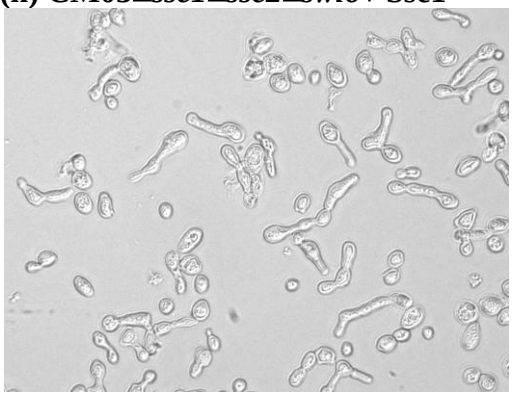

(i) CM03Δ*sse1*Δ*sse2* + Sse1^{G342D}

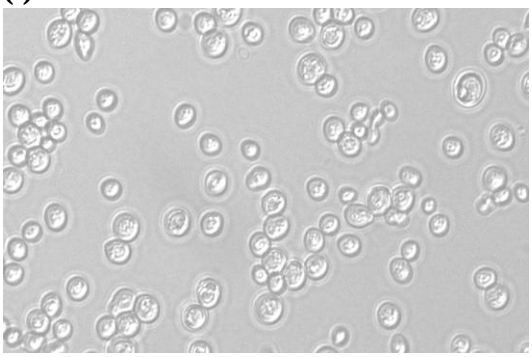

(j) CM03Δ*sse1*Δ*sse2*Δ*swi6* + Sse1^{G342D}

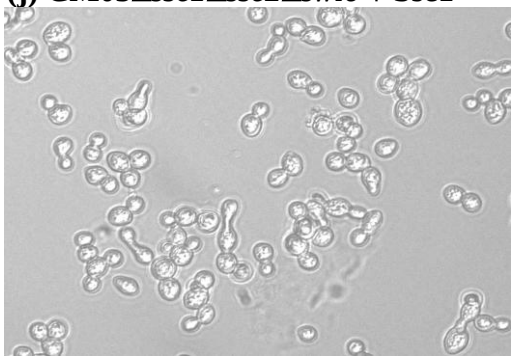

(k) CM03Δ*sse1*Δ*sse2* + Sse1^{T365I}

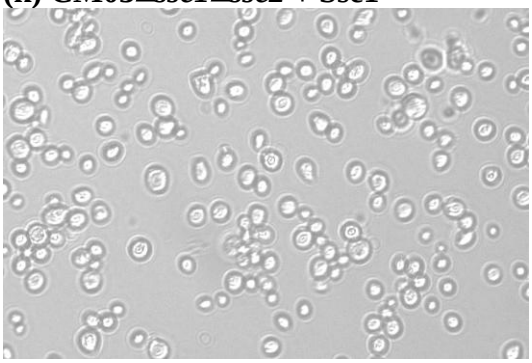

(l) CM03Δ*sse1*Δ*sse2*Δ*swi6* + Sse1^{T365I}

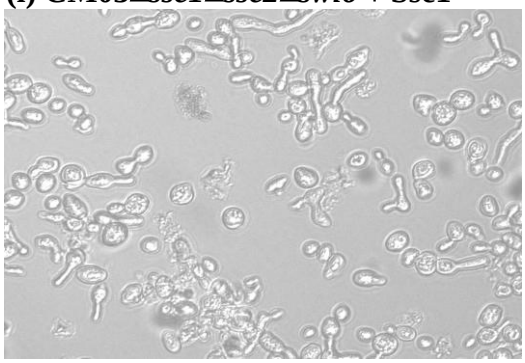

40X magnification

Figure 4.40.b. Analysis of yeast cellular morphology changes when *swi6* is deleted. CM03Δ*sse1*Δ*sse2* and CM03Δ*sse1*Δ*sse2*Δ*swi6* were transformed with Sse1, Sse2 and four Sse1 mutants. Cells were selected on SC - leucine, incubated at 30^{o}C for 2 days and replicated onto 5-FOA. Strains were maintained on SC - leucine and prepared by streaking on glass slides with 20 μl dH_2O. Cells were analysed at 40X under light microscopy.

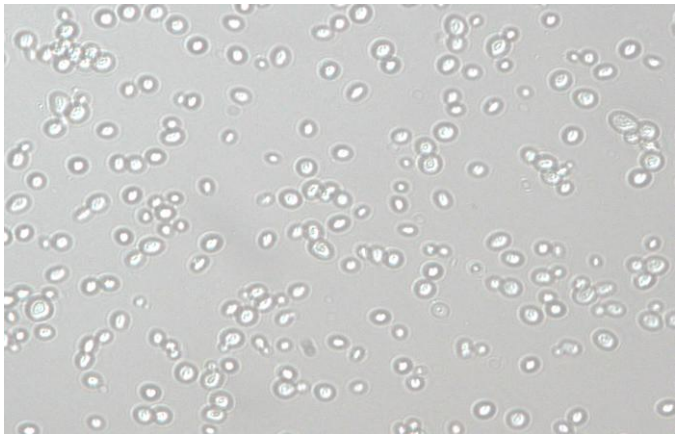

40X magnification

Figure 4.36.c. Analysis of BY4741 strain when *swi6* is knocked-out. Cells were prepared by streaking on glass slides with 20 μl dH_2O and analysed at 40X under light microscopy.

The Hsp110 group of molecular chaperones serve as heat-induced stress factors in many eukaryotic species including mammals (Lee-Yoon *et al*., 1995). In yeast, *SSE1* gene is moderately expressed at normal growth temperatures and induced at higher levels upon heat shock. *SSE2* is virtually undetectable until it is induced 20-fold upon heat stress (Mukai *et al*., 1993; Shirayama *et al*., 1993). Deletion of *SSE1* leads to slow-growing temperature-sensitive cells (Mukai *et al*., 1993). Due to the nature of Sse1 the initial aim was to test if any of the Sse1 mutants were incapable at providing cellular thermostability. Results from 37^{o}C comparative growth analysis revealed that the mutants $Sse1^{G342D}$ and $Sse1^{G616D}$ were ts. Comparative growth analysis at 39^{o}C allowed us to further classify all the mutants as they all displayed varying degrees of sensitivity at this temperature with $Sse1^{G41D}$, $Sse1^{G50D}$, $Sse1^{G342D}$ and $Sse1^{G616D}$ completely non-viable. These results confirmed a role of Sse1 in cellular thermotolerance and it is interesting how each Sse1 mutant showed thermal stress at different magnitudes. Sensitivity to thermal stress could be due to disruption

to Sse1 protein stability and interaction with other molecular chaperones due to heat denaturation. Sse1^{G342D} and Sse1^{G616D} were both temperature-sensitive at 37^{o}C in CM02. These non-viable phenotypes could result from improper Sse1 heat shock protein function. It was later investigated whether these mutants were ts in CM03 BY4741 background and Sse1^{G342D} was not ts but only slightly slow-growing at 37^{o}C. The differences in growth of mutant G342D in two strains could be due to strain background differences but how exactly is unknown. The next step involved investigating whether these mutants cause any other cell sensitivity in CM02.

Yeast cope well with environmental stress such as heat and osmotic shock by activating MAP kinase cascades (Chen and Thorner, 2007). When yeast grow on hypoosmotic medium such as YPD, the MAP kinase CWI signaling pathway is activated. CWI signaling mediates cell wall biosynthesis and repair (Levin, 2005). Mutants which disrupt this pathway need osmotic stabilisers such as 1 M sorbitol in order to grow (Davenport *et al*., 1995). Mutants G342D and G616D were osmoremedial at 37^{o}C when grown on YPD with 1 M sorbitol. This result indicated that the Sse1 protein may play a role in cell wall integrity. Other groups have found that mutants causing cell lysis at increased temperatures are often located in genes involved in cell wall maintenance (Paravicini *et al*., 1992). This theory was investigated further by testing the ts mutants sensitivity to cell wall damaging agents. Exposure of yeast to chemical agents such as congo red initiates CWI signaling and mutants of this cascade often display sensitivity to these agents (Levin, 2005). The results from this experiment were inconclusive as CM02 expressing WT Sse1 was sensitive to the chemicals and an accurate comparison between WT and mutant growth could not be made. The chemical concentrations used were lower than those used by other groups and the strain background was different to those used by others.

CM02 observed a general strain sensitivity, particularly to congo red and calcofluor white. This could be due to a background sensitivity in CM02 making it particularly sensitive to cell wall stress. Further on in this Chapter a number of SNPs were identified in the G600 genome which could be accountable for this strain sensitivity.

It was also investigated whether high copy inducers of CWI signaling could restore growth in temperature-sensitive Sse1 mutants. Pkc1 and Bck1 are essential components of CWI signaling and their constitutive expression on plasmid DNA did partially recover G342D and G616D growth at 37^{o}C. This indicated that these mutants could be affecting CWI signaling, through the MAP kinase pathway, as activation of Pkc1 and Bck1 leads to the up-regulation of genes involved in cell wall repair (Irie *et al*., 1993). However, the constitutive expression of Pkc1 seemed to have a greater effect on mutant growth at 37^{o}C than Bck1. Perhaps this was due to the fact that Pkc1 fulfills more than one role in cellular homeostasis and its activation stimulates the up-regulation of a multitude of genes through many signaling pathways. Despite these positive results no accurate conclusion could be made. The sensitivity of G600 and CM02 to the chemical agents was concerning and suggested an underlying genetic problem with this strain. The recovery of Sse1 mutant ts by Pkc1 and Bck1 was not reproduced in CM03.

These results prompted the creation of a new BY4741Δ*sse1*Δ*sse2* strain for testing Sse1 mutant phenotypes. Shaner *et al*. (2008) also used a BY4741 background strain for testing Sse1 mutant sensitivity to congo red and calcofluor white. They found a comparable difference in sensitivity between WT Sse1 and Δ*sse1*/*sse1* mutant strains when grown on these agents. All previous tests performed in CM02 were repeated in BY4741 Δ*sse1*/*sse2* strain (CM03). The first difference observed was that the Sse1 mutant G342D was not fully ts but only slightly slow-growing. Sse1^{G342D}

and Sse1^{G616D} temperature-sensitive growth was fully recovered on 1 M sorbitol but the activation of Bck1 and Pkc1 resulted in no growth recovery at 37^{o}C. When tested on chemical cell wall perturbing agents CM03 grew substantially better than CM02 although its response to each individual chemical was not uniform. There were no obvious differences in growth between WT Sse1 and Sse1 mutants on chemical agents. BY4741Δ*slt2* was used as a control and it was non-viable on 5 μg/ml congo red. CM03 survived on congo red at concentrations up to 25 μg/ml. The stability of Sse1 mutants on congo red compared to Δ*slt2* suggested that the Sse1 mutants are not affecting CWI signaling at all, or that their effects are not easily detectable, as they should have displayed similar phenotypes to Δ*slt2*. However Δ*slt2* was selective in what it was sensitive to as it only showed sensitivity to congo red and calcofluor white. It was clear from these results that different chemical stresses do not have a uniform response in CWI signaling mutants such as Δ*slt2* (Fuchs and Mylonakis, 2009). The recovery of Pkc1 and Bck1 in CM02 did hint at CWI signaling but this may have been due to a strain background issue and not the mutants alone. A number of SNPs were identified in G600 with one located in Pkc1. This could possibly account for growth recovery in the presence of activated Pkc1 and Bck1.

CWI signaling is known to cross-talk with other cellular pathways in response to stress such as protein kinase A, TOR and HOG signaling (Fuchs and Mylonakis, 2009). It has also been suggested that Slt2 activation is independent of Pkc1 and Bck1. Harrison and collegues tested Pkc1 and Bck1 mutant strains and found Slt2 induction and phosphorylation in response to heat shock (Harrison *et al*., 2004). Perhaps CWI signaling is dispensable and allows lateral influences to activate Slt2? (Fuchs and Mylonakis, 2009). The activation of CWI signaling also depends on the type of stress that initiates the response. Osmotic stress and exposure to zymolase

involves both HOG and CWI signaling whereas caffeine stress induces a CWI response through Slt2 phosphorylation in a TOR dependent manner (Fuchs and Mylonakis, 2009). The lack of sensitivity of CM03 to caffeine re-emphasised no role in CWI signaling. The complexity of the CWI signaling network and numerous interacting components makes it difficult to pinpoint exactly how and why the Sse1 mutants may be affecting signaling. Perhaps Sse1 mutants are not affecting a single stress pathway in a specific manner but causing a more complicated effect through multiple interacting pathways?

The Sse1 mutants were further assessed to determine if they affect other cell signaling pathways. Hsp90 is a cellular chaperone that plays a central role in cell signaling and in providing cell thermostability (Nathan *et al*., 1997; Zhao *et al*., 2005). Sse1 has been physically and genetically linked with Hsp90 and is implicated in the maturation and client fate of Hsp90 substrates (Liu *et al*., 1999; Lee *et al*., 2004; Shaner *et al*., 2008; Mandal *et al*., 2010). Like Sse1 mutants, Hsp90 mutants exhibit osmoremedial temperature-sensitive growth (Piper *et al*., 2006; Truman *et al*., 2007). A number of tests were carried out to assess whether Sse1 mutants affect Hsp90 signaling and the results suggested that they do not interfere with Hsp90 signaling. Whether the mutants were disrupting PKA signaling was also tested. Yeast cell growth on glucose medium results in the hyperactivation of the PKA pathway which is ultimately associated with decreased tolerance to thermal stress. Sse1 and Sse2 may decrease PKA activity in times of heat shock when chaperone levels are highly induced. Sse1 has been linked with PKA signaling, as a negative regulator, and the ts effects of Δ*sse1* can be suppressed by decreasing PKA signaling (Trott *et al*., 2005). Sse1 mutants G342D and G616D growth was improved at 37^{o}C and they grew as well as WT Sse1 when selected on YP-glycerol. YP-glycerol down-regulates

normal PKA signaling and it is perhaps suppressing a ts phenotype exerted by Sse1 mutants on YP-glucose. So mutations to Sse1 such as G616D may be preventing Sse1 from regulating PKA thus leading to a ts phenotype.

The availability of two Δ*sse1*Δ*sse2* strains allowed a comparative analysis to be carried out between both CM02 and CM03. Firstly, strain temperature sensitivity and sensitivity to cell wall damaging agents was looked at. Mutant $Sse1^{G342D}$ was non-viable in CM02 at 37^{o}C but only slightly slow-growing in CM03. This indicates that $Sse1^{G342D}$ is having an enhanced effect when expressed in CM02. CM03 + Sse1 grew on cell wall perturbing agents at a much greater rate than CM02 + Sse1. CM02 was unstable on relatively low concentrations of congo red and SDS (Figure 4.22). These differences in environmental stress coping mechanisms are indicative of genetic mutations to cell wall stress signaling. Differences were also observed in the strains ability to complement different proteins with similar NEF function. In Chapter 3 it was concluded that Fes1 and HSPH1 could not support non-viable growth in CM02Δ*sse1*Δ*sse2*. The tests were repeated in CM03 and found that both proteins could support deletion of *sse1*/*sse2*. As previous work has shown that Fes1 could partially/fully complement Sse deletion it was concluded that Fes1 over-expression can complement deletion of *sse1* and *sse2*. HSPH1 is the human homolog of yeast Sse1 and they share functional characteristics so it does seem plausible that it can compensate for loss of Sse1 in yeast as it was expressed on a high copy plasmid vector. These results confirmed the previous belief that CM02 has a background strain weakness making it highly sensitive. An additional comparative observation was made with the Sse1 mutant Q458*. This was analysed as a difference in the level of nonsense suppression between the two strains. Truncated protein $Sse1^{Q458trunc}$ was created and expressed in CM02 and CM03 and it could not support growth. This was

not surprising as Sse1 could not form a fully functional protein with such a huge truncation. However, the Sse1^{Q458*} stop codon mutant could support growth in CM02 but not in CM03. It can be speculated that perhaps the premature stop codon was subjected to a relatively high level of readthrough in CM02. Highly efficient nonsense suppression in an *ade2.1* strain means that the cell is [*PSI*$^{+}$] caused by aggregation of Sup35 (Tuite and Cox, 2007). However, Sse1 mutant Q458* was originally isolated as a [*psi*$^{-}$] mutant therefore there is still a certain level of functional Sup35 in the cell. A number of factors could enhance readthrough in strain CM02 including the presence of *SUQ5* mutation. CM02 contains *SUQ5* and CM03 does not. *SUQ5* is a serine tRNA nonsense suppressor resulting in the incorporation of a serine residue at certain stop codons. Therefore, there is the possibility that Q458* is actually translated as Q458S in CM02. This would account for the readthrough and possible [*psi*$^{-}$] phenotype of this mutant. To confirm this theory a Q458S mutant could be induced into WT *SSE1* DNA by site-directed mutagenesis to assess whether the mutant has a [*psi*$^{-}$] phenotype. The Sse1^{Q458trunc} DNA was cloned into the plasmid pC210 at *Nde1* and *Sph1* sites. The C-terminal sequence of this truncated form of *SSE1* is composed of approximately 175 bp of *SSA1* terminator sequence which then leads onto pC210 plasmid sequence after a *Hind*III site. The next in-frame stop codon is approximately 100 bp after the Sse1 truncated protein. If this nonsense Q458-TAA stop codon was subjected to readthrough then the Sse1 protein would possibly have a 100 bp C-terminal extension composed of Ssa1 protein. This could also impact the Q458* truncated protein phenotype in CM02 and CM03.

Using next generation sequencing approximately 6,500 SNPs were identified in G600 compared reference strain S288C (BY4741 is directly related to this strain). This translated into approximately 1,500 non-synonymous amino acid changes

distributed across G600 coding DNA. A number of plausible hypotheses for mutations that could change the sensitivity to cell wall damaging agents can be made. Five changes were identified in the protein kinases Akl1 and Hsl1, kinases that phosphorylate Sse1 and Sse2. Changes to Sse phosphorylation could alter the proteins stability, location and function. Four mutations were also identified in protein kinase Pkc1. This protein initiates cell stress signals from the cell wall and through the the CWI pathway, leading to the up-regulation of stress response genes. SNPs in Pkc1 could potentially explain why CM02 was so sensitive to cell wall damaging agents. No SNPs were identified in heat shock proteins. A single mutation was also identified in Ira2 protein. This protein plays a role in cAMP/PKA signaling and a mutation to it may affect CM02 thermotolerance and sensitivity. CM02 grew better than CM03 on non-fermentable carbon which reduces PKA activity. Perhaps this mutation is affecting CM02 in a way that makes it better able to grow in the absence of glucose.

G600 also contains a number of Inactivating Stop Codon Mutations (ISCMs) which can have major implications on mRNA translation and function. Four ORFS in G600 contained single internal nonsense mutations, one of them being *ade2.1*. Two of these genes were YNL106C and YBR074W. Both were severely truncated by 532 and 653 amino acids respectively. If YNL106C and YBR074W play a role in cell wall signaling then their truncation could affect one of these pathways and thus lead to strain sensitivity. Whether or not YBR074W expression could suppress G600 sensitivity to cell wall damaging agents was tested. G600 [PSI^{+}] grew relatively the same whether YBR074W was over-expressed or not. However G600 [psi^{-}] was non-viable on small quantities of congo red, SDS and calcofluor white. This sensitivity was partially recovered by the over-expression of YBR074W. This provided a new perspective on G600 sensitivity. It appears that some of G600

sensitivity is related to the cellular levels of [*PSI*$^{+}$]. When Sup35 is nonfunctional and G600 is [*PSI*$^{+}$] perhaps there is decreased translation termination at the ISCMs leading to some functional YBR074W protein available in the cell. This could have an impact on phenotypic results for Sse1 [*psi*$^{-}$] mutants in CM02 as their growth and sensitivity could be affected by the level of nonsense suppression at ISCMs. However, there must be something else affecting G600 sensitivity as it is not just a [*psi*$^{-}$] phenotype making the strains more sensitive. Sse1 [*psi*$^{-}$] mutant G616D was ts and recovered by sorbitol in both CM02 and CM03 showing no difference in growth or recovery in both strains so sensitivity of strain G600 is not just [*PSI*$^{+}$] related.

As Sse1^{G616D} was confirmed temperature-sensitive in CM03 it was an objective to screen for other possible *sse1* ts mutants. The screen was carried out meticulously and all the controls behaved as predicted. The secondary screen confirmed that four isolates were ts and each was sequenced as Sse1^{G616D}. It seemed unusual that only one mutation was isolated that could cause Sse1 to be thermosensitive, but the screen was approaching saturation as Sse1^{G616D} was isolated more than once. Perhaps the screen could have been performed at a higher temperature in order to isolate more ts mutants. However, this could have resulted in many ts mutants with unknown structural problems so it was carried out at 37^{o}C to isolate specific cell wall signaling mutants. This result confirmed that mutant G616D is altering the Sse1 chaperones ability to deal with the consequence of thermal stress either directly or indirectly through interaction with other chaperones. In Chapter 3, G616D was suggested to disrupt Hsp70 interaction perhaps indicating that its temperature sensitivity is due to a loss of Hsp70 interaction.

The growth and morphological effects that Δ*swi6* has on yeast expressing Sse1 mutants was also investigated. Swi6 is a component of the SBF and MBF

transcription factors that activate gene expression in the late G_1 phase of cell cycle progression (Breeden, 1996). Swi6 is also involved in CWI signaling and is activated by Mpk1 in response to cellular stress (Madden *et al*., 1997). *swi6* was successfully knocked out in CM03 but attempts at creating CM03Δ*swi6*Δ*swi4* was unsuccessful. Shaner *et al*. (2008) successfully created Δ*swi6*Δ*swi4* but the difference between this strain and Shaner *et al*. (2008) was that the CM03 strain was deleted for *SSE2*. The CM03 strain used to knock out *SWI4* in was BY4741Δ*sse1*Δ*sse2*Δ*swi6* + pRS316*SSE1* compared to BY4741 Δ*swi6* used by Shaner *et al*. (2008). It may have been the absence of *SSE2* that prevented the viability of this deletion therefore Δ*sse2*Δ*swi6*Δ*swi4* is a lethal knockout.

Swi6 deletion had major growth effects on CM03Δ*sse1* (Δ*sse1*Δ*sse2* + Sse2) at basal temperatures and disrupted Sse1 mutant growth at 37^{o}C and 39^{o}C. Shaner *et al.* (2008) also observed this phenotype but in their strain background Δ*swi6*Δ*sse1* grew poorer than the CM03 strain at 30^{o}C and 37^{o}C. The only difference between the two strains was that CM03 had *SSE2* expressed on a plasmid vector, under its own promoter, and Shaner *et al*. (2008) had genomic *SSE2*. This could account for the small differences in growth. Sse1 mutants G41D, G50D and T365I could support growth at 39^{o}C when expressed alone but were completely non-viable when *swi6* was deleted. As both Swi6 and Sse1 are involved in cell wall signaling perhaps their combined deletion/mutation is affecting signaling through this pathway. However, the mutants must be affecting some other biological process as a non-stress temperature of 30^{o}C resulted in poor growth for CM03Δ*sse1*Δ*swi6* (Δ*sse1*Δ*sse2*Δ*swi6* + Sse2). These results concur with Shaner *et al*. (2008).

Swi6 is known to control the expression of many cell cycle regulating proteins and its deletion has been implicated in abnormal bud elongation morphology

(Nasmyth and Dirick, 1991; Andrews and Moore, 1992; Blacketer *et al*., 1995). Changes in yeast morphology is indicative of alterations to cell cycle control and cell signaling activity (Blacketer *et al*., 1995). CM03 with mutations to *sse1* and *sse2* alone produced normal circular budding cells and seemed to have little obvious impact on normal cell morphology. However, the additional deletion of *swi6* had a huge impact resulting in cells with disrupted structure, size and bud formation (Figure 4.40). The combination of Δ*swi6* and *sse* mutants/deletions created amorphous elongated yeast cells. The most severe abnormalities was seen for Δ*sse1*Δ*sse2*Δ*swi6* + Sse2, Δ*swi6*Δ*sse1*Δ*sse2* + $Sse1^{G50D}$ and Δ*swi6*Δ*sse1*Δ*sse2* + $Sse1^{T365I}$ where approximately 80% of cells were amorphous or elongated, indicative of defects to cell cycle regulation (Shaner *et al*., 2008). Shaner *et al*. (2008) found that reintroducing WT Sse1 into Δ*sse1*Δ*swi6* restored normal cell morphology by approximately 90% indicating that it is a combination of the two mutations creating the abnormalities but that Δ*swi6* alone does impact cell structure. They also found that the over-expression of Fes1 restored a normal phenotype in approximately 90% of Δ*sse1*Δ*swi6* cells indicating a possible role for NEF activity in regulating cell morphology. Shaner *et al*. (2008) expressed mutant $Sse1^{G233D}$ in Δ*sse1*Δ*swi6* and found that cells still suffered severe morphological defects. This mutant is known to disrupt NEF activity. The Sse1 mutant T365I exhibited the most severe morphological defects in Δ*sse1*Δ*sse2*Δ*swi6* and in Chapter 3 it was hypothesised that this mutant disrupts Hsp70 interaction and NEF activity. This supports Shaner *et al*. (2008) suggestion that NEF activity is important for normal cell morphology. However, mutant G50D also exhibited severe amorphous elongated cells and it is not believed to disrupt NEF activity.

Recently, using a variety of genetic, bioinformatic and biochemical techniques Alberti *et al*. (2009) identified a number of novel yeast prion proteins. This involved isolating proteins with prion-like Q/N-rich domains. These prion forming domains (PrDs) are rich in Q/N residues and can be transferred to other proteins to create new prions (Li and Linquist, 2000; Alberti *et al*., 2009). Alberti *et al*. (2009) found that Slt2 and Rlm1 have the potential to form prion proteins. If they are true prions then Sse1 mutant chaperones could have unknown effects on their stability and possible cell phenotypes. If they are true prions then that could suggest why there was sensitivity in CWI signaling.

In this Chapter the temperature-sensitive effects of Sse1 mutants on the cell were assessed. It was investigated whether the mutants were disrupting MAP kinase signaling, Hsp90 signaling and PKA signaling. This led to the conclusion that yeast cell wall signaling processes are complicated and influenced by numerous factors making it hard to pinpoint and exact mechanism of disruption. Therefore mutations to Sse1 which make the cell ts could be affecting a multitude of factors which all accumulate to create the resulting sensitive phenotype. This Chapter helped reveal the major differences in the laboratory strain G600 compared to commonly used BY4741. This prompted the sequence analysis of the G600 genome leading to genetic analysis which is still ongoing. It provided possible answers to questions as to potentially why this strain has different characteristics to BY4741 and why [*PSI*$^{+}$] may have an effect on strain sensitivity.

CHAPTER 5
COMPARATIVE ANALYSIS OF *SSE1* AND *SSE2* IN ABILITY TO PROPAGATE PRIONS AND AN INITIAL INTRODUCTION INTO POSTTRANSLATIONAL MODIFICATION OF HSP110

5.0 Introduction

The main objective of the experiments described in this Chapter was to carry out a comparative analysis of Sse1 and Sse2 by assessing their role in prion propagation and the role protein phosphorylation plays in their cellular functions. Posttranslational modifications such as phosphorylation have the potential to impact how these chaperones function in prion propagation and in providing cellular thermostability.

In yeast, Hsp110 is represented by Sse1 and Sse2 molecular chaperones (Polier *et al*., 2008). *SSE1* and *SSE2* work together to create an essential gene pair (Trott *et al*., 2005) that respond to heat stress and function as NEFs (Mukai *et al*., 1993; Sadlish *et al*., 2008). Sse1 is the more well-studied protein of the two and it appears to play a more dominant role in cellular activity (Mukai *et al*., 1993). Few groups have compared Sse1 and Sse2 in their ability to propagate yeast prions or in their role as heat shock activated proteins. Mukai *et al*. (1993) were one of the first groups to study Hsp110 in yeast. They discovered that the deletion of *SSE1* resulted in temperature sensitivity. Mukai *et al*. (1993) also investigated the response of Sse1 and Sse2 to cellular heat shock. They concluded that *SSE1* is constitutively expressed at basal temperatures and *SSE2* mRNA was hardly detectable at 30^{o}C. However, both Hsp110 isoforms are up-regulated in response to thermal stress. Since then other groups have confirmed these observations and research into Hsp110 molecular chaperones has revealed that they are vital proteins, playing roles in many cellular pathways. The significance of these chaperones in yeast cell viability is emphasised by the fact that deletion of both proteins results in cell lethality (Shaner *et al*., 2004; Raviol *et al*., 2006b).

Sse2 does function as a NEF alongside Sse1, however it stimulates nucleotide release ~50% less than Sse1 (Dragovic *et al*., 2006; Sadlish *et al*., 2008). It has also been suggested that up-regulated Sse2 may be sufficient to refold firefly luciferase in the absence of Sse1 (Raviol *et al*., 2006b). However, Polier *et al*. (2010) concluded that Sse2 fails to stabilise the luciferase substrate under heat stress, possibly due to small structural differences between the proteins. The proteins are structurally similar but somehow Sse2 has a smaller role when it comes to Hsp110 activity. In the absence of Sse1 the level of [*PSI*$^{+}$] propagons diminishes with soluble Sup35 levels rising. This indicates that Sse2 is incapable at propagating [*PSI*$^{+}$] at an equal rate to Sse1 (Sadlish *et al*., 2008).

The differences in the Sse1 and Sse2 proteins ability to propagate [*PSI*$^{+}$] and support growth may also be due to the amount of molecular interactions they make within the cell. It has been confirmed that Sse1 does interact with more biological entities than Sse2 (Gong *et al*., 2009). The small differences in protein structure could also account for functional differences. As Sse2 is only stress induced, it may have originally evolved as a 'backup' chaperone for Sse1 by helping out in times of stress. It is presumed that the *SSE* genes resulted from gene-duplication in the *Saccharomyces* progenitor species (Polier *et al*., 2010).

In this study, the abilities of Sse1 and Sse2 to propagate [*PSI*$^{+}$], provide growth and withstand thermal stress were compared. It was also aimed to investigate the response of Sse2 to mutations, originally isolated in Sse1, and how mutations which make Sse2 more structurally similar to Sse1 affect its phenotype. Another objective was to investigate how phosphorylation affects the ability of chaperones to propagate [*PSI*$^{+}$]. In this Chapter, kinases which phosphorylate Hsp110 proteins were analysed and how posttranslational modification of Hsp110 may affect prion

propagation was also examined. The objective was to gain insight into this phenomenom by mutating particular kinases and phosphorylation sites and observing the responding phenotypes.

5.1 A comparative analysis of Sse1 and Sse2's influence on growth and [*PSI*$^+$]

The function of Sse2 in prion biology is less understood than Sse1 (Fan *et al*., 2007). Sse1 remains the main Hsp110 chaperone in yeast as its deletion results in slow-growing temperature sensitivity whereas deletion of Sse2 has no obvious growth defects (Mukai *et al*., 1993). Few groups have looked at the comparative differences between yeast expressing either Sse1 or Sse2. In this section the two proteins were compared in their ability to provide cellular growth, at normal and adverse temperatures, and in their ability to promote [*PSI*$^+$] propagation as the only Hsp110 isoform.

5.1.1 Cloning *SSE2* into pRS315

SSE2 was cloned into plasmid vector pRS315 using homologous recombination methods described in section 2.23. G600 genomic DNA was isolated and *SSE2* promoter and coding sequence were amplified by PCR using primers listed in Table 2.12.b and PCR cycle 2 in Table 2.11. The PCR product was 2365 bp with 60 bp overhangs homologous to pRS315 sequence. pRS315 plasmid DNA was prepared as described in sections 2.23.3 and 2.23.4 and cloning was carried out by transforming digested vector and PCR insert into strain G600 (as described in section 2.23.5). Five potential *SSE2* clones were isolated and Figure 5.1 illustrates the results of *Bam*H1 digestion. *Bam*H1 digestion should result in a large DNA fragment approximately

(i) pRS315-*SSE2* construct digested with *Bam*H1 enzyme

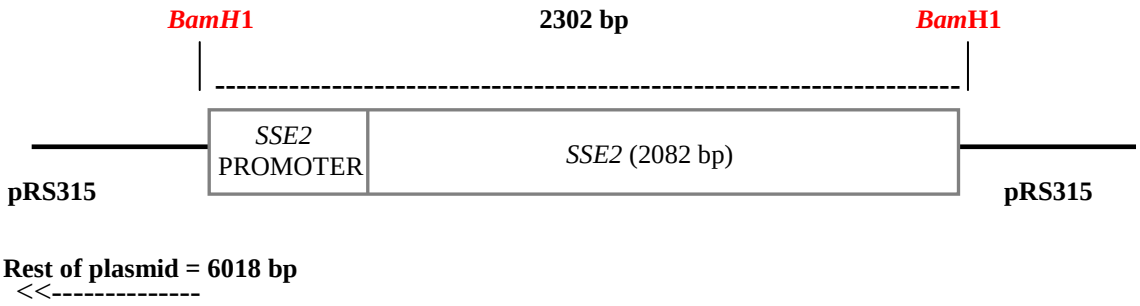

(ii) Agarose gel electrophoresis of digested vectors

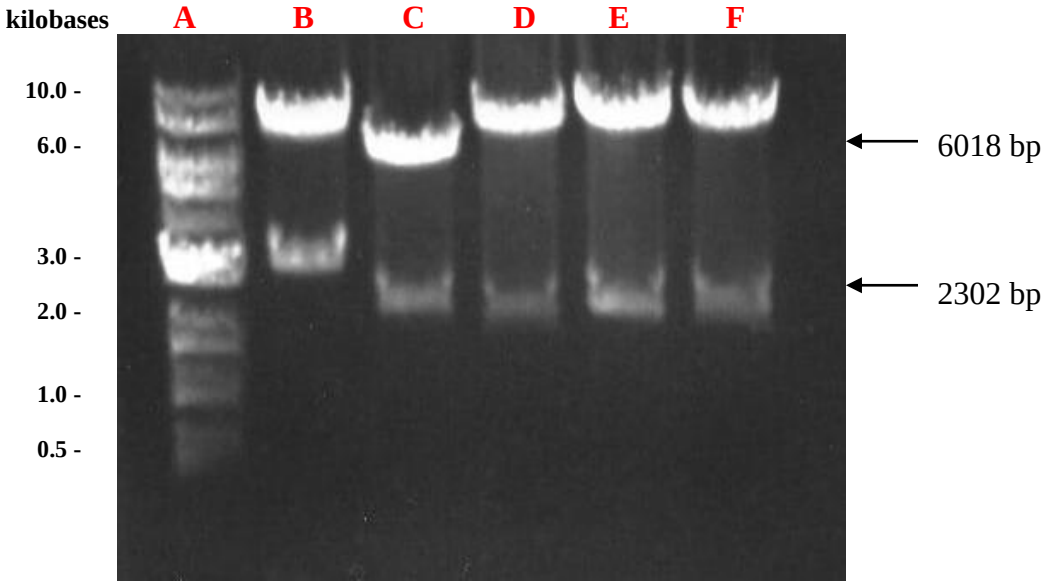

Figure 5.1. Diagnostic restriction digest of potential *SSE2* clones.

(i) pRS315-*SSE2* construct with expected bp sizes after restriction digest with *Bam*H1. *Bam*H1 sites were included in the cloning primers before the *SSE2* promoter and after the *SSE2* stop codon. This should result in two linearised DNA bands of 6018 bp (pRS315) and 2302 bp (*SSE2*).
(ii) Agarose gel electrophoresis of five potential *SSE2* plasmid clones. Each isolate was digested with restriction enzyme *Bam*H1.
Lane A: 1kb molecular weight marker.
Lane B: *Bam*H1 digestion of potential *SSE2* clone 1A. Clone was negative as bands were approximately 3kb and 8kb.
Lane C: *Bam*H1 digestion of potential *SSE2* clone 1C. Bands appeared positive as an *SSE2* clone. Cloned *SSE2* + promoter region = 2302 bp and pRS315 = 6018 bp. Clone 1C was later sequenced and confirmed as an *SSE2* clone.
Lane D-F: *Bam*H1 digestion of potential *SSE2* clones 1E, 2A and 2E. Smaller bands appeared as a positive size for *SSE2* but upper bands were too large to be confirmed as pRS315.

6018 bp in size, representing pRS315, and a smaller band approximately 2302 bp representing *SSE2* clone. Isolate 1C was later confirmed as an *SSE2* clone by sequence analysis. The *SSE2* gene was ready to be phenotypically analysed in CM02 by plasmid shuffle. Figure 5.2 illustrates the construct of pRS315-*SSE2* plasmid vector.

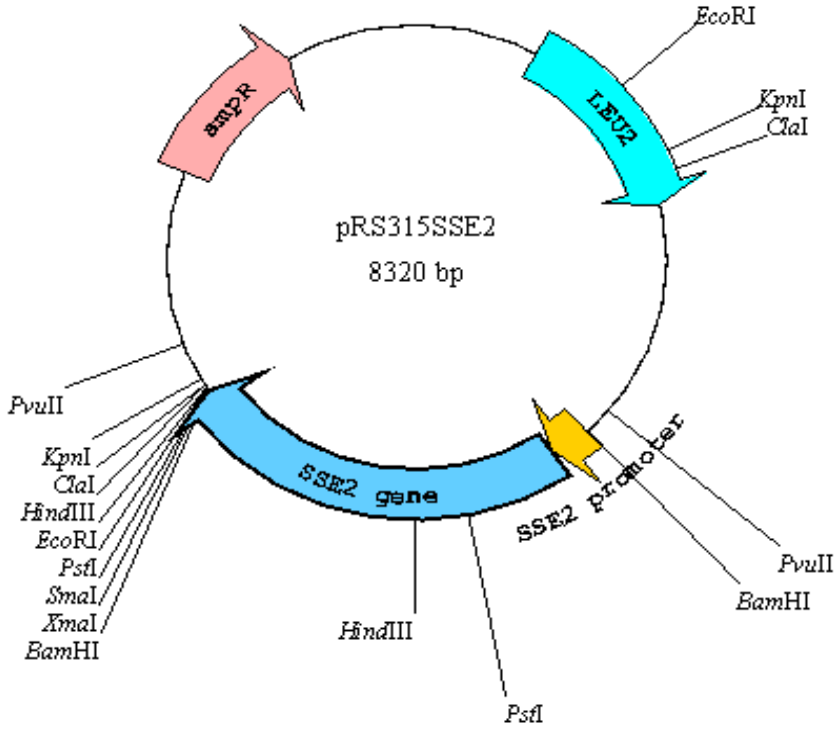

Figure 5.2. Plasmid construct of pRS315*SSE2*.

5.1.2 A comparison of [*PSI*$^+$] in CM02 + Sse1 and CM02 + Sse2

pRS315*SSE2* and pRS315*SSE1* were transformed into CM02. 5-FOA selection of transformants selected against pRS316*SSE1*. CM02 cells expressing pRS315*SSE2* without *SSE1* took 3-4 days to grow on 5-FOA at 30^{o}C. Once the strains were made their initial [*PSI*$^+$] phenotype was assessed by streaking onto YPD (Figure

5.3). Their [*PSI*$^{+}$] phenotype was subjectively analysed by their red/white colour, as described in section 2.13. [*PSI*$^{+}$] was further assessed by spotting Sse1 and Sse2 strains onto medium with limiting adenine (SC) and medium with no adenine (SC - adenine). Sse2 appeared red and [*psi*$^{-}$] on SC medium when expressed alone in CM02 (Figure 5.4). As Sse2 failed to grow on SC - adenine it suggested that Sse2 cannot maintain [*PSI*$^{+}$] propagation when expressed alone in CM02 (Figure 5.4).

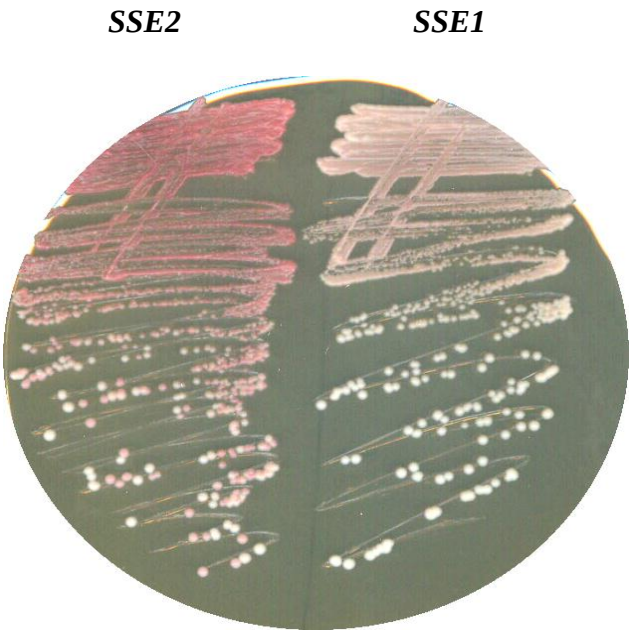

Figure 5.3. Assessment of [*PSI*$^{+}$] in CM02 expressing Sse1 and Sse2. CM02 was transformed with pRS315*SSE1* or pRS315*SSE2* and incubated at 30^{o}C for 2 days on SC - leucine medium. Transformants were replicated onto 5-FOA to select against pRS316*SSE1*. Yeast strains were streaked onto YPD medium and incubated for 2 days at 30^{o}C and 2 days at room temperature. [*PSI*$^{+}$] was subjectively measured by the red/white hypothesis.

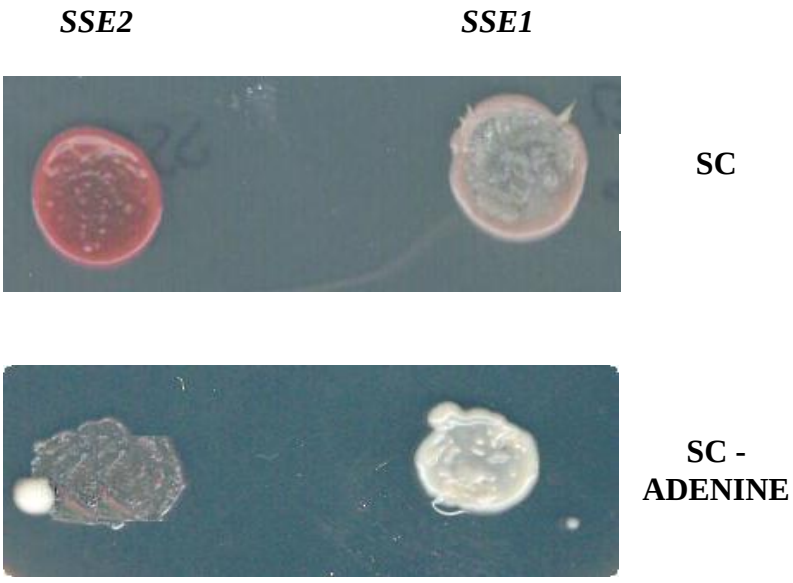

Figure 5.4. Assessment of [*PSI*$^+$] in CM02 + Sse1 and CM02 + Sse2 by comparing growth on SC - adenine medium. CM02 was transformed with pRS315*SSE1* or pRS315*SSE2* and incubated at 30^{o}C for 2 days on SC - leucine medium. Transformants were replicated onto 5-FOA to select against pRS316*SSE1*. Yeast were spotted onto SC and SC - adenine medium in 10 µl dH_2O and incubated for 2 days at 30^{o}C followed by 2 days at room temperature. CM02 + Sse2 failed to grow on medium lacking adenine indicating that it has no aggregated Sup35 and translation of *ADE2* gene is being halted at the abberent stop codon.

To further assess Sse1 and Sse2 [*PSI*$^+$] phenotypes a [*psi*$^-$] 621 strain was mated with CM02 + Sse1 and CM02 + Sse2 and the diploids were selected on SD + adenine medium. [*PSI*$^+$] is dominant so if any [*PSI*$^+$] was present in the Sse2 strain then the diploids should have appeared white. Sse1 was white when mated with [*psi*$^-$] 621 which confirmed the presence of [*PSI*$^+$]. However Sse2 appeared red when mated with 621 and the diploid failed to grow on SC – adenine suggesting again that Sse2 is completely [*psi*$^-$] (Figure 5.5 and 5.6).

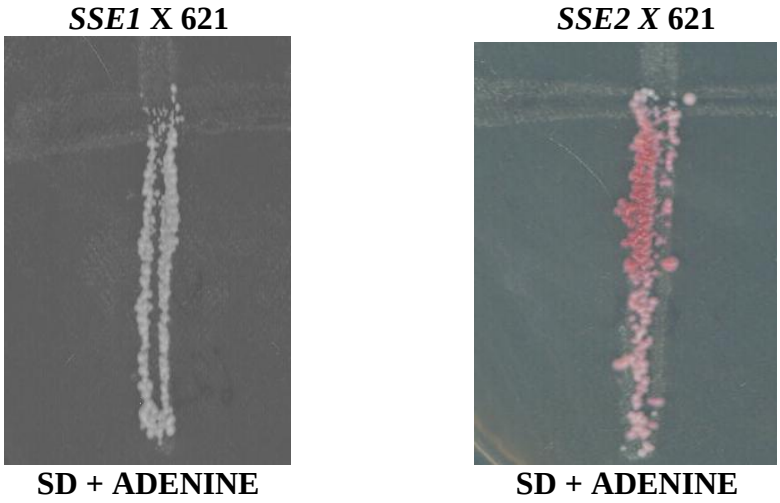

Figure 5.5. Mating 621 [*psi*$^-$] strain with Sse1 and Sse2 to create diploids. Yeast strain 621 was cured on 3 mM GdnHCl and mated with CM02 + Sse1 or Sse2 on SD + adenine medium. [*PSI*$^+$] is dominant and always propagated onto daughter cells. Sse1 is [*PSI*$^+$] as diploids appeared white. Sse2 is [*psi*$^-$] as diploids appeared red.

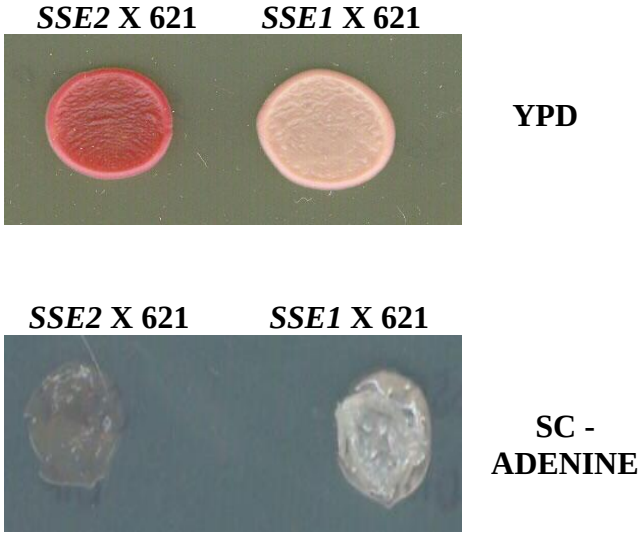

Figure 5.6. Diploid cells spotted onto YPD and SC - adenine to assess if [*PSI*$^+$] is present. Diploid strains from Figure 5.5 were mixed with 10 µl of dH_2O and spotted onto YPD and SC - adenine. This reconfirmed that Sse1 is [*PSI*$^+$] and Sse2 is [*psi*$^-$].

5.1.3 A comparison of growth and thermostability in CM02 + Sse1 and CM02 + Sse2

CM02 was transformed with pRS315*SSE1*, pRS315*SSE2* and pRS315. Transformants were replicated onto 5-FOA and each strain was monitored for growth at 30^{o}C over 4 days. By day 1 Sse1 cells were growing well and there was no growth for either the negative control or for cells expressing Sse2. CM02 + Sse2 colonies appeared after 4 days at 30^{o}C indicating that CM02 + Sse2 was slower to grow on medium with limiting adenine. Once the colonies were restreaked onto SC - leucine the strain grew as normal.

Growth curves were generated by monitoring CM02 + Sse1 and CM02 + Sse2 growth in liquid media over 8 hours. Both strains were incubated at 30^{o}C and 37^{o}C and cell concentrations were monitored by OD_{600nm} in a spectrophotometer. The growth curves illustrate that cells expressing Sse2 were slightly slower growing than cells expressing Sse1, at normal growth temperatures and at high temperatures (Figure 5.7). The average cell doubling time at 37^{o}C was 100 minutes for Sse1 and 132 minutes for Sse2 (Table 5.1). Comparative growth analysis was performed on Sse1 and Sse2 at 30^{o}C, 37^{o}C and 39^{o}C (Figure 5.8) revealing that CM02 + Sse2 cells grow slowly even at 30^{o}C. Sse2 cells were non-viable at 39^{o}C and slow-growing at 37^{o}C.

(a) 30°C

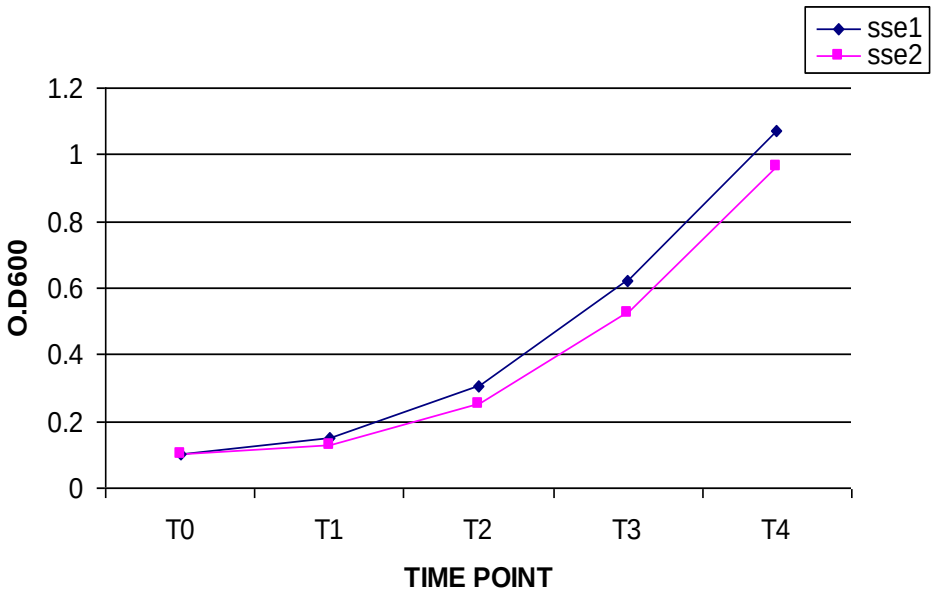

(b) 37°C

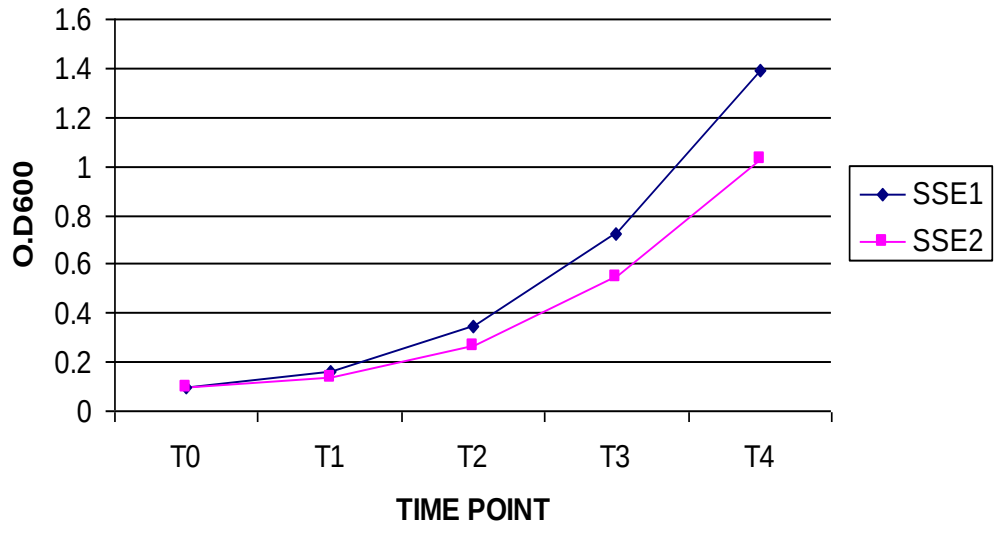

Figure 5.7. Growth curves for Sse1 and Sse2 at 30°C and 37°C. Cells were inoculated at OD_{600nm} = 0.1 and grown at 30°C and 37°C shaking. OD_{600nm} was assessed every 2 hours for cell concentrations. T_0 = inoculation timepoint and T_4 = last OD reading after eight hours. Sse1 grew slightly better than Sse2 at 30°C and 37°C.

Table 5.1. Cell generation time (GT) for Sse1 and Sse2.

	30°C average GT (minutes)	37°C average GT (minutes)
Sse1	**116**	**100**
Sse2	**134**	**132**

Sse1 grew well at both 30°C and 37°C and doubled slightly less than every two hours. Sse2 average doubling time took more than 2 hours and was a lot slower than Sse1.

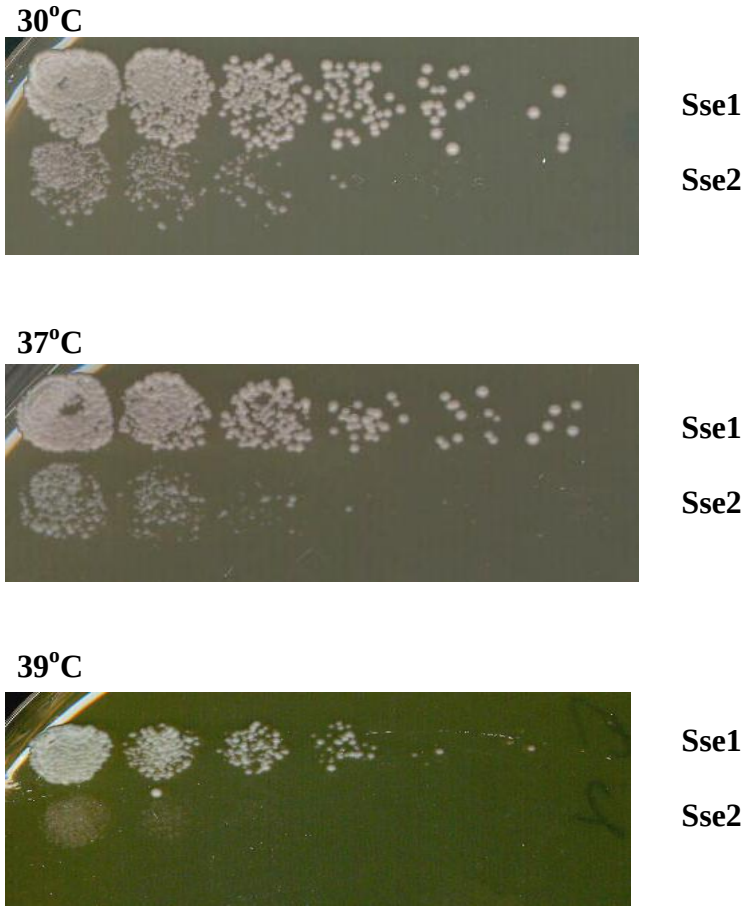

Figure 5.8. Temperature-sensitive analysis of CM02 + Sse1 and CM02 + Sse2. Yeast were serial diluted on YPD medium and incubated for 2 days at 30°C, 37°C and 39°C. Sse2 was non-viable at 39°C and slightly sensitive and slow-growing at 30°C and 37°C.

5.2 Functional effects of introducing Sse1 prion-impairing mutations into Sse2

Sse1 and Sse2 sequence are 76% identical (Polier *et al*., 2010) (Figure 5.9). Twelve of the thirteen Sse1 mutants isolated in this study are located in residues which are conserved in Sse2. Sse1 residue E504 is not conserved in Sse2. It was hypothesised that one possibility why Sse2 cannot promote [*PSI*$^{+}$] propagation is because it has this residue difference to Sse1. Mutation E504K was originally isolated in a screen for mutants which affect Sse1's ability to maintain [*PSI*$^{+}$]. By site-directed mutagenesis Sse2^{Q504E} mutant was created, making Sse2 more similar to Sse1. Sse2^{Q504E} mutant strain initially appeared slow-growing in CM02 Δ*sse1*Δ*sse2*. When it was first transformed and replicated onto 5-FOA the colonies took a long time to grow (Figure 5.10). CM02 + Sse2^{Q504E} [*PSI*$^{+}$] phenotype was analysed subjectively by colour on limiting adenine medium and was compared to WT Sse1 and WT Sse2 for its [*PSI*$^{+}$] phenotype (Figure 5.11). It appeared that this mutation did improve the ability of Sse2 to promote [*PSI*$^{+}$] propagation as it appeared pink in colour. It also displayed some growth on SC – adenine medium confirming its improved [*PSI*$^{+}$] phenotype (not shown). When analysed for its affect on cellular thermostability the growth of mutant Sse2^{Q504E} was similar to WT Sse2 (Figure 5.12).

The effects caused by the mutation G616D on Sse2 were also assessed. In Sse1 this mutation disrupted the ability of Sse1 to propagate [*PSI*$^{+}$] and disrupted cellular thermotolerance. The mutant Sse2^{G616D} was created by site-directed mutagenesis and it also appeared slow-growing in CM02 Δ*sse1*Δ*sse2* when first transformed into cells (Figure 5.10). When analysed on limiting adenine for its [*PSI*$^{+}$] phenotype, mutant Sse2^{G616D} appeared similar to [*psi*$^{-}$] WT Sse2 as it was red in colour (Figure 5.11). However, it did display severe thermosensitivity greater than

Figure 5.9. Comparison of Sse1 and Sse2 protein sequence. They are 76% identical. Sse1 is the top sequence and Sse2 is the bottom sequence. All Sse1 mutant residues are conserved in Sse2 with the exception of E504 (highlighted).

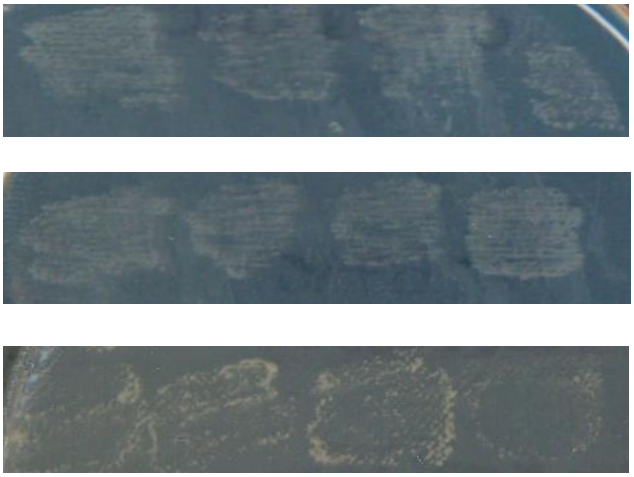

Figure 5.10. Growth of Sse2 mutants on 5-FOA after 3 days incubation at 30°C. Sse2 and mutants were transformed into CM02 and incubated on SC - leucine medium for 2 days at 30°C. Transformants were replicated onto 5-FOA, to select against pRS316*SSE1*, and incubated at 30°C for 2 days. Sse2 mutants struggled to grow and colonies did not appear until an additional 2 days at room temperature.

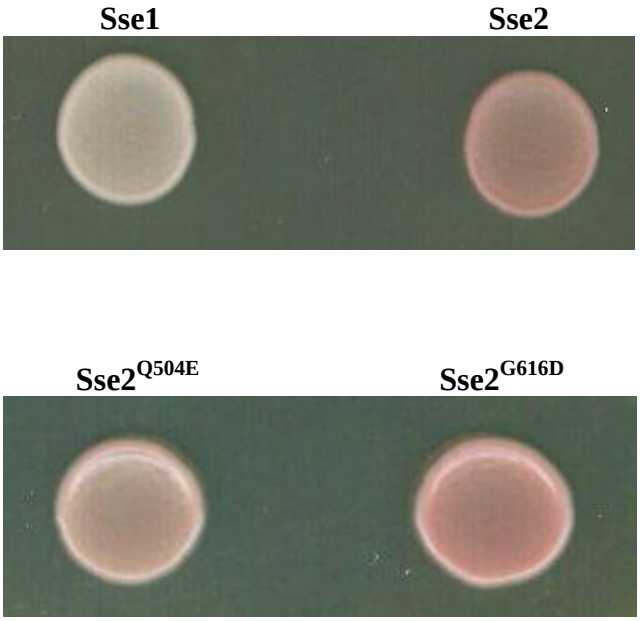

Figure 5.11. Sse2 mutant [*PSI*$^+$] phenotypes on YPD medium**.** After initial transformation the mutants were restreaked onto SC - leucine medium followed by restreaking onto YPD medium. The mutants were spotted in 10 µl dH_2O onto YPD medium and incubated for 2 days at 30°C followed by 2 days at room temperature. Mutant Sse2^{G616D} appeared [*psi*$^-$] and similar in colour to wild type Sse2. However mutant Sse2^{Q504E} had an improved [*PSI*$^+$] appearance compared to wild type Sse2.

WT Sse2, as it was non-viable at 37^{o}C and slow-growing at 30^{o}C (Figure 5.12). This residue appears to have conserved function in both Sse1 and Sse2 as it creates an unstable temperature-sensitive phenotype.

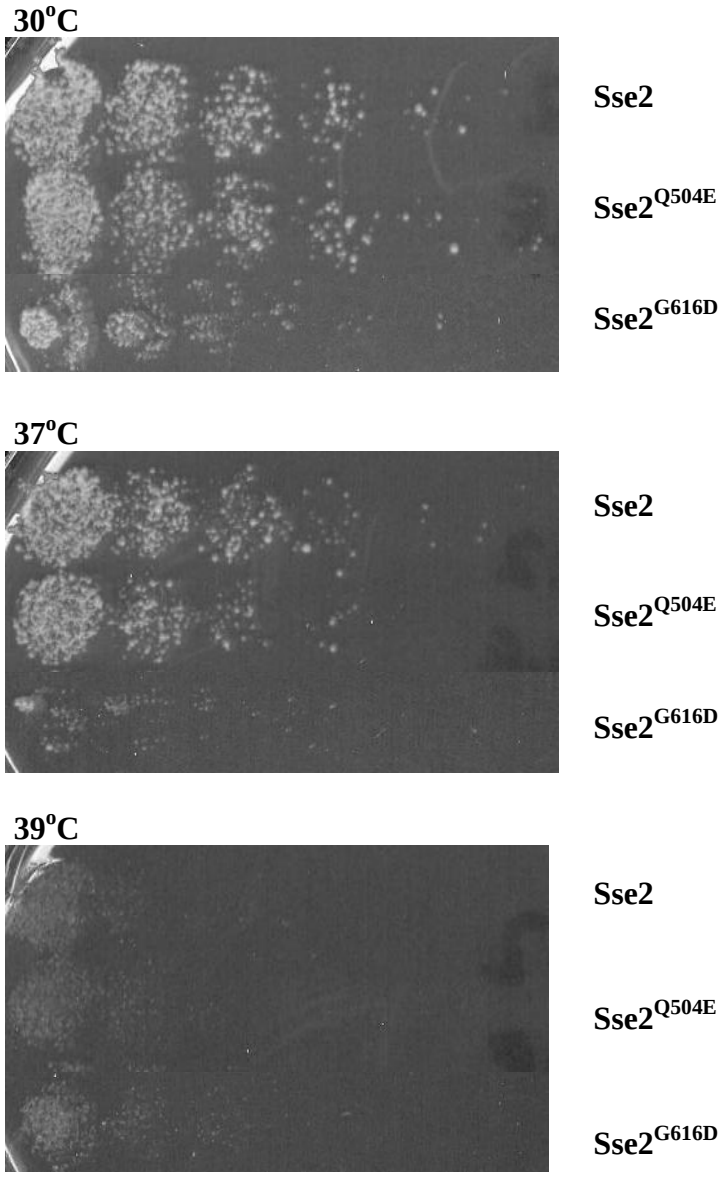

Figure 5.12. Comparative growth analysis of Sse2 mutants to assess temperature sensitivity. Sse2, Sse2^{Q504E} and Sse2^{G616D} were serial diluted onto YPD medium and incubated at 30^{o}C, 37^{o}C and 39^{o}C for 2 days. Sse2 mutant Q504E grew similarly to wild type as it showed sensitivity to 30^{o}C and 37^{o}C and was non-viable at 39^{o}C. However mutant G616D was very sensitive at 30^{o}C and non-viable at 37^{o}C and 39^{o}C.

5.3 Initial investigation into Sse1 and Sse2 phosphorylation

In this section the role of protein kinases suggested to phosphorylate Sse1 and Sse2 were investigated and the implications this phosphorylation has on growth and [*PSI*$^{+}$] was assessed. The Phosphorylome Database is the source where this information was obtained (Ptacek *et al*., 2005)

Protein phosphorylation is a post-translational modification that is ubiquitous in eukaryotic cells (Rubinstein and Schmidt, 2007). Protein kinases account for approximately 2% of genes in the eukaryotic genome and they constitute one of the largest eukaryotic protein families (Manning *et al*., 2002). Protein phosphorylation regulates a plethora of cell signaling and biological processes (Rubinstein and Schmidt, 2007). Using proteome chip technology Ptacek *et al*. (2005) revealed that each yeast protein kinase they investigated recognised an average of 47 substrates. The majority of these substrates (73%) were phosphorylated by less than three kinases indicating a high level of kinase-substrate specificity (Ptacek *et al*., 2005).

Phosphorylation of proteins such as heat shock proteins could modulate their biological activity, cellular location and interaction with other proteins (Cohen, 2000). It has been shown that phosphorylation of Hsp90 impairs its ATPase activity and its ability to chaperone client proteins. Hsp90 phosphorylation has also been shown to be important for cell cycle regulation (Mollapour *et al*., 2010). Sse1 and Sse2 have important [*PSI*$^{+}$] related functions and cell integrity functions that most likely rely on the location and interaction of both chaperones. In this section the implications that Sse1/Sse2 kinase protein deletions have on cellular growth and on [*PSI*$^{+}$] phenotypes were investigated.

Using proteome chip technology and mass spectrometry Ptacek *et al*. (2005) identified the substrates recognised by most protein kinases in yeast. As predicted by the Phosphorylome Database three kinases Akl1, Kin2 and Hsl1 phosphorylate either Sse1 or Sse2. Akl1 is a serine/threonine kinase involved in actin cytoskeleton organisation and is a member of the Ark kinase family of proteins (Cope *et al*., 1999; Henry *et al*., 2003). Akl is predicted to interact with and phosphorylate Sse1 (Ptacek *et al*., 2005). Kin2 is also a serine/threonine kinase involved in regulating cellular exocytosis (Elbert *et al*., 2005). Kin2 is structurally and functionally related to Kin1. They both belong to the Snf1 family of Ca^{2+}/calmodulin-dependent kinase II group (CaMK) (Hanks *et al*., 1988; Lamb *et al*., 1991). Kin2 is predicted to phosphorylate both Sse1 and Sse2 (Ptacek *et al*., 2005). Hsl1 is a Nim1-related protein kinase that regulates cytokinesis at the yeast bud neck (Barral *et al*., 1999). Hsl1, along with Hsl7, targets and phosphorylates the protein Swe1 ultimately leading to Swe1 protein degradation (Mcmillan *et al*., 1999). Hsl1 has also been predicted to phosphorylate Sse2 (Ptacek *et al*., 2005).

5.3.1 Deletion of protein kinases Akl1, Kin2 and Hsl1 in G600

Genes encoding *AKL1*, *KIN2* and *HSL1* were singularly knocked out in G600 using *kanMX* knockout constructs. This was performed using homologous recombination knockout techniques described in section 2.19. PCR products of knockout cassettes were obtained using Euroscarf genomic DNA and primers listed in Table 2.12.d. The PCR products were transformed into G600 **a** (*AKL1*) and G600 α (*HSL1* and *KIN2*) and transformants were selected on G418 medium. Six colonies per plate were selected and their DNA isolated for analysis. Potential *akl1* knockouts were amplified with primers AKL1F/R resulting in four isolates (Lane D-G)

corresponding to the correct knockout size of 1989 bp (Figure 5.14). The other two isolates were WT *AKL1* and an unknown product. The potential four knockouts were confirmed as *akl1* knockouts using primers that anneal to the flanking regions of the knockout construct. This gel is of poor quality and is not included in the illustrated results. AKL1F with KAN01R resulted in a 353 bp DNA band and AKL1R with KAN02F resulted in a 742 bp band.

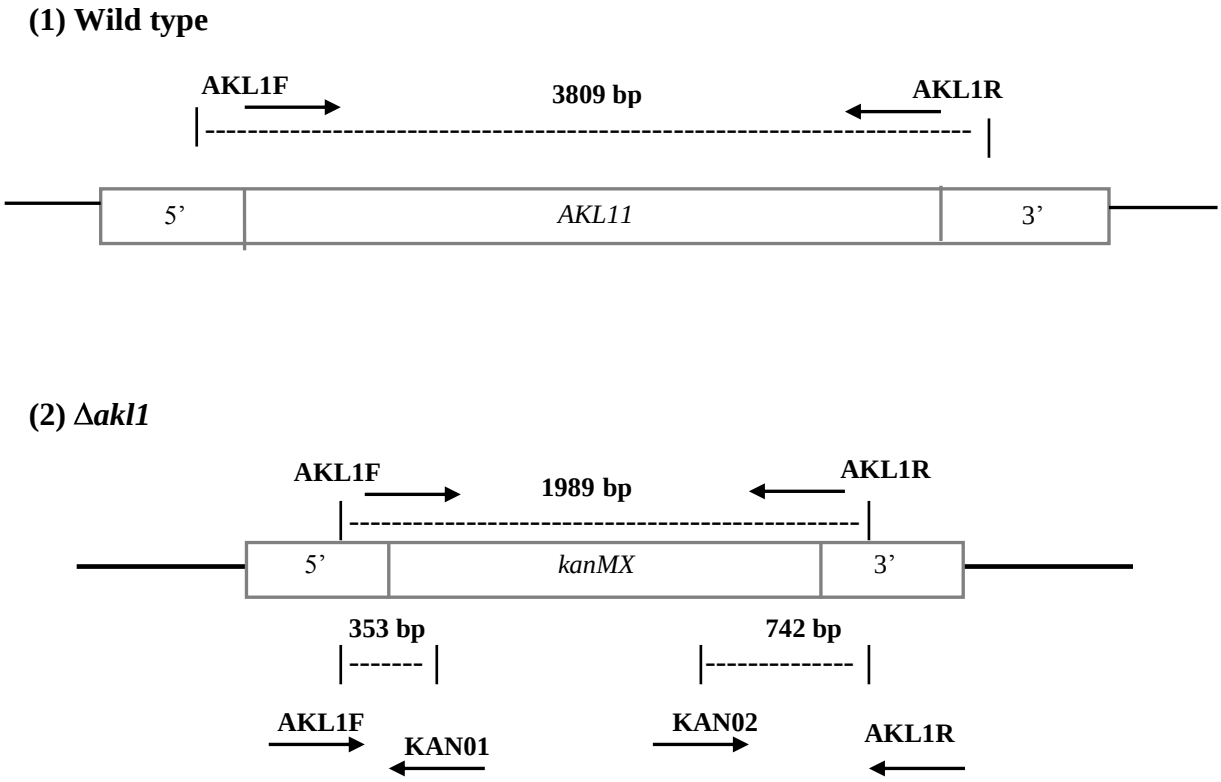

Figure 5.13. Illustration shows the expected wild type *AKL1* and Δ*akl1* PCR fragment sizes. (1) *AKL1* wild type DNA coding sequence is 3327 bp. Primers AKL1F and AKL1R are located upstream and downstream of *AKL1* coding sequence. PCR using these primers should result in a DNA band of approximately 3809 bp. (2) illustrates an *akl1* knockout construct with *kanMX* gene replacing the coding sequence of *AKL1*. PCR using primers AKL1F and AKL1R should result in a band approximately 1989 bp in size. Internal KAN01R and KAN02F primers used with external AKL1R and AKL1F primers should result in two bands of 353 bp and 742 bp. This confirms that *AKL1* is replaced with *kanMX*.

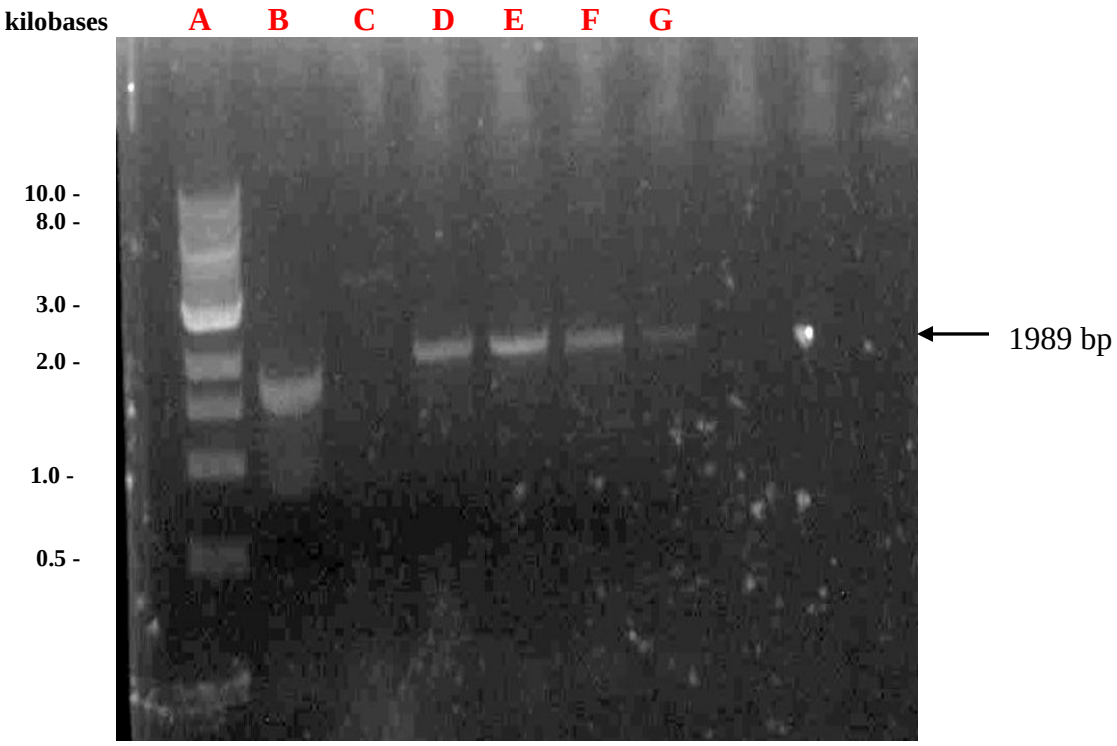

Figure 5.14. Diagnostic PCR for Δ*akl1* knockout strain.

Lane A: 1kb DNA molecular marker.

Lane B: Potential Δ*akl1* using primers AKL1F/R and DNA from isolate 1. DNA band did not correspond to the size of knockout construct.

Lane C: Potential Δ*akl1* using primers AKL1F/R and DNA from isolate 2. DNA band did not correspond to the size of the knockout construct but to that of WT *AKL1*.

Lane D-G: Potential Δ*akl1* using primers AKL1F/R and DNA from isolate 3-6. DNA bands did correspond to the size of knockout construct (1989 bp). All four isolates were later confirmed as Δ*akl1* by further diagnostic PCRs using internal KAN01 and KAN02 primers.

kin2 and *hsl1* knockouts were performed at the same time using two different strains. The diagnostic PCR results for Δ*hsl1* are in Lane B-E in Figure 5.17 and confirm the isolation of a G600Δ*hsl1* strain. The diagnostic PCR results for Δ*kin2* are

in Lane F-I also in Figure 5.17 and confirm the isolation of a G600Δ*kin2* strain. Figures 5.15 and 5.16 annotate how these fragment sizes were obtained.

(1) Wild type

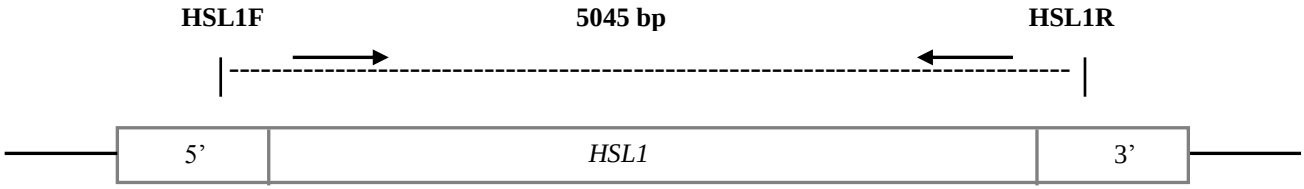

(2) Δ*hsl1*

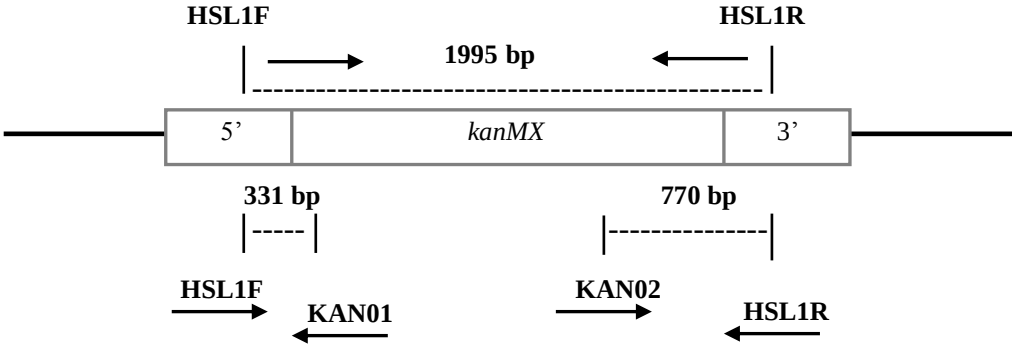

Figure 5.15. Illustration shows the expected wild type *HSL1* and Δ*hsl1* PCR fragment sizes. (1) *HSL1* wild type DNA coding sequence is 4557 bp. Primers HSL1F and HSL1R are located upstream and downstream of *HSL1* coding sequence. PCR using these primers should result in a DNA band of approximately 5045 bp. (2) illustrates a *hsl1* knockout construct with *kanMX* gene replacing the coding sequence of *HSL1*. PCR using primers HSL1F and HSL1R should result in a band approximately 1995 bp in size. Internal KAN01R and KAN02F primers used with external HSL1R and HSL1F primers should result in two bands of 331 bp and 770 bp. This confirms that *HSL1* is replaced with *kanMX*.

(1) Wild type

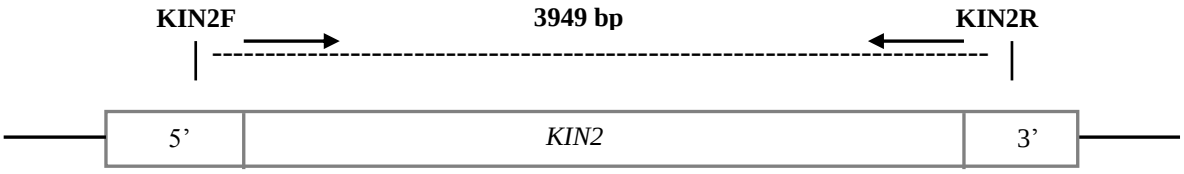

(2) Δ*kin2*

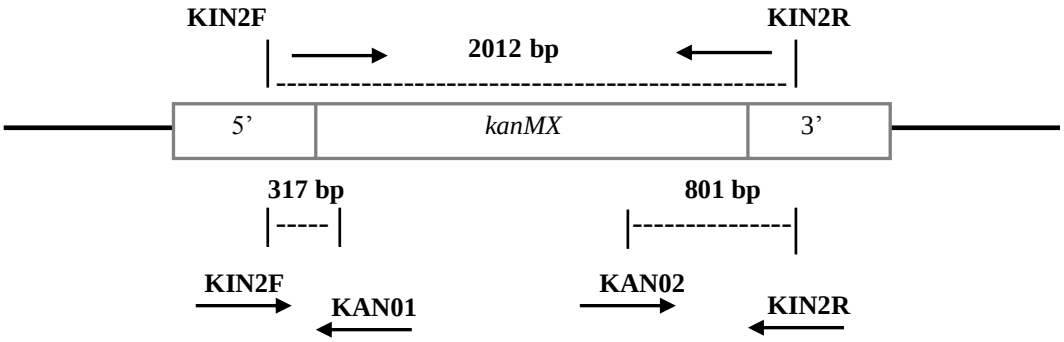

Figure 5.16. Illustration shows the expected wild type *KIN2* and Δ*kin2* PCR fragment sizes. (1) *KIN2* wild type DNA coding sequence is 3444 bp. Primers KIN2F and KIN2R are located upstream and downstream of *KIN2* coding sequence. PCR using these primers should result in a DNA band of approximately 3949 bp. (2) illustrates a *kin2* knockout construct with *kanMX* gene replacing the coding sequence of *KIN2*. PCR using primers KIN2F and KIN2R should result in a band approximately 2012 bp in size. Internal KAN01R and KAN02F primers used with external KIN2R and KIN2F primers should result in two bands of 317 bp and 801 bp. This confirms that *KIN2* is replaced with *kanMX*.

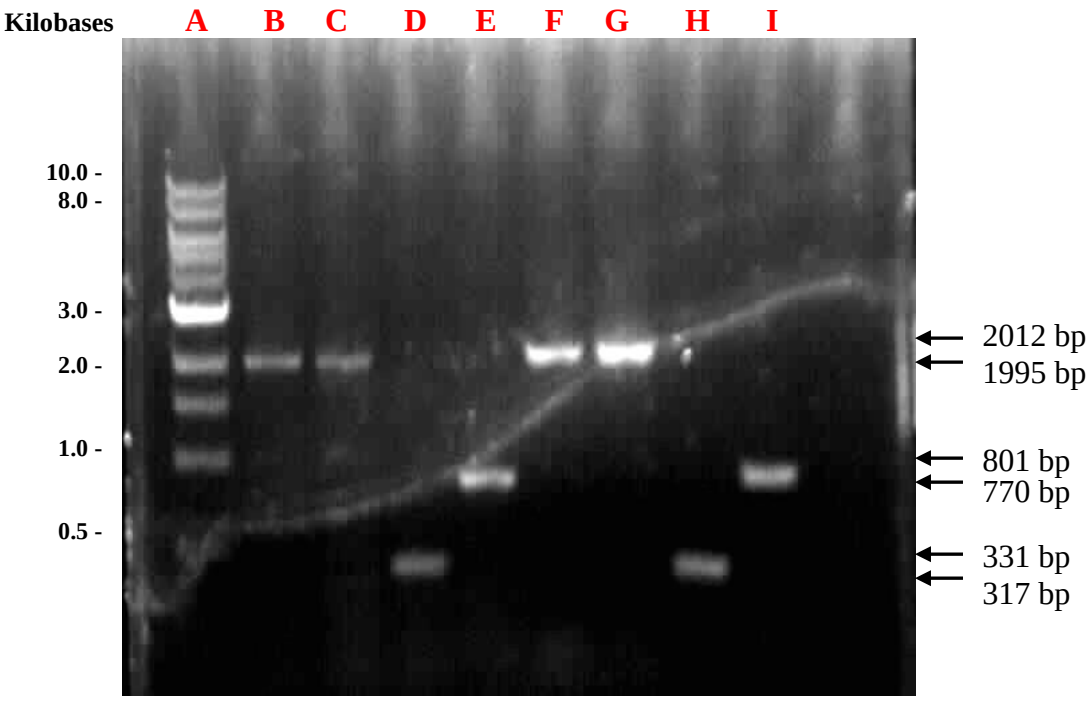

Figure 5.17. Diagnostic PCR for Δ*hsl1* and Δ*kin2* knockout strains.

Lane A: 1kb DNA molecular marker.

Lane B: Potential Δ*hsl1* using primers HSL1F/R and DNA from isolate 1. DNA band corresponds to the size of Δ*hsl1* knockout construct (1995 bp).

Lane C: Potential Δ*hsl1* using primers HSL1F/R and DNA from isolate 2. DNA band corresponds to the size of Δ*hsl1* knockout construct (1995 bp).

Lane D: PCR product represents the left flanking region of Δ*hsl1* (331 bp). DNA was from isolate 1 and primers used were HSL1F and KAN01R.

Lane E: PCR product represents the right flanking region of Δ*hsl1* (770 bp). DNA was from isolate 1 and primers used were HSL1R and KAN02F.

Lane F: Potential Δ*kin2* using primers KIN2F/R and DNA from isolate 3. DNA band corresponds to the size of Δ*kin2* knockout construct (2012 bp).

Lane G: Potential Δ*kin2* using primers KIN2F/R and DNA from isolate 5. DNA band corresponds to the size of Δ*kin2* knockout construct (2012 bp).

Lane H: PCR product represents left flanking region of Δ*kin2* (317 bp). DNA was from isolate 3 and primers used were KIN2F and KAN01R.

Lane I: PCR product represents right flanking region of Δ*kin2* (801 bp). DNA was from isolate 3 and primers used were KIN2R and KAN02F.

5.3.2 Analysis of the phenotypic effects caused by protein kinase deletion

Proteins need to interact with other biomolecules in order to execute their various biological functions (Ito *et al*., 2001). Deleting kinases which interact with and phosphorylate Sse proteins may lead to the disruption of Sse1/Sse2 function. As Sse proteins play a role in thermotolerance the effects that Δ*akl1,* Δ*kin2* and Δ*hsl1* deletions have on cellular thermostability were tested. As these kinases also interact with other proteins it would be difficult to conclude that any phenotypic changes are solely Sse related. Comparative growth analysis tests revealed that Δ*kin2* and Δ*hsl1* grew relatively well at restrictive temperatures but Δ*akl1* was slightly sensitive and grew slower than the other knockout strains (Figure 5.18).

The effect that kinase knockouts have on cellular [*PSI*$^{+}$] was also examined. Knockout strains were streaked onto YPD medium alongside G600 control and cells were incubated at 30^{o}C for 2 days. [*PSI*$^{+}$] phenotypes were subjectively measured on limiting adenine medium using the red/white colony colour. Δ*akl1* appeared to weaken [*PSI*$^{+}$] in G600 whereas the other kinase knockouts seemed to have no effect on [*PSI*$^{+}$] (Figure 5.19). From these tests it was concluded that Δ*akl1* appeared to be slightly [*PSI*$^{+}$] weak and demonstrated slow growth.

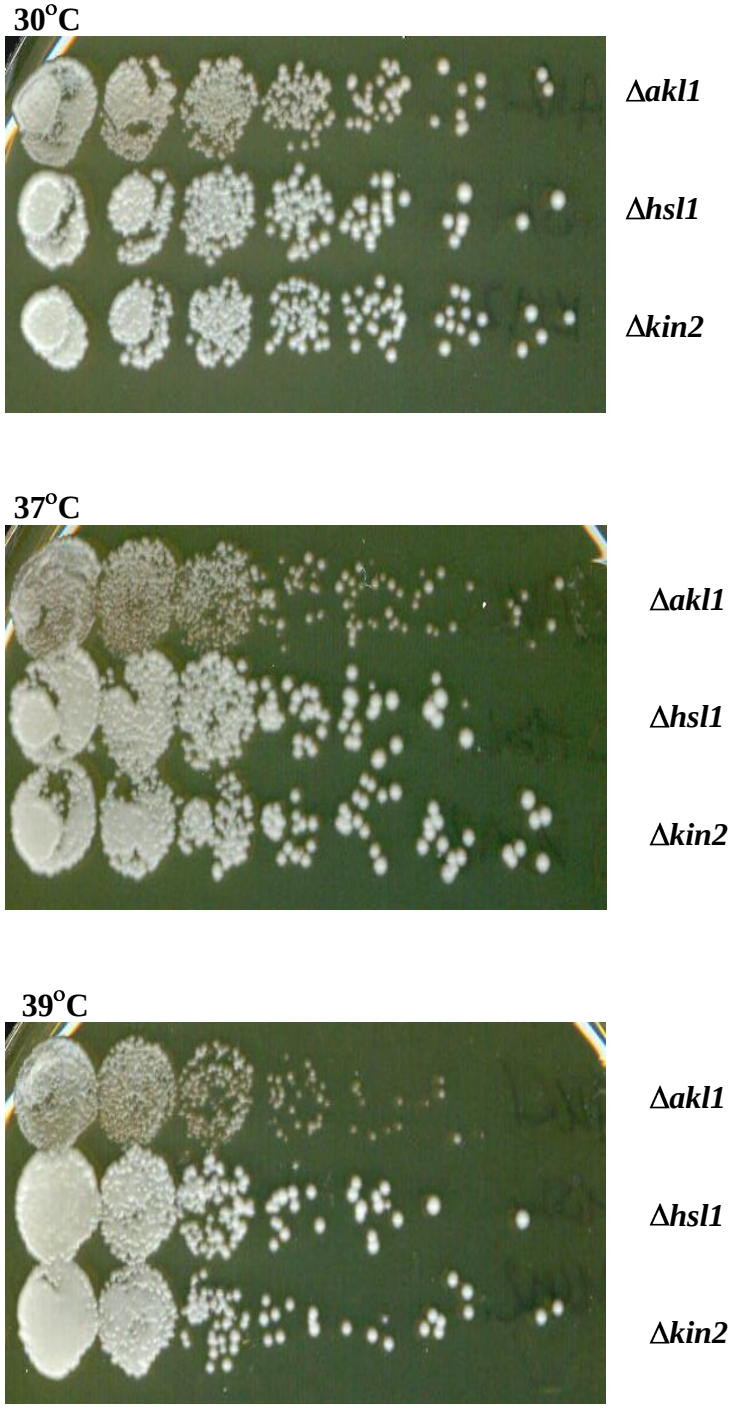

Figure 5.18. Comparative growth analysis of Δ*akl1*, Δ*hsl1* and Δ*kin2* temperature sensitivity. Kinase knockout strains were serial diluted onto YPD medium and incubated at 30°C, 37°C and 39°C for 2 days. Δ*akl1* was slightly slow-growing at 37°C and 39°C.

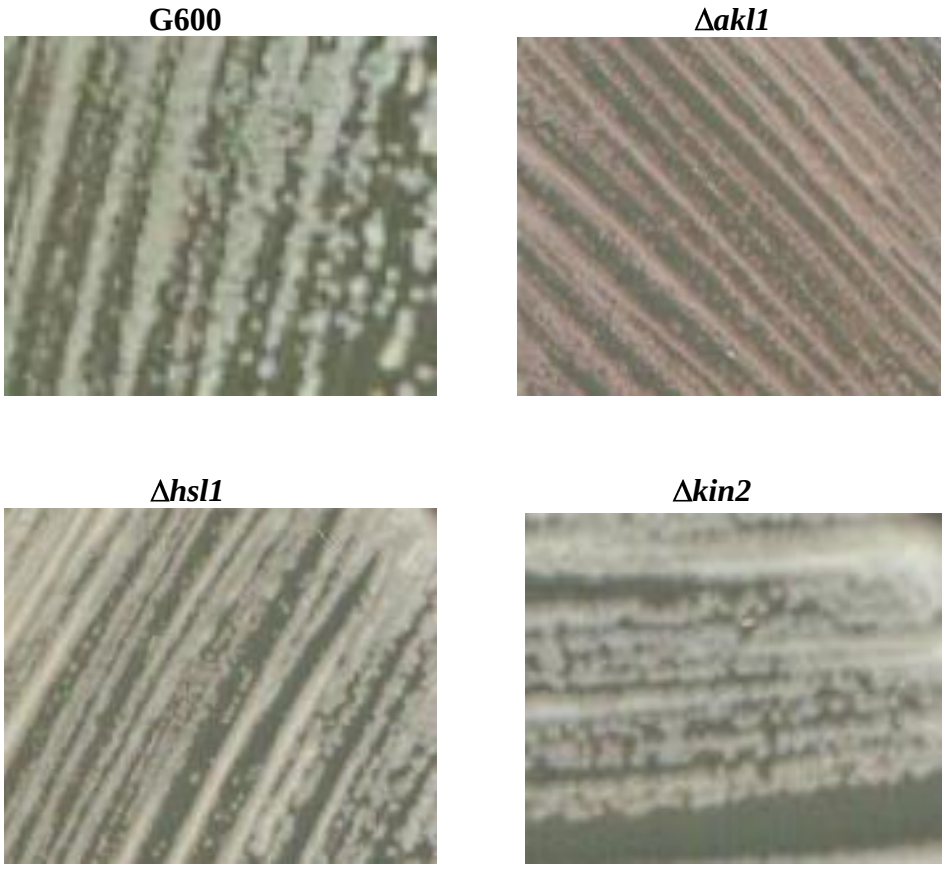

Figure 5.19. [*PSI*$^+$] phenotypes in kinase knockout strains. G600, Δ*akl1*, Δ*hsl1* and Δ*kin2* were streaked onto YPD medium and incubated at 30^{o}C for 2 days. Δ*akl1* mutant showed a weak [*PSI*$^+$] phenotype by its pink colony colour.

5.3.3 Creating kinase double knockout mutants

Double knockout strains were created by mating G600Δ*akl1* (*Mat* **a**) with either G600Δ*kin2* or G600Δ*hsl1* (both *Mat* α). As all three genes were knocked out with *kanMX* each strain was transformed with a different control plasmid as a selectable marker. Δ*akl1* was transformed with pRS315, Δ*kin2* with pRS316 and Δ*hsl1* with pRS423. Strains were mated on selective medium, incubated for 2 days at 30^{o}C and then replicated onto SD medium. Amino acids were added to the medium so that diploids would survive and haploids die (Figure 5.20). For example, Δ*akl1*Δ*hsl1*

were replicated onto SD + adenine, tryptophan and uracil as haploid cells would not survive in the absence of leucine and histidine. Diploids were sporulated on sporulating medium with the addition of adenine, tryptophan and uracil or adenine, tryptophan and histidine.

Random spore analysis resulted in the isolation of red, white and pink colonies (Figure 5.21). Ten colonies were picked from each plate and DNA extracted for PCR analysis. Colony 5 from Δ*akl1*Δ*kin2* plate was confirmed as a double knockout by diagnostic PCR (Figure 5.22). Colony 7 from Δ*akl1*Δ*hsl1* plate was confirmed as a double knockout by diagnostic PCR (Figure 5.23). The absence of wild type kinase DNA bands from the diagnostic gels reconfirmed that the strains were sporulated correctly and that the mutants were haploid. PCR fragment sizes in Figures 5.22 and 5.23 can be annotated from Figures 5.13, 5.15 and 5.16 which illustrate how the various DNA bands were obtained. Interestingly both colonies confirmed as knockouts were white.

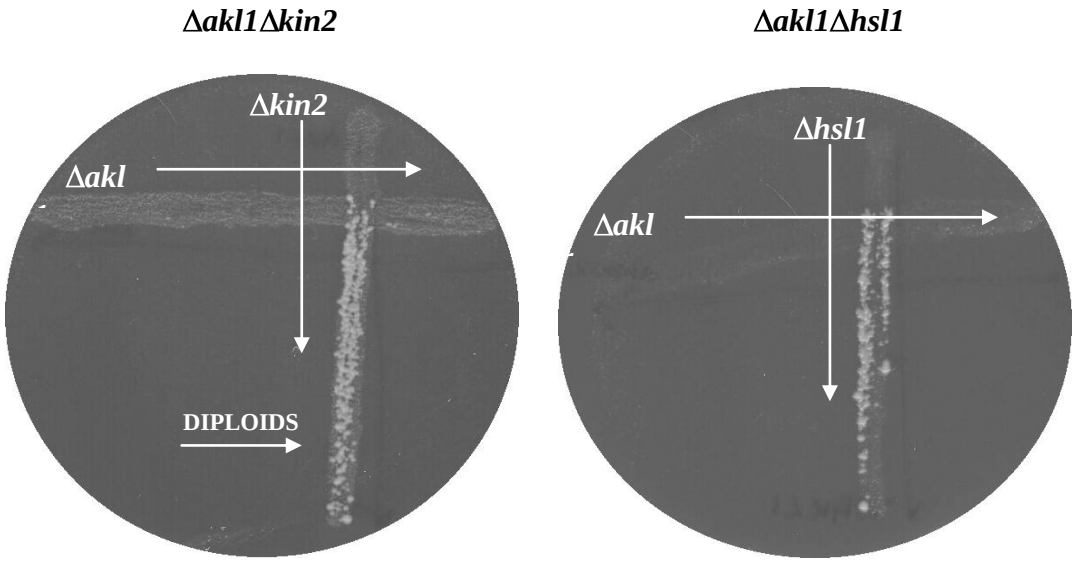

Figure 5.20. Diploid strains were created by mating on selective media.

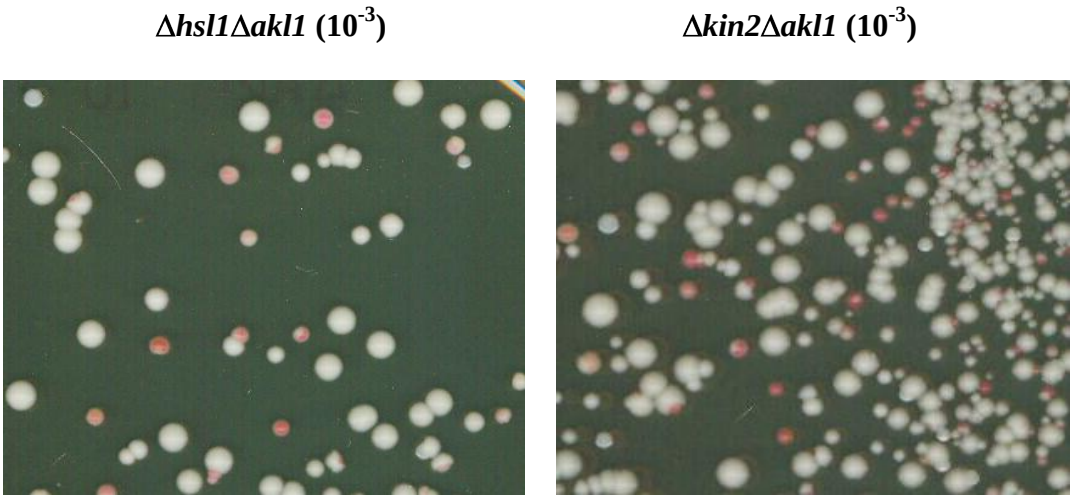

Figure 5.21. Random spore analysis of potential double knockout strains. Individual colonies represent a mixture of either haploid spores with potential to express the double knockout of interest or diploids which were unsuccessfully sporulated. Colonies appeared red, pink and white and at least one representative colony from each colour was picked for further analysis.

5.3.4 Analysis of the temperature-sensitive effects of double kinase knockouts

It was speculated that perhaps the deletion of two Sse phosphorylating kinases would have a bigger impact on cell temperature sensitivity or cell viability. Mutant strains Δ*akl1*Δ*hsl1* and Δ*akl1*Δ*kin2* were analysed by comparative growth assays on YPD medium after 2 days incubation at 30^{o}C, 37^{o}C and 39^{o}C. However, the double kinase knockout strains grew relatively well at these temperatures (Figure 5.24). It was previously observed that Δ*akl1* struggled to grow and looked quite sick at 37^{o}C and 39^{o}C. However, it appeared to grow better in the presence of Δ*hsl1* and Δ*kin2* mutants.

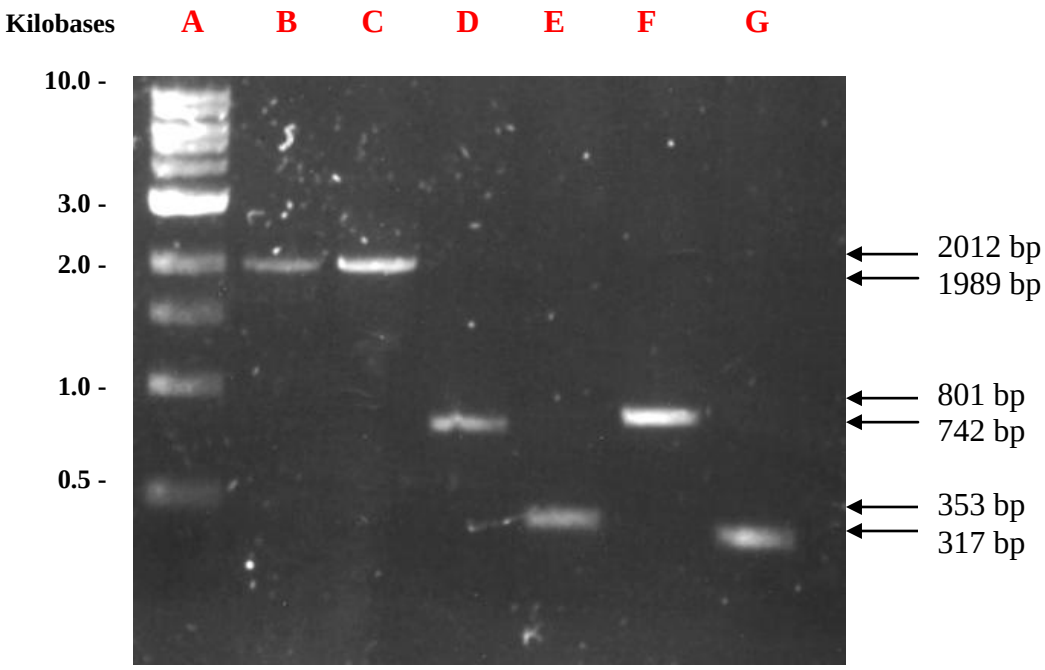

Figure 5.22. Diagnostic PCR for double knockout strain Δ*akl1*Δ*kin2*.

Lane A: 1kb DNA molecular marker.

Lane B: Potential Δ*akl1* using primers AKL1F/R and DNA isolate 5 for Δ*akl1*Δ*kin2*. Product size was approximately 1989 bp which corresponds to *kanMX* knockout construct size.

Lane C: Potential Δ*kin2* using primers KIN2F/R and DNA isolate 5 for Δ*akl1*Δ*kin2*. Product size was approximately 2012 bp which corresponds to *kanMX* knockout construct size.

Lane D: DNA isolate 5 amplified with primers AKL1R and KAN02F. PCR product was approximately 742 bp and reflects the right flanking region of *akl1* knockout construct.

Lane E: DNA isolate 5 amplified with primers AKL1F and KAN01R. PCR product was approximately 353 bp and reflects the left flanking region of *akl1* knockout construct.

Lane F: DNA isolate 5 amplified with primers KIN2R and KAN02F. PCR product was approximately 801 bp and reflects the right flanking region of *kin2* knockout construct.

Lane G: DNA isolate 5 amplified with primers KIN2F and KAN01R. PCR product was approximately 317 bp and reflects the left flanking region of *kin2* knockout construct.

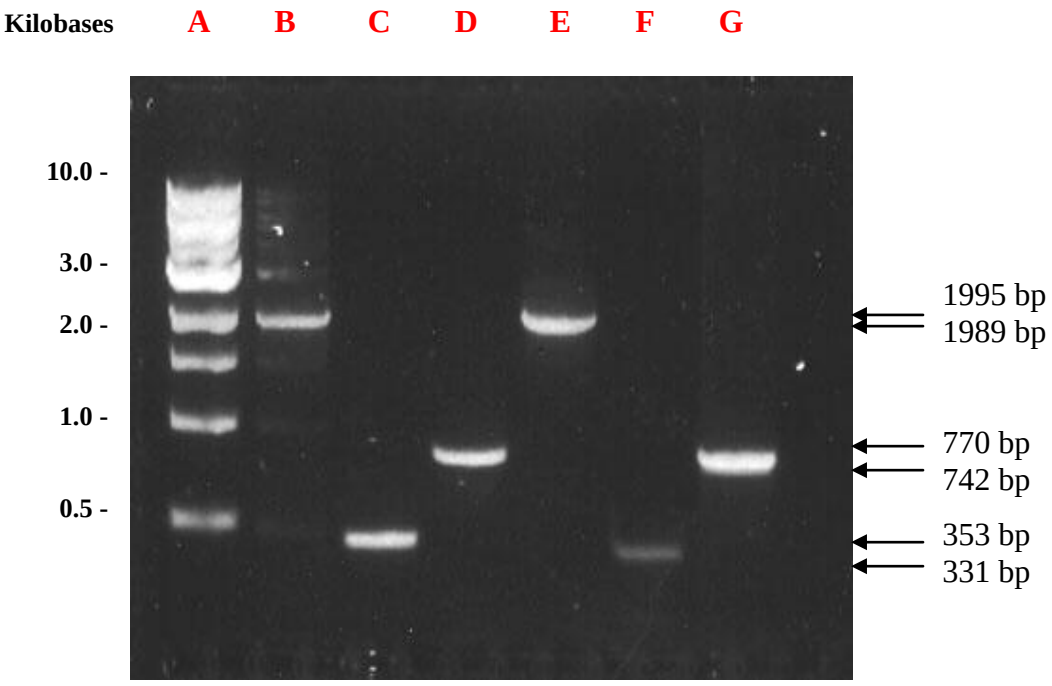

Figure 5.23. Diagnostic PCR for double knockout strain Δ*akl1*Δ*hsl1*.

Lane A: 1kb DNA molecular marker.

Lane B: Potential Δ*akl1* using primers AKL1F/R and DNA isolate 7 for Δ*akl1*Δ*hsl1*. Product size was approximately 1989 bp which corresponds to *kanMX* knockout construct size.

Lane C: DNA isolate 7 amplified with primers AKL1F and KAN01R. PCR product was approximately 353 bp and reflects the left flanking region of *akl1* knockout construct.

Lane D: DNA isolate 7 amplified with primers AKL1R and KAN02F. PCR product was approximately 742 bp and reflects the right flanking region of *akl1* knockout construct.

Lane E: Potential Δ*hsl1* using primers HSL1F/R and DNA isolate 7 for Δ*akl1*Δ*hsl1*. Product size was approximately 1995 bp which corresponds to *kanMX* knockout construct size.

Lane F: DNA isolate 7 amplified with primers HSL1R and KAN02F. PCR product was approximately 770 bp and reflects the right flanking region of *hsl1* knockout construct.

Lane G: DNA isolate 7 amplified with primers HSL1F and KAN01R. PCR product was approximately 331 bp and reflects the left flanking region of *hsl1* knockout construct.

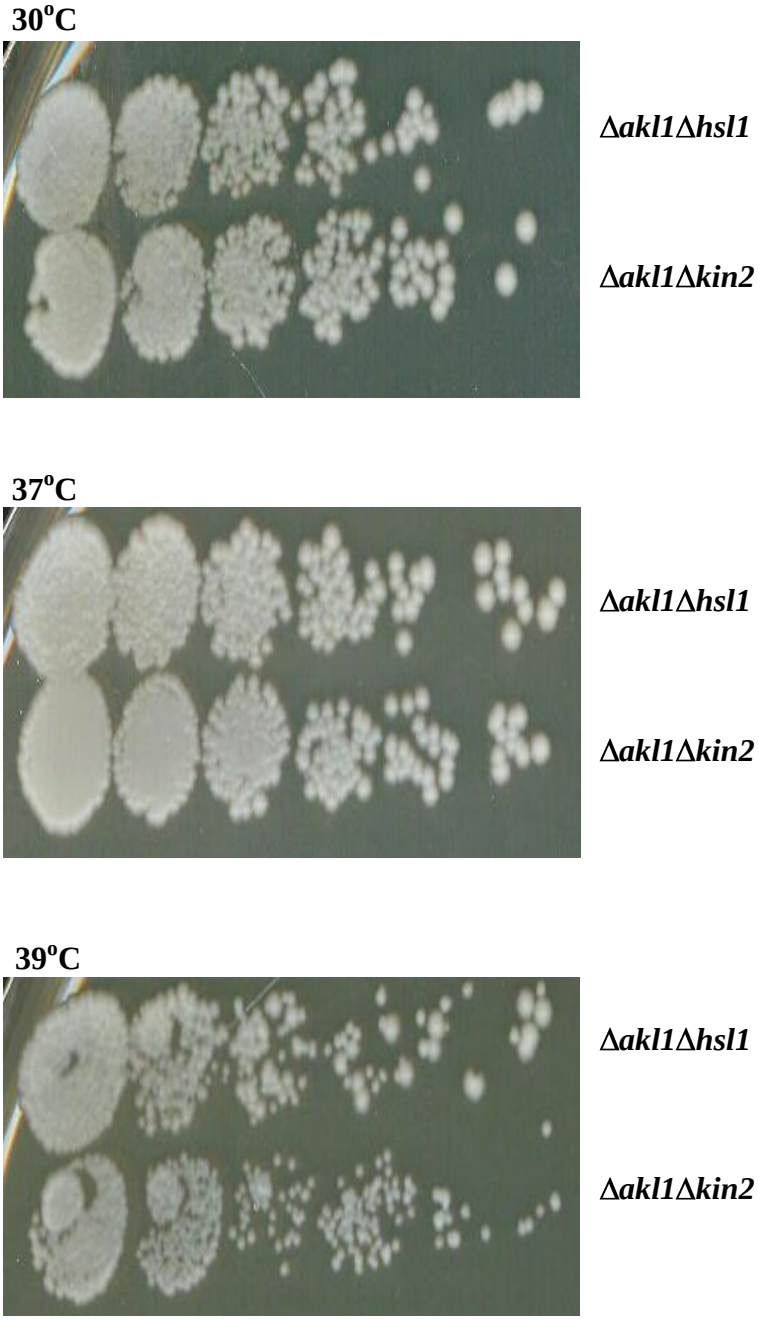

Figure 5.24. Comparative growth analysis of the effects of protein kinase knockouts on strain G600. Double knockout strains were serial diluted onto YPD medium and incubated at 30°C, 37°C and 39°C for 2 days. Double knockout mutants were not ts at 37°C or 39°C.

5.3.5 Analysis of [*PSI*$^+$] in G600 protein kinase mutants

Single and double kinase mutants were spotted onto YPD medium alongside WT G600. The plates were incubated for 2 days at 30^{o}C followed by 2 days at room temperature. All mutants appeared [*PSI*$^+$]. Δ*akl1* appeared pink when streaked on YPD in Figure 5.19 however when spotted onto YPD it appeared only slightly [*PSI*$^+$] weak (Figure 5.25). Interestingly, the addition of a second kinase mutation to G600Δ*akl1* made the strain more [*PSI*$^+$]. It appears that single and double deletions of kinases that phosphorylate Sse1 and Sse2 do not have a huge effect on [*PSI*$^+$].

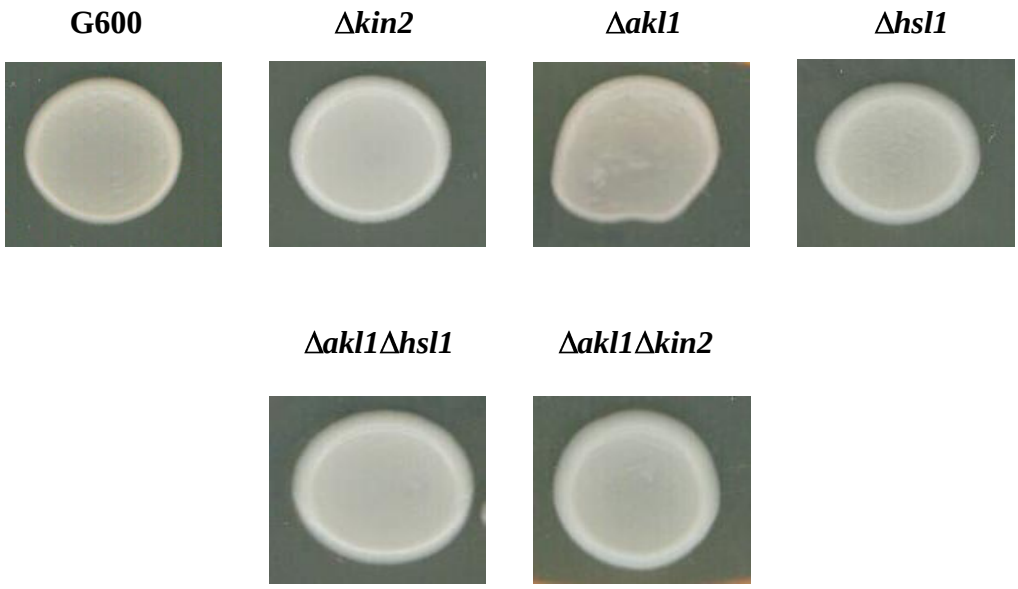

Figure 5.25. [*PSI*$^+$] phenotypic analysis in protein kinase mutant strains. All single and double knockout mutants were spotted onto YPD medium in 10 µl of dH_2O. The plates were incubated at 30^{o}C for 2 days followed by 2 days at room temperature. All knockout strains were [*PSI*$^+$]. Δ*akl1* appeared only slightly [*PSI*$^+$] weak.

To further analyse [*PSI*$^+$] in the kinase mutants each strain was spotted on SC - adenine medium (Figure 5.26). The plates were incubated at 30^{o}C for 2 days followed by 2 days at room temperature. All mutants were expected to grow as they

all displayed a [*PSI*$^{+}$] phenotype on YPD medium. However, single mutants Δ*kin2* and Δ*hsl1* did not grow. The test was repeated again and the same phenotype appeared. Single mutant Δ*akl1* and double mutants Δ*akl1*Δ*kin2* and Δ*akl1*Δ*hsl1* all grew well on SC - adenine medium (Figure 5.26). These results were contradictory as Δ*kin2* and Δ*hsl1* displayed a [*PSI*$^{+}$] phenotype on YPD but a [*psi*$^{-}$] phenotype on SC - adenine.

Perhaps deleting *kin2* and *hsl1* impaired the adenine biosynthesis pathway somehow, and without supplemented adenine these mutants cannot grow. There is also the possibility that the mutants are actually [*psi*$^{-}$] and they appear white on YPD because there is some sort of factor impairing the formation of the red pigment. There are possibly other conditions that a cell requires, other than the *ade2* mutation, in order to produce the red pigment. Any genetic disruption to these processes could ultimately lead to a white phenotype.

The kinase mutants were streaked onto YPD + 3 mM GdnHCl agar and incubated at 30^{o}C for 2 days followed by 2 days at room temperature. The only strains to cure were G600 WT and G600Δ*akl1* (Figure 5.27). Perhaps the other mutants are successfully cured but the red pigment is not produced. There is also the possibility that these mutants are petite mutants and this may be the reason why they are white but Ade^{-}. These results were quite unexpected and it is hard to make a conclusion as to exactly what is genetically/biochemically occurring. Possible future work is discussed in Chapter 6.

Preliminary results with single mutant Δ*hsl1* suggested that its genetic abnormality is dominant. Δ*hsl1* and Δ*akl1* were mated with [*psi*$^{-}$] G620/G621 strains and the diploids were cured on 3 mM GdHCl. Δ*akl1* successfully cured but Δ*hsl1* remained white.

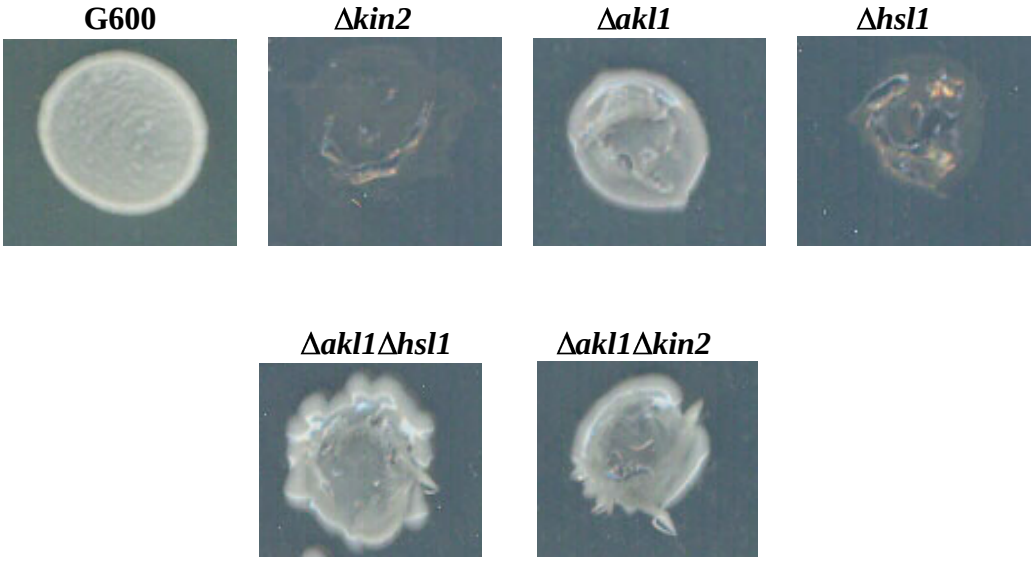

Figure 5.26. [*PSI*$^{+}$] phenotypic analysis in kinase knockout strains. All knockout strains were spotted onto SC - adenine in 10 μl of dH_2O. The plates were incubated for 2 days at 30^{o}C followed by 2 days at room temperature. Single Δ*kin2* and Δ*hsl1* strains failed to grow on SC - adenine but grew with the addition of Δ*akl1* second deletion. This result was not expected as both mutants appeared [*PSI*$^{+}$] on YPD medium, but failure to grow on medium without adenine is indicative of a [*psi*$^{-}$] strain.

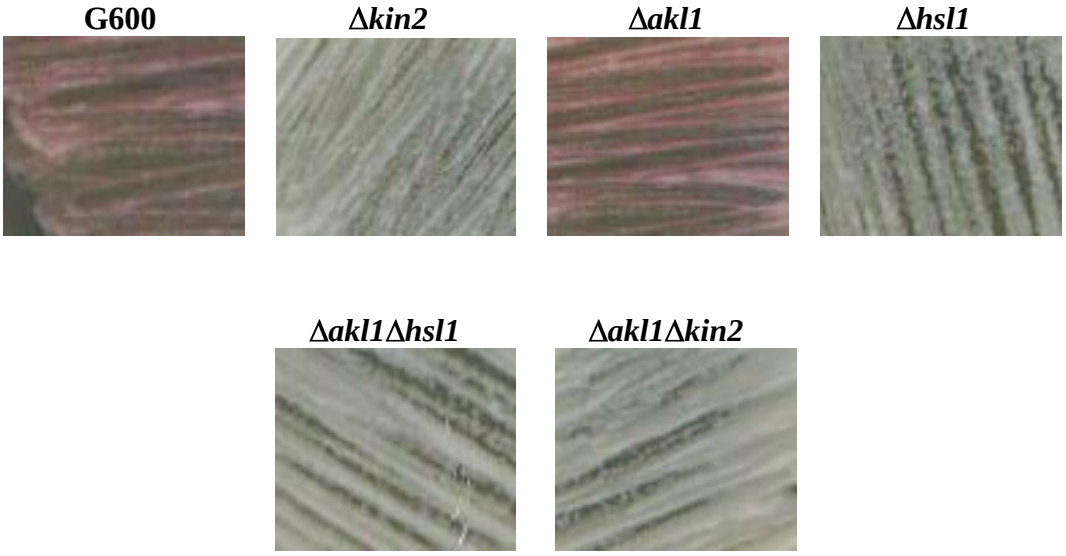

Figure 5.27. Analysis of the curability of kinase mutants on 3 mM GdnHCl. G600 WT and kinase mutants were streaked onto YPD + 3 mM GdnHCl and incubated at 30^{o}C for days. [*PSI*$^{+}$] was analysed after the strains were left for 2 days at room temperature. The only mutant that successfully turned red (cured) was single mutant Δ*akl1*.

5.4 Analysis of Sse1 and Sse2 phosphorylation sites

Protein phosphorylation is a universal mechanism which is essential for regulating cell behaviour in yeast and other eukaryotes. Protein kinases target their substrates by binding to short pieces of their linear protein sequence (Mok *et al.*, 2010). In this section the effects of altering these sites were examined and how this impacts the ability of Sse1 and Sse2 to propagate [*PSI*$^{+}$] and maintain cellular integrity.

5.4.1 Sse phosphorylation site location and the generation of mutations which alter these sites

The Sse serine residues which are phosphorylated *in vivo* by protein kinases were chosen to be analysed. Using the Phosphopep database the precise codons which the kinases are presumed to modify were identified. The phosphopep database has identified nearly 9,000 phosphorylation sites in the yeast proteome. Most sites in the database were identified from peptides which were separated by their isoelectric points and analysed using LTQ-FT and LTQ-Orbtitrap Mass Spectrometry instruments. Kinases phosphorylate these sites by adding a phosphate group onto the hydroxyl group of serine. These sites were S85 and S384 in Sse1 and S384, S679 and S682 in Sse2 (Figure 5.28). These sites were altered to alanine and glutamic acid residues. This was achieved by site-directed mutagenesis (Figure 5.29 and Figure 5.31). The reason why alanine and glutamic acid were chosen is because alanine is refractory to phosphorylation and glutamic acid mimics phosphorylation (phosphomimetic) so they have opposing effects.

The mutants were transformed into CM02 and selected on SC - leucine for 2 days at 30^{o}C. Transformants were replicated onto 5-FOA to select against

pRS316*SSE1*. Sse1 mutants grew well on this medium for 2 days (Figure 5.30) however the Sse2 mutants struggled to grow even after 4 days incubation (Figure 5.32). Small colonies appeared after the plates were left at room temperature for 2 days. These colonies were picked off and restreaked onto fresh SC - leucine where they all grew well.

Sse1

MSTPFGLDLGNNNSVLAVARNRGIDIVVNEVSNRSTPSVVGFGPKNRYLGETGKNKQTSN
IKNTVANLKRIIGLDYHHPDFEQE**S**KHFTSKLVELDDKKTGAEVRFAGEKHVFSATQLAA
MFIDKVKDTVKQDTKANITDVCIAVPPWYTEEQRYNIADAARIAGLNPVRIVNDVTAAGV
SYGIFKTDLPEGEEKPRIVAFVDIGHSSYTCSIMAFKKGQLKVLGTACDKHFGGRDFDLA
ITEHFADEFKTKYKIDIRENPKAYNRILTAAEKLKKVLSANTNAPFSVESVMNDVDVSSQ
LSREELEELVKPLLERVTEPVTKALAQAKLSAEEVDFVEIIGGTTRIPTLKQSISEAFGK
PLSTTLNQDEAIAKGAAFICAIH**S**PTLRVRPFKFEDIHPYSVSYSWDKQVEDEDHMEVFP
AGSSFPSTKLITLNRTGDFSMAASYTDITQLPPNTPEQIANWEITGVQLPEGQDSVPVKL
KLRCDPSGLHTIEEAYTIEDIEVEEPIPLPEDAPEDAEQEFKKVTKTVKKDDLTIVAHTF
GLDAKKLNELIEKENEMLAQDKLVAETEDRKNTLEEYIYTLRGKLEEEYAPFASDAEKTK
LQGMLNKAEEWLYDEGFDSIKAKYIAKYEELASLGNIIRGRYLAKEEEKKQAIRSKQEAS
QMAAMAEKLAAQRKAEAEKKEEKKDTEGDVDMD*

Sse2

MSTPFGLDLGNNNSVLAVARNRGIDVVVNEVSNRSTPSLVGFGPRNRYLGESGKTKQTSN
VKNTVENLKRIIGLKFKDPEFDIENKFFTSKLVQLKNGKVGVEVEFGGKTHVFSATQLTA
MFIDKVKHTVQEETKSSITDVCLAVPVWYSEEQRYNIADAARIAGLNPVRIVNDVTAAAV
SYGVFKNDLPGPEEKPRIIGLVDIGHSTYTCSIMAFRKGEMKVLGTAYDKHFGGRDFDRA
ITEHFADQFKDKYKIDIRKNPKAYNRILIAAEKLKKVLSANTTAPFSVESVMDDIDVSSQ
LSREELEELVEPLLKRVTYPITNALAQAKLTVNDIDFVEIIGGTTRIPVLKKSISDVFGK
PLSSTLNQDEAVAKGAAFICAIH**S**PTLRVRPFKFEDIDPYSVSYTWDKQVDDEDRLEVFP
ANSSYPSTKLITLHRTGDFSMKAVYTHPSKLPKGTSTTIAKWSFTGVKVPKDQDFIPVKV
KLRCDPSGLHIIENAYTTEDITVQEPVPLPEDAPEDAEPQFKEVTKTIKKDVLGMTAKTF
ALNPVELNDLIEKENELRNQDKLVAETEDRKNALEEYIYTLRAKLDDEYSDFASDAEKEK
LKNMLATTENWLYGDGDDSTKAKYIAKYEELASLGNIIRGRYLAKEEEKRQALRANQETS
KMNDIAEKLAEQRRARAA**S**DD**S**DDNNDENMDLD*

Figure 5.28. Phosphorylation sites located on the Sse1 and Sse2 protein sequence. Sse1 is the top sequence and Sse2 is the bottom. Sites were confirmed using the Phosphopep database. All phosphorylation sites are serine residues.

S85A

TTCGAGCAAGAAGCTAAGCACTTCACCTCTAAGTTGGTTGAATTGG

TTCGAGCAAGAATCTAAGCACTTCACCTCTAAGTTGGTTGAATTGG

S85E

TTCGAGCAAGAAGAAAAGCACTTCACCTCTAAGTTGGTTGAATTGG

TTCGAGCAAGAATCTAAGCACTTCACCTCTAAGTTGGTTGAATTGG

S384A

TTTATTTGCGCCATTCACGCTCCAACTCTAAGAGTTAGACCATTCAA

TTTATTTGCGCCATTCACTCTCCAACTCTAAGAGTTAGACCATTCAA

S384E

TTTATTTGCGCCATTCACGAACCAACTCTAAGAGTTAGACCATTCAA

TTTATTTGCGCCATTCACTCTCCAACTCTAAGAGTTAGACCATTCAA

Figure 5.29. Location of *SSE1* phosphorylation site mutants. Serine codons are highlighted and are in the top sequence. The mutants were generated by site-directed mutagenesis. This figure illustrates a select region of DNA sequence from *SSE1* gene with the exact mutation on the bottom row. These codon mutations correspond to the particular amino acid site of phosphorylation.

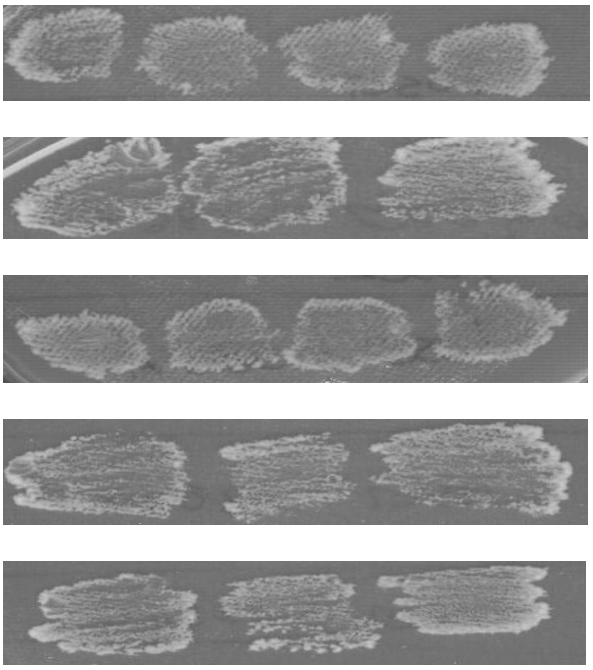

Figure 5.30. Growth status of Sse1 phosphorylation mutants in CM02. CM02 was transformed with each mutant, selected on SC - leucine and incubated at 30^{o}C for 2 days. The plates were replicated onto 5-FOA, to select against pRS316*SSE1*, and incubated at 30^{o}C for 2 days. Sse1 phosphorylation mutants could support growth.

S384A

CGCTTTCATATGTGCCATTCACGCTCCAACTTTAAGGGTCAGGCCG

CGCTTTCATATGTGCCATTCACTCTCCAACTTTAAGGGTCAGGCCG

S384E

CGCTTTCATATGTGCCATTCACGAACCAACTTTAAGGGTCAGGCCG

CGCTTTCATATGTGCCATTCACTCTCCAACTTTAAGGGTCAGGCCG

S679A

ACGCGCTGCAGCTGATGATAGCGATGACAACAATGATGAAAACAT

ACGCGCTGCAAGTGATGATAGCGATGACAACAATGATGAAAACAT

S679E

ACGCGCTGCAGAAGATGATAGCGATGACAACAATGATGAAAACAT

ACGCGCTGCAAGTGATGATAGCGATGACAACAATGATGAAAACAT

S682A

AAGTGATGATGCCGATGACAACAATGATGAAAACATGGACCTTGA

AAGTGATGATAGCGATGACAACAATGATGAAAACATGGACCTTGA

S682E

AAGTGATGATGACGATGACAACAATGATGAAAACATGGACCTTGA

AAGTGATGATAGCGATGACAACAATGATGAAAACATGGACCTTGA

Figure 5.31. Location of *SSE2* phosphorylation site mutants. Serine codons are highlighted and are in the top sequence. Mutants were generated by site-directed mutagenesis. This figure illustrates a select region of DNA sequence from *SSE2* gene with the exact mutation on the bottom rows. These codon mutations correspond to the particular amino acid site of phosphorylation.

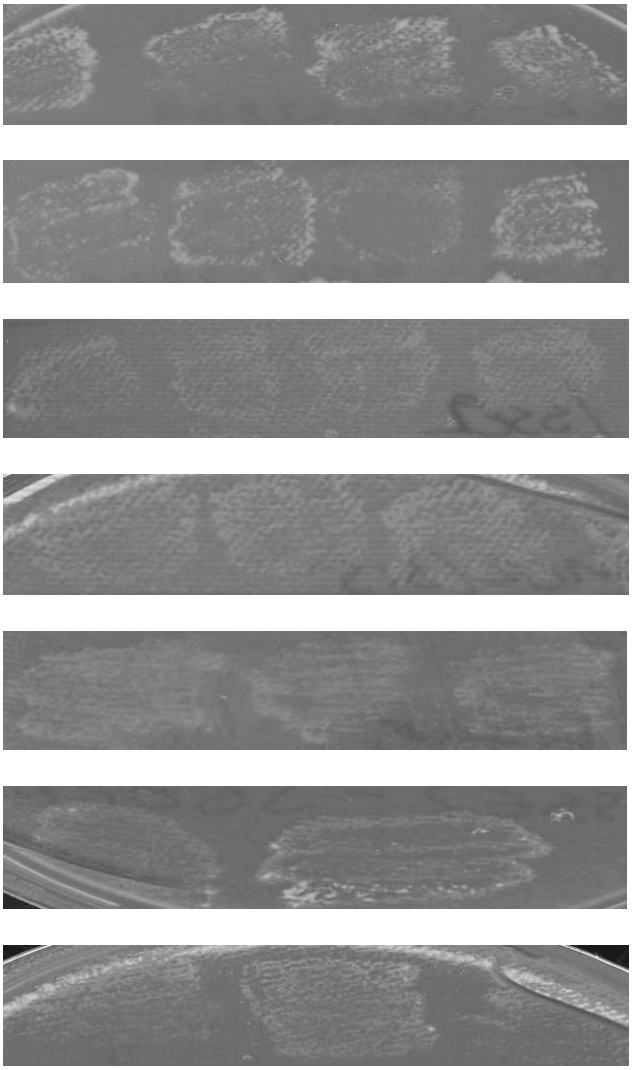

Figure 5.32. Growth status of Sse2 phosphorylation mutants in CM02. CM02 was transformed with each mutant, selected on SC - leucine and incubated at 30^{o}C for 2 days. The plates were replicated onto 5-FOA, to select against pRS316*SSE1*, and incubated at 30^{o}C for 4 days. Sse2 phosphorylation mutants struggled to support growth even after 4 days incubation. The plates were left at room temperature for 2 days and colonies were selected and restreaked onto fresh medium.

5.4.2 Investigation into the effects of phosphorylation site mutants on cellular thermostability

As Sse1 and Sse2 play a role in responding to thermal stress an objective was to test the effect the mutations have on the ability of Sse to maintain thermostability. CM02 with Sse1 and Sse2 phosphorylation site mutants were serial

diluted onto YPD and incubated at 30°C, 37°C and 39°C for 2 days. Sse1 mutants all grew at a similar rate to WT Sse1 at all temperatures (Figure 5.33).

Screening for temperature-sensitive mutants in Sse2 is slightly more difficult since WT Sse2 is slow-growing and non-viable at 39°C already. However, Sse2 mutant S384E was temperature-sensitive and slow-growing at 30°C. In comparison S384A grew slightly better than WT Sse2 which showed growth at all temperatures (Figure 5.34). All other Sse2 mutants displayed similar growth to WT Sse2 (Figure 5.35 and 5.36). S384E was also created in Sse1 but did not result in a temperature-sensitive phenotype (Figure 5.33).

5.4.3. Analysis of [*PSI*$^+$] phenotypes in Sse1 and Sse2 phosphorylation site mutants

Sse1 mutants were streaked onto YPD and incubated at 30°C for 2 days. The mutants displayed a colour phenotype similar to WT Sse1 and were deemed as [*PSI*$^+$] mutants (Figure 5.37). The mutants also cured efficiently on 3 mM GdnHCl which confirmed that nothing effected the *ade2* red pigment development (Figure 5.38).

In comparison the Sse2 mutants were spotted onto YPD in 10 μl of dH_2O and they displayed varying degrees of [*PSI*$^+$] (Figure 5.39). Mutants S384A and S682E appeared red [*psi*$^-$] which was confirmed by their lack of growth on SC - adenine (Figure 5.40). However two mutants, S679E and S682A, appeared pink and [*PSI*$^+$] was present in the cell as these mutants grew successfully on SC - adenine (Figure 5.40). However, all of the Sse2 mutants did appear to have slightly greater [*PSI*$^+$] phenotypes than WT Sse2.

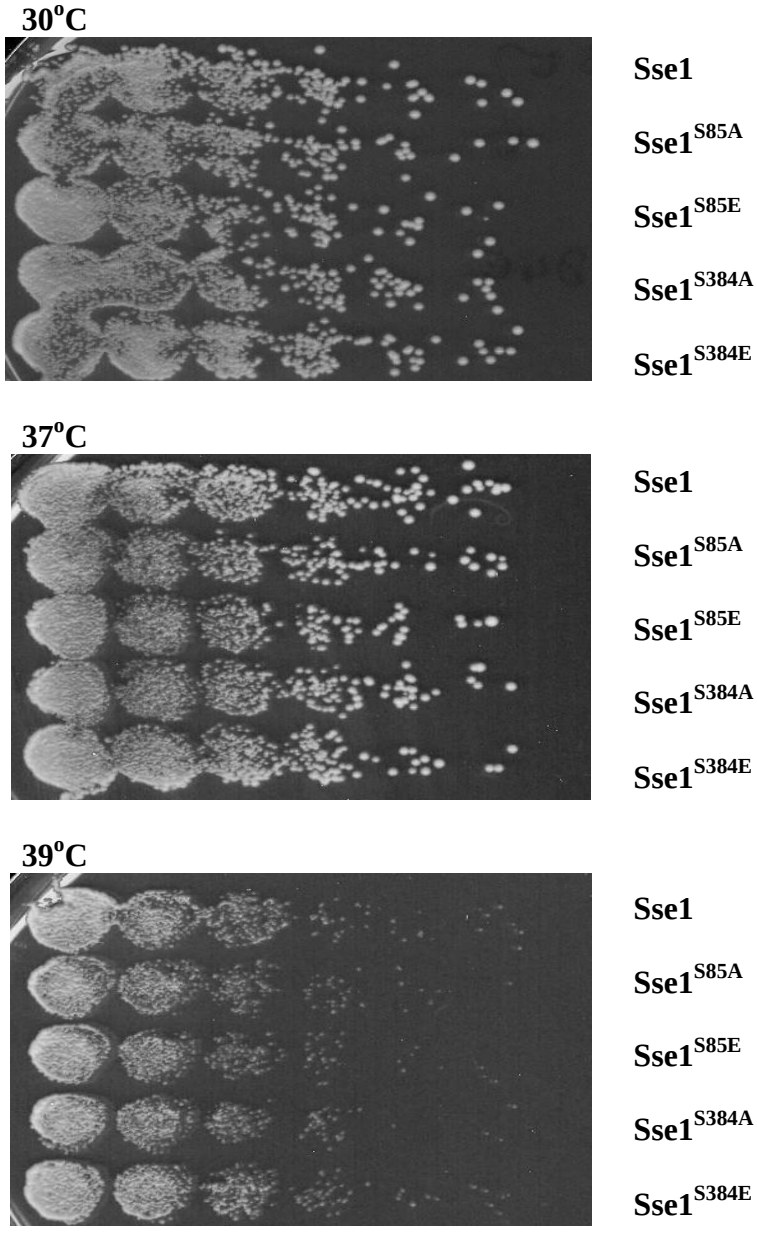

Figure 5.33. Comparative growth analysis of the temperature-sensitive effects caused by Sse1 phosphorylation site mutants. Sse1 mutants were serial diluted onto YPD medium and incubated at 30°C, 37°C and 39°C for 2 days. Mutants had no effect on the ability of Sse1 to maintain thermostability.

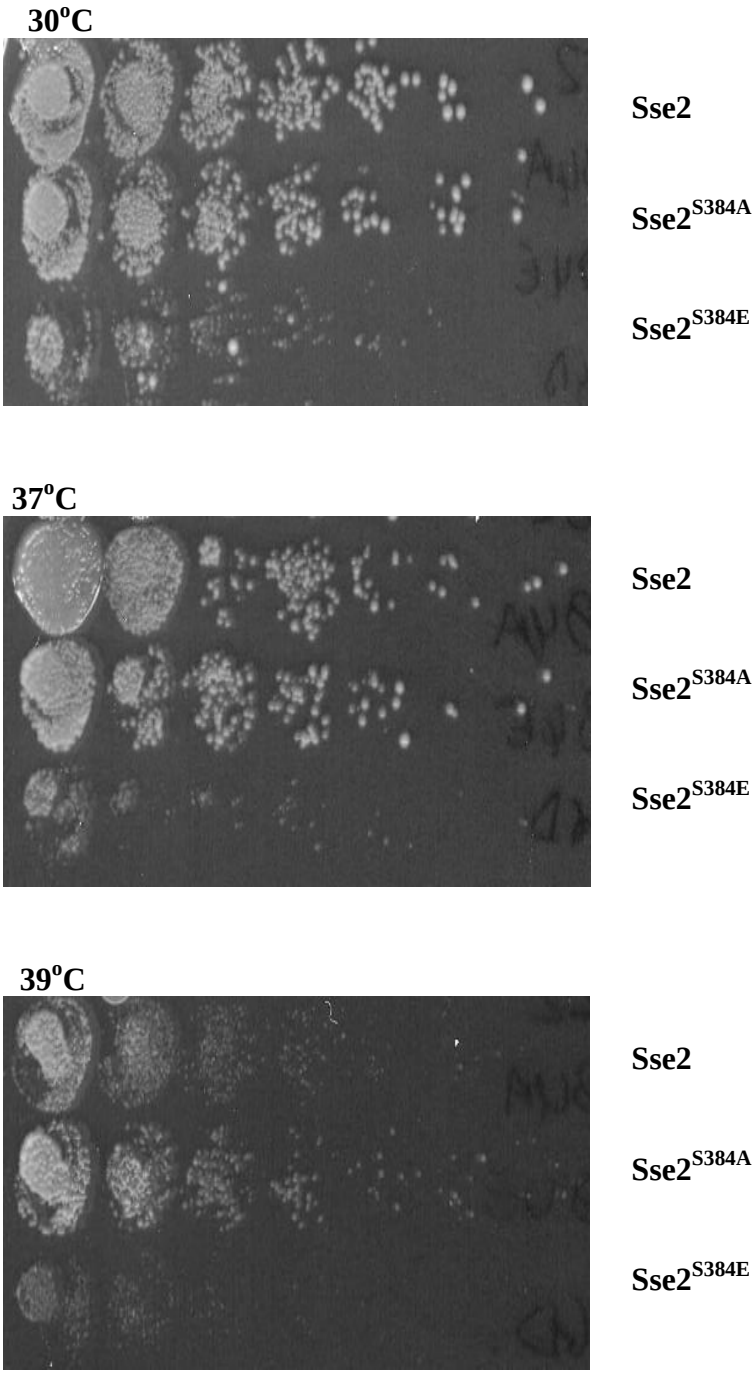

Figure 5.34. Comparative growth analysis of the temperature-sensitive effects caused by Sse2 phosphorylation site mutants. Sse2 mutants were serial diluted onto YPD medium and incubated at 30°C, 37°C and 39°C for 2 days. Mutant Sse2^{S384E} had an effect on Sse2 at temperatures as low as 30°C. In comparison mutant Sse2^{S384A} grew well and even slightly better than WT Sse2 at 39°C. WT Sse2 showed small amounts of growth at 39°C on this plate which is not reflected in the other plates in this test.

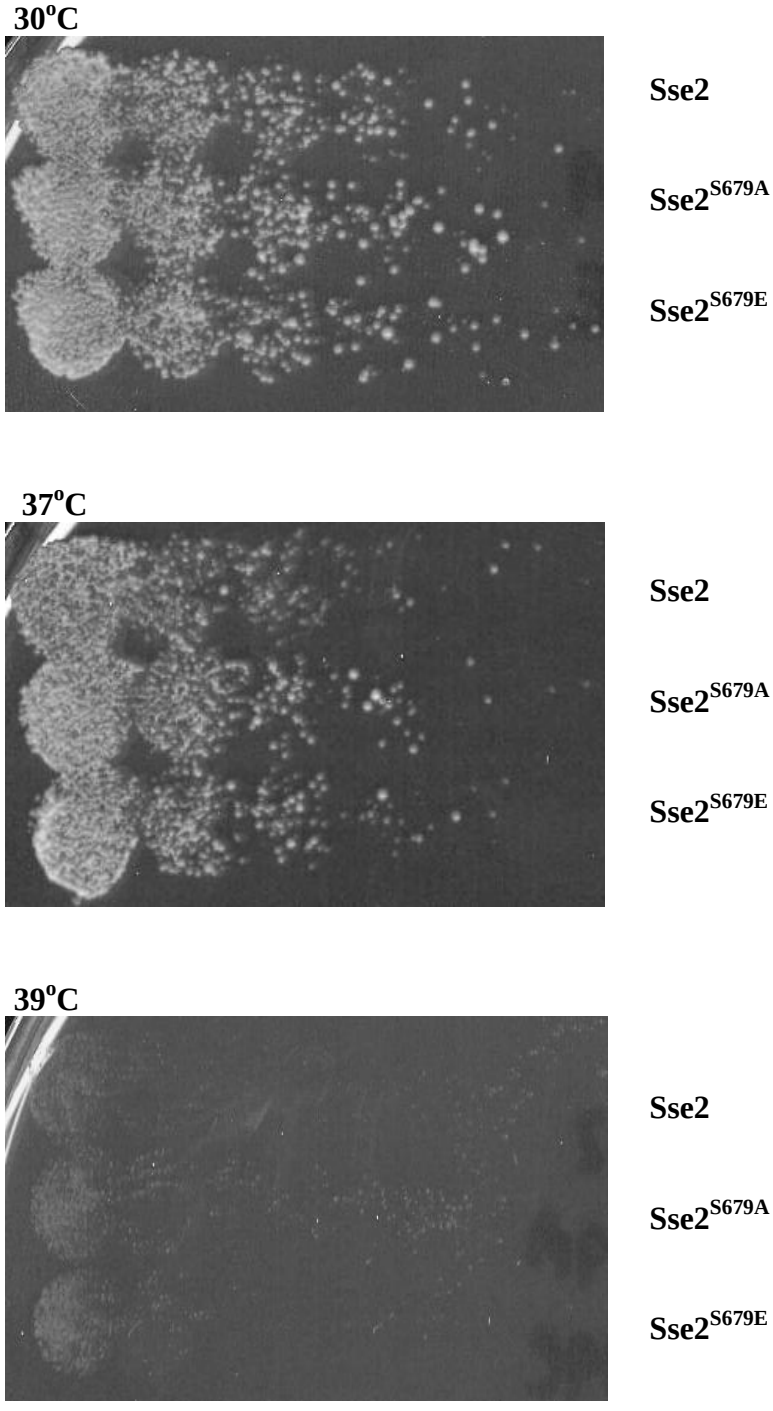

Figure 5.35. Comparative growth analysis of the temperature-sensitive effects caused by Sse2 phosphorylation site mutants. Sse2 mutants were serial diluted onto YPD medium and incubated at 30°C, 37°C and 39°C for 2 days. Phosphorylation site mutants $Sse2^{S679A}$ and $Sse2^{S679E}$ behaved similarly to WT Sse2 in that they were slow-growing at 37°C and non-viable at 39°C.

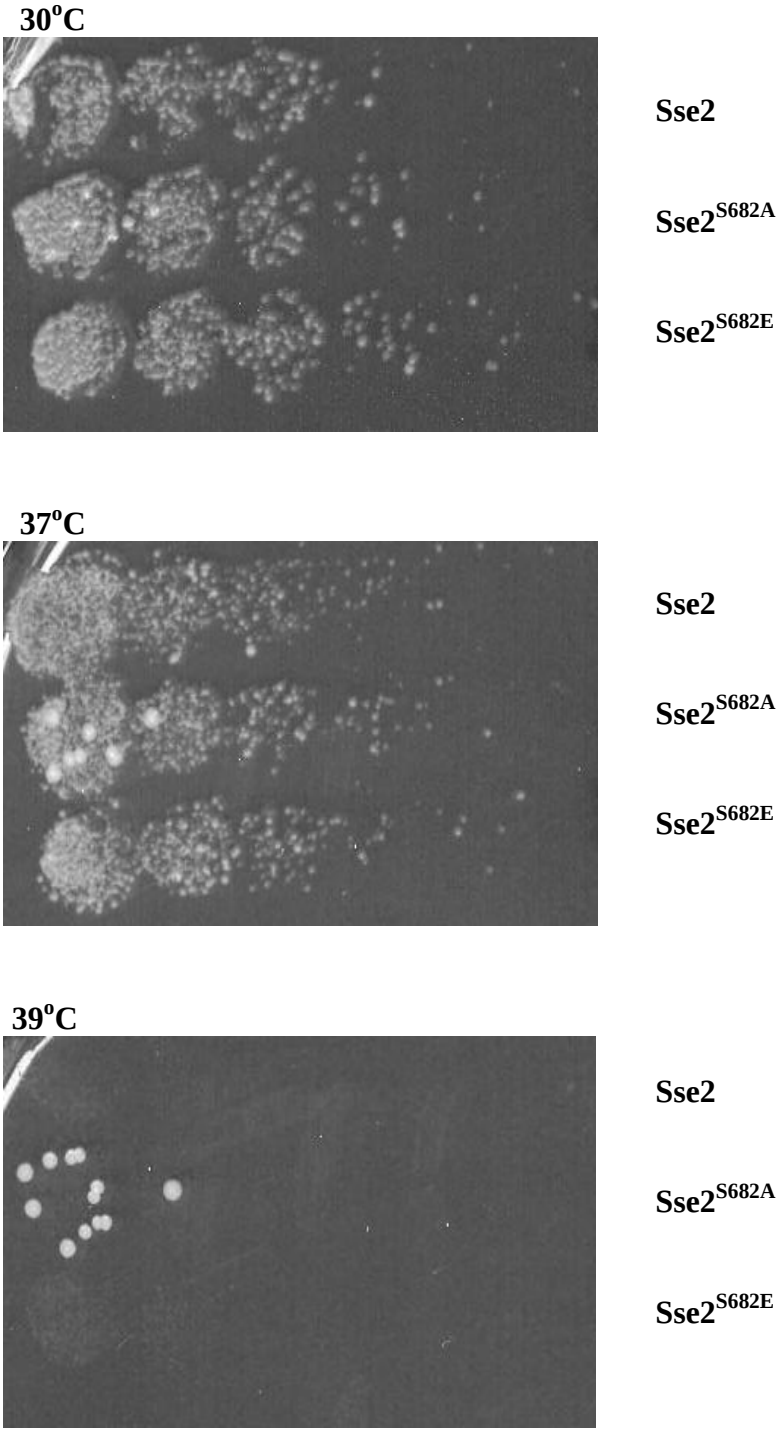

Figure 5.36. Coimparative growth analysis of the temperature-sensitive effects caused by Sse2 phosphorylation site mutants. Sse2 mutants were serial diluted onto YPD medium and incubated at 30°C, 37°C and 39°C for 2 days. Phosphorylation site mutants $Sse2^{S682A}$ and $Sse2^{S682E}$ behaved similarly to WT Sse2 in that they were slow-growing at 37°C and non-viable at 39°C.

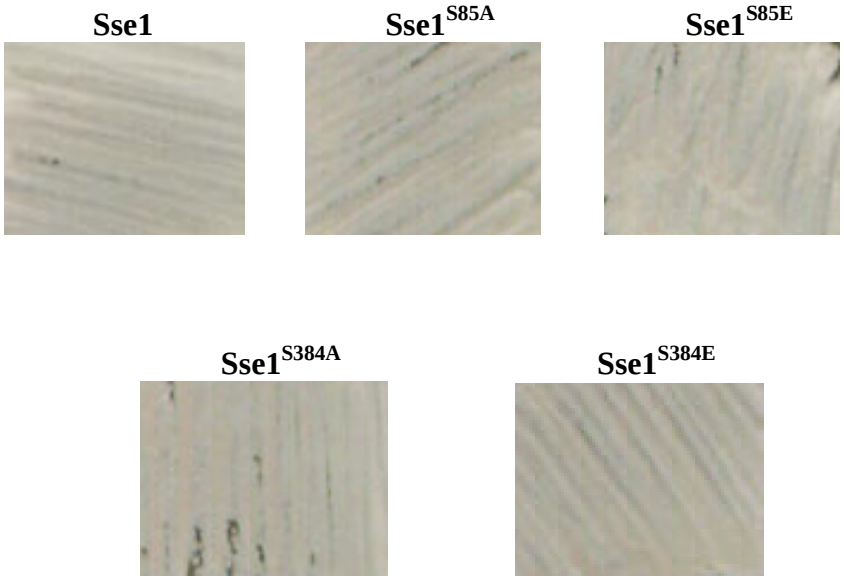

Figure 5.37. [*PSI*$^{+}$] phenotypic analysis of Sse1 phosphorylation mutants. Mutants were streaked onto YPD and incubated at 30^{o}C for 2 days. Mutations to the phosphorylation sites of Sse1 appear to cause no disruption to [*PSI*$^{+}$] propagation.

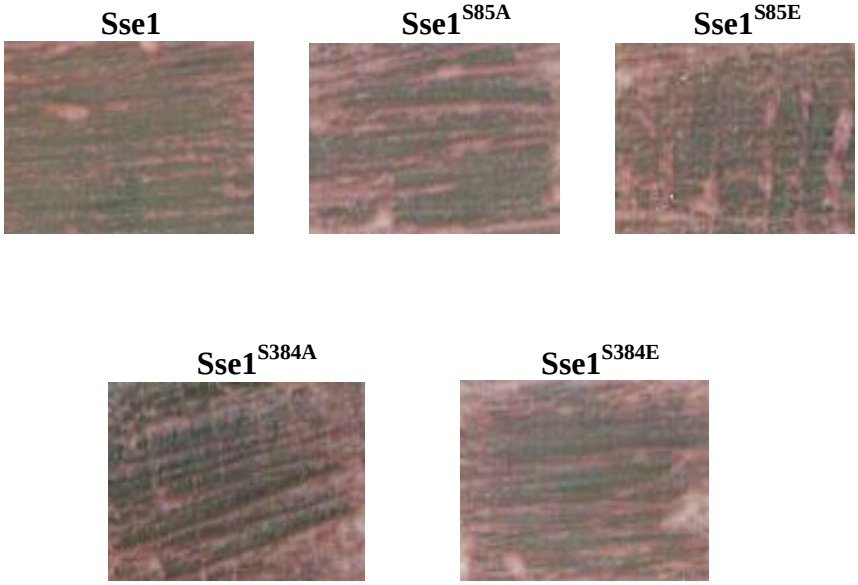

Figure 5.38. Analysis of Sse1 phosphorylation mutant curability on 3 mM GdnHCl. Mutants were streaked onto YPD + 3 mM GdnHCl and incubated at 30^{o}C for 2 days. WT Sse1 and Sse1 mutants successfully cured on this medium.

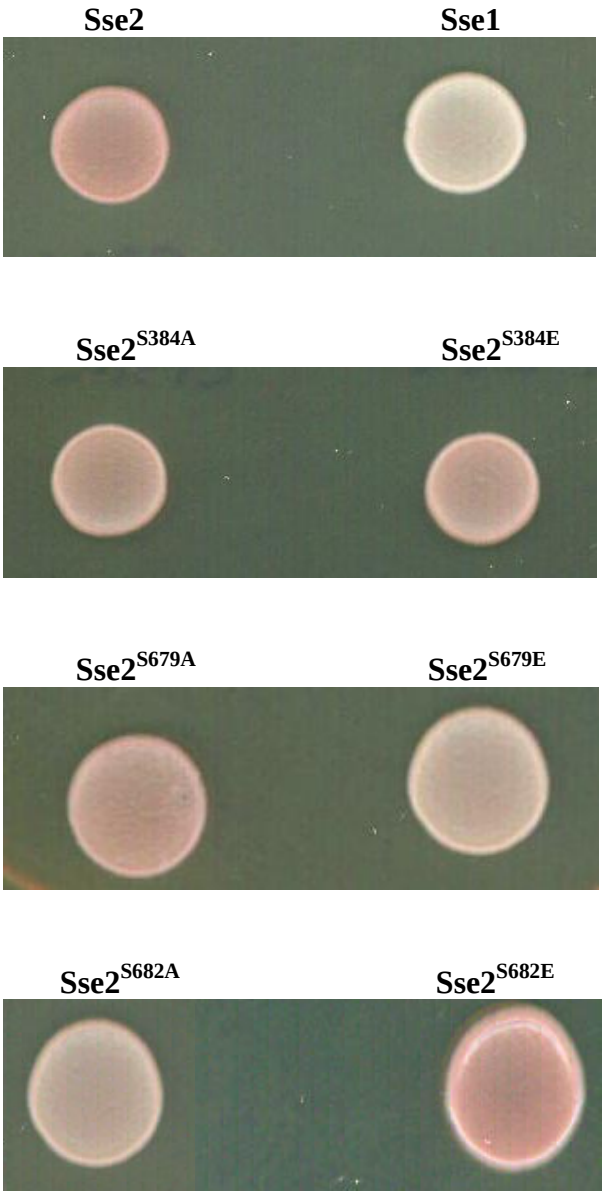

Figure 5.39. Analysis of [*PSI*$^+$] in Sse2 phosphorylation site mutants. CM02 + Sse1, Sse2 and Sse2 mutants were spotted onto YPD in 10 μl dH_2O. The plates were incubated at 30^{o}C for 2 days and left at room temperature for 2 days prior to analysis. All Sse2 mutants appeared slightly more [*PSI*$^+$] than WT Sse2, particularly Sse2^{S679E} and Sse2^{S682A}.

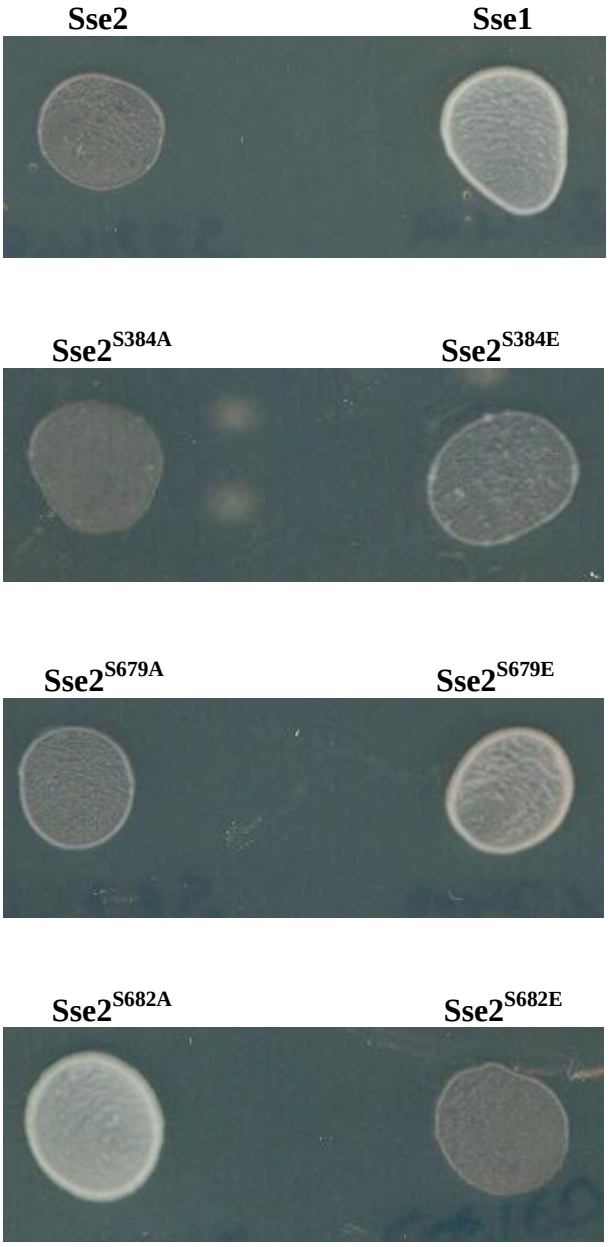

Figure 5.40. Analysis of [*PSI*$^+$] in Sse2 phosphorylation site mutants. CM02 + Sse1, Sse2 and Sse2 mutants were spotted onto SC - adenine in 10 μl dH_2O. The plates were incubated at 30^{o}C for 2 days and left at room temperature for 2 days prior to analysis. Sse2 mutants S384A and S682E failed to grow like WT Sse2 control. Mutants S384E and S679A showed small amounts of growth and mutants S679E and S682A grew as well as WT Sse1. These results correspond with those in Figure 5.39 in that certain Sse2 mutations make the strain more [*PSI*$^+$].

Mutants S384E and S679A appeared dark pink on YPD and had a small amount of growth on SC - adenine. All mutants were mated with [*psi*$^-$] strain G621 resulting in mutants S384E, S679E and S682A demonstrating a dominant [*PSI*$^+$] phenotype. The ability to isolate Sse2 mutants which improve the proteins ability to propagate [*PSI*$^+$] alone is very interesting, particularly since these mutations affect kinases binding to Sse2. It appears that if you differentially phosphorylate Sse2 it can start to propagate [*PSI*$^+$] again and could possibly be the reason why Sse2 cannot propagate [*PSI*$^+$] in the first place.

5.5 Chapter discussion

In Chapters 3 and 4 the focus was mainly on the role Sse1 plays in yeast prion propagation and cell integrity. In this Chapter Sse1 and Sse2 have been compared in their ability to provide the cell with Hsp110 functions when expressed as the sole Hsp110 isoform.

Cloning *SSE2* enabled a comparative analysis of Sse1 and Sse2 phenotypes in CM02 to be carried out. *SSE2* was successfully cloned into pRS315 under the control of its own promoter. This enabled the transformation of *SSE2*, alongside *SSE1*, into cells and shuffle out WT *SSE1*. Sse1 and Sse2 were first compared by assessing their ability to promote [*PSI*$^+$] propagation. When spotted onto YPD Sse2 appeared [*psi*$^-$] in comparison to Sse1. Sse2 also failed to grow on SC - adenine medium, indicative of a [*psi*$^-$] strain. When Sse1 and Sse2 strains were mated with a [*psi*$^-$] strain the Sse2 diploids were red and failed to grow on SC - adenine, confirming again the hypothesis that Sse2 is incapable at propagating [*PSI*$^+$]. As Sse2 is expressed at low levels under normal environmental conditions its low cellular presence may not be sufficient

enough to propagate [*PSI*$^{+}$]. It has been shown that Sse2 is ~50% less efficient as Sse1 at Ssa1 nucleotide exchange (Dragovic *et al*., 2006) and Polier *et al*. (2010) recently showed that Sse2 is capable of binding unfolded firefly luciferase but fails to stabilise it for Hsp70-mediated folding. Perhaps the limited expression of Sse2 protein at basal temperatures, its lack of holdase function and its insufficient NEF function inhibits its ability to maintain and propagate [*PSI*$^{+}$].

As Sse1 and Sse2 have been recorded as having different expression levels at different temperatures (Mukai *et al*., 1993) the growth rates of cells expressing Sse1 and Sse2 were compared in CM02. This was performed at 30^{o}C and 37^{o}C. Cells with WT Sse1 grew relatively fast at 30^{o}C and 37^{o}C with generation times of 116 and 100 minutes respectively. It appears that heat stress caused the Sse1 strain to grow at a faster rate. In comparison, Sse2 had growth rates of 134 minutes at 30^{o}C and 132 minutes at 37^{o}C so it was slower growing at both temperatures. This was not a surprising result as Sse2 expression is up-regulated at increased temperatures so no differences were observed between growth at 30^{o}C and 37^{o}C. Comparative growth analysis at 30^{o}C, 37^{o}C and 39^{o}C confirmed this, as Sse2 was slow-growing at 30^{o}C and 37^{o}C and was completely non-viable at 39^{o}C. These results concur with previous reports by Liu *et al*. (1999), Shaner *et al*. (2004) and Raviol *et al*. (2005). As Sse2 is a stress induced protein its expression is up-regulated by transcription factors such as Hsf1 and Msn2 (Wu and Li, 2008) at 37^{o}C and not 30^{o}C, perhaps this is why Sse2 could grow similarly at both temperatures. It seems that Sse2 is either not expressed at a high enough level to cope with temperature stress or its structure disables it from making critical interactions necessary for normal cell growth. These findings agree with those made by Shaner *et al*. (2004) and Raviol *et al*. (2006).

Sse1 mutant E504K is located at the only amino acid residue not conserved in Sse2. E504K was previously isolated as an Sse1 mutant with a [*PSI*$^{+}$] weak phenotype. It was theorised that if this residue is important for Sse1 to function in [*PSI*$^{+}$] propagation then perhaps Sse2 could maintain [*PSI*$^{+}$] if it expressed residue E504. Changing Sse2 Q504 to E504 resulted in cells that grew at a similar rate to WT Sse2 but expressed an enhanced [*PSI*$^{+}$] phenotype (Figure 5.11). Therefore Sse2 mutant Q504E has a specific affect on [*PSI*$^{+}$] and does not enhance Sse2 growth indicating that Hsp110 residues are specific in their interactions and molecular functions. In Chapter 3 it could not be established exactly how this residue is important for Sse1 function and how the mutation disrupts the Sse1 structure. However, this residue is clearly important in [*PSI*$^{+}$] propagation as its presence in Sse2 enhanced some function that led to an improved [*PSI*$^{+}$] phenotype.

Mutant G616D was isolated in Sse1 as a [*psi*$^{-}$] ts mutant and this residue is conserved in Sse2. The aim was to investigate whether this residue has conserved function in both Sse1 and Sse2. G616D was introduced into the Sse2 structure leading to a ts phenotype more extreme than that seen in WT Sse2. Sse2^{G616D} was slow-growing at 30^{o}C and non-viable at 37^{o}C (Figure 5.12). This residue appears to have conserved function in both Sse1 and Sse2. In Sse1 this mutant possibly disrupted Hsp70 binding and subsequent NEF function and its 30^{o}C ts phenotype in Sse2 could also be due to a lack of NEF function.

Another area explored was how Sse phosphorylation affects [*PSI*$^{+}$] propagation and thermostability. Surprisingly, single and double deletions of kinase proteins Akl1, Kin2 and Hsl1 did not appear to have a severe effect on cell growth or on [*PSI*$^{+}$]. It soon became clear that the mutants had an unusual phenotype as all but Δ*akl1* failed to cure on 3 mM GdnHCl and mutants Δ*kin2* and Δ*hsl1* failed to grow on

SC – adenine when they appeared [*PSI*$^{+}$] on limiting adenine. The adenine biosynthesis pathway is complicated and disruptions to it could ultimately affect a cells phenotype. There is the possibility that Δ*kin2* and Δ*hsl1* are [*psi*$^{-}$] but failed to produce the red pigment associated with this phenotype. This would explain how the mutants grew as white cells on YPD, failed to grow on SC – adenine and failed to cure on GdnHCl. If this were the case then double mutants Δ*akl1*Δ*kin2* and Δ*akl1*Δ*hsl1* stabilised this [*PSI*$^{+}$] disruption as they successfully grew on SC – adenine. But these double mutants also failed to cure on GdnHCl still indicating a problem with red pigment formation. There is also the possibility that they are [*PSI*$^{+}$] mutants but failed to grow on SC – adenine as their mutation impairs the adenine biosynthesis pathway somehow, and without supplemented adenine these mutants cannot grow. There is something genetically complex occurring with these mutants and future work will need to be done in order to establish exactly what this is.

In this Chapter the Sse1/Sse2 serine residues which are suggested as being phosphorylated *in vivo* by protein kinases were examined. The phosphopep database has identified five phosphorylation sites in Sse1 and Sse2 by mass spectrometry analysis. However, it is important to note that these phosphorylation sites have not yet been formally shown by ^{32}P labeling *in vivo*. The residues were altered to alanine and glutamic acid residues by site-directed mutagenesis. The concept behind these amino acid substitutions was that alanine mutants would fail to be phosphorylated and glutamic acid mutants would mimic permanent phosphorylation. Sse1 phosphorylation site mutants displayed no impairment to either temperature sensitivity or to [*PSI*$^{+}$] phenotypes. In comparison, Sse2 phosphorylation site mutant S384E was slow-growing at 30^{o}C and 37^{o}C. This same mutation in Sse1 had no effect on cell growth. Sse2 mutant S384A enhanced cell growth at 37^{o}C and 39^{o}C.

Interestingly, mutants S384A and S384E are located at the same residue but resulted in two completely different phenotypes probably due to variations in protein phosphorylation. It appears that a lack of phosphorylation at S384 enhances the ability of Sse2 to withstand thermal stress and permanently activating phosphorylation (S384E) increases Sse2 temperature sensitivity. This is significant as it is not only the mutation that is having the effect on Sse2 but the resulting phenotype is dependent on the type of amino acid change occurring. As these two phenotypes were observed, there is an indication that posttranslational modification of Sse2 does have an impact on its function in thermotolerance. There is the possibility that this mutation may not just be disrupting kinase binding but also disrupting the Sse2 structure in a way that improves/disrupts its ability to withstand thermal stress. It also appears that Sse2 is more sensitive to these mutations than Sse1, in respect to thermostability, perhaps because Sse2 is already more sensitive to thermal stress than Sse1.

Sse2 phosphorylation site mutants also resulted in improved [*PSI*$^{+}$] propagation. Mutants S679E and S682A appeared pink on limiting adenine and grew well on medium lacking adenine. Most of the other Sse2 phosphorylating mutants did appear slightly more [*PSI*$^{+}$] than WT Sse2 even if they did not fully grow on SC - adenine. Once again it appears that differentially phosphorylating Sse2 enhances its function, but this time it was enhancing [*PSI*$^{+}$] propagation. Inhibiting and promoting phosphorylation of Sse2 did not result in a uniform patterned phenotype as some residues functioned better with phosphorylation and others without. There is the possibility that the mutations are altering the Sse2 structure in a way that enables Sse2 to enhance [*PSI*$^{+}$] propagation or a combination of structure and posttranslational modification.

From this Chapter it can be concluded that Sse1 and Sse2 may be structurally similar but are different in their ability to propagate prions, in their response to thermal stress and in their response to mutation. Sse1 does play a more dominant role in the cell and mutations which make Sse2 more structurally similar to Sse1 do improve Sse2's ability to promote [*PSI*$^{+}$] propagation. It remains elusive as to how phosphorylation affects Sse1 and Sse2 function. Both the disruption and induction of phosphorylation appeared to have no impact on Sse1 functions. In comparison, certain phosphorylation site mutants affected Sse2 in a way that enhanced [*PSI*$^{+}$] and also affected cell thermotolerance. Probably the most interesting mutant was located at S384 as it had opposing cellular effects dependent on whether it was phosphorylated or not.

CHAPTER SIX
DISCUSSION

6.1 General discussion

Previous work within the laboratory has revealed how molecular chaperones such as Hsp70 and Hsp104 have key roles in the maintenance and propagation of yeast prions. Such work has been supported by a plethora of research over the past decade which emphasises the significant role played by heat shock proteins in propagating yeast prions (Rikhvanov *et al*., 2007). Heat shock proteins are extensively characterised in *Saccharomyces cerevisiae* and the discovery that certain yeast proteins exhibit prion conformations has allowed scientists to uncover the nature of the relationship between prion and chaperone. Over the past few years evidence suggests that the molecular chaperone Hsp110 plays a critical role in yeast prion propagation (Fan *et al*., 2007; Kryndushkin and Wickner, 2007; Sadlish *et al*., 2008). As it has only been recently implicated in prion propagation we sought to determine the nature of the Hsp110 protein and how its expression affects yeast prion propagation, mainly through genetic analysis.

6.1.1 The Sse1 mutants and their phenotypic consequences

The most important discovery made from this study was how a group of single Sse1 mutants could impair the ability of yeast to propagate both [*PSI*$^{+}$] and [*URE3*] prions. Random mutagenesis screening resulted in the isolation of a group of thirteen Sse1 single mutants which displayed varying degrees of [*PSI*$^{+}$] loss. This highlighted the importance of particular Sse1 amino acid residues and how their correct orientation ultimately affects how the protein exerts its prion promoting effects. These mutations were located across the SBD and NBD of Sse1 and not localised at one particular region. This emphasised how the whole Sse1 structure is important for its role in [*PSI*$^{+}$] propagation. Mutants with the most severe loss of

[*PSI*$^{+}$] were D236N, G342D, S440L and G616D. The [*psi*$^{-}$] mutants were all predicted as disrupting ATP binding and Hsp70 binding, with some structural effects unclear from the 3D analysis.

This group of Sse1 mutants also affected the ability of [*URE3*] to propagate. The over-expression of Sse1 effectively cures [*URE3*] (Kryndushkin and Wickner, 2007) but when the Sse1 mutants were over-expressed they could not suppress [*URE3*] to the same extent as WT Sse1. The mutants appeared to exert a dominant negative effect over the genomic WT copy of *SSE1* with mutants G41D, D236N and G342D having the biggest effect. The fact that all mutants had a similar effect on [*URE3*] suggested that a number of Sse1 functions such as NEF activity, Hsp70 interaction and interdomain interaction may all be necessary for Sse1's curing effect on [*URE3*]. However it soon became clear, from structural data, that the mutants were potentially affecting a number of different Sse1 functions and interactions which highlighted the complicated nature in which Sse1 overproduction cures [*URE3*].

This work also highlighted how Sse1's correct amino acid sequence is required to make the interactions it needs to carry out its prion promoting functions. The Sse1 mutants were successfully modeled on the Sse1 3D crystal structure. This molecular modeling helped to determine the potential structural implications of the new mutants. The mutations were suggested as causing disruption to amino acid charge, polarity and hydrophobicity and also disrupted interdomain interactions and possible Hsp70 interactions. The mutants with the most obvious structural disruptions were G342D and G343D, which were located at the ATP binding pocket and possibly cause disruption to ATP binding. Mutants T365I and E370K appeared to directly disrupt Hsp70 binding. Mutant E554K may also disrupt Hsp70 binding as it is located at the interface of an Hsp70 binding site but this mutation only produced a [*PSI*$^{+}$]

weak phenotype. G41D and G616D may also disrupt Sse1-Hsp70 binding. It was unclear as to exactly how the other mutants were disrupting Sse1 structure and function but what was evident from the data obtained was that Hsp70 interaction, ATP binding and subsequent NEF activity are most likely the main functions that are necessary for prion propagation and are possibly being affected by these mutations. The fact that other mutants were isolated with no obvious disruption to Hsp70 or ATP binding suggested that Sse1 may play an independent role in prion propagation. These results led to the conclusion that Sse1 is a molecular chaperone that plays a major role in yeast prion propagation both indirectly through Hsp70 and possibly directly through interaction with [*PSI*$^{+}$].

As well as the Sse1 mutants [*PSI*$^{+}$]-related phenotypes, their cellular growth phenotypes were also assessed. As Sse1 and Sse2 are necessary for cellular growth and Sse1 deletion compromises the cells ability to withstand thermal stress (Mukai *et al*., 1993), it was aimed to establish whether any of the Sse1 mutants affected normal cellular homeostasis. Temperature sensitivity growth analysis in G600 background strain CM02 resulted in the mutants demonstrating various levels of sensitivity to 37^{o}C and 39^{o}C. Most mutants were slow-growing at 39^{o}C, which is possibly because the mutants disrupt Sse1 in a way that makes them sensitive to thermal aggregation, but mutants G342D and G616D were ts at 37^{o}C. Mutant G616D was the most interesting mutant as it was non-viable in both CM02 and CM03 at 37^{o}C, whereas the G342D ts phenotype was not reproduced in CM03. These results suggested that the mutants not only disrupt prion propagation but also normal cellular homeostasis, possibly through interfering with Sse1's ability to bind and refold denatured proteins. These mutations could also potentially be indirectly disrupting the protein disaggregation system by interfering with the functionality of other molecular

chaperones such as Hsp104 or Hsp70. Or perhaps the particular mutations are disrupting a different function of Sse1 in maintaining cellular homeostasis. Results also suggested that Sse1 ts mutants such as G616D may be mutants of the PKA pathway. Sse1 is involved in maintaining the down-regulation of PKA signaling and G616D may disrupt Sse1's normal function in this pathway and cause cell temperature sensitivity.

From the work presented in this thesis it can be concluded that Sse1 mutants G342D and G616D were possibly the most disruptive to the Sse1 structure and function and warrant further investigation. Table 6.1 summarises eight key mutants isolated in this study and what phenotypic effects they had on the cell. The key mutants were selected as the most [*PSI*$^{+}$] weak mutants which also demonstrated other cellular impairments and protein structural effects.

6.1.2 Hsp110 shares functional characteristics with yeast Fes1 protein and mammalian HSPH1 protein

Another aspect explored was whether proteins with similar functions could functionally compensate for Sse1 and Sse2. Initially in Chapter 3 it appeared that the NEF Fes1 and the human Hsp110 protein HSPH1 could not compensate for the combined loss of Sse1 and Sse2 in yeast. However, when repeated in a different background strain both Fes1 and HSPH1 could support growth in CM03Δ*sse1*Δ*sse2*. This highlighted the genetic background differences between BY4741 and G600. As BY4741 is widely used by other groups and G600 displayed other sensitivities it was confirmed that the yeast NEF Fes1 and a mammalian Hsp110 homolog HSPH1 could

Table 6.1. Overview of the key Sse1 mutations and their phenotypic consequences.

MUTATION	[*PSI*$^+$] PHENOTYPE	TEMPERATURE -SENSITIVE (TS) GROWTH	DISRUPT ABILITY OF *SSE1* TO CURE [*URE3*]?	STRUCTURAL EFFECTS
G41D	[*psi*$^-$] COLOUR SCORE OF 8	TS IN CM02 AT 39^{o}C	YES	POSSIBLE DISRUPTION TO HSP70 BINDING?
G50D	[*psi*$^-$] COLOUR SCORE OF 8	TS IN CM02 AT 39^{o}C	YES	UNKNOWN. POSSIBLE DISRUPTION TO HSP70:HSP110 BINDING INTERFACE?
D236N	[*psi*$^-$] COLOUR SCORE OF 10	TS IN CM02 AT 39^{o}C	YES. BIGGEST LOSS OF [*URE3*] CURING.	UNKNOWN. POSSIBLY A LOSS OF ATP BINDING?
G342D	[*psi*$^-$] COLOUR SCORE OF 10	TS IN CM02 AT 37^{o}C AND 39^{o}C	YES	DISRUPTS ATP BINDING
T365I	[*psi*$^-$] COLOUR SCORE OF 7	SLOW-GROWING IN CM02 AT 39^{o}C	YES	DISRUPTS HSP70 BINDING
E370K	[*psi*$^-$] COLOUR SCORE OF 9	TS IN CM02 AT 39^{o}C	YES	DISRUPTS ATP AND HSP70 BINDING
S440L	[*psi*$^-$] COLOUR SCORE OF 10	SLOW-GROWING IN CM02 AT 39^{o}C	YES	UNCLEAR
G616D	[*psi*$^-$] COLOUR SCORE OF 10	TS IN CM02 AND CM03 AT 37^{o}C AND 39^{o}C. POSSIBLY A PKA MUTANT??	YES	UNCLEAR. MAY DISRUPT HSP70 BINDING

Colour score: 0 = [*PSI*$^+$]/white. 10 = [*psi*$^-$]/red.

provide growth when over-expressed, in a normally lethal, Δ*sse1*Δ*sse2* strain. Other groups such as Raviol *et al*. (2006b) and Sadlish *et al*. (2008) also confirmed that Fes1 could functionally compensate for Hsp110 which also supported this theory. From these results it can be concluded that Sse1 shares enough conserved function with its mammalian counterpart thus allowing HSPH1 to compensate for the loss of yeast Hsp110. This highlighted how Hsp110 proteins may have conserved functions such as NEF activity and the ability to bind and interact with Hsp70. This result emphasised the relevance of studying molecular chaperones in yeast systems as they do share functional characteristics with their mammalian equivalents. The fact that yeast protein Fes1 compensated for Hsp110 deletion highlights the conserved nature of these proteins even though they are structurally dissimilar. This suggested that perhaps it is the increased NEF function provided by Fes1 that is enough to rescue the Δ*sse1*Δ*sse2* lethal phenotype. Or perhaps Fes1 provides another function similar to Sse1 that we are unaware of. Fes1 was also over-expressed in the Sse1 mutants to see if increased NEF activity could recover [*PSI*$^{+}$]. The only mutant with an improved [*PSI*$^{+}$] phenotype was G616D. This suggested that perhaps G616D may be the only mutant whose [*psi*$^{-}$] phenotype is mainly due to a loss of NEF activity.

6.1.3 Hsp110 may play a role in yeast cellular homeostasis and strain G600 has background sensitivity.

Another aim of this study was to establish why certain Sse1 mutants were temperature-sensitive and whether this had any link with the role of Sse1 in cellular signaling pathways. These experiments not only highlighted that Hsp110 may play a role in cell signaling pathways and in cellular morphology, but also resulted in the discovery that strain G600 and BY4741 are comparably different which may be

related to acquired mutations in G600. 37^{o}C ts mutants G342D and G616D had osmoremedial temperature sensitivity suggesting a disruption to CWI signaling but tests on the mutants sensitivity to cell wall damaging agents resulted in a strain sensitivity problem. This led to the creation of a new BY4741 background Δ*sse1*Δ*sse2* strain. The G616D mutant had a reproducible ts phenotype in CM03 however G342D only appeared slow-growing and not completely ts at 37^{o}C, re-emphasising again the differences in strain backgrounds. At 37^{o}C G616D failed to grow in the presence of constitutively activated members of the CWI signaling cascade, *BCK1* and *PKC1* and the mutants showed little difference in their ability to grow on the chemical medium when compared to wild type Sse1. These results suggested that the mutants disrupted something different to CWI signaling.

Sse1 has been linked with protein kinase A (PKA) signaling and it has been shown that the temperature-sensitive effects of Δ*sse1* can be alleviated by reducing PKA signaling (Trott *et al*., 2005). This prompted the analysis of whether or not decreasing PKA activity could restore G342D and G616D temperature sensitivity in both CM02 and CM03. PKA activity is decreased by growth on non-fermentable carbon sources. When the mutants were grown on YP-glycerol they grew as well as WT Sse1 at 30^{o}C and 37^{o}C, in both CM02 and CM03. Trott *et al*. (2005) suggested that Sse1 may be a negative regulator of PKA so it is possible that the Sse1 ts mutants are not functioning properly as negative regulators of this pathway and thus demonstrate ts phenotypes on glucose medium at 37^{o}C because PKA is over-activated. These results were promising and could potentially establish why mutants G342D and G616D have a slow-growing or non-viable phenotype at increased temperatures. G616D could be located at a point in the Sse1 structure critical for

Sse1's role in regulating PKA signaling. This result was suggestive of a PKA signaling problem and warrants further investigation.

As discussed before, CM02 and CM03 demonstrated comparable growth and sensitivity differences. They were different in their ability to complement Hsp110 deletion with Fes1 and HSPH1 and they also displayed temperature-sensitive differences when expressing mutant G342D. CM02 and CM03 also showed comparable differences in sensitivity to cell wall damaging agents, when expressing WT Sse1. This evidence taken together confirmed the belief that CM02 has a background strain weakness making it particularly sensitive. However this characteristic was not observed in the PKA signaling tests as CM02 grew a lot better than CM03 on non-fermentable carbon medium. Another difference observed in the strains was their response to the expression of the Sse1 mutant Q458* but this may have been due to a difference in the level of nonsense suppression between the strains. A number of factors could contribute to increased readthrough in CM02 including the presence of the nonsense suppressor mutant *SUQ5*. When a truncated version of Q458* was created it could not support growth in either of the strains which confirmed that the stop codon mutant could possibly be subjected to increased readthrough in CM02.

Substantial differences observed between G600 and BY4741 background sensitivity prompted a genomic analysis of G600 to be carried out. This revealed that G600 contains 6,500 SNPs equating to approximately 1,500 non-synonymous amino acid changes. Amino acid changes were identified in a number of proteins that could potentially impact Sse1/Sse2 function and strain sensitivity. Changes were identified in proteins which phosphorylate Sse1 and Sse2, in the CWI signaling counterpart Pkc1 and in the PKA signaling protein Ira2. A number of ORFs had altered stop

codons, leading to protein elongation at the C-terminus, which could affect G600 molecular and cellular processes. Inactivating stop codon mutations (ISCMs) were also identified which could contribute to G600 sensitivity if the protein affected is necessary for cell signaling processes. Gene YBR074W encodes a vacuolar proteolytic enzyme and contained a 653 amino acid truncation in G600. Interestingly, when expressed on plasmid DNA, YBRO74W did improve G600 [*psi*$^-$] strain growth on SDS and congo red, suggesting that insufficient translation of YBRO74W may affect the strain sensitivity to chemical stress. An overall increased sensitivity of G600 [*psi*$^-$] cells compared to [*PSI*$^+$] cells on chemical medium was also observed, suggesting that some of G600 sensitivity may rely on cellular levels of [*PSI*$^+$]. These results were indicative that ISCMs in G600 may be the reason why it is a sensitive strain and [*psi*$^-$] strains may be more sensitive because of the increased functional Sup35 promoting translation termination at these ISCMs. This theory warrants further investigation which is discussed in section 6.3.

Sse1 may interact with the transcription factor SBF (Swi4-Swi6) in a way that supports cell growth and proliferation (Shaner *et al*., 2008). Swi6 is also involved in CWI signaling (Madden *et al*., 1997). The effect Swi6 deletion has on the cell, in the presence of Sse1 and Sse2 mutants, was tested in strain CM03. Comparative growth analysis revealed that deleting Swi6 has a major impact on Δ*sse1* cells at all temperatures but had little effect on Δ*sse2* cells even at 39^{o}C. Four Sse1 mutants were also tested in the presence of Δ*swi6*. They were all non-viable at 39^{o}C and slow-growing at other temperatures but did not exhibit as severe of an effect as Δ*sse1*Δ*swi6*. These results suggested that it is the combined loss of Sse1 and Swi6 that is having the negative effect on cell thermostability as Δ*sse1* grows relatively well at 30^{o}C and Δ*sse2*Δ*swi6* also grows well. These results were similar to those produced

by Shaner *et al*. (2008). Somehow the combined loss of function of Sse1 and Swi6 has a major impact on cell thermostability, either through CWI signaling or some other process. Normal cell morphology was also disrupted in Δ*swi6*Δ*sse1*, Δ*swi6*Δ*sse2* and Δ*swi6*Δ*sse1*Δ*sse2* + *sse1* mutants. They had a large, amorphous and elongated structure with some mutants exhibiting more severe effects than others. *sse1*, *sse2* delete strains and *sse1* mutants were tested alone and expressed normal circular budding cell morphology. Despite Shaner *et al*. (2008) stating that Δ*swi6* alone disrupts cell morphology no obvious physical changes were observed in BY4741Δ*swi6*. From these results it was concluded that the combined effect of *swi6* and *sse1*/*sse2* mutations has a huge impact on cell structure resulting in disrupted cell size and shape. It is possible that Sse1 NEF function may contribute to cell shape and morphology as complete loss of NEF (Δ*sse1*) and possible NEF mutant T365I had the most severe affect on cell structure and shape, in the presence of Δ*swi6*.

6.1.4. Sse1 and Sse2 proteins may have comparable differences in their roles in [*PSI*$^+$] propagation and cellular homeostasis

The comparative functional differences between *SSE1* and *SSE2* were analysed as little is known about these. Firstly, the abilities of Sse1 and Sse2 to provide cell growth and to promote [*PSI*$^+$] were compared. *SSE2* expressed alone in CM02 was incapable of maintaining [*PSI*$^+$] but in comparison *SSE1* expressed alone had a [*PSI*$^+$] phenotype, indicative of the major functional difference between these two homologous proteins. Although they are structurally similar and are both divergent members of the Hsp70 superfamily, Sse1 was more potent in its ability to propagate [*PSI*$^+$]. Perhaps because *SSE2* has low expression levels or low nucleotide

exchange function it is less able to function in yeast prion propagation. When comparing growth rates *SSE2* generation time was slower than *SSE1* at 30^{o}C and 37^{o}C. There was little difference in generation time in *SSE2* cells when grown at either 30^{o}C or 37^{o}C which was reflected in the subsequent comparative growth analysis. *SSE2* was ts at 39^{o}C but slow-growing at both 30^{o}C and 37^{o}C. It could be that Sse2 is less able to function as a 'holdase' of denatured proteins when the cell is exposed to increased temperatures. This could be why Δ*sse1* cells are more thermosensitive, as Sse2 is incapable at functioning in the protein disaggregation response to cellular stress (Shaner *et al*., 2004; Raviol *et al*., 2006). These results highlighted the importance of Sse1 and how it is the most important Hsp110 isoform in [*PSI*$^{+}$] propagation and in cell stress responses.

It was proposed that as Sse1 and Sse2 are 76% identical (Polier *et al*., 2010) it may be the small differences which make Sse2 incapable of promoting [*PSI*$^{+}$] propagation. The only Sse1 mutant location which was not conserved in Sse2 was E504. As this residue is important for Sse1 to function in [*PSI*$^{+}$] propagation it was theorised that Sse2 may also function better if it expressed E504 rather than Q504. Tests showed that Sse2^{Q504E} had an improved [*PSI*$^{+}$] phenotype compared to WT Sse2 but failed to provide Sse2 with better thermostability. This result suggested that Hsp110 proteins differ in their function between [*PSI*$^{+}$] propagation and thermostability as recovery of one phenotype did not result in recovery of the other. Residue G616 is conserved between Sse1 and Sse2 and to test if they have conserved function the G616D mutation was introduced into the Sse2 structure. The Sse2^{G616D} mutant remained [*psi*$^{-}$] but also exhibited a ts phenotype much worse than WT Sse2. It was concluded from these results that Sse1 and Sse2 do share conservation in their

function but possibly if Sse2 was more structurally similar to Sse1 it may be better able to promote [*PSI*$^{+}$] propagation.

Another enigmatic area explored was the effects phosphorylation has on the ability of Hsp110 to carry out its functions. Single and double deletions of the kinases proteins Akl1, Kin2 and Hsl1 had no major impact on [*PSI*$^{+}$] or on cell thermostability. Problems were encountered when it was discovered that single Δ*kin2* and Δ*hsl1* mutants failed to grow on SC – adenine medium even though they appeared [*PSI*$^{+}$] and single and double Δ*kin2* and Δ*hsl1* mutants failed to cure on GdnHCl. A number of potential possibilities as to why these unexpected phenotypes have appeared has been considered and will be further discussed in section 6.3.

The Sse1/Sse2 sites where phosphates bind to were identified using the Phosphopep database. These sites were altered in two ways, one that mimics constitutively active phosphorylation (E) or another which inhibits phosphorylation (A) completely. Sse1 phosphorylation site mutants displayed no effects on either temperature sensitivity or on [*PSI*$^{+}$]. In comparison, Sse2 phosphorylation site mutants did affect growth at restrictive temperatures. Mutant S384E was more ts than WT Sse2, therefore enhancing phosphorylation at this residue negatively affected temperature sensitivity. In comparison mutant S384A had enhanced growth at restrictive temperatures and it was resistant to phosphorylation. This characteristic appears unique to Sse2 as the same mutants were induced in Sse1 but did not have an effect. Most of the Sse2 phosphorylation site mutants also resulted in improved [*PSI*$^{+}$] propagation. The mutants appeared pink on limiting adenine and demonstrated full/partial growth on medium lacking adenine. Once again Sse2 mutants have a divergence in function as ones that improve growth and thermostability (S384A) did not exhibit the greatest improvement in [*PSI*$^{+}$] propagation. It appears from these

results that differentially phosphosphorylating Sse2 affects its ability to promote [*PSI*$^{+}$] propagation and withstand thermal stress. However there did not seem to be any preference for phosphorylation activation or deactivation as a combination of the mutants demonstrated the altered phenotypes. This work highlighted another difference between Sse1 and Sse2, as Sse2 seemed more sensitive to altering phosphorylation. It can only be presumed that the phenotypic results from these experiments were a result of posttranslational modification by protein phosphorylation. It is also possible that these mutations are causing structural alterations to the Sse2 protein that interfere with other interactions or functions that are not related to phosphorylation. The impact of phosphorylation on Sse2 needs to be further investigated.

6.2 A hypothesis for the role of Hsp110 in prion propagation

Previous work published by other groups has proven Hsp110 as a prion promoting chaperone (Fan *et al*., 2007; Sadlish *et al*., 2008). Other work also suggests that Sse1 plays an important role in cell signaling functions (Shaner *et al*., 2008). The work demonstrated in this thesis furthers our understanding of the role played by Hsp110 in yeast prion propagation and in cellular homeostasis. It is proposed that Sse1 plays an integral role in [*PSI*$^{+}$] and [*URE3*] propagation by interacting with Hsp70 at critical points necessary to drive nucleotide exchange. It is this nucleotide exchange that allows Hsp70 to bind and release prion aggregates and subsequently allows them pass onto daughter cells. ATP binding is also important for Sse1 to functionally interact with Hsp70 as mutations which disrupted ATP binding led to a loss of [*PSI*$^{+}$]. Mutational and structural analysis also led to the conclusion that Sse1

may play an Hsp70-independent role in prion propagation as certain mutants displayed [*PSI*$^{+}$] weak phenotypes but were not located at amino acid positions believed to be important for NEF function. Sse1 could functionally interact with [*PSI*$^{+}$] protein aggregates in a way that aids its folding and propagation and certain amino acid residues could be critical for this interaction. It is also proposed that Sse1 is important for cellular tolerance to heat stress possibly by the up-regulation of Sse1 expression during times of stress and aiding in the protein disaggregation system. Sse1 may also play a role in PKA signaling and may function alongside Hsp90 in maintaining cellular homeostasis and signaling through a number of cascades. Sse1 may also function alongside SBF transcription factors in the maintenance of cell shape and morphology. Together Sse1 and Sse2 are critical for cell survival but it is Sse1 that plays a more important role than Sse2 in prion propagation. Figure 6.1 illustrates the proposed functions played by Sse1 in prion propagation and in other cellular processes.

The results from this study can also be utilised to help further our understanding of the role played by Hsp110 in mammalian prion propagation. Yeast and mammalian Hsp110 both function as NEFs for Hsp70 (Dragovic *et al*., 2006) and in mammals HSPH1 may aid in prion propagation by providing this essential function. The fact that yeast Sse1 may have prion-related functions separate from its NEF function also implies the possibility that mammalian HSPH1 may also interact with PrP^{sc} intermediates in a way that promotes its stability and progression. Understanding the mechanisms by which Sse1 functions in yeast prion propagation could help to determine the nature of the relationship between mammalian HSPH1 and prion disease.

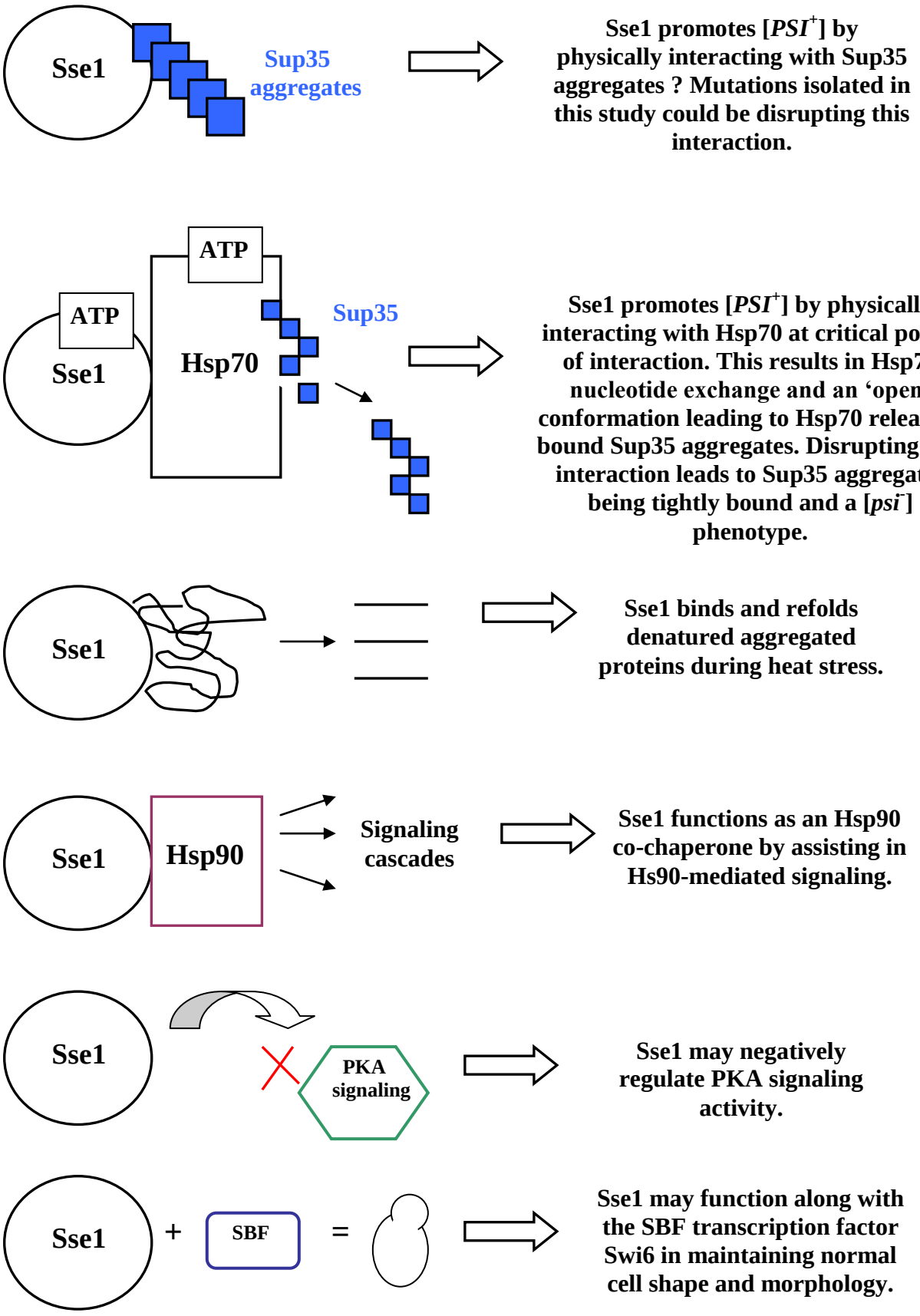

Figure 6.1. The proposed functions of Sse1 in yeast.

6.3 Future work

While the importance of Hsp110 as a molecular chaperone has been demonstrated mainly by genetic means there remains much scope for studying the nature of Hsp110 and the Hsp110 mutants by biochemical analysis. Purification of the Sse1 and Sse2 mutant proteins would allow us to test what effects the mutations are having on the ability of Sse1/Sse2 to hydrolyse ATP and function as NEFs. This would give a greater insight into the direct impact these mutations are having on the Sse1/Sse2 structure and subsequent functions. Sse1 mutants of particular interest would be ones implicated as disrupting NEF activity or ATPase activity. Sse2 mutant Q504E is interesting as it improved the ability of Sse2 to maintain [*PSI*$^{+}$] propagation. Purifying this protein, along with WT Sse2, would allow the rate of ATPase activity or nucleotide exchange to be measured and would determine if there is any improvement in the mutant versus WT.

The temperature-sensitive Sse1 mutant G616D was osmoremedial on 1 M sorbitol but tests failed to confirm any sensitivity to cell wall damaging medium in this mutant. Osmoremedial mutants often signify a disruption to the cell wall or cell organelles making the cell 'leaky'. By biochemical analysis this mutant strain could be tested to see if it is suffering from cytoplasm leakage and if so what the nature of the contents is. Mutant G616D was also recovered on non-fermentable glycerol indicating that it may be disrupting the ability of Sse1 to negatively regulate PKA signaling. Testing PKA activity in G616D mutant could help establish this theory. Ira2 protein is involved in PKA signaling and this protein was identified as having a non-synonymous change in G600. The *IRA2* gene could be incorporated into CM02 to see if this has an impact on growth. This mutation could be responsible for why G342D was ts in CM02 but not CM03.

The sensitivity of G600 to cell wall damaging agents was slightly improved when gene YBR074W was expressed. Other genes identified with nonsense mutations such as YNL106C could be transformed into G600 and tested alone and with YBR074W for improved growth on cell wall perturbing medium. If these genes are severely truncated in G600 then they could be responsible for disrupting cell homeostasis in G600.

Insight into the role of phosphorylation in chaperone function led to some interesting results. It appears that differentially phosphorylating Sse2 may impact its ability to maintain [*PSI*$^{+}$] and its thermostability. Future work could involve looking at these phosphorylation sites in more detail and perhaps performing some biochemical analysis on Sse2 when in a phosphorylated and non-phosphorylated state. This could be done by GFP tagging the Sse2 protein mutants and looking at differences in cellular location when in a phosphorylated and non-phosphorylated state. The mutants could also be measured for their rate of ATP hydrolysis using an ATPase assay. This would indicate if phosphorylation has any impact on the ability of Sse2 to exchange ATP in the peptide binding cycle.

Problems were encountered with kinase knockout strains. Due to time constraints no conclusion was made as to how they were affecting the cell. There are a number of things that could be explored such as whether disrupting these genes has an indirect effect on the adenine biosynthesis pathway, thus resulting in cells dying on SC – adenine. Are the mutants disrupting the pathway responsible for formation of the red pigment? It appears that Δ*hsl1* inability to cure on GdnHCl may be a dominant genetic defect as mating this mutant with a cured strain resulted in white colonies that were still unable to cure. These diploids could be sporulated to see if the colony colour segregates normally and also repeat the test for Δ*kin2*. From preliminary results

it appears that Δ*hsl1* and Δ*kin2* may be [*psi*$^{-}$] but somehow failing to produce the red pigment. This mutation could be introduced into a different strain such as 74D to see if the same phenotype occurs or whether it is a strain specific defect.

BIBLIOGRAPHY

AGUZZI, A. 2003. Prions and the immune system: a journey through gut, spleen, and nerves. *Adv Immunol,* 81**,** 123-71.

ALBERTI, S., HALFMANN, R., KING, O., KAPILA, A. & LINDQUIST, S. 2009. A systematic survey identifies prions and illuminates sequence features of prionogenic proteins. *Cell,* 137**,** 146-58.

ALLEN, K., WEGRZYN, R., CHERNOVA, T., MÜLLER, S., NEWNAM, G., WINSLETT, P., WITTICH, K., WILKINSON, K. & CHERNOFF, Y. 2005. Hsp70 chaperones as modulators of prion life cycle: novel effects of Ssa and Ssb on the Saccharomyces cerevisiae prion [PSI+]. *Genetics,* 169**,** 1227-42.

ALPER, T., HAIG, D. & CLARKE, M. 1966. The exceptionally small size of the scrapie agent. *Biochem Biophys Res Commun,* 22**,** 278-84.

ALPERS, M., 1987. Epidemiology and Chemical aspects of Kuru. In: S. Prusiner, & M. McKinley., eds. *Prions: novel infectious pathogens causing scrapie and Creutzfeldt Jakob disease*. San Diego, CA, USA: Academic Press, pp. 451-65.

ANDREASSON, C., FIAUX, J., RAMPELT, H., DRUFFEL-AUGUSTIN, S. & BUKAU, B. 2008. Insights into the structural dynamics of the Hsp110-Hsp70 interaction reveal the mechanism for nucleotide exchange activity. *Proceedings of the National Academy of Sciences of the United States of America,* 105**,** 16519-16524.

ANDREWS, B. & HERSKOWITZ, I. 1989. The yeast SWI4 protein contains a motif present in developmental regulators and is part of a complex involved in cell-cycle-dependent transcription. *Nature,* 342**,** 830-3.

ANDREWS, B. & MOORE, L. 1992. Interaction of the yeast Swi4 and Swi6 cell cycle regulatory proteins in vitro. *Proc Natl Acad Sci U S A,* 89**,** 11852-6.

BACH, S., TALAREK, N., ANDRIEU, T., VIERFOND, J., METTEY, Y., GALONS, H., DORMONT, D., MEIJER, L., CULLIN, C. & BLONDEL, M. 2003. Isolation of drugs active against mammalian prions using a yeast-based screening assay. *Nat Biotechnol,* 21**,** 1075-81.

BAGRIANTSEV, S. N., GRACHEVA, E. O., RICHMOND, J. E. & LIEBMAN, S. W. 2008. Variant-specific PSI+ infection is transmitted by Sup35 polymers within PSI+ aggregates with heterogeneous protein composition. *Molecular Biology of the Cell,* 19**,** 2433-2443.

BARRAL, Y., PARRA, M., BIDLINGMAIER, S. & SNYDER, M. 1999. Nim1-related kinases coordinate cell cycle progression with the organization of the peripheral cytoskeleton in yeast. *Genes Dev,* 13**,** 176-87.

BAXA, U., WICKNER, R., STEVEN, A., ANDERSON, D., MAREKOV, L., YAU, W. & TYCKO, R. 2007. Characterization of beta-sheet structure in Ure2p1-89 yeast prion fibrils by solid-state nuclear magnetic resonance. *Biochemistry,* 46**,** 13149-62.

BENKEMOUN, L. & SAUPE, S. 2006. Prion proteins as genetic material in fungi. *Fungal Genet Biol,* 43**,** 789-803.

BLACKETER, M., MADAULE, P. & MYERS, A. 1995. Mutational analysis of morphologic differentiation in Saccharomyces cerevisiae. *Genetics,* 140**,** 1259-75.

BONS, N., MESTRE-FRANCES, N., BELLI, P., CATHALA, F., GAJDUSEK, D. & BROWN, P. 1999. Natural and experimental oral infection of nonhuman primates by bovine spongiform encephalopathy agents. *Proc Natl Acad Sci U S A,* 96**,** 4046-51.

BRACHMANN, A., BAXA, U. & WICKNER, R. 2005. Prion generation in vitro: amyloid of Ure2p is infectious. *EMBO J,* 24**,** 3082-92.

BRADFORD, M. 1976. A rapid and sensitive method for the quantification of microgram quantities of protein utilizing the principles of protein-dye binding. *Anal Biochem,* 72, 248-54.

BREEDEN, L. 1996. Start-specific transcription in yeast. *Curr Top Microbiol Immunol,* 208**,** 95-127.

BREEDEN, L. & NASMYTH, K. 1987. Similarity between cell-cycle genes of budding yeast and fission yeast and the Notch gene of Drosophila. *Nature,* 329**,** 651-4.

BROACH, J. & DESCHENES, R. 1990. The function of ras genes in Saccharomyces cerevisiae. *Adv Cancer Res,* 54**,** 79-139.

BRODSKY, J., WERNER, E., DUBAS, M., GOECKELER, J., KRUSE, K. & MCCRACKEN, A. 1999. The requirement for molecular chaperones during endoplasmic reticulum-associated protein degradation demonstrates that protein export and import are mechanistically distinct. *J Biol Chem,* 274**,** 3453-60.

BROWN, P., CATHALA, F., RAUBERTAS, R., GAJDUSEK, D. & CASTAIGNE, P. 1987. The epidemiology of Creutzfeldt-Jakob disease: conclusion of a 15-year investigation in France and review of the world literature. *Neurology,* 37**,** 895-904.

BROWN, P., PREECE, M., BRANDEL, J., SATO, T., MCSHANE, L., ZERR, I., FLETCHER, A., WILL, R., POCCHIARI, M., CASHMAN, N., D'AIGNAUX, J., CERVENÁKOVÁ, L., FRADKIN, J., SCHONBERGER, L. & COLLINS, S. 2000. Iatrogenic Creutzfeldt-Jakob disease at the millennium. *Neurology,* 55**,** 1075-81.

BROWN, P., PREECE, M. & WILL, R. 1992. "Friendly fire" in medicine: hormones, homografts, and Creutzfeldt-Jakob disease. *Lancet,* 340**,** 24-7.

BRUCE, M., WILL, R., IRONSIDE, J., MCCONNELL, I., DRUMMOND, D., SUTTIE, A., MCCARDLE, L., CHREE, A., HOPE, J., BIRKETT, C., COUSENS, S., FRASER, H. & BOSTOCK, C. 1997. Transmissions to mice indicate that 'new variant' CJD is caused by the BSE agent. *Nature,* 389**,** 498-501.

BUDKA, H., AGUZZI, A., BROWN, P., BRUCHER, J., BUGIANI, O., GULLOTTA, F., HALTIA, M., HAUW, J., IRONSIDE, J. & JELLINGER, K. 1995. Neuropathological diagnostic criteria for Creutzfeldt-Jakob disease (CJD) and other human spongiform encephalopathies (prion diseases). *Brain Pathol,* 5**,** 459-66.

BYRNE, L., COLE, D., COX, B., RIDOUT, M., MORGAN, B. & TUITE, M. 2009. The number and transmission of [PSI] prion seeds (propagons) in the yeast Saccharomyces cerevisiae. *Plos One,* 4, 1-10.

BÖSL, B., GRIMMINGER, V. & WALTER, S. 2005. Substrate binding to the molecular chaperone Hsp104 and its regulation by nucleotides. *Journal of Biological Chemistry*, 280, 38170-176.

BÖSL, B., GRIMMINGER, V. & WALTER, S. 2006. The molecular chaperone Hsp104--a molecular machine for protein disaggregation. *J Struct Biol,* 156**,** 139-48.

CABIB, E., DRGONOVÁ, J. & DRGON, T. 1998. Role of small G proteins in yeast cell polarization and wall biosynthesis. *Annu Rev Biochem,* 67**,** 307-33.

CABIB, E. & DURAN, A. 1975. Simple and sensitive procedure for screening yeast mutants that lyse at nonpermissive temperatures. *J Bacteriol,* 124**,** 1604-6.

CAUGHEY, B. & LANSBURY, P. 2003. Protofibrils, pores, fibrils, and neurodegeneration: separating the responsible protein aggregates from the innocent bystanders. *Annu Rev Neurosci,* 26**,** 267-98.

CHEN, R. & THORNER, J. 2007. Function and regulation in MAPK signaling pathways: lessons learned from the yeast Saccharomyces cerevisiae. *Biochim Biophys Acta,* 1773**,** 1311-40.

CHERNOFF, Y., DERKACH, I. & INGE-VECHTOMOV, S. 1993. Multicopy SUP35 gene induces de-novo appearance of psi-like factors in the yeast Saccharomyces cerevisiae. *Curr*

Genet, 24**,** 268-70.

CHERNOFF, Y., LINDQUIST, S., ONO, B., INGE-VECHTOMOV, S. & LIEBMAN, S. 1995. Role of the chaperone protein Hsp104 in propagation of the yeast prion-like factor [psi+]. *Science,* 268**,** 880-4.

CHERNOFF, Y., NEWNAM, G., KUMAR, J., ALLEN, K. & ZINK, A. 1999. Evidence for a protein mutator in yeast: role of the Hsp70-related chaperone ssb in formation, stability, and toxicity of the [PSI] prion. *Mol Cell Biol,* 19**,** 8103-12.

COHEN, P. 2000. The regulation of protein function by multisite phosphorylation--a 25 year update. *Trends Biochem Sci,* 25**,** 596-601.

COLLINGE, J. 2001. Prion diseases of humans and animals: their causes and molecular basis. *Annu Rev Neurosci,* 24**,** 519-50.

COLLINGE, J. 2005. Molecular neurology of prion disease. *J Neurol Neurosurg Psychiatry,* 76**,** 906-19.

COLLINGE, J., WHITFIELD, J., MCKINTOSH, E., BECK, J., MEAD, S., THOMAS, D. & ALPERS, M. 2006. Kuru in the 21st century--an acquired human prion disease with very long incubation periods. *Lancet,* 367**,** 2068-74.

COLLINS, S., DOUGLASS, A., VALE, R. & WEISSMAN, J. 2004. Mechanism of prion propagation: amyloid growth occurs by monomer addition. *PLoS Biol,* 2**,** e321.

COOPER, T. 2002. Transmitting the signal of excess nitrogen in Saccharomyces cerevisiae from the Tor proteins to the GATA factors: connecting the dots. *FEMS Microbiol Rev,* 26**,** 223-38.

COPE, M., YANG, S., SHANG, C. & DRUBIN, D. 1999. Novel protein kinases Ark1p and Prk1p associate with and regulate the cortical actin cytoskeleton in budding yeast. *J Cell Biol,*

144**,** 1203-18.

CORVERA, S., D'ARRIGO, A. & STENMARK, H. 1999. Phosphoinositides in membrane traffic. *Curr Opin Cell Biol,* 11**,** 460-5.

COSCHIGANO, P. & MAGASANIK, B. 1991. The URE2 gene product of Saccharomyces cerevisiae plays an important role in the cellular response to the nitrogen source and has homology to glutathione s-transferases. *Mol Cell Biol,* 11**,** 822-32.

COUSTOU, V., DELEU, C., SAUPE, S. & BEGUERET, J. 1997. The protein product of the het-s heterokaryon incompatibility gene of the fungus Podospora anserina behaves as a prion analog. *Proc Natl Acad Sci U S A,* 94**,** 9773-8.

COX, B. 1965. PSI, a cytoplasmic suppressor of super-suppressor in yeast. *Heredity,* 20, 505-521.

COX, B., NESS, F. & TUITE, M. 2003. Analysis of the generation and segregation of propagons: entities that propagate the [PSI+] prion in yeast. *Genetics,* 165**,** 23-33.

CUFF, J. & BARTON, G. 2000. Application of multiple sequence alignment profiles to improve protein secondary structure prediction. *Proteins,* 40**,** 502-11.

CYR, D. 2008. Swapping nucleotides, tuning Hsp70. *Cell,* 133**,** 945-7.

DALSTRA, H., SWART, K., DEBETS, A., SAUPE, S. & HOEKSTRA, R. 2003. Sexual transmission of the [Het-S] prion leads to meiotic drive in Podospora anserina. *Proc Natl Acad Sci U S A,* 100**,** 6616-21.

DAVENPORT, K., SOHASKEY, M., KAMADA, Y., LEVIN, D. & GUSTIN, M. 1995. A second osmosensing signal transduction pathway in yeast. Hypotonic shock activates the PKC1 protein kinase-regulated cell integrity pathway. *J Biol Chem,* 270**,** 30157-61.

DE NOBEL, H., RUIZ, C., MARTIN, H., MORRIS, W., BRUL, S., MOLINA, M. & KLIS, F. 2000. Cell wall perturbation in yeast results in dual phosphorylation of the Slt2/Mpk1 MAP kinase and in an Slt2-mediated increase in FKS2-lacZ expression, glucanase resistance and thermotolerance. *Microbiology,* 146 (Pt 9)**,** 2121-32.

DEPACE, A., SANTOSO, A., HILLNER, P. & WEISSMAN, J. 1998. A critical role for amino-terminal glutamine/asparagine repeats in the formation and propagation of a yeast prion. *Cell,* 93**,** 1241-52.

DERKATCH, I., BRADLEY, M., HONG, J. & LIEBMAN, S. 2001. Prions affect the appearance of other prions: the story of [PIN(+)]. *Cell,* 106**,** 171-82.

DERKATCH, I., BRADLEY, M., ZHOU, P., CHERNOFF, Y. & LIEBMAN, S. 1997. Genetic and environmental factors affecting the de novo appearance of the [PSI+] prion in Saccharomyces cerevisiae. *Genetics,* 147**,** 507-19.

DERKATCH, I., CHERNOFF, Y., KUSHNIROV, V., INGE-VECHTOMOV, S. & LIEBMAN, S. 1996. Genesis and variability of [PSI] prion factors in Saccharomyces cerevisiae. *Genetics,* 144**,** 1375-86.

DOBSON, C. 2003. Protein folding and misfolding. *Nature,* 426**,** 884-90.

DODOU, E. & TREISMAN, R. 1997. The Saccharomyces cerevisiae MADS-box transcription factor Rlm1 is a target for the Mpk1 mitogen-activated protein kinase pathway. *Mol Cell Biol,* 17**,** 1848-59.

DOEL, S., MCCREADY, S., NIERRAS, C. & COX, B. 1994. The dominant PNM2- mutation which eliminates the psi factor of Saccharomyces cerevisiae is the result of a missense mutation in the SUP35 gene. *Genetics,* 137**,** 659-70.

DONNELLY, C., FERGUSON, N., GHANI, A. & ANDERSON, R. 2002. Implications of BSE

infection screening data for the scale of the British BSE epidemic and current European infection levels. *Proc Biol Sci,* 269**,** 2179-90.

DOYLE, S., SHORTER, J., HOSKINS, J., LINDQUIST, S. & WICKNER, S. 2007. Asymmetric deceleration of ClpB or Hsp104 ATPase activity unleashes protein-remodeling activity. *Struct Mol Biol,* 14, 114-122.

DRAGOVIC, Z., BROADLEY, S. A., SHOMURA, Y., BRACHER, A. & HARTL, F. U. 2006. Molecular chaperones of the Hsp110 family act as nucleotide exchange factors of Hsp70s. *Embo Journal,* 25**,** 2519-2528.

DU, Z., PARK, K., YU, H., FAN, Q. & LI, L. 2008. Newly identified prion linked to the chromatin-remodeling factor Swi1 in Saccharomyces cerevisiae. *Nat Genet,* 40**,** 460-5.

EAGLESTONE, S., COX, B. & TUITE, M. 1999. Translation termination efficiency can be regulated in Saccharomyces cerevisiae by environmental stress through a prion-mediated mechanism. *EMBO J,* 18**,** 1974-81.

EASTON, D., KANEKO, Y. & SUBJECK, J. 2000. The hsp110 and Grp1 70 stress proteins: newly recognized relatives of the Hsp70s. *Cell Stress Chaperones,* 5**,** 276-90.

ELBERT, M., ROSSI, G. & BRENNWALD, P. 2005. The yeast par-1 homologs kin1 and kin2 show genetic and physical interactions with components of the exocytic machinery. *Mol Biol Cell,* 16**,** 532-49.

ERHARDT, M., WEGRZYN, R. & DEUERLING, E. 2010. Extra N-terminal residues have a profound effect on the aggregation properties of the potential yeast prion protein Mca1. *PLoS One,* 5, 9929-9939.

ERREDE, B., CADE, R., YASHAR, B., KAMADA, Y., LEVIN, D., IRIE, K. & MATSUMOTO, K. 1995. Dynamics and organization of MAP kinase signal pathways. *Mol*

Reprod Dev, 42, 477-85.

FAN, Q., PARK, K. W., DU, Z. Q., MORANO, K. A. & LI, L. M. 2007. The role of Sse1 in the de novo formation and variant determination of the PSI+ prion. *Genetics,* 177**,** 1583-1593.

FECHTELER, T., DENGLER, U. & SCHOMBURG, D. 1995. Prediction of protein three-dimensional structures in insertion and deletion regions: a procedure for searching data bases of representative protein fragments using geometric scoring criteria. *J Mol Biol,* 253**,** 114-31.

FERREIRA, P., NESS, F., EDWARDS, S., COX, B. & TUITE, M. 2001. The elimination of the yeast [PSI+] prion by guanidine hydrochloride is the result of Hsp104 inactivation. *Mol Microbiol,* 40**,** 1357-69.

FIROOZAN, M., GRANT, C., DUARTE, J. & TUITE, M. 1991. Quantification of readthrough of termination codons in yeast using a novel gene fusion assay. *Yeast,* 7, 173-183.

FUCHS, B. & MYLONAKIS, E. 2009. Our paths might cross: the role of the fungal cell wall integrity pathway in stress response and cross talk with other stress response pathways. *Eukaryot Cell,* 8**,** 1616-25.

GAJDUSEK, D. 1977. Unconventional viruses and the origin and disappearance of kuru. *Science,* 197**,** 943-60.

GHANI, A., DONNELLY, C., FERGUSON, N. & ANDERSON, R. 2003. Updated projections of future vCJD deaths in the UK. *BMC Infect Dis,* 3**,** 4.

GIBBS, C. J., GAJDUSEK, D. & LATARJET, R. 1978. Unusual resistance to ionizing radiation of the viruses of kuru, Creutzfeldt-Jakob disease, and scrapie. *Proc Natl Acad Sci U S A,* 75**,** 6268-70.

GLOVER, J. & LINDQUIST, S. 1998. Hsp104, Hsp70, and Hsp40: a novel chaperone system

that rescues previously aggregated proteins. *Cell,* 94**,** 73-82.

GOECKELER, J., PETRUSO, A., AGUIRRE, J., CLEMENT, C., CHIOSIS, G. & BRODSKY, J. 2008. The yeast Hsp110, Sse1p, exhibits high-affinity peptide binding. *FEBS Lett,* 582**,** 2393-6.

GOECKELER, J. L., STEPHENS, A., LEE, P., CAPLAN, A. J. & BRODSKY, J. L. 2002. Overexpression of yeast Hsp110 homolog Sse1p suppresses ydj1-151 thermosensitivity and restores Hsp90-dependent activity. *Molecular Biology of the Cell,* 13**,** 2760-2770.

GONG, Y., KAKIHARA, Y., KROGAN, N., GREENBLATT, J., EMILI, A., ZHANG, Z. & HOURY, W. 2009. An atlas of chaperone-protein interactions in Saccharomyces cerevisiae: implications to protein folding pathways in the cell. *Mol Syst Biol,* 5**,** 275.

GUINAN, E. & JONES, G. 2009. Influence of Hsp70 chaperone machinery on yeast prion propagation. *Protein Pept Lett,* 16**,** 583-6.

HALFMANN, R., ALBERTI, S. & LINDQUIST, S. 2010. Prions, protein homeostasis, and phenotypic diversity. *Trends Cell Biol,* 20**,** 125-33.

HANKS, S., QUINN, A. & HUNTER, T. 1988. The protein kinase family: conserved features and deduced phylogeny of the catalytic domains. *Science,* 241**,** 42-52.

HARRISON, J., ZYLA, T., BARDES, E. & LEW, D. 2004. Stress-specific activation mechanisms for the "cell integrity" MAPK pathway. *J Biol Chem,* 279**,** 2616-22.

HATTENDORF, D. & LINDQUIST, L. 2002. Cooperative kinetics of both Hsp104 ATPase domains and interdomain communication revealed by AAA sensor-1 mutants. *EMBO J,* 21, 12-21.

HENRY, K., D'HONDT, K., CHANG, J., NIX, D., COPE, M., CHAN, C., DRUBIN, D. & LEMMON, S. 2003. The actin-regulating kinase Prk1p negatively regulates Scd5p, a suppressor of clathrin deficiency, in actin organization and endocytosis. *Curr Biol,* 13**,** 1564-9.

HILL, A., DESBRUSLAIS, M., JOINER, S., SIDLE, K., GOWLAND, I. & COLLINGE, J. 1997. The same prion strain causes vCJD and BSE. *Nature*, 389, 448-50.

HILL, A., BUTTERWORTH, R., JOINER, S., JACKSON, G., ROSSOR, M., THOMAS, D., FROSH, A., TOLLEY, N., BELL, J., SPENCER, M., KING, A., AL-SARRAJ, S., IRONSIDE, J., LANTOS, P. & COLLINGE, J. 1999. Investigation of variant Creutzfeldt-Jakob disease and other human prion diseases with tonsil biopsy samples. *Lancet,* 353**,** 183-9.

HOSODA, N., KOBAYASHI, T., UCHIDA, N., FUNAKOSHI, Y., KIKUCHI, Y., HOSHINO, S. & KATADA, T. 2003. Translation termination factor eRF3 mediates mRNA decay through the regulation of deadenylation. *J Biol Chem,* 278**,** 38287-91.

HUTCHISON, C., PHILIPS, S., EDGELL, M., GILLAM, S., JAHNKE, J. & SMITH, M. 1978. Mutagenesis at a specific position in a DNA sequence. *J Biol Chem,*253, 6551-6560.

IGUAL, J., JOHNSON, A. & JOHNSTON, L. 1996. Coordinated regulation of gene expression by the cell cycle transcription factor Swi4 and the protein kinase C MAP kinase pathway for yeast cell integrity. *EMBO J,* 15**,** 5001-13.

IRIE, K., TAKASE, M., LEE, K., LEVIN, D., ARAKI, H., MATSUMOTO, K. & OSHIMA, Y. 1993. MKK1 and MKK2, which encode Saccharomyces cerevisiae mitogen-activated protein kinase-kinase homologs, function in the pathway mediated by protein kinase C. *Mol Cell Biol,* 13**,** 3076-83.

IRONSIDE, J. & HEAD, M. 2004. Neuropathology and molecular biology of variant Creutzfeldt-Jakob disease. *Curr Top Microbiol Immunol,* 284**,** 133-59.

ITO, T., CHIBA, T., OZAWA, R., YOSHIDA, M., HATTORI, M. & SAKAKI, Y. 2001. A comprehensive two-hybrid analysis to explore the yeast protein interactome. *Proc Natl Acad Sci U S A*, 98**,** 4569-74.

JARRETT, J., BERGER, E. & LANSBURY, P. J. 1993. The carboxy terminus of the beta amyloid protein is critical for the seeding of amyloid formation: implications for the pathogenesis of Alzheimer's disease. *Biochemistry*, 32**,** 4693-7.

JIANG, J., PRASAD, K., LAFER, E. & SOUSA, R. 2005. Structural basis of interdomain communication in the Hsc70 chaperone. *Mol Cell*, 20**,** 513-24.

JOHNSTON, M. & CARLSTON, M., 1992. Carbon regulation in Saccharomyces cerevisiae. In: T. Broach, J. Pringle, & E. Jones., eds. *Molecular and Cellular Biology of the yeast Saccharomyces*. Cold Spring harbour, NY: Cold Spring Harbour Laboratory press.

JOHNSTON, G., EHRHARDT, C., LORINCZ, A. & CARTER, B. 1979. Regulation of cell size in the yeast Saccharomyces cerevisiae. *J Bacteriol*, 137**,** 1-5.

JONES, E. & FINK, G, 1982. Regulation of amino acid and nucleotide biosynthesis in yeast. In: J. Strathern, E. Jones & J. Broach., eds. *The molecular biology of the yeast Saccharomyces: metabolism and gene expression.* Cold Spring Harbour, NY: Cold Spring Harbour Laboratory Press, pp. 181-299.

JONES, G. & MASISON, D. 2003. Saccharomyces cerevisiae Hsp70 mutations affect [PSI+] prion propagation and cell growth differently and implicate Hsp40 and tetratricopeptide repeat cochaperones in impairment of [PSI+]. *Genetics*, 163**,** 495-506.

JONES, G., SONG, Y., CHUNG, S. & MASISON, D. 2004. Propagation of Saccharomyces cerevisiae [PSI+] prion is impaired by factors that regulate Hsp70 substrate binding. *Mol Cell Biol*, 24**,** 3928-37.

JONES, G. & TUITE, M. 2005. Chaperoning prions: the cellular machinery for propagating an infectious protein? *Bioessays,* 27**,** 823-32.

JUNG, G., JONES, G., WEGRZYN, R. & MASISON, D. 2000. A role for cytosolic hsp70 in yeast [PSI(+)] prion propagation and [PSI(+)] as a cellular stress. *Genetics,* 156**,** 559-70.

JUNG, U., SOBERING, A., ROMEO, M. & LEVIN, D. 2002. Regulation of the yeast Rlm1 transcription factor by the Mpk1 cell wall integrity MAP kinase. *Mol Microbiol,* 46**,** 781-9.

KABANI, M., BECKERICH, J. & BRODSKY, J. 2002. Nucleotide exchange factor for the yeast Hsp70 molecular chaperone Ssa1p. *Mol Cell Biol,* 22**,** 4677-89.

KAJAVA, A., BAXA, U., WICKNER, R. & STEVEN, A. 2004. A model for Ure2p prion filaments and other amyloids: the parallel superpleated β-structure. *Proc. Natl. Acad. Sci. USA,* 101, 7885-90.

KAMADA, Y., JUNG, U., PIOTROWSKI, J. & LEVIN, D. 1995. The protein kinase C-activated MAP kinase pathway of Saccharomyces cerevisiae mediates a novel aspect of the heat shock response. *Genes Dev,* 9**,** 1559-71.

KAMPINGA, H., HAGEMAN, J., VOS, M., KUBOTA, H., TANGUAY, R., BRUFORD, E., CHEETHAM, M., CHEN, B. & HIGHTOWER, L. 2009. Guidelines for the nomenclature of the human heat shock proteins. *Cell Stress Chaperones,* 14**,** 105-11.

KETELA, T., GREEN, R. & BUSSEY, H. 1999. Saccharomyces cerevisiae mid2p is a potential cell wall stress sensor and upstream activator of the PKC1-MPK1 cell integrity pathway. *J Bacteriol,* 181**,** 3330-40.

KING, C. & DIAZ-AVALOS, R. 2004. Protein-only transmission of three yeast prion strains. *Nature,* 428, 319-23.

KOCH, C., MOLL, T., NEUBERG, M., AHORN, H. & NASMYTH, K. 1993. A role for the transcription factors Mbp1 and Swi4 in progression from G1 to S phase. *Science,* 261**,** 1551-7.

KOCH, C. & NASMYTH, K. 1994. Cell cycle regulated transcription in yeast. *Curr Opin Cell Biol,* 6**,** 451-9.

KRISHNAN, R. & LINDQUIST, S. 2005. Structural insights into a yeast prion illuminate nucleation and strain diversity. *Nature,* 435, 765-72.

KRYNDUSHKIN, D., ALEXANDROV, I., TER-AVANESYAN, M. & KUSHNIROV, V. 2003. Yeast [PSI+] prion aggregates are formed by small Sup35 polymers fragmented by Hsp104. *J Biol Chem,* 278, 49636-43.

KRYNDUSHKIN, D., SMIRNOV, V., TER-AVANESYAN, M. & KUSHNIROV, V. 2002. Increased expression of Hsp40 chaperones, transcriptional factors, and ribosomal protein Rpp0 can cure yeast prions. *J Biol Chem,* 277**,** 23702-8.

KRYNDUSHKIN, D. & WICKNER, R. B. 2007. Nucleotide exchange factors for Hsp70s are required for [URE3] prion propagation in Saccharomyces cerevisiae. *Molecular Biology of the Cell,* 18**,** 2149-2154.

KUSHNIROV, V., KRYNDUSHKIN, D., BOGUTA, M., SMIRNOV, V. & TER-AVANESYAN, M. 2000. Chaperones that cure yeast artificial [PSI+] and their prion-specific effects. *Curr Biol,* 10**,** 1443-6.

LACROUTE, F. 1971. Non-Mendelian mutation allowing ureidosuccinic acid uptake in yeast. *J Bacteriol,* 106**,** 519-22.

LAMB, A., TIBBETTS, M. & HAMMOND, C. 1991. The product of the KIN1 locus in Saccharomyces cerevisiae is a serine/threonine-specific protein kinase. *Yeast,* 7**,** 219-28.

LEE, H., BROWN, P., CERVENÁKOVÁ, L., GARRUTO, R., ALPERS, M., GAJDUSEK, D. & GOLDFARB, L. 2001. Increased susceptibility to Kuru of carriers of the PRNP 129 methionine/methionine genotype. *J Infect Dis,* 183**,** 192-196.

LEE, K. & LEVIN, D. 1992. Dominant mutations in a gene encoding a putative protein kinase (BCK1) bypass the requirement for a Saccharomyces cerevisiae protein kinase C homolog. *Mol Cell Biol,* 12**,** 172-82.

LEE, P., SHABBIR, A., CARDOZO, C. & CAPLAN, A. 2004. Sti1 and Cdc37 can stabilize Hsp90 in chaperone complexes with a protein kinase. *Mol Biol Cell,* 15**,** 1785-92.

LEE-YOON, D., EASTON, D., MURAWSKI, M., BURD, R. & SUBJECK, J. 1995. Identification of a major subfamily of large hsp70-like proteins through the cloning of the mammalian 110-kDa heat shock protein. *J Biol Chem,* 270**,** 15725-33.

LEIDHOLD, C., VON JANOWSKY, B., BECKER, D., BENDER, T. & VOOS, W. 2006. Structure and function of Hsp78, the mitochondrial ClpB homolog. *J Struct Biol,* 156**,** 149-64.

LENGELER, K., DAVIDSON, R., D'SOUZA, C., HARASHIMA, T., SHEN, W., WANG, P., PAN, X., WAUGH, M. & HEITMAN, J. 2000. Signal transduction cascades regulating fungal development and virulence. *Microbiol Mol Biol Rev,* 64**,** 746-85.

LEVIN, D. 2005. Cell wall integrity signaling in Saccharomyces cerevisiae. *Microbiol Mol Biol Rev,* 69**,** 262-91.

LEVIN, D. & BARTLETT-HEUBUSCH, E. 1992. Mutants in the S. cerevisiae PKC1 gene display a cell cycle-specific osmotic stability defect. *J Cell Biol,* 116**,** 1221-9.

LEVIN, D., BOWERS, B., CHEN, C., KAMADA, Y. & WATANABE, M. 1994. Dissecting the protein kinase C/MAP kinase signalling pathway of Saccharomyces cerevisiae. *Cell Mol Biol Res,* 40**,** 229-39.

LEVIN, D., FIELDS, F., KUNISAWA, R., BISHOP, J. & THORNER, J. 1990. A candidate protein kinase C gene, PKC1, is required for the S. cerevisiae cell cycle. *Cell,* 62**,** 213-24.

LEVITT, M. 1992. Accurate modeling of protein conformation by automatic segment matching. *J Mol Biol,* 226**,** 507-33.

LI, L. & LINDQUIST, S. 2000. Creating a protein-based element of inheritance. *Science,* 287**,** 661-4.

LIAN, H. Y., JIANG, Y., ZHANG, H., JONES, G. W. & PERRETT, S. 2006. The yeast prion protein Ure2: Structure, function and folding. *Biochimica Et Biophysica Acta-Proteins and Proteomics,* 1764**,** 535-545.

LIEBMAN, S. & SHERMAN, F. 1979. Extrachromosomal psi+ determinant suppresses nonsense mutations in yeast. *J Bacteriol,* 139**,** 1068-71.

LINDQUIST, S., KROBITSCH, S., LI, L. & SONDHEIMER, N. 2001. Investigating protein conformation-based inheritance and disease in yeast. *Philos Trans R Soc Lond B Biol Sci,* 356**,** 169-76.

LITI, G., CARTER, D., MOSES, A., WARRINGER, J., PARTS, L., JAMES, S., DAVEY, R., ROBERTS, I., BURT, A., KOUFOPANOU, V., TSAI, I., BERGMAN, C., BENSASSON, D., O'KELLY, M., VAN OUDENAARDEN, A., BARTON, D., BAILES, E., NGUYEN, A., JONES, M., QUAIL, M., GOODHEAD, I., SIMS, S., SMITH, F., BLOMBERG, A., DURBIN, R. & LOUIS, E. 2009. Population genomics of domestic and wild yeasts. *Nature,* 458**,** 337-41.

LIU, Q. L. & HENDRICKSON, W. A. 2007. Insights into Hsp70 chaperone activity from a crystal structure of the yeast Hsp110 Sse1. *Cell,* 131**,** 106-120.

LIU, X. D., MORANO, K. A. & THIELE, D. J. 1999. The yeast Hsp110 family member, SSE1, is an Hsp90 cochaperone. *Journal of Biological Chemistry,* 274**,** 26654-26660.

LOOVERS, H. M., GUINAN, E. & JONES, G. W. 2007. Importance of the Hsp70 ATPase domain in yeast prion propagation. *Genetics,* 175**,** 621-630.

LUM, R., TKACH, J., VIERLING, E. & GLOVER, J. 2004. Evidence for an unfolding/threading mechanism for protein disaggregation by Saccharomyces cerevisiae Hsp104. *J Biol Chem,* 279**,** 29139-46.

MADDEN, K., SHEU, Y., BAETZ, K., ANDREWS, B. & SNYDER, M. 1997. SBF cell cycle regulator as a target of the yeast PKC-MAP kinase pathway. *Science,* 275**,** 1781-4.

MANDAL, A., GIBNEY, P., NILLEGODA, N., THEODORAKI, M., CAPLAN, A. & MORANO, K. 2010. Hsp110 chaperones control client fate determination in the hsp70-Hsp90 chaperone system. *Mol Biol Cell,* 21**,** 1439-48.

MANNING, G., PLOWMAN, G., HUNTER, T. & SUDARSANAM, S. 2002. Evolution of protein kinase signaling from yeast to man. *Trends Biochem Sci,* 27**,** 514-20.

MARTÍN, H., RODRIGUEZ-PACHON, J., RUIZ, C., NOMBELA, C. & MOLINA, M. 2000. Regulatory mechanisms for modulation of signaling through the cell integrity Slt2-mediated pathway in Saccharomyces cerevisiae. *J Biol Chem,* 275, 1511-9.

MASISON, D. & WICKNER, R. 1995. Prion-inducing domain of yeast Ure2p and protease resistance of Ure2p in prion-containing cells. *Science,* 270**,** 93-5.

MAYER, M., BREHMER, D., GÄSSLER, C. & BUKAU, B. 2001. Hsp70 chaperone machines. *Adv Protein Chem,* 59**,** 1-44.

MAYER, M. & BUKAU, B. 1999. Molecular chaperones: the busy life of Hsp90. *Curr Biol,* 9**,** R322-5.

MAYER, M. & BUKAU, B. 2005. Hsp70 chaperones: cellular functions and molecular mechanism. *Cell Mol Life Sci,* 62**,** 670-84.

M'GOWAN, J. 1914. *Investigation into the disease of sheep called scrapie*. Edinburgh: William Blackwood and sons.

MCKINLEY, M., MEYER, R., KENAGA, L., RAHBAR, F., COTTER, R., SERBAN, A. & PRUSINER, S. 1991. Scrapie prion rod formation in vitro requires both detergent extraction and limited proteolysis. *J Virol,* 65**,** 1340-51.

MCMILLAN, J., LONGTINE, M., SIA, R., THEESFELD, C., BARDES, E., PRINGLE, J. & LEW, D. 1999. The morphogenesis checkpoint in Saccharomyces cerevisiae: cell cycle control of Swe1p degradation by Hsl1p and Hsl7p. *Mol Cell Biol,* 19**,** 6929-39.

MEAD, S. 2006. Prion disease genetics. *Eur J Hum Genet,* 14**,** 273-81.

MEAD, S., POULTER, M., UPHILL, J., BECK, J., WHITFIELD, J., WEBB, T., CAMPBELL, T., ADAMSON, G., DERIZIOTIS, P., TABRIZI, S., HUMMERICH, H., VERZILLI, C., ALPERS, M., WHITTAKER, J. & COLLINGE, J. 2009. Genetic risk factors for variant Creutzfeldt-Jakob disease: a genome-wide association study. *Lancet Neurol,* 8**,** 57-66.

MEAD, S., STUMPF, M., WHITFIELD, J., BECK, J., POULTER, M., CAMPBELL, T., UPHILL, J., GOLDSTEIN, D., ALPERS, M., FISHER, E. & COLLINGE, J. 2003. Balancing selection at the prion protein gene consistent with prehistoric kurulike epidemics. *Science,* 300**,** 640-3.

MEIMARIDOU, E., GOOLJAR, S. & CHAPPLE, J. 2009. From hatching to dispatching: the multiple cellular roles of the Hsp70 molecular chaperone machinery. *J Mol Endocrinol,* 42**,** 1-9.

MELLOR, H. & PARKER, P. 1998. The extended protein kinase C superfamily. *Biochem J,* 332 (Pt 2)**,** 281-92.

MEYER, R., MCKINLEY, M., BOWMAN, K., BRAUNFELD, M., BARRY, R. & PRUSINER, S. 1986. Separation and properties of cellular and scrapie prion proteins. *Proc Natl Acad Sci U S A,* 83**,** 2310-4.

MICHELITSCH, M. & WEISSMAN, J. 2000. A census of glutamine/asparagine-rich regions: implications for their conserved function and the prediction of novel prions. *Proc Natl Acad Sci U S A,* 97**,** 11910-5.

MILLSON, S., TRUMAN, A., KING, V., PRODROMOU, C., PEARL, L. & PIPER, P. 2005. A two-hybrid screen of the yeast proteome for Hsp90 interactors uncovers a novel Hsp90 chaperone requirement in the activity of a stress-activated mitogen-activated protein kinase, Slt2p (Mpk1p). *Eukaryot Cell,* 4**,** 849-60.

MOK, J., KIM, P., LAM, H., PICCIRILLO, S., ZHOU, X., JESCHKE, G., SHERIDAN, D., PARKER, S., DESAI, V., JWA, M., CAMERONI, E., NIU, H., GOOD, M., REMENYI, A., MA, J., SHEU, Y., SASSI, H., SOPKO, R., CHAN, C., DE VIRGILIO, C., HOLLINGSWORTH, N., LIM, W., STERN, D., STILLMAN, B., ANDREWS, B., GERSTEIN, M., SNYDER, M. & TURK, B. 2010. Deciphering protein kinase specificity through large-scale analysis of yeast phosphorylation site motifs. *Sci Signal,* 3**,** ra12.

MOLLAPOUR, M., TSUTSUMI, S. & NECKERS, L. 2010. Hsp90 phosphorylation, Wee1, and the cell cycle. *Cell Cycle,* 9.

MUKAI, H., KUNO, T., TANAKA, H., HIRATA, D., MIYAKAWA, T. & TANAKA, C. 1993. Isolation and characterization of sse1 and sse2, new members of the yeast Hsp70 multigene family. *Gene,* 132**,** 57-66.

NAKAYASHIKI, T., KURTZMAN, C., EDSKES, H. & WICKNER, R. 2005. Yeast prions [URE3] and [PSI+] are diseases. *Proc Natl Acad Sci U S A,* 102**,** 10575-80.

NAMY, O., DUCHATEAU-NGUYEN, G., HATIN, I., HERMANN-LE DENMAT, S., TERMIER, M. & ROUSSET, J. 2003. Identification of stop codon readthrough genes in Saccharomyces cerevisiae. *Nucleic Acids Res,* 31, 2289-96.

NASMYTH, K. & DIRICK, L. 1991. The role of SWI4 and SWI6 in the activity of G1 cyclins in yeast. *Cell,* 66**,** 995-1013.

NATHAN, D., VOS, M. & LINDQUIST, S. 1997. In vivo functions of the Saccharomyces cerevisiae Hsp90 chaperone. *Proc Natl Acad Sci U S A,* 94**,** 12949-56.

NELSON, R., ZIEGELHOFFER, T., NICOLET, C., WERNER-WASHBURNE, M. & CRAIG, E. 1992. The translation machinery and 70 kd heat shock protein cooperate in protein synthesis. *Cell,* 71, 97-105.

NEMECEK, J., NAKAYASHIKI, T. & WICKNER, R. 2009. A prion of yeast metacaspase homolog (Mca1p) detected by a genetic screen. *Proc Natl Acad Sci U S A,* 106**,** 1892-6.

NONAKA, H., TANAKA, K., HIRANO, H., FUJIWARA, T., KOHNO, H., UMIKAWA, M., MINO, A. & TAKAI, Y. 1995. A downstream target of RHO1 small GTP-binding protein is PKC1, a homolog of protein kinase C, which leads to activation of the MAP kinase cascade in Saccharomyces cerevisiae. *EMBO J,* 14**,** 5931-8.

OH, H., CHEN, X. & SUBJECK, J. 1997. Hsp110 protects heat-denatured proteins and confers cellular thermoresistance. *J Biol Chem,* 272**,** 31636-40.

OH, H., EASTON, D., MURAWSKI, M., KANEKO, Y. & SUBJECK, J. 1999. The chaperoning activity of hsp110. Identification of functional domains by use of targeted deletions. *J Biol Chem,* 274**,** 15712-8.

OOMS, L., MCCOLL, B., WIRADJAJA, F., WIJAYARATNAM, A., GLEESON, P., GETHING, M., SAMBROOK, J. & MITCHELL, C. 2000. The yeast inositol polyphosphate 5-

phosphatases inp52p and inp53p translocate to actin patches following hyperosmotic stress: mechanism for regulating phosphatidylinositol 4,5-bisphosphate at plasma membrane invaginations. *Mol Cell Biol,* 20**,** 9376-90.

OSHEROVICH, L. & WEISSMAN, J. 2002. The utility of prions. *Dev Cell,* 2**,** 143-51.

PALMER, M., DRYDEN, A., HUGHES, J. & COLLINGE, J. 1991. Homozygous prion protein genotype predisposes to sporadic Creutzfeldt-Jakob disease. *Nature,* 352**,** 340-2.

PAN, K., BALDWIN, M., NGUYEN, J., GASSET, M., SERBAN, A., GROTH, D., MEHLHORN, I., HUANG, Z., FLETTERICK, R. & COHEN, F. 1993. Conversion of alpha-helices into beta-sheets features in the formation of the scrapie prion proteins. *Proc Natl Acad Sci U S A,* 90**,** 10962-6.

PAN, X., HARASHIMA, T. & HEITMAN, J. 2000. Signal transduction cascades regulating pseudohyphal differentiation of Saccharomyces cerevisiae. *Curr Opin Microbiol,* 3**,** 567-72.

PARAVICINI, G., COOPER, M., FRIEDLI, L., SMITH, D., CARPENTIER, J., KLIG, L. & PAYTON, M. 1992. The osmotic integrity of the yeast cell requires a functional PKC1 gene product. *Mol Cell Biol,* 12**,** 4896-905.

PARSELL, D., KOWAL, A. & LINDQUIST S. 1994a. Saccharomyces cerevisiae Hsp104 protein: Purification and characterization of ATP-induced structural changes. *J Biol Chem*, 269, 4480-7.

PARSELL, D., KOWAL, A., SINGER, M. & LINDQUIST, S. 1994b. Protein disaggregation mediated by heat-shock protein Hsp104. *Nature,* 372**,** 475-8.

PARSELL, D. & LINDQUIST, S. 1993. The function of heat-shock proteins in stress tolerance: degradation and reactivation of damaged proteins. *Annu Rev Genet,* 27**,** 437-96.

PATEL, B., GAVIN-SMYTH, J. & LIEBMAN, S. 2009. The yeast global transcriptional co-repressor protein Cyc8 can propagate as a prion. *Nat Cell Biol,* 11**,** 344-9.

PATINO, M., LIU, J., GLOVER, J. & LINDQUIST, S. 1996. Support for the prion hypothesis for inheritance of a phenotypic trait in yeast. *Science,* 273**,** 622-6.

PAUSHKIN, S., KUSHNIROV, W., SMIRNOV, V. & TER-AVANESYAN, M. 1996. Propagation of the yeast prion-like [psi+] determinant is mediated by oligomerization of the SUP35-encoded polypeptide chain release factor. *EMBO J,* 15, 3127-34.

PEARL, L. & PRODROMOU, C. 2000. Structure and in vivo function of Hsp90. *Curr Opin Struct Biol,* 10**,** 46-51.

PEARL, L. & PRODROMOU, C. 2001. Structure, function, and mechanism of the Hsp90 molecular chaperone. *Adv Protein Chem,* 59**,** 157-86.

PERRETT, S. & JONES, G. W. 2008. Insights into the mechanism of prion propagation. *Current Opinion in Structural Biology,* 18**,** 52-59.

PIPER, P., TRUMAN, A., MILLSON, S. & NUTTALL, J. 2006. Hsp90 chaperone control over transcriptional regulation by the yeast Slt2(Mpk1)p and human ERK5 mitogen-activated protein kinases (MAPKs). *Biochem Soc Trans,* 34**,** 783-5.

POLIER, S., DRAGOVIC, Z., HARTL, F. & BRACHER, A. 2008. Structural basis for the cooperation of Hsp70 and Hsp110 chaperones in protein folding. *Cell,* 133**,** 1068-79.

POLIER, S., HARTL, F. & BRACHER, A. 2010. Interaction of the Hsp110 molecular chaperones from S. cerevisiae with substrate protein. *J Mol Biol,* 401**,** 696-707.

PRATT, W. 1998. The hsp90-based chaperone system: involvement in signal transduction from a variety of hormone and growth factor receptors. *Proc Soc Exp Biol Med,* 217**,** 420-34.

PRUSINER, S. 1982. Novel proteinaceous infectious particles cause scrapie. *Science,* 216**,** 136-44.

PRUSINER, S. 1989. Scrapie prions. *Annu Rev Microbiol,* 43**,** 345-74.

PRUSINER, S. 1997. Prion diseases and the BSE crisis. *Science,* 278**,** 245-51.

PRUSINER, S. 1998. Prions. *Proc Natl Acad Sci U S A,* 95**,** 13363-83.

PRUSINER, S. 2004. *Prion Biology and Diseases*. 2nd ed. New York: Cold Spring Harbour Laboratory Press.

PTACEK, J., DEVGAN, G., MICHAUD, G., ZHU, H., ZHU, X., FASOLO, J., GUO, H., JONA, G., BREITKREUTZ, A., SOPKO, R., MCCARTNEY, R., SCHMIDT, M., RACHIDI, N., LEE, S., MAH, A., MENG, L., STARK, M., STERN, D., DE VIRGILIO, C., TYERS, M., ANDREWS, B., GERSTEIN, M., SCHWEITZER, B., PREDKI, P. & SNYDER, M. 2005. Global analysis of protein phosphorylation in yeast. *Nature,* 438**,** 679-84.

QUEITSCH, C., HONG, S., VIERLING, E. & LINDQUIST, S. 2000. Heat shock protein 101 plays a crucial role in thermotolerance in Arabidopsis. *Plant Cell,* 12, 479-492.

RAVIOL, H., BUKAU, B. & MAYER, M. 2006a. Human and yeast Hsp110 chaperones exhibit functional differences. *FEBS Lett,* 580**,** 168-74.

RAVIOL, H., SADLISH, H., RODRIGUEZ, F., MAYER, M. P. & BUKAU, B. 2006b. Chaperone network in the yeast cytosol: Hsp110 is revealed as an Hsp70 nucleotide exchange factor. *Embo Journal,* 25**,** 2510-2518.

RESENDE, C., OUTEIRO, T., SANDS, L., LINDQUIST, S. & TUITE, M. 2003. Prion protein polymorphisms in Saccharomyces cerevisiae. *Mol Microbiol,* 49, 1005-17.

RIESNER, D. 2003. Biochemistry and structure of PrP(C) and PrP(Sc). *Br Med Bull,* 66**,** 21-33.

RIKHVANOV, E., ROMANOVA, N. & CHERNOFF, Y. 2007. Chaperone effects on prion and nonprion aggregates. *Prion,* 1**,** 217-22.

ROMANOVA, N. & CHERNOFF, Y. 2009. Hsp104 and prion propagation. *Protein Pept Lett,* 16**,** 598-605.

RUBENSTEIN, E. & SCHMIDT, M. 2007. Mechanisms regulating the protein kinases of Saccharomyces cerevisiae. *Eukaryot Cell,* 6**,** 571-83.

SADLISH, H., RAMPELT, H., SHORTER, J., WEGRZYN, R. D., ANDREASSON, C., LINDQUIST, S. & BUKAU, B. 2008. Hsp110 Chaperones Regulate Prion Formation and Propagation in S-cerevisiae by Two Discrete Activities. *Plos One,* 3.

SANTANGELO, G. 2006. Glucose signaling in Saccharomyces cerevisiae. *Microbiol Mol Biol Rev,* 70**,** 253-82.

SCHATZ, P., SOLOMON, F. & BOTSTEIN, D. 1988. Isolation and characterization of conditional-lethal mutations in the TUB1 alpha-tubulin gene of the yeast Saccharomyces cerevisiae. *Genetics,* 120**,** 681-95.

SCHEIBEL, T., BLOOM, J. & LINDQUIST, S. 2004. The elongation of yeast prion fibers involves separable steps of association and conversion. *Proc Natl Acad Sci U S A,* 101**,** 2287-92.

SCHEIBEL, T. & LINDQUIST, S. 2001. The role of conformational flexibility in prion propagation and maintenance for Sup35p. *Nat Struct Biol,* 8**,** 958-62.

SCHIRMER, E., HOMANN, O., KOWAL, A. & LINDQUIST, S. 2004. Dominant gain-of-function mutations in Hsp104p reveal crucial roles for the middle region. *Mol Biol Cell,* 15, 2061-72.

SCHIRMER, E., QUEITSCH, C., KOWAL, A., PARSELL, D. & LINDQUIST, S. 1998. The ATPase activity of Hsp104, effects of environmental conditions and mutations. *J Biol Chem,* 273, 15546-52.

SCHLUMPBERGER, M., PRUSINER, S. & HERSKOWITZ, I. 2001a. Induction of distinct [URE3] yeast prion strains. *Mol Cell Biol,* 21**,** 7035-46.

SCHNEPER, L., DÜVEL, K. & BROACH, J. 2004. Sense and sensibility: nutritional response and signal integration in yeast. *Curr Opin Microbiol,* 7**,** 624-30.

SCHUERMANN, J. P., JIANG, J. W., CUELLAR, J., LLORCA, O., WANG, L. P., GIMENEZ, L. E., JIN, S. P., TAYLOR, A. B., DEMELER, B., MORANO, K. A., HART, P. J., VALPUESTA, J. M., LAFER, E. M. & SOUSA, R. 2008. Structure of the Hsp110 : Hsc70 nucleotide exchange machine. *Molecular Cell,* 31**,** 232-243.

SCHWIMMER, C. & MASISON, D. 2002. Antagonistic interactions between yeast [PSI(+)] and [URE3] prions and curing of [URE3] by Hsp70 protein chaperone Ssa1p but not by Ssa2p. *Mol Cell Biol,* 22**,** 3590-8.

SERIO, T. & LINDQUIST, S. 2000. Protein-only inheritance in yeast: something to get [PSI+]-ched about. *Trends Cell Biol,* 10**,** 98-105.

SHANER, L., GIBNEY, P. A. & MORANO, K. A. 2008. The Hsp110 protein chaperone Sse1 is required for yeast cell wall integrity and morphogenesis. *Current Genetics,* 54**,** 1-11.

SHANER, L., SOUSA, R. & MORANO, K. A. 2006. Characterization of Hsp70 binding and nucleotide exchange by the yeast Hsp110 chaperone Sse1. *Biochemistry,* 45**,** 15075-15084.

SHANER, L., TROTT, A., GOECKELER, J. L., BRODSKY, J. L. & MORANO, K. A. 2004. The function of the yeast molecular chaperone Sse1 is mechanistically distinct from the closely related Hsp70 family. *Journal of Biological Chemistry,* 279**,** 21992-22001.

SHANER, L., WEGELE, H., BUCHNER, J. & MORANO, K. A. 2005. The yeast Hsp110 Sse1 functionally interacts with the Hsp70 chaperones Ssa and Ssb. *Journal of Biological Chemistry,* 280**,** 41262-41269.

SHEWMAKER, F., WICKNER, R. & TYCKO, R. 2006. Amyloid of the prion domain of Sup35p has an in-register parallel beta-sheet structure. *Proc Natl Acad Sci U S A,* 103**,** 19754-9.

SHIRAYAMA, M., KAWAKAMI, K., MATSUI, Y., TANAKA, K. & TOH-E, A. 1993. MSI3, a multicopy suppressor of mutants hyperactivated in the RAS-cAMP pathway, encodes a novel HSP70 protein of Saccharomyces cerevisiae. *Mol Gen Genet,* 240**,** 323-32.

SHORTER, J. & LINDQUIST, S. 2005. Prions as adaptive conduits of memory and inheritance. *Nat Rev Genet,* 6**,** 435-50.

SHORTER, J. & LINDQUIST, S. 2006. Destruction or potentiation of different prions catalyzed by similar Hsp104 remodeling activities. *Mol Cell,* 23**,** 425-38.

SHORTER, J. & LINDQUIST, S. 2008. Hsp104, Hsp70 and Hsp40 interplay regulates formation, growth and elimination of Sup35 prions. *Embo Journal,* 27**,** 2712-2724.

SIKORSKI, R. & HIETER, P. 1989. A system of shuttle vectors and yeast host strains designed for efficient manipulation of DNA in Saccharomyces cerevisiae. *Genetics,* 122**,** 19-27.

SONDHEIMER, N. & LINDQUIST, S. 2000. Rnq1: an epigenetic modifier of protein function in yeast. *Mol. Cell,* 5, 163-172.

SONG, O., WANG, X., WATERBORG, J. & STERNGLANZ, R. 2003. An Nalpha-acetyltransferase responsible for acetylation of the N-terminal residues of histones H4 and H2A. *J Biol Chem,* 278**,** 38109-12.

SQUIRES, C.L., PEDERSEN, S., ROSS, B. & SQUIRES, C. 1991. ClpB is the Escherichia coli heat shock protein F84.1. *J Bacteriol,* 173, 4254-62.

STAHL, N., BORCHELT, D., HSIAO, K. & PRUSINER, S. 1987. Scrapie prion protein contains a phosphatidylinositol glycolipid. *Cell*, 51, 229-240.

STAHL, N., BALDWIN, M., TEPLOW, D., HOOD, L., GIBSON, B., BURLINGAME, A. & PRUSINER, S. 1993. Structural studies of the scrapie prion protein using mass spectrometry and amino acid sequencing. *Biochemistry,* 32**,** 1991-2002.

STANSFIELD, I., JONES, K., KUSHNIROV, V., DAGKESAMANSKAYA, A., POZNYAKOVSKI, A., PAUSHKIN, S., NIERRAS, C., COX, B., TER-AVANESYAN, M. & TUITE, M. 1995. The products of the SUP45 (eRF1) and SUP35 genes interact to mediate translation termination in Saccharomyces cerevisiae. *EMBO J,* 14**,** 4365-73.

STOLZ, L., HUYNH, C., THORNER, J. & YORK, J. 1998. Identification and characterization of an essential family of inositol polyphosphate 5-phosphatases (INP51, INP52 and INP53 gene products) in the yeast Saccharomyces cerevisiae. *Genetics,* 148**,** 1715-29.

STRASSBURG, K., WALTHER, D., TAKAHASHI, H., KANAYA, S. & KOPKA, J. 2010. Dynamic transcriptional and metabolic responses in yeast adapting to temperature stress. *OMICS,* 14**,** 249-59.

TANAKA, M., CHIEN, P., NABER, N., COOKE, R. & WEISSMAN, J. 2004. Conformational variations in an infectious protein determine prion strain differences. *Nature,* 18, 323-8.

TER-AVANESYAN, M., DAGKESAMANSKAYA, A., KUSHNIROV, V. & SMIRNOV, V. 1994. The SUP35 omnipotent suppressor gene is involved in the maintenance of the non-Mendelian determinant [psi+] in the yeast Saccharomyces cerevisiae. *Genetics,* 137**,** 671-6.

TESSIER, P. & LINDQUIST, S. 2009. Unraveling infectious structures, strain variants and species barriers for the yeast prion [PSI+]. *Nat Struct Mol Biol,* 16**,** 598-605.

THEVELEIN, J. & DE WINDE, J. 1999. Novel sensing mechanisms and targets for the cAMP-protein kinase A pathway in the yeast Saccharomyces cerevisiae. *Mol Microbiol,* 33**,** 904-18.

TORRES, L., MARTÍN, H., GARCÍA-SAEZ, M., ARROYO, J., MOLINA, M., SÁNCHEZ, M. & NOMBELA, C. 1991. A protein kinase gene complements the lytic phenotype of Saccharomyces cerevisiae lyt2 mutants. *Mol Microbiol,* 5**,** 2845-54.

TROTT, A., SHANER, L. & MORANO, K. A. 2005. The molecular chaperone Sse1 and the growth control protein kinase Sch9 collaborate to remalate protein kinase a activity in Saccharomyces cerevisiae. *Genetics,* 170**,** 1009-1021.

TRUCKSES, D., GARRENTON, L. & THORNER, J. 2004. Jekyll and Hyde in the microbial world. *Science,* 306**,** 1509-11.

TRUE, H. 2006. The battle of the fold: chaperones take on prions. *Trends Genet,* 22**,** 110-7.

TRUE, H. & LINDQUIST, S. 2000. A yeast prion provides a mechanism for genetic variation and phenotypic diversity. *Nature,* 407**,** 477-83.

TRUMAN, A., MILLSON, S., NUTTALL, J., MOLLAPOUR, M., PRODROMOU, C. & PIPER, P. 2007. In the yeast heat shock response, Hsf1-directed induction of Hsp90 facilitates the activation of the Slt2 (Mpk1) mitogen-activated protein kinase required for cell integrity. *Eukaryot Cell,* 6**,** 744-52.

TUITE, M. 2000. Cell biology. Sowing the protein seeds of prion propagation. *Science,* 289**,** 556-7.

TUITE, M. & COX, B. 2003. Propagation of yeast prions. *Nat Rev Mol Cell Biol,* 4**,** 878-90.

TUITE, M. & COX, B. 2007. The genetic control of the formation and propagation of the [PSI+] prion of yeast. *Prion,* 1**,** 101-9.

TUITE, M. & KOLOTEVA-LEVIN, N. 2004. Propagating prions in fungi and mammals. *Mol Cell,* 14**,** 541-52.

VALLERON, A., BOELLE, P., WILL, R. & CESBRON, J. 2001. Estimation of epidemic size and incubation time based on age characteristics of vCJD in the United Kingdom. *Science,* 294**,** 1726-8.

VERNA, J., LODDER, A., LEE, K., VAGTS, A. & BALLESTER, R. 1997. A family of genes required for maintenance of cell wall integrity and for the stress response in Saccharomyces cerevisiae. *Proc Natl Acad Sci U S A,* 94**,** 13804-9.

VOS, M., HAGEMAN, J., CARRA, S. & KAMPINGA, H. 2008. Structural and functional diversities between members of the human HSPB, HSPH, HSPA, and DNAJ chaperone families. *Biochemistry,* 47**,** 7001-11.

WADSWORTH, J. & COLLINGE, J. 2010. Molecular pathology of human prion disease. *Acta Neuropathol*.

WADSWORTH, J., HILL, A., BECK, J. & COLLINGE, J. 2003. Molecular and clinical classification of human prion disease. *Br Med Bull,* 66**,** 241-54.

WADSWORTH, J., JOINER, S., HILL, A., CAMPBELL, T., DESBRUSLAIS, M., LUTHERT, P. & COLLINGE, J. 2001. Tissue distribution of protease resistant prion protein in variant Creutzfeldt-Jakob disease using a highly sensitive immunoblotting assay. *Lancet,* 358**,** 171-80.

WAKATSUKI, T. & HATAYAMA, T. 1998. Characteristic expression of 105-kDa heat shock protein (HSP105) in various tissues of nonstressed and heat-stressed rats. *Biol Pharm Bull,* 21**,** 905-10.

WALES, T. & ENGEN, J. 2006. Hydrogen exchange mass spectrometry for the analysis of protein dynamics. *Mass Spectrom Rev,* 25**,** 158-70.

WALTER, S. & BUCHNER, J. 2002. Molecular chaperones--cellular machines for protein folding. *Angew Chem Int Ed Engl,* 41**,** 1098-113.

WANG, Y., PIERCE, M., SCHNEPER, L., GÜLDAL, C., ZHANG, X., TAVAZOIE, S. & BROACH, J. 2004. Ras and Gpa2 mediate one branch of a redundant glucose signaling pathway in yeast. *PLoS Biol,* 2**,** E128.

WATANABE, Y., TAKAESU, G., HAGIWARA, M., IRIE, K. & MATSUMOTO, K. 1997. Characterisation of a serum response factor-like protein in Saccharomyces serevisiae, Rlm1, which has a transcriptional activity regulated by the Mpk1 (Slt2) mitogen-activated protein kinase pathway. *Mol Cell Biol,* 17, 2615-2623.

WATSON, J., BAKER, T., BELL, S., GANN, A., LEVINE, M. & LOSICK, R., 2008. Model Organisms. In *Molecular Biology of the Gene*. 6th ed. New York: Cold Spring Harbour Laboratory Press, pp 795-797.

WEISSMANN, C. 1995. Molecular biology of transmissible spongiform encephalopathies. *Prog Brain Res,* 105**,** 15-22.

WEISSMANN, C. 2004. The state of the prion. *Nat Rev Microbiol,* 2, 861-71.

WEISSMANN, C. & AGUZZI, A. 2005. Approaches to therapy of prion diseases. *Annu Rev Med,* 56**,** 321-44.

WERNER-WASHBURNE, M., STONE, D. & CRAIG, E. 1987. Complex interactions among members of an essential subfamily of hsp70 genes in Saccharomyces cerevisiae. *Mol Cell Biol,* 7, 2568-77.

WICKNER, R. 1994. [URE3] as an altered URE2 protein: evidence for a prion analog in Saccharomyces cerevisiae. *Science,* 264**,** 566-9.

WICKNER, R. 2005. Scrapie in ancient China? *Science,* 309**,** 874.

WICKNER, R., EDSKES, H., SHEWMAKER, F., KRYNDUSHKIN, D. & NEMECEK, J. 2009. Prion variants, species barriers, generation and propagation. *J Biol,* 8**,** 47.

WICKNER, R., EDSKES, H., SHEWMAKER, F. & NAKAYASHIKI, T. 2007a. Prions of fungi: inherited structures and biological roles. *Nat Rev Microbiol,* 5**,** 611-8.

WICKNER, R., EDSKES, H., SHEWMAKER, F., NAKAYASHIKI, T., ENGEL, A., MCCANN, L. & KRYNDUSHKIN, D. 2007b. Yeast prions: evolution of the prion concept. *Prion,* 1**,** 94-100.

WICKNER, R., MASISON, D. & EDSKES, H. 1995. [PSI] and [URE3] as yeast prions. *Yeast,* 11**,** 1671-85.

WICKNER, R., TAYLOR, K., EDSKES, H., MADDELEIN, M., MORIYAMA, H. & ROBERTS, B. 2000. Prions of yeast as heritable amyloidoses. *J Struct Biol,* 130**,** 310-22.

WIEDERHOLD, E., GANDHI, T., PERMENTIER, H., BREITLING, R., POOLMAN, B. & SLOTBOOM, D. 2009. The yeast vacuolar membrane proteome. *Mol Cell Proteomics,* 8**,** 380-92.

WILL, R., IRONSIDE, J., ZEIDLER, M., COUSENS, S., ESTIBEIRO, K., ALPEROVITCH, A., POSER, S., POCCHIARI, M., HOFMAN, A. & SMITH, P. 1996. A new variant of Creutzfeldt-Jakob disease in the UK. *Lancet,* 347**,** 921-5.

WRIGHT, C., FEWELL, S., SULLIVAN, M., PIPAS, J., WATKINS, S. & BRODSKY, J. 2007. The Hsp40 molecular chaperone Ydj1p, along with the protein kinase C pathway, affects cell-

wall integrity in the yeast Saccharomyces cerevisiae. *Genetics,* 175**,** 1649-64.

WU, W. & LI, W. 2008. Identifying gene regulatory modules of heat shock response in yeast. *BMC Genomics,* 9, 439-454.

XU, Y. & LINDQUIST, S. 1993. Heat-shock protein hsp90 governs the activity of pp60v-src kinase. *Proc Natl Acad Sci U S A,* 90**,** 7074-8.

YAM, A., ALBANÈSE, V., LIN, H. & FRYDMAN, J. 2005. Hsp110 cooperates with different cytosolic HSP70 systems in a pathway for de novo folding. *J Biol Chem,* 280**,** 41252-61.

YAMAGISHI, N., ISHIHARA, K. & HATAYAMA, T. 2004. Hsp105 alpha suppresses Hsc70 chaperone activity by inhibiting Hsc70 ATPase activity. *Journal of Biological Chemistry,* 279**,** 41727-41733.

YAMAGISHI, N., ISHIHARA, K., SAITO, Y. & HATAYAMA, T. 2003. Hsp105 but not Hsp70 family proteins suppress the aggregation of heat-denatured protein in the presence of ADP. *FEBS Lett,* 555**,** 390-6.

ZAMAN, S., LIPPMAN, S., SCHNEPER, L., SLONIM, N. & BROACH, J. 2009. Glucose regulates transcription in yeast through a network of signaling pathways. *Mol Syst Biol,* 5**,** 245.

ZHAO, R., DAVEY, M., HSU, Y., KAPLANEK, P., TONG, A., PARSONS, A., KROGAN, N., CAGNEY, G., MAI, D., GREENBLATT, J., BOONE, C., EMILI, A. & HOURY, W. 2005. Navigating the chaperone network: an integrative map of physical and genetic interactions mediated by the hsp90 chaperone. *Cell,* 120**,** 715-27.

ZHU, X., DÉMOLIS, N., JACQUET, M. & MICHAELI, T. 2000. MSI1 suppresses hyperactive RAS via the cAMP-dependent protein kinase and independently of chromatin assembly factor-1. *Curr Genet,* 38**,** 60-70.

ZLOTNIK, I. & STAMP, J. 1961. Scrapie disease of sheep. *World Neurol,* 2**,** 895-907.